Chemistry–A European Journal

Supporting Information

Identification of Isomeric *N*-Glycans by Conformer Distribution Fingerprinting using Ion Mobility Mass Spectrometry

Javier Sastre Toraño[+],[a] Oier Aizpurua-Olaizola[+],[a, e] Na Wei,[b] Tiehai Li,[b] Luca Unione,[a] Gonzalo Jiménez-Osés,[c] Francisco Corzana,[d] Victor J. Somovilla,[a] Juan M. Falcon-Perez,[e] and Geert-Jan Boons*[a, b]

Contents

1. Experimental Procedures

1.1 Chemicals and reagents

Fetuin from bovine serum, MS-grade formic acid, MS-grade acetic acid, dimethyl sulfoxide (DMSO), 2-aminoanthrallic acid (2-AA), and sodium cyanoborohydride were purchased from Sigma Aldrich (Hamburg, Germany). MS-grade acetonitrile (ACN) was acquired from Biosolve (Dieuz, France), trifluoro acetic acid (TFA) from Argos Organics (Geel, Belgium) and PNGase F from E. coli was acquired from Roche (Basel, Switzerland). Reaction buffers of 1% NP-40, denaturation buffer (0.5% SDS, 40 mM dithiothreitol (DTT) and glycobuffer (50 mM sodium phosphate) were purchased from New England BioLabs (Ipswich, US). Ammonium formate was obtained from Fluka (Seelze, Germany), C_{18} SPE Sep-Pak® Vac (1cc) columns from Waters Corporation (Milford, US), PGC SPE Hypercarb Hypersep (1cc) columns from Thermo Scientific (Rockwood, USA) and PD Minitrap G-10 cartridges from GE Healthcare (Uppsala, Sweden). Ultra-pure water was obtained from a MerckMillipore Synergy® water purification system (Burlington, US).

1.2 Enzymatic synthesis of complex *N*-glycan standards

The well-defined *N*-glycans **1-15** were prepared by an enzymatic approach (scheme S1). Starting from a sialoglycopeptide (SGP) isolated from the egg yolk powder,[1] removal of the peptide using PNGase F afforded glycan **10**. Treatment of **10** by neuraminidase to cleave the terminal sialic acids provided glycan **6**. Subsequently, removal of two galactoses of **6** by treatment with galactosidase from *A. niger* gave glycan **1**. Core fucosylation of **1** using recombinant FUT8 and guanosine 5′ -diphospho-β-L-fucose(GDP-Fuc) in presence of calf intestine alkaline phosphatase (CIAP) afforded glycan **2**, and treatment of **2** with B4GalT1 and uridine 5′ -diphosphogalactose (UDP-Gal) afforded **7** (scheme S1A). With compound **6** in hand, two strategies for the selective modification of bottom antenna due to inherent branch selectivity of glycosyltransferase and glycosidase were used to prepare asymmetric glycans **8** and **3** (scheme S1B). Selective α2,6-sialylation of **6** at the bottom antenna based on a high preference of ST6Gal1[2] in presence of cytidine-5′ -monophospho-*N*-acetylneuraminic acid (CMP-Neu5Ac, 1.0 eq) and CIAP afforded an asymmetric *N*-glycan **8**. And selective removal of the galactose at bottom antenna of **6** was achieved using a galactosidase from *E. coli*[3] provide asymmetrical glycan **3**. In addition, α2,3-sialylation of terminal two galactoses of **6** using ST3Gal4 in presence of CMP-Neu5Ac and CIAP afforded glycan **11**. Based on the same strategies, core fucosylated *N*-glycans **4**, **9** and **14** were also prepared smoothly (scheme S1C). In addition, treatment of **7** using ST6Gal1 in presence of excess CMP-Neu5Ac (2.5 eq) and CIAP installed two α2,6-Neu5Ac at terminal Gal to afford **15** (scheme S1D).

Scheme S1. Enzymatic synthesis of N-glycan standards

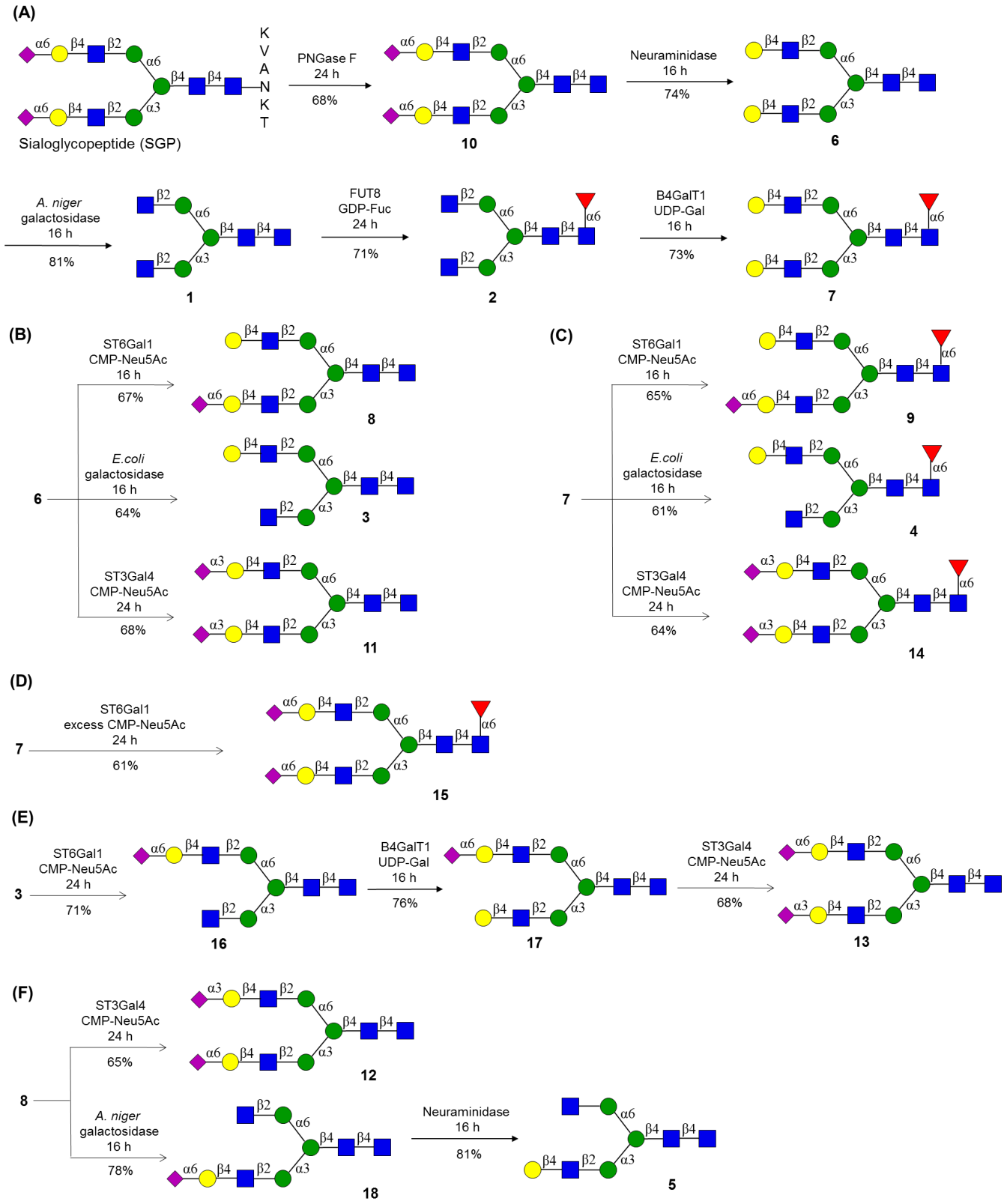

Asymmetric glycan **3** was characterized with terminal GlcNAc and LacNAc moiety at bottom antenna and upper antennae, respectively. Many glycosyltransferases modify LacNAc but not terminal GlcNAc moieties, thus α2,6-sialylation of **3** at upper antennae using ST6Gal1 in presence of CMP-Neu5Ac and CIAP afforded glycan **16**. Due to α2,6-sialoside blocking further modification by mammalian glycosyl transferases, installation of galactose using B4GalT1 and UDP-Gal in the presence of $MnCl_2$ and CIAP gave glycan **17** with the resulting LacNAc moiety at bottom antennae, which was further α2,3-sialylated by ST3Gal4 in presence of CMP-Neu5Ac and CIAP to afford asymmetric glycan **13** (scheme S1E).

Next, another di-sialylated isomer **12** was also prepared by treatment of **8** using ST3Gal4 in presence of CMP-Neu5Ac and CIAP. In addition, treatment of **8** with galactosidase from *A. niger* cleaved galactose at upper antenna provided glycan **18**, which was further modified by neuraminidase to afford glycan **5** (scheme S1F). It is important to note that all synthesized *N*-glycans were purified by HPLC using a HILIC column (XBrigde® Amide 5 μm, 10 mm x 250 mm, Waters).

1.3 General protocols for enzymatic reactions

General procedure for removal of pepetide of SGP using PNGase F

To a sialoglycopeptide (SGP) substrate (5-10 mM) in a PBS buffer solution (50 mM, pH 7.4) containing BSA (1% volume total) was added PNGase F (1% *wt*/wt relative to acceptor substrate), and the mixture was incubated for 24 h at 37°C. Reaction progress was monitored by ESI-MS, if starting material remained after 24 h, another portion of PNGase F was added until no starting material could be detected. The reaction mixture was centrifuged, and the resulting supernatant was loaded on Bio-Gel P4 column (eluent: 0.1 M NH_4HCO_3). Product containing fractions were combined and lyophilized for further purification by HPLC.

General procedure for removal of terminal Neu5Ac using neuraminidase

To a solution of *N*-glycan (5-10 mM) in sodium acetate buffer solution (50 mM, pH 5.5) containing $CaCl_2$ (5 mM) was added α2-3,6,8,9 neuraminidase A (1 U/μL, P0722L, NEW ENGLAND BioLabs®Inc.), and the mixture was incubated at 37 ºC for 16 h. Reaction progress was monitored by ESI-MS, if starting material remained after 16 h, another portion of neuraminidase was added until no starting material could be detected. Once the reaction finished, the neuraminidase was inactivated at 65 ºC for 10 min. The reaction mixture was centrifuged, and the resulting supernatant was loaded on Bio-Gel P4 column (eluent: 0.1 NH_4HCO_3). Product containing fractions were combined and lyophilized for further purification by HPLC.

General procedure for removal of teriminal Gal using galactosidase from *A. niger*

To a solution of *N*-glycan (5-10 mM) in sodium acetate buffer solution (50 mM, pH 4.5) containing BSA (1% volume total) was added β-galactosidase (0.5 U/μL) from *Aspergillus niger* (Megazyme # E-BGLAN), and the mixture was incubated at 37 ºC for 16 h. Reaction progress was monitored by ESI-MS, if starting material remained after 16 h, another portion of β-galactosidase was added until no starting material could be detected. Once the reaction finished, the β-galactosidase was inactivated at 65 ºC for 10 min. The reaction mixture was centrifuged,

and the resulting supernatant was loaded on Bio-Gel P4 column (eluent: 0.1 NH_4HCO_3). Product containing fractions were combined and lyophilized for further purification by HPLC.

General procedure for the selective cleavage of Gal using *E. coli* β-galactosidase

To a solution of *N*-glycan (5-10 mM) in a Tris buffer solution (50 mM, pH 7.3) containing $MgCl_2$ (5 mM) was added *E. coli* β-galactosidase (0.3 U/μL, Sigma-Aldrich, G4155), and the mixture was incubated for 16 h at 37°C. Once the reaction finished, the β-galactosidase was inactivated at 65 °C for 10 min. The reaction mixture was centrifuged, and the resulting supernatant was loaded on Bio-Gel P4 column (eluent: 0.1 NH_4HCO_3). Product containing fractions were combined and lyophilized for further purification by HPLC.

General procedure for the installation of α1,6 Fuc using FUT8

To a solution of *N*-glycan acceptor (5-10 mM) and GDP-Fuc (1.5 eq) in MES buffer solution (100 mM, pH 7.0) containing $MnCl_2$ (10 mM) and BSA (1% volume total) was added FUT8 (1% *wt/wt* relative to acceptor substrate) and CIAP (1% volume total), and the mixture was incubated at 37 °C for 24 h. Reaction progress was monitored by ESI-MS, if starting material remained after 24 h, another portion of FUT8 was added until no starting material could be detected. The reaction mixture was centrifuged, and the resulting supernatant was loaded on Bio-Gel P4 column (eluent: 0.1 NH_4HCO_3). Product containing fractions were combined and lyophilized for further purification by HPLC.

General procedure for the installation of β1,4 Gal using B4GalT1

To a solution of *N*-glycan acceptor (5-10 mM) and UDP-Gal (1.2 eq per Gal) in Tris buffer solution (100 mM, pH 7.5) containing $MnCl_2$ (10 mM) and BSA (1% volume total) was added B4GalT1 (1% *wt/wt* relative to acceptor substrate) and CIAP (1% volume total), and the mixture was incubated at 37 °C for 16 h. Reaction progress was monitored by ESI-MS, if starting material remained after 16 h, another portion of FUT8 was added until no starting material could be detected. The reaction mixture was centrifuged, and the resulting supernatant was loaded on Bio-Gel P4 column (eluent: 0.1 NH_4HCO_3). Product containing fractions were combined and lyophilized for further purification by HPLC.

General procedure for the selective installation of α2,6 Neu5Ac using ST6Gal1

To a solution of *N*-glycan acceptor (5-10 mM) and CMP-Neu5Ac (1.1 eq) in a sodium cacodylate buffer solution (50 mM, pH 7.2) containing BSA (1% total volume) was added ST6Gal1 (1% *wt/wt* relative to acceptor substrate) and CIAP (1% volume total), and the reaction mixture was incubated at 37 °C for 16 h. The mixture was centrifuged, and the resulting supernatant was loaded on Bio-Gel P4 column (eluent: 0.1 NH_4HCO_3). Product containing fractions were combined and lyophilized for further purification by HPLC.

General Procedure for the installation of α2,3 Neu5Ac using ST3Gal4

To a solution of *N*-glycan acceptor (5-10 mM) and CMP-Neu5Ac (1.5 eq per Neu5Ac) in a sodium cacodylate buffer solution (50 mM, pH 7.2) containing BSA (1% total volume) was added ST3Gal4 (2% *wt/wt* relative to acceptor substrate) and CIAP (1% volume total), and the reaction mixture was incubated at 37 °C for 24 h. Reaction progress was monitored by ESI-MS, if starting material remained after 24 h, another portion of ST3Gal4 was added until no starting material could be detected. The reaction mixture was centrifuged, and the resulting supernatant was loaded on Bio-Gel P4 column (eluent: 0.1 NH_4HCO_3). Product containing fractions were combined and lyophilized for further purification by HPLC.

General Procedure for the installation of α2,6 Neu5Ac using ST6Gal1

To a solution of *N*-glycan acceptor (5-10 mM) and CMP-Neu5Ac (1.5 eq per Neu5Ac) in a sodium cacodylate buffer solution (50 mM, pH 7.2) containing BSA (1% total volume) was added ST6Gal1 (2% *wt/wt* relative to acceptor substrate) and CIAP (1% volume total), and the reaction mixture was incubated at 37 °C for 16 h. Reaction progress was monitored by ESI-MS, if starting material remained after 16 h, another portion of ST3Gal4 was added until no starting material could be detected. The reaction mixture was centrifuged, and the resulting supernatant was loaded on Bio-Gel P4 column (eluent: 0.1 NH_4HCO_3). Product containing fractions were combined and lyophilized for further purification by HPLC.

1.4 NMR characterization data

Nuclear magnetic resonance spectra were recorded with Varian Varian/Agilent 600 (at 600 MHz) spectrometer, and operated at 25 ^{0}C. Samples were dissolved into 99.9% deuterium oxide (D_2O). Spectra were assigned using ^{1}H-NMR, 2D-NMR including gCOSY, HSQCAD and zTOCSY experiments. Chemical shifts were referenced to internal DSS at 0 ppm for compound **1**, and assigned the GlcNAc-1α H-1 to 5.182 ppm.

The residues of the oligosaccharides were labeled as showed. Starting from the reducing terminal, GlcNAc-1, GlcNAc-2, the β-mannoside was labeled as Man-3, the α-3 mannoside as Man-4, the α-6 mannoside as Man-4', the *N*-acetylglucosamine residues as GlcNAc-5 and GlcNAc-5', followed by the galactosides residues as Gal-6 and Gal-6', the core fucoside residue as Fuc.

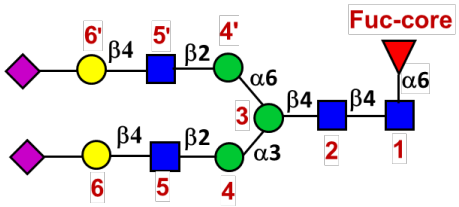

The detailed NMR characterization data of compounds **1-15** is listed below.

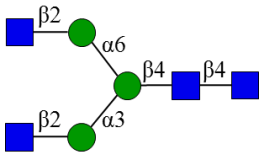

1

Table S1. ^{1}H NMR of compound **1**

1	H1	H2	H3	H4	H5	H6
GlcNAc-1α	5.182	3.872	3.632	NA	NA	NA
Man-4	5.107	4.182	3.892	3.612	3.735	NA
Man-4'	4.912	4.103	3.858	3.611	NA	NA
Man-3	4.764	4.244	3.777	3.626	NA	NA
GlcNAc-1β	4.688	3.683	3.646	3.511	NA	NA
GlcNAc-2	4.599	3.778	3.752	3.605	NA	NA
GlcNAc-5	4.546	3.672	3.696	3.547	NA	NA
GlcNAc-5'	4.546	3.726	3.765	3.547	NA	NA

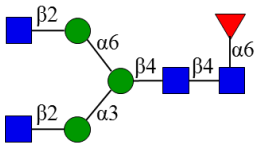

2

Table S2. ^{1}H NMR of compound **2**

2	H1	H2	H3	H4	H5	H6	Fuc-CH_3
GlcNAc-1α	5.182	3.888	3.791	NA	NA	NA	—
Man-4	5.117	4.190	3.904	3.621	3.745	NA	—
Man-4'	4.920	4.109	3.901	3.621	NA	NA	—
Man-3	4.776	4.256	3.779	3.634	NA	NA	—
GlcNAc-1β	4.696	3.695	3.675	NA	NA	NA	—
GlcNAc-2	4.669	3.786	3.761	3.603	NA	NA	—
GlcNAc-5	4.556	3.671	3.705	3.549	NA	NA	—
GlcNAc-5'	4.556	3.724	3.705	3.549	NA	NA	—
Fuc	4.934	3.791	3.908	3.803	4.118	—	1.216

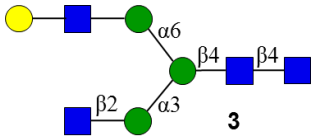

Table S3. ^{1}H NMR of compound **3**

3	H1	H2	H3	H4	H5	H6
GlcNAc-1α	5.182	3.871	3.630	NA	NA	NA
Man-4	5.110	4.183	3.897	3.615	3.743	NA
Man-4’	4.922	4.106	3.882	3.612	NA	NA
Man-3	4.761	4.243	3.774	3.613	NA	NA
GlcNAc-1β	4.690	3.686	3.625	3.512	NA	NA
GlcNAc-2	4.601	3.786	3.743	3.607	NA	NA
GlcNAc-5	4.548	3.691	3.683	NA	NA	NA
GlcNAc-5’	4.576	3.741	3.733	NA	NA	NA
Gal-6’	4.466	3.537	3.668	3.924	NA	NA

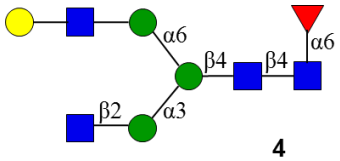

4

Table S4. ^{1}H NMR of compound **4**

4	H1	H2	H3	H4	H5	H6	Fuc-CH_3
GlcNAc-1α	5.182	3.902	3.794	NA	NA	NA	—
Man-4	5.118	4.191	3.906	3.624	3.746	NA	—
Man-4’	4.927	4.111	3.905	3.623	NA	NA	—
Man-3	4.770	4.254	3.782	3.630	NA	NA	—
GlcNAc-1β	4.696	3.708	3.684	NA	NA	NA	—
GlcNAc-2	4.669	3.794	3.762	3.602	NA	NA	—
GlcNAc-5	4.557	3.699	3.701	3.572	NA	NA	—
GlcNAc-5’	4.585	3.752	3.743	3.572	NA	NA	—
Gal-6’	4.475	3.548	3.674	3.933	NA	NA	—
Fuc	4.895	3.794	3.912	3.804	4.119	—	1.216

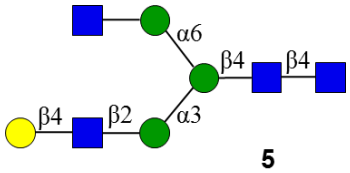

5

Table S5. ^{1}H NMR of compound **5**

5	H1	H2	H3	H4	H5	H6
GlcNAc-1α	5.182	3.871	3.630	NA	NA	NA
Man-4	5.112	4.186	3.897	3.614	3.742	NA
Man-4'	4.913	4.104	3.883	3.613	NA	NA
Man-3	4.766	4.245	3.774	3.623	NA	NA
GlcNAc-1β	4.690	3.687	3.621	3.512	NA	NA
GlcNAc-2	4.602	3.788	3.742	3.606	NA	NA
GlcNAc-5	4.575	3.740	3.727	NA	NA	NA
GlcNAc-5'	4.547	3.697	3.689	NA	NA	NA
Gal-6	4.462	3.534	3.664	3.921	NA	NA

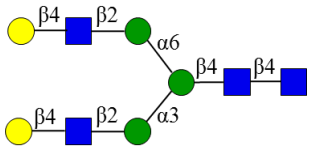

6

Table S6. ^{1}H NMR of compound **6**

6	H1	H2	H3	H4	H5	H6
GlcNAc-1α	5.182	3.871	3.631	NA	NA	NA
Man-4	5.111	4.185	3.898	3.614	3.739	NA
Man-4’	4.922	4.105	3.885	3.611	NA	NA
Man-3	4.760	4.244	3.766	3.616	NA	NA
GlcNAc-1β	4.689	3.684	3.623	3.513	NA	NA
GlcNAc-2	4.596	3.788	3.743	3.606	NA	NA
GlcNAc-5	4.574	3.736	3.727	3.568	NA	NA
GlcNAc-5’	4.574	3.736	3.727	3.568	NA	NA
Gal-6	4.469	3.539	3.664	3.923	NA	NA
Gal-6’	4.457	3.539	3.664	3.923	NA	NA

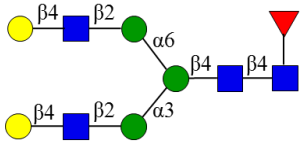

7

Table S7. ^{1}H NMR of compound **7**

7	H1	H2	H3	H4	H5	H6	Fuc-CH_3
GlcNAc-1α	5.182	3.901	3.795	NA	NA	NA	—
Man-4	5.121	4.195	3.905	3.619	3.746	NA	—
Man-4’	4.929	4.111	3.896	3.622	NA	NA	—
Man-3	4.771	4.256	3.781	3.629	NA	NA	—
GlcNAc-1β	4.696	3.708	3.684	NA	NA	NA	—
GlcNAc-2	4.670	3.794	3.744	3.600	NA	NA	—
GlcNAc-5	4.584	3.748	3.733	3.574	NA	NA	—
GlcNAc-5’	4.584	3.748	3.733	3.574	NA	NA	—
Gal-6	4.480	3.546	3.672	3.929	NA	NA	—
Gal-6’	4.466	3.546	3.672	3.929	NA	NA	—
Fuc	4.896	3.792	3.911	3.805	4.117	—	1.216

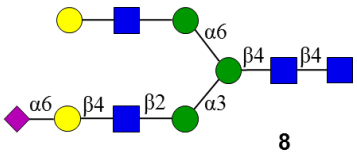

8

Table S8. ^{1}H NMR of compound **8**

8	H1	H2	H3	H4	H5	H6
GlcNAc-1α	5.182	3.868	3.628	NA	NA	NA
Man-4	5.128	4.190	3.892	3.615	3.741	NA
Man-4’	4.924	4.106	3.886	3.611	NA	NA
Man-3	4.764	4.249	3.775	3.620	NA	NA
GlcNAc-1β	4.688	3.684	3.619	3.513	NA	NA
GlcNAc-2	4.604	3.794	3.748	3.620	NA	NA
GlcNAc-5	4.575	3.746	3.717	3.564	NA	NA
GlcNAc-5’	4.594	3.746	3.717	3.564	NA	NA
Gal-6	4.466	3.527	3.672	3.919	NA	NA
Gal-6’	4.439	3.540	3.666	3.922	NA	NA
α2,6-Neu5Ac	—	—	2.660, 1.715	3.646	3.802	3.694

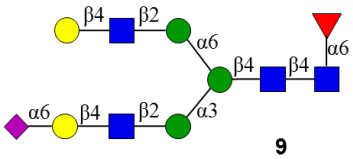

9

Table S7. ^{1}H NMR of compound **9**

9	H1	H2	H3	H4	H5	H6	Fuc-CH_3
GlcNAc-1α	5.182	3.897	3.794	NA	NA	NA	—
Man-4	5.136	4.197	3.902	3.624	3.748	NA	—
Man-4’	4.929	4.109	3.904	3.619	NA	NA	—
Man-3	4.774	4.258	3.783	3.634	NA	NA	—
GlcNAc-1β	4.693	3.707	3.684	NA	NA	NA	—
GlcNAc-2	4.668	3.793	3.745	3.602	NA	NA	—
GlcNAc-5	4.583	3.755	3.761	3.603	NA	NA	—
GlcNAc-5’	4.606	3.749	3.740	3.572	NA	NA	—
Gal-6	4.473	3.550	3.672	3.929	NA	NA	-
Gal-6’	4.447	3.538	3.672	3.929	NA	NA	-
Fuc	4.894	3.792	3.910	3.807	4.110	-	1.215
α2,6-Neu5Ac	—	—	2.668, 1.724	3.655	3.803	3.702	-

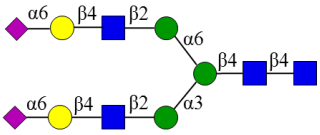

10

Table S10. ^{1}H NMR of compound **10**

10	H1	H2	H3	H4	H5	H6
GlcNAc-1α	5.182	3.869	3.625	NA	NA	NA
Man-4	5.126	4.191	3.894	3.616	3.741	NA
Man-4’	4.942	4.111	3.887	3.614	NA	NA
Man-3	4.767	4.251	3.776	3.632	NA	NA
GlcNAc-1β	4.686	3.686	3.618	3.511	NA	NA
GlcNAc-2	4.605	3.788	3.748	3.618	NA	NA
GlcNAc-5	4.596	3.747	3.649	3.592	NA	NA
GlcNAc-5’	4.596	3.747	3.649	3.592	NA	NA
Gal-6	4.436	3.534	3.662	3.921	NA	NA
Gal-6’	4.436	3.534	3.662	3.921	NA	NA
α2,6-Neu5Ac	—	—	2.663, 1.714	3.651	3.800	3.670
α2,6-Neu5Ac’	—	—	2.663, 1.714	3.651	3.800	3.670

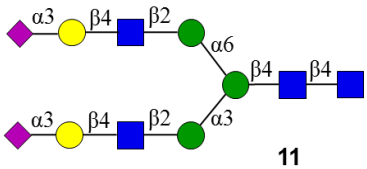

11

Table S11. ^{1}H NMR of compound **11**

11	H1	H2	H3	H4	H5	H6
GlcNAc-1α	5.182	3.869	3.625	NA	NA	NA
Man-4	5.109	4.186	3.892	3.611	3.738	NA
Man-4’	4.919	4.110	3.892	3.606	3.737	NA
Man-3	4.759	4.243	3.777	3.606	NA	NA
GlcNAc-1β	4.689	3.683	3.617	3.511	NA	NA
GlcNAc-2	4.599	3.801	3.741	3.602	NA	NA
GlcNAc-5	4.562	3.744	3.686	3.564	NA	NA
GlcNAc-5’	4.562	3.744	3.686	3.564	NA	NA
Gal-6	4.438	3.565	4.097	3.949	NA	NA
Gal-6’	4.438	3.565	4.097	3.949	NA	NA
α2,3-Neu5Ac	—	—	2.752, 1.795	3.683	3.839	3.666
α2,3-Neu5Ac’	—	—	2.752, 1.795	3.683	3.839	3.666

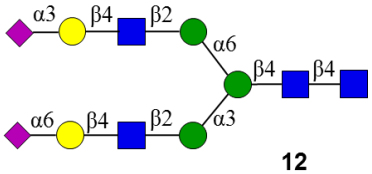

12

Table S12. ^{1}H NMR of compound **12**

12	H1	H2	H3	H4	H5	H6
GlcNAc-1α	5.182	3.867	3.625	NA	NA	NA
Man-4	5.126	4.190	3.894	3.612	3.738	NA
Man-4’	4.918	4.113	3.878	3.609	NA	NA
Man-3	4.762	4.246	3.777	3.612	NA	NA
GlcNAc-1β	4.687	3.685	3.617	3.513	NA	NA
GlcNAc-2	4.596	3.755	3.746	3.616	NA	NA
GlcNAc-5	4.565	3.753	3.680	3.563	NA	NA
GlcNAc-5’	4.565	3.753	3.680	3.563	NA	NA
Gal-6	4.436	3.527	3.661	3.915	NA	NA
Gal-6’	4.543	3.563	4.104	3.952	NA	NA
α2,3-Neu5Ac	—	—	2.751, 1.795	3.681	3.840	3.665
α2,6-Neu5Ac	—	—	2.659, 1.715	3.646	3.797	3.674

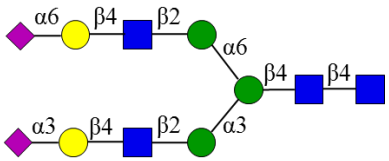

13

Table S13. ^{1}H NMR of compound **13**

13	H1	H2	H3	H4	H5	H6
GlcNAc-1α	5.182	3.870	3.627	NA	NA	NA
Man-4	5.110	4.186	3.904	3.604	3.757	NA
Man-4’	4.941	4.111	3.893	3.611	3.741	NA
Man-3	4.766	4.246	3.769	NA	NA	NA
GlcNAc-1β	4.686	3.685	3.617	3.511	NA	NA
GlcNAc-2	4.602	3.754	3.657	3.603	NA	NA
GlcNAc-5	4.566	3.737	3.721	3.571	NA	NA
GlcNAc-5’	4.438	3.563	4.110	3.952	NA	NA
Gal-6	4.537	3.563	4.110	3.952	NA	NA
Gal-6’	4.438	3.530	3.664	3.925	NA	NA
α2,6-Neu5Ac	—	—	2.664, 1.727	3.659	3.804	3.706
α2,3-Neu5Ac	—	—	2.750, 1.800	3.688	3.842	3.646

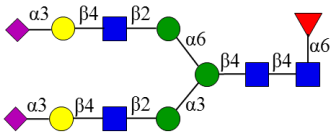

14

Table S14. ^{1}H NMR of compound **14**

14	H1	H2	H3	H4	H5	H6	Fuc-CH_3
GlcNAc-1α	5.182	3.900	3.784	NA	NA	NA	—
Man-4	5.117	4.192	3.901	3.614	3.742	NA	—
Man-4’	4.924	4.114	3.902	3.611	NA	NA	—
Man-3	4.768	4.252	3.782	3.620	NA	NA	—
GlcNAc-1β	4.693	3.709	3.685	NA	NA	NA	—
GlcNAc-2	4.666	3.795	3.760	3.596	NA	NA	—
GlcNAc-5	4.574	3.746	3.706	3.570	NA	NA	—
GlcNAc-5’	4.574	3.746	3.706	3.570	NA	NA	—
Gal-6	4.549	3.573	4.114	3.959	NA	NA	—
Gal-6’	4.549	3.573	4.114	3.959	NA	NA	—
Fuc	4.898	3.794	3.907	3.806	4.118	—	1.218
α2,3-Neu5Ac	—	—	2.759, 1.804	3.692	3.846	3.638	—
α2,3-Neu5Ac’	—	—	2.759, 1.804	3.692	3.846	3.638	—

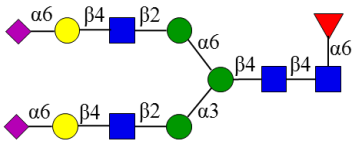

15

Table S15. ^{1}H NMR of compound **15**

15	H1	H2	H3	H4	H5	H6	Fuc-CH_3
GlcNAc-1α	5.182	3.898	3.786	NA	NA	NA	—
Man-4	5.134	4.198	3.901	3.624	3.746	NA	—
Man-4’	4.943	4.114	3.901	3.617	NA	NA	—
Man-3	4.777	4.261	3.781	3.648	NA	NA	—
GlcNAc-1β	4.692	3.706	3.683	3.600	NA	NA	—
GlcNAc-2	4.669	3.792	3.748	3.603	NA	NA	—
GlcNAc-5	4.606	3.757	3.657	3.593	NA	NA	—
GlcNAc-5’	4.606	3.757	3.657	3.593	NA	NA	—
Gal-6	4.446	3.545	3.657	3.593	NA	NA	—
Gal-6’	4.446	3.545	3.657	3.593	NA	NA	—
Fuc	4.894	3.795	3.906	3.805	4.111	—	1.216
α2,6-Neu5Ac	—	—	2.671, 1.723	3.654	3.804	3.682	—
α2,6-Neu5Ac’	—	—	2.671, 1.723	3.654	3.804	3.682	—

1.5 NMR spectra

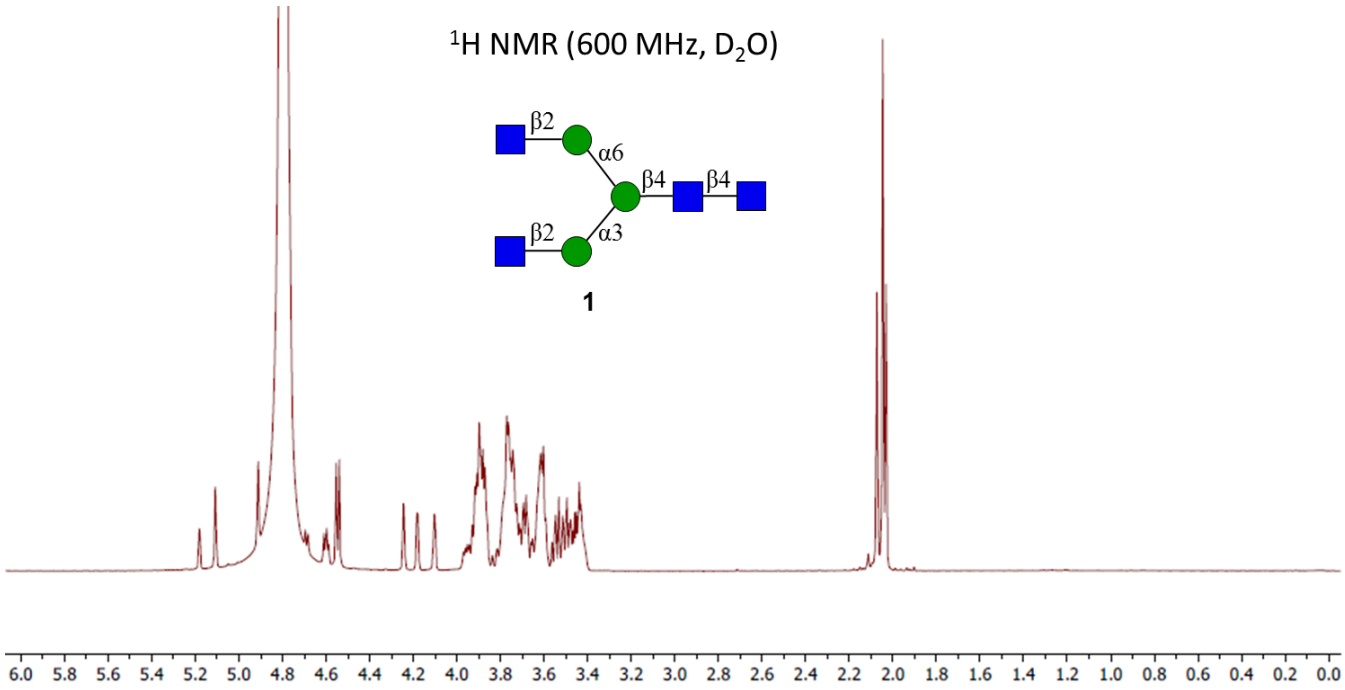

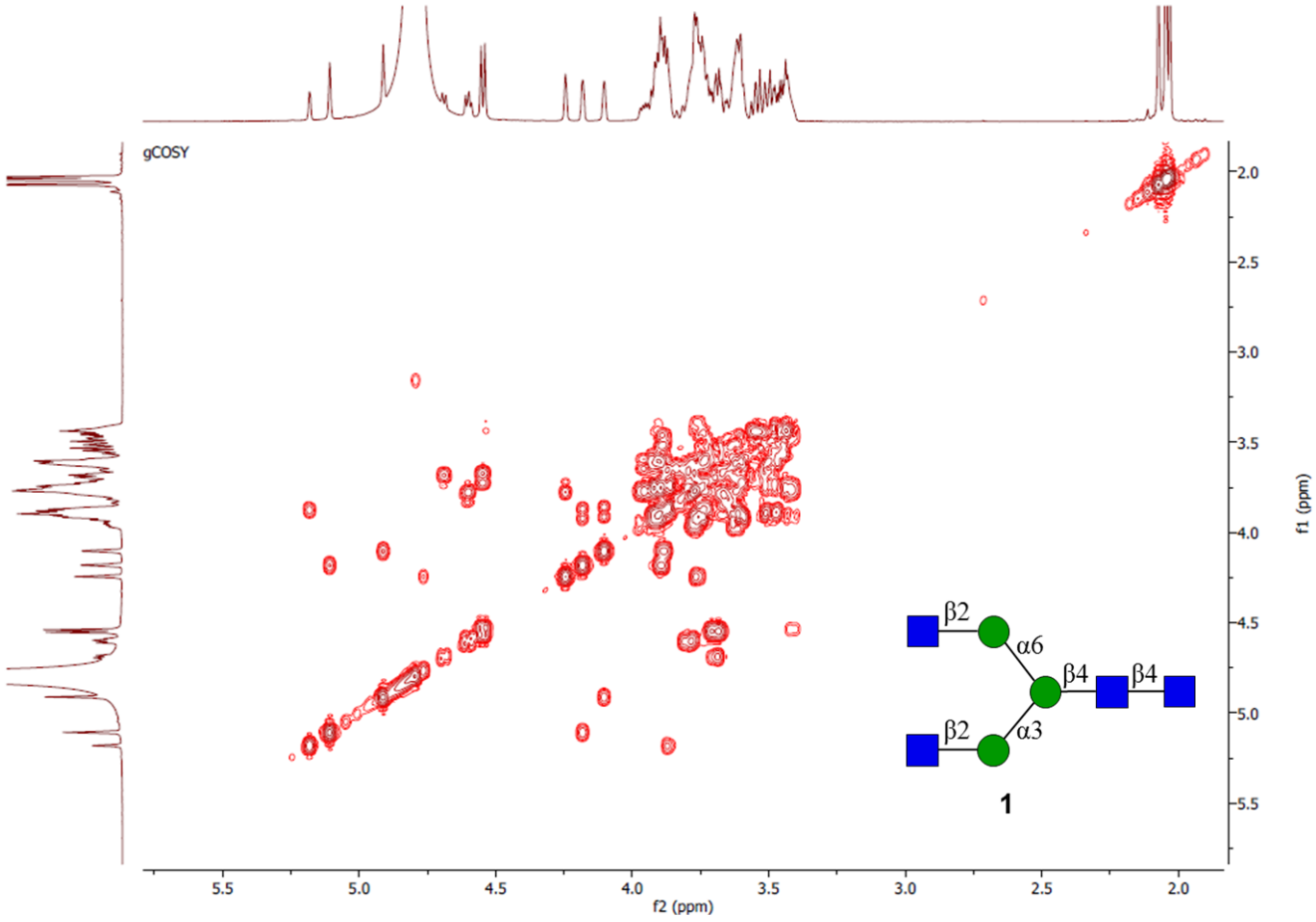

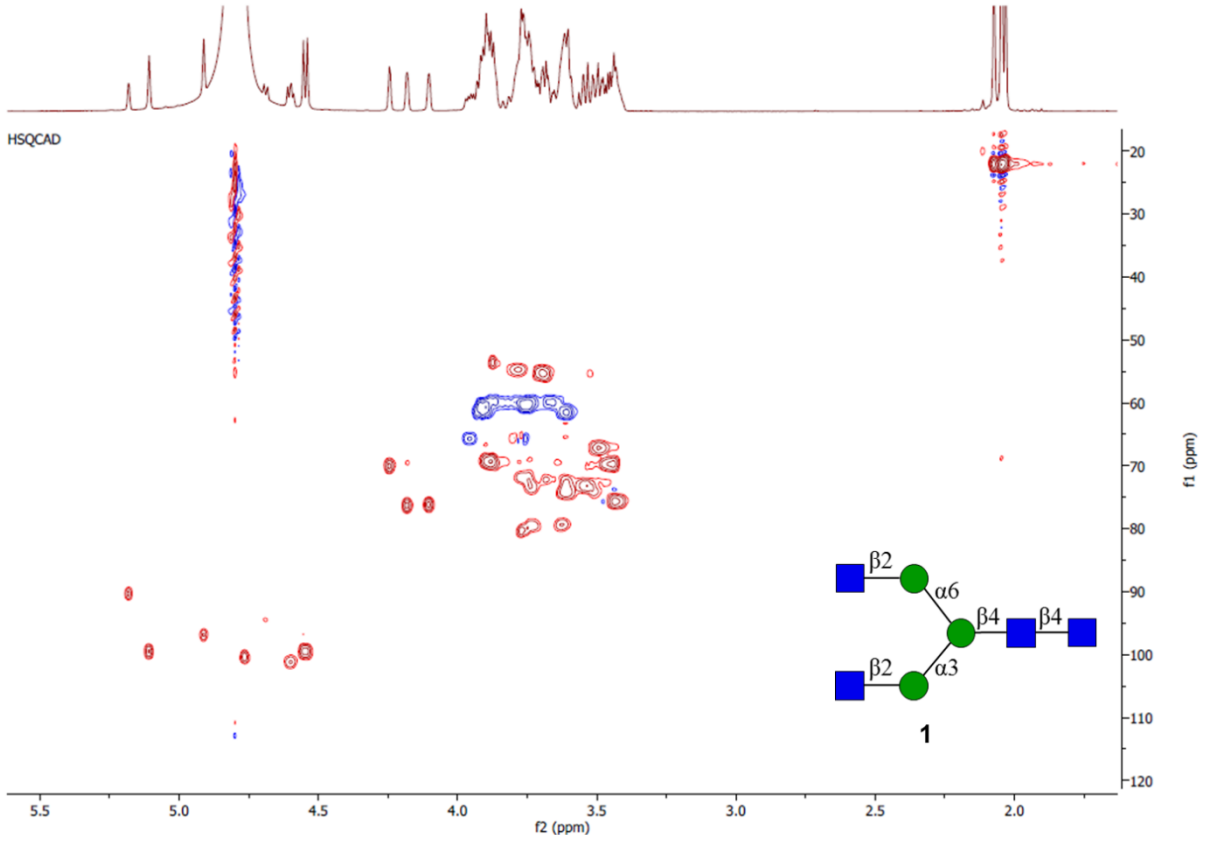

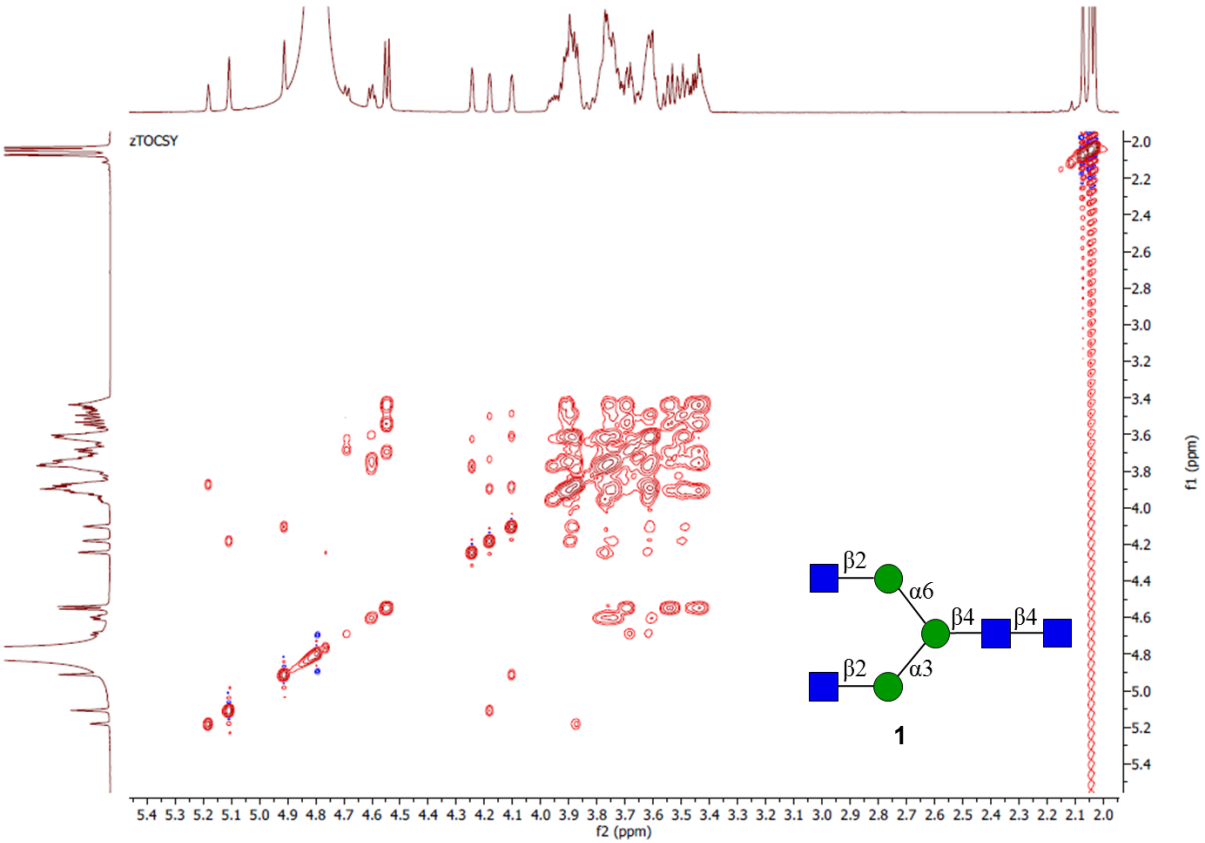

NMR spectra Compound 1

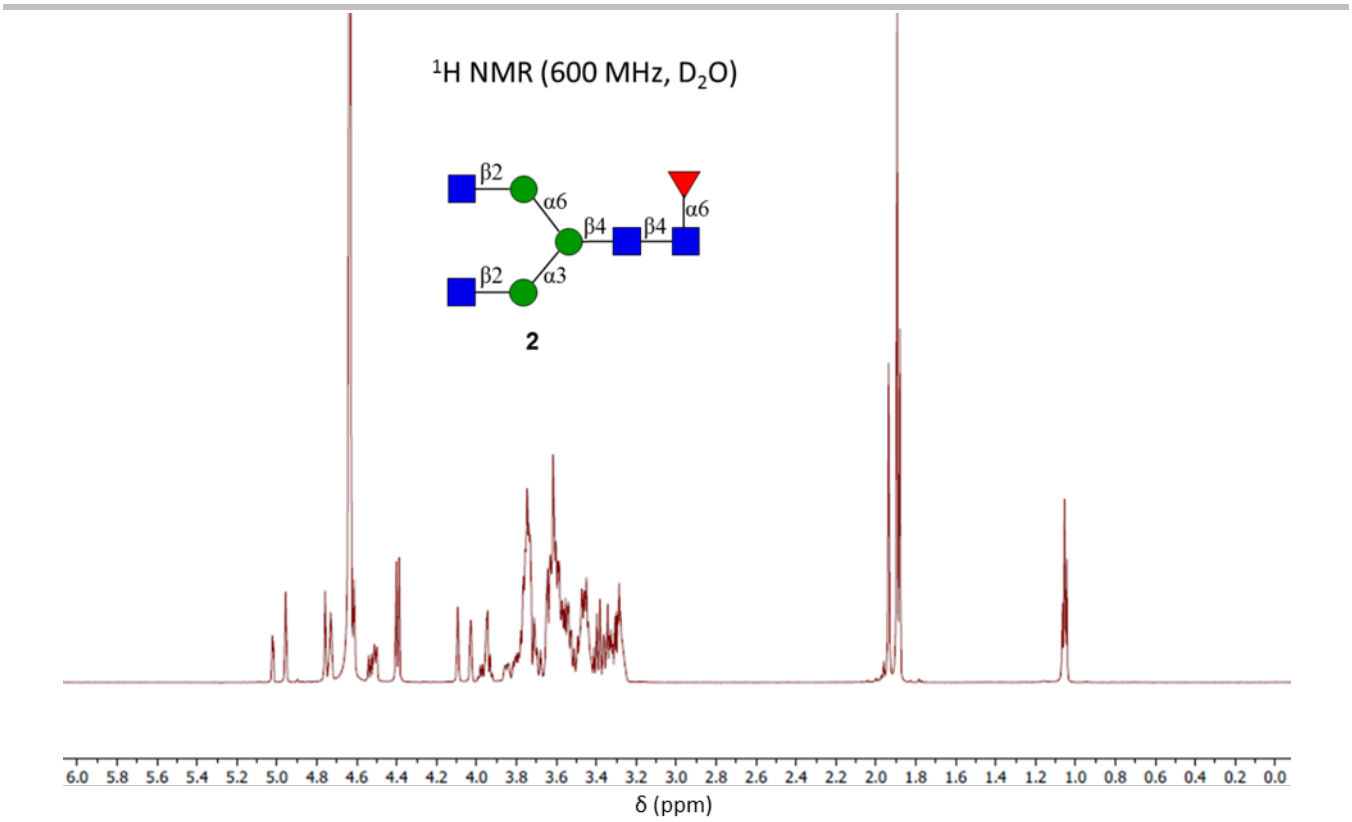
^{1}H NMR (600 MHz, D_2O)
β2
α6
β4
β4
α6
β2
α3
2
6.0 5.8 5.6 5.4 5.2 5.0 4.8 4.6 4.4 4.2 4.0 3.8 3.6 3.4 3.2 3.0 2.8 2.6 2.4 2.2 2.0 1.8 1.6 1.4 1.2 1.0 0.8 0.6 0.4 0.2 0.0
δ (ppm)

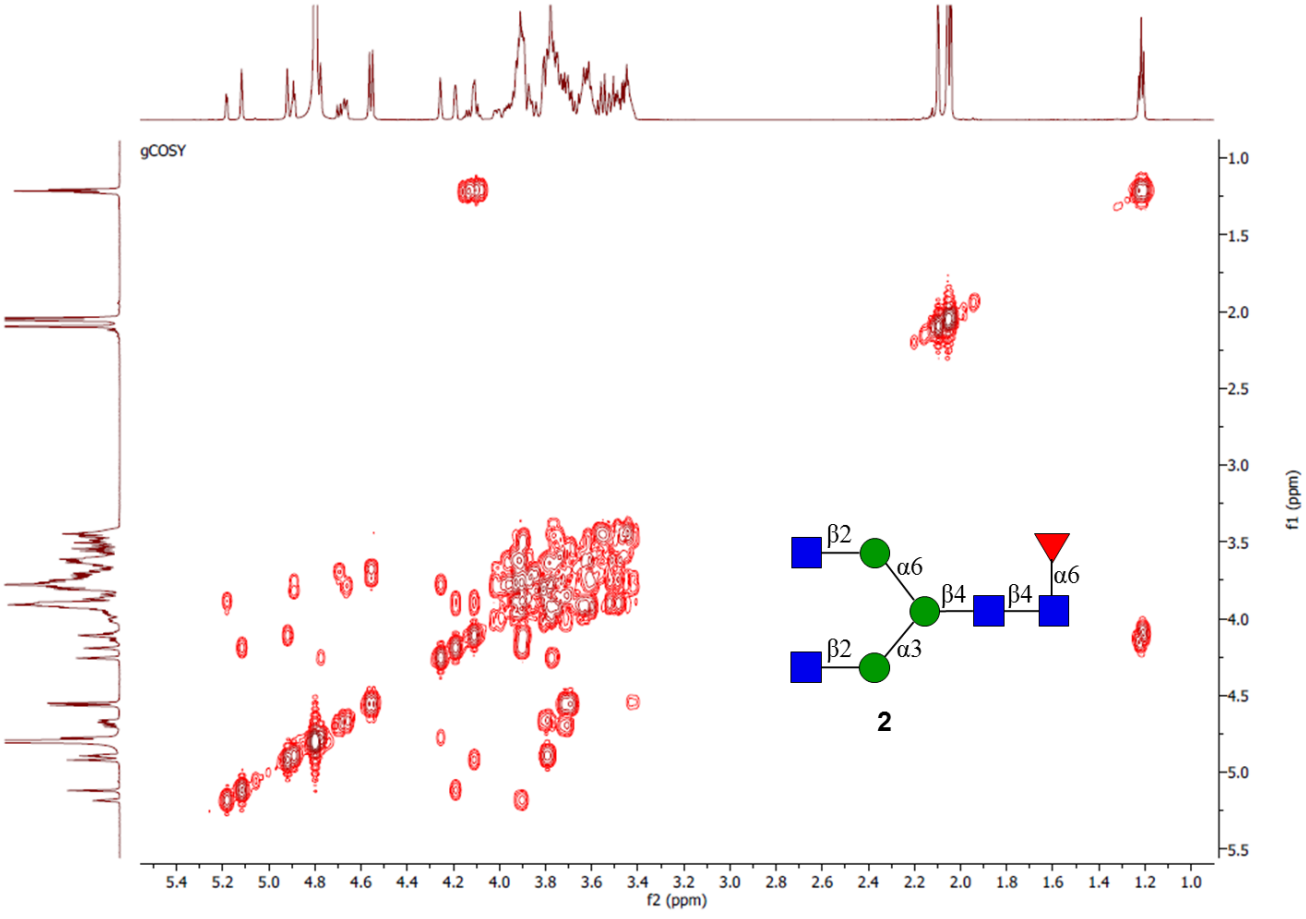
gCOSY
β2
α6
β4
β4
α6
β2
α3
2
5.4 5.2 5.0 4.8 4.6 4.4 4.2 4.0 3.8 3.6 3.4 3.2 3.0 2.8 2.6 2.4 2.2 2.0 1.8 1.6 1.4 1.2 1.0
f2 (ppm)
1.0 1.5 2.0 2.5 3.0 3.5 4.0 4.5 5.0 5.5
f1 (ppm)

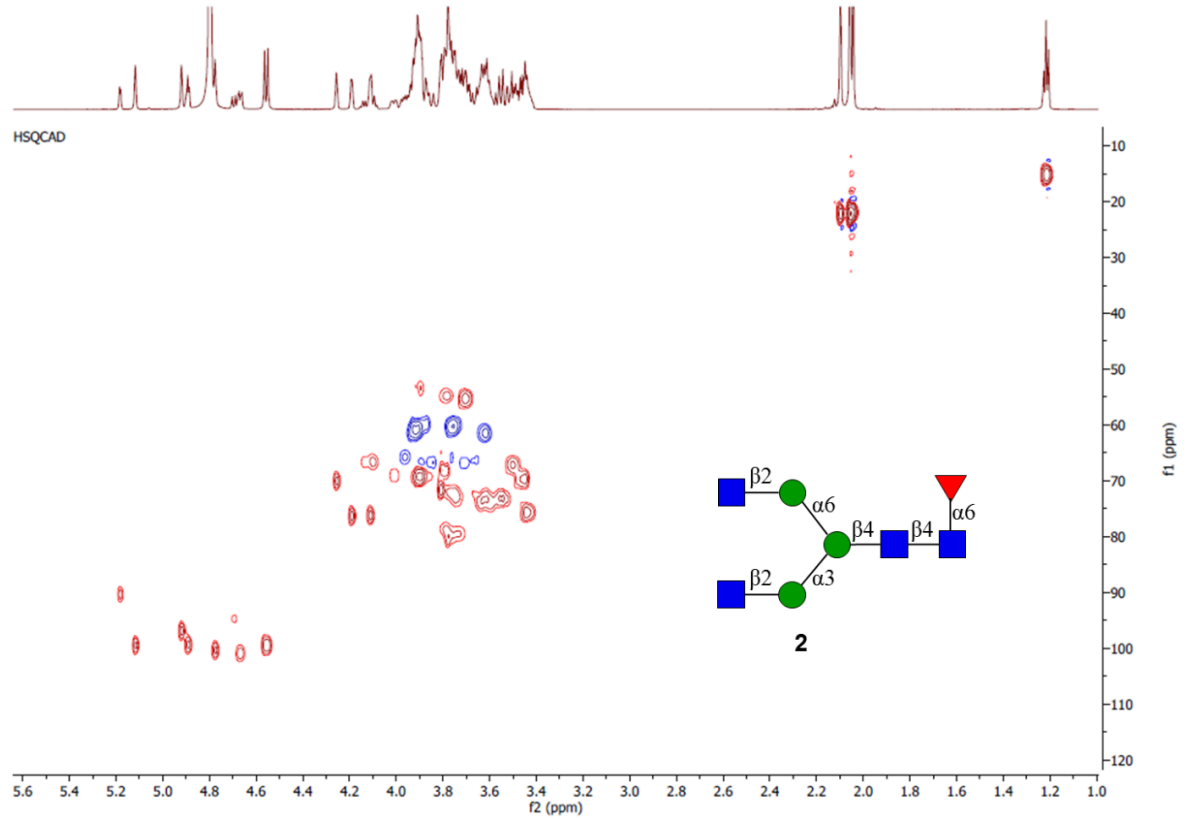

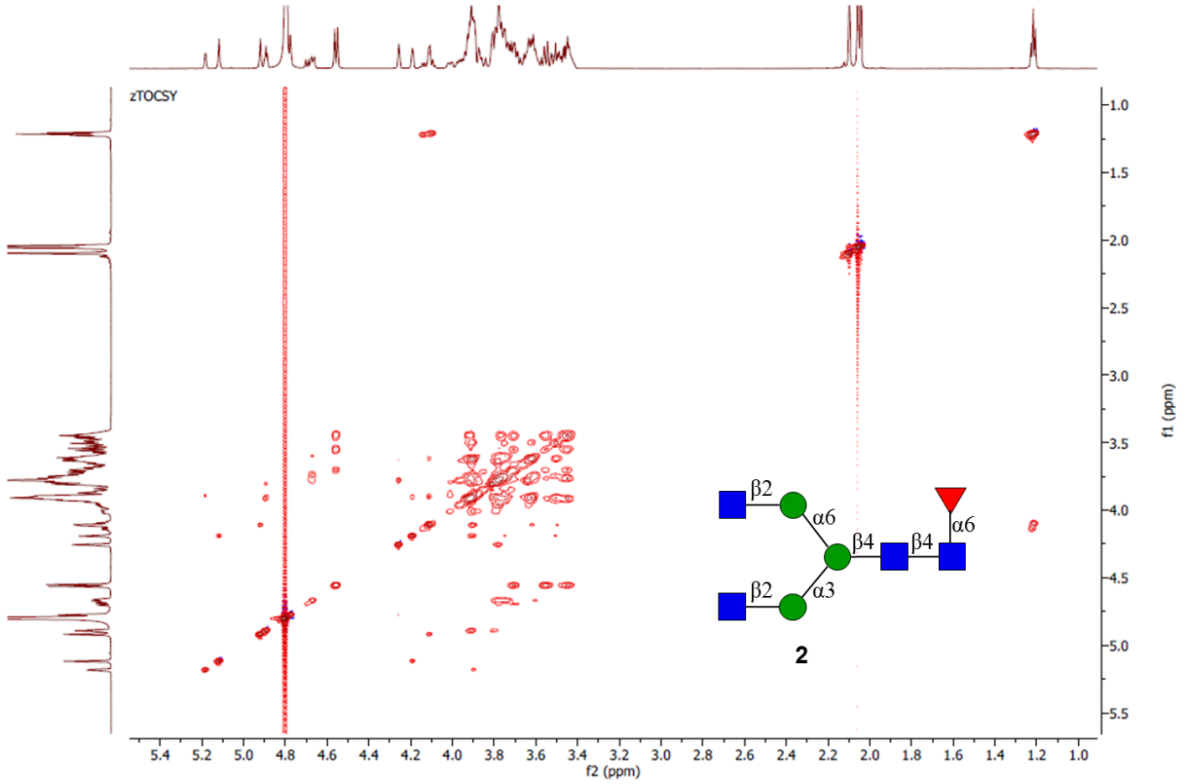

NMR spectra compound 2

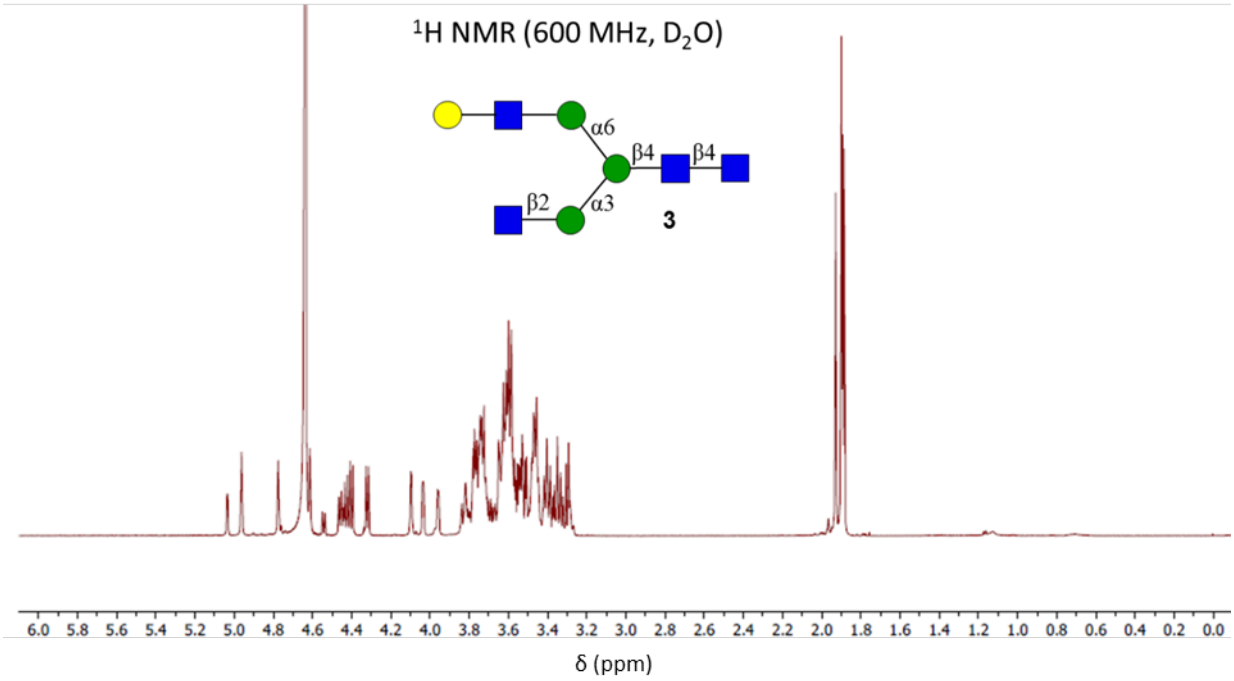
^{1}H NMR (600 MHz, D_2O)
α6
β4
β4
β2
α3
3
δ (ppm)

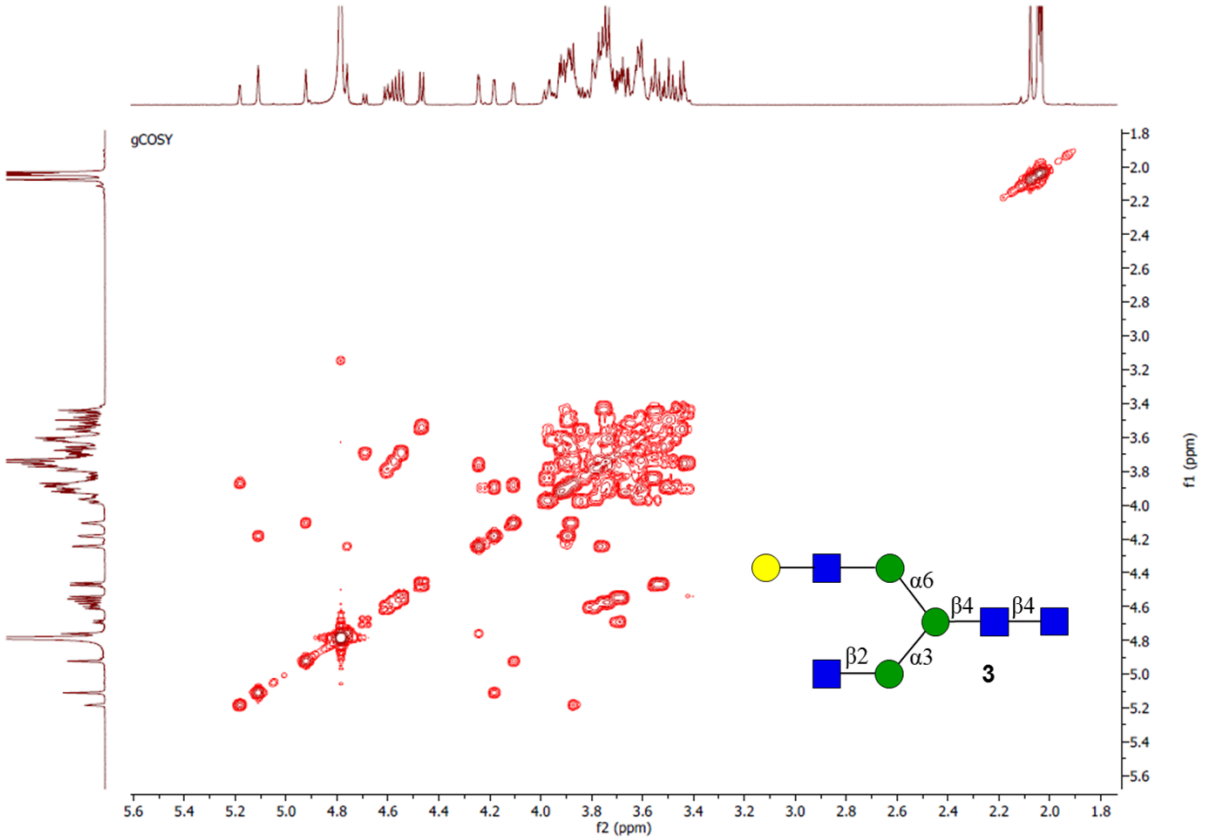
gCOSY
α6
β4
β4
β2
α3
3
f2 (ppm)
f1 (ppm)

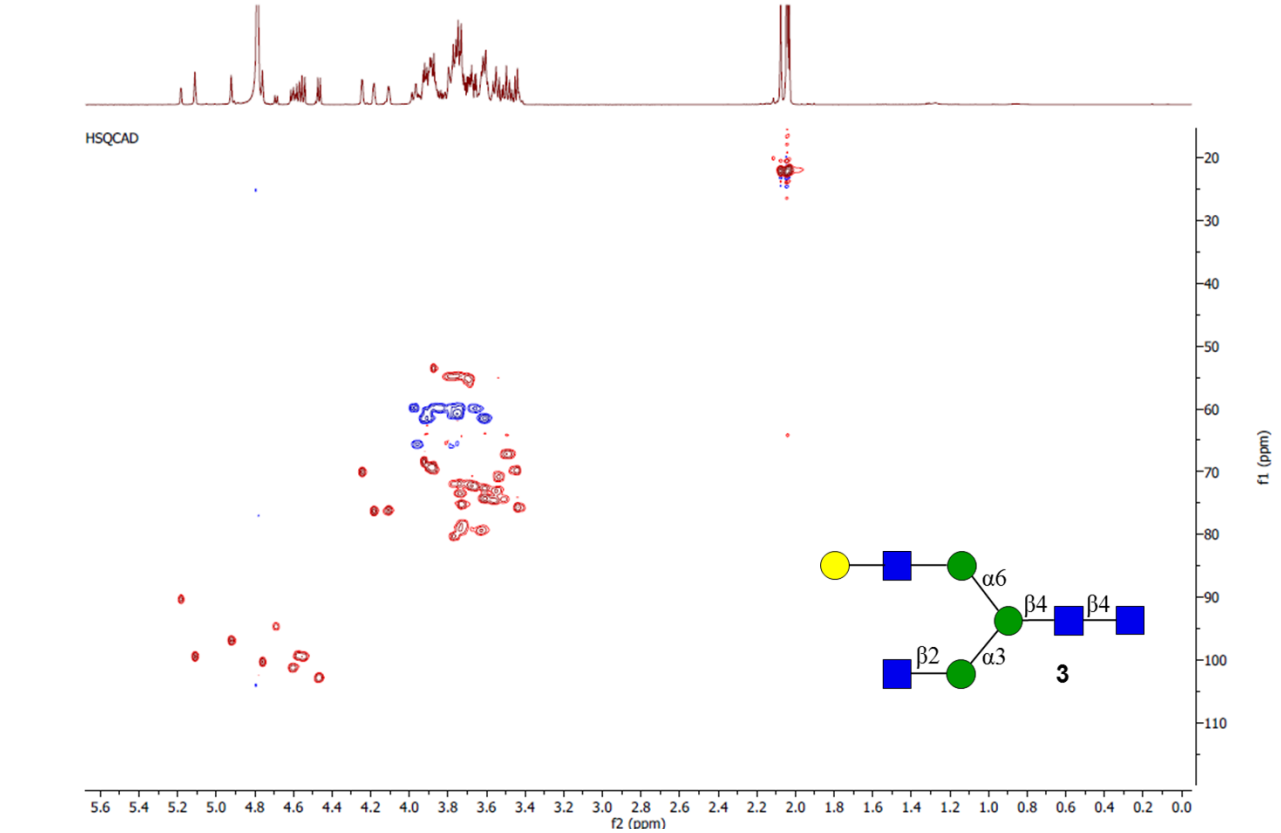

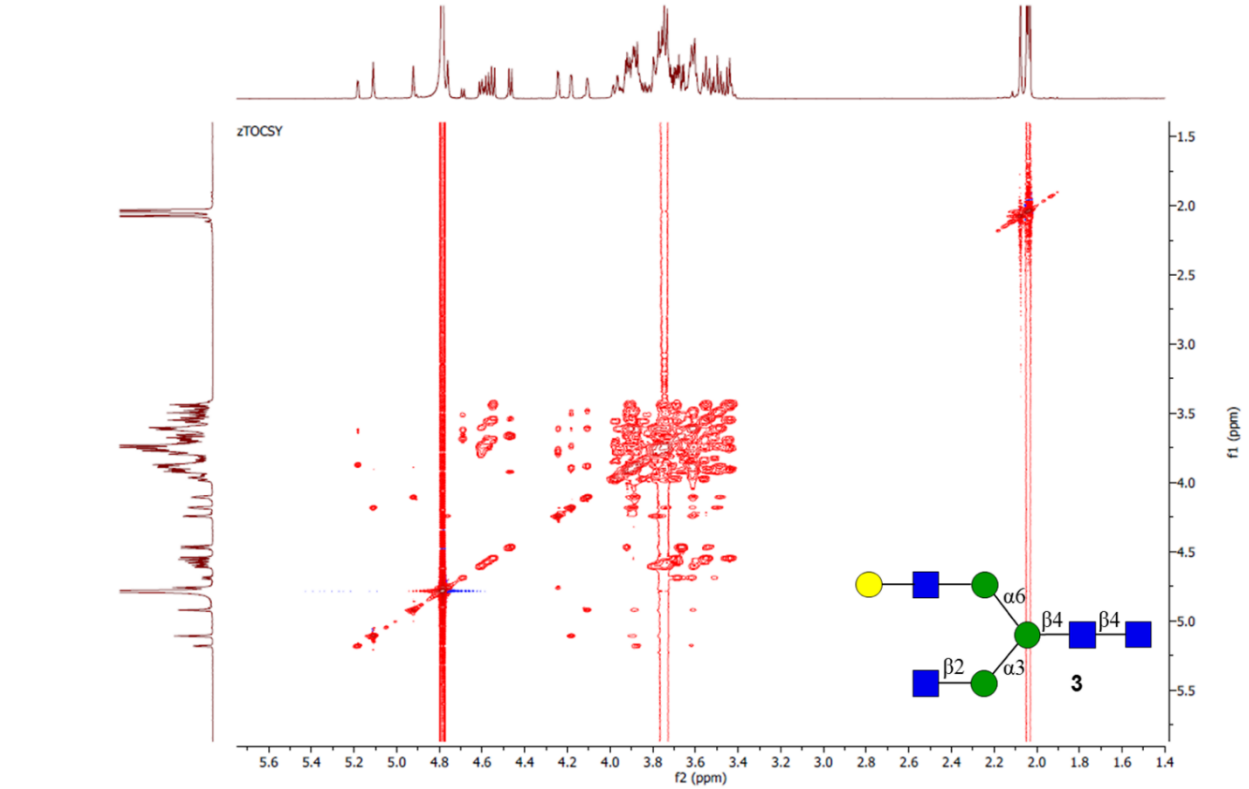

NMR spectra compound 3

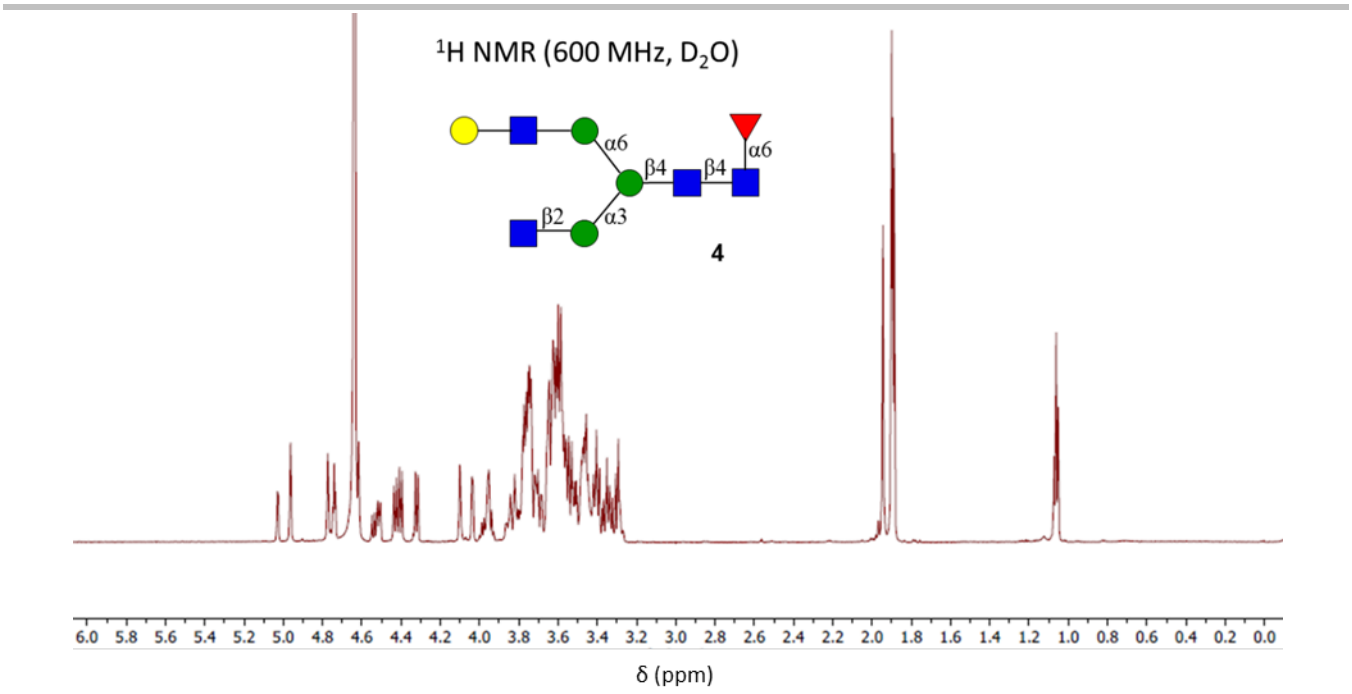
^{1}H NMR (600 MHz, D_2O)
α6
β4
β4
α6
β2
α3
4
δ (ppm)

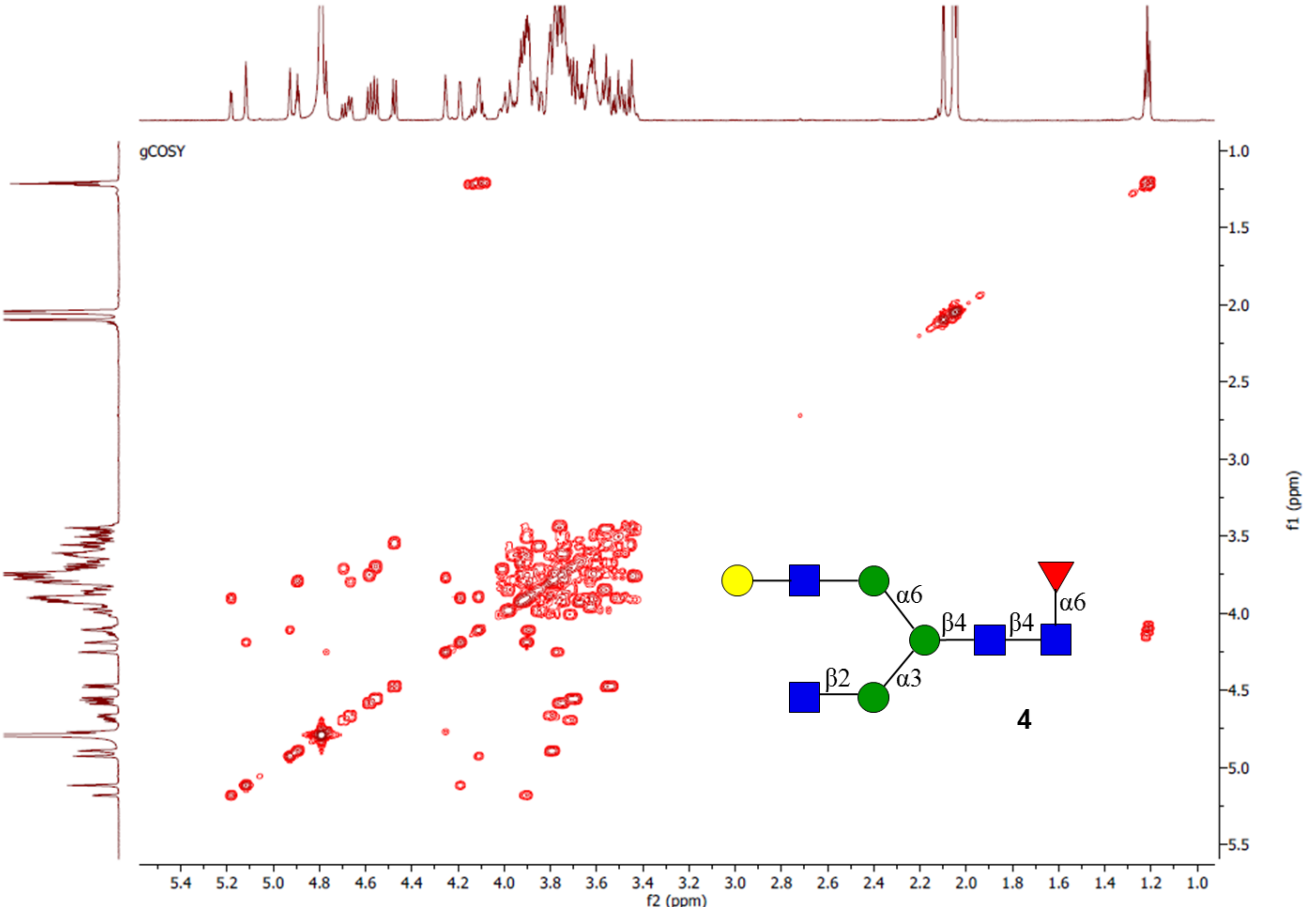
gCOSY
α6
β4
β4
α6
β2
α3
4
f2 (ppm)
f1 (ppm)

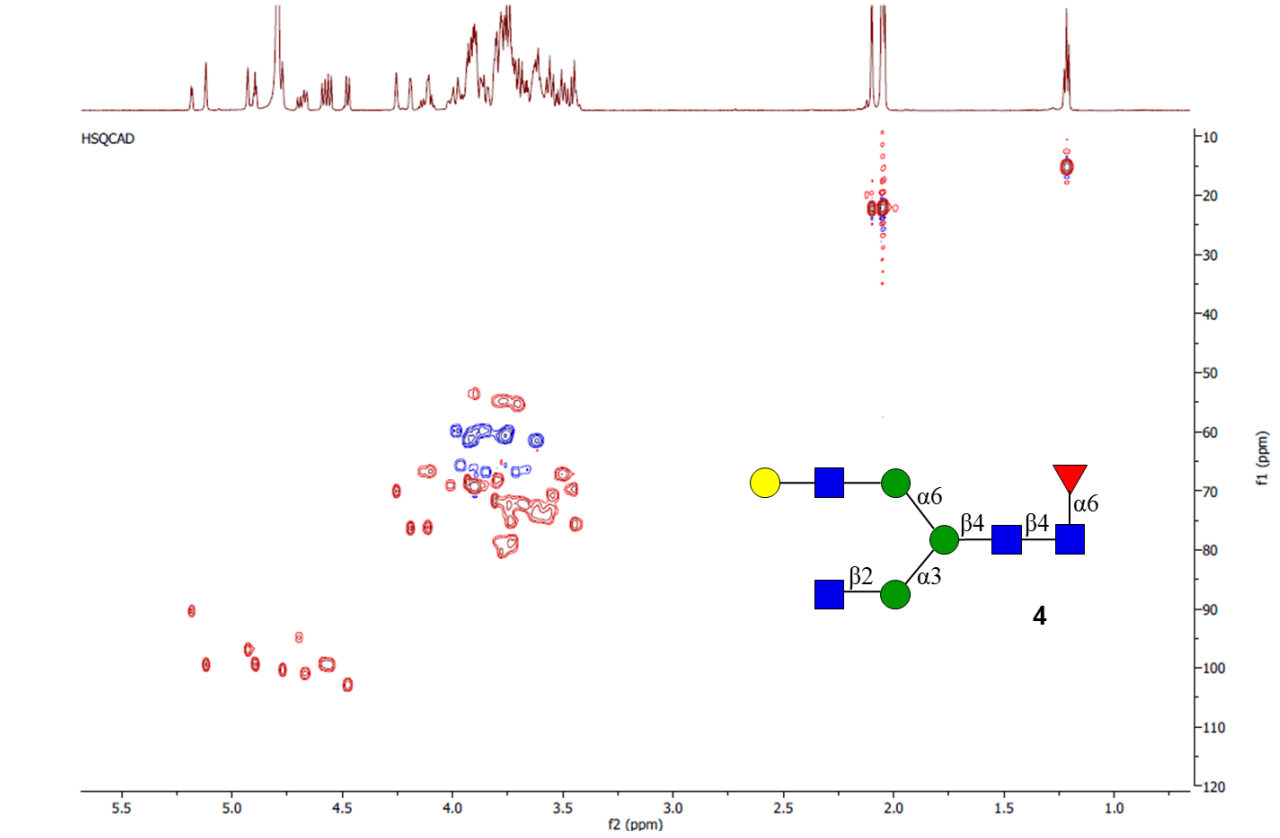

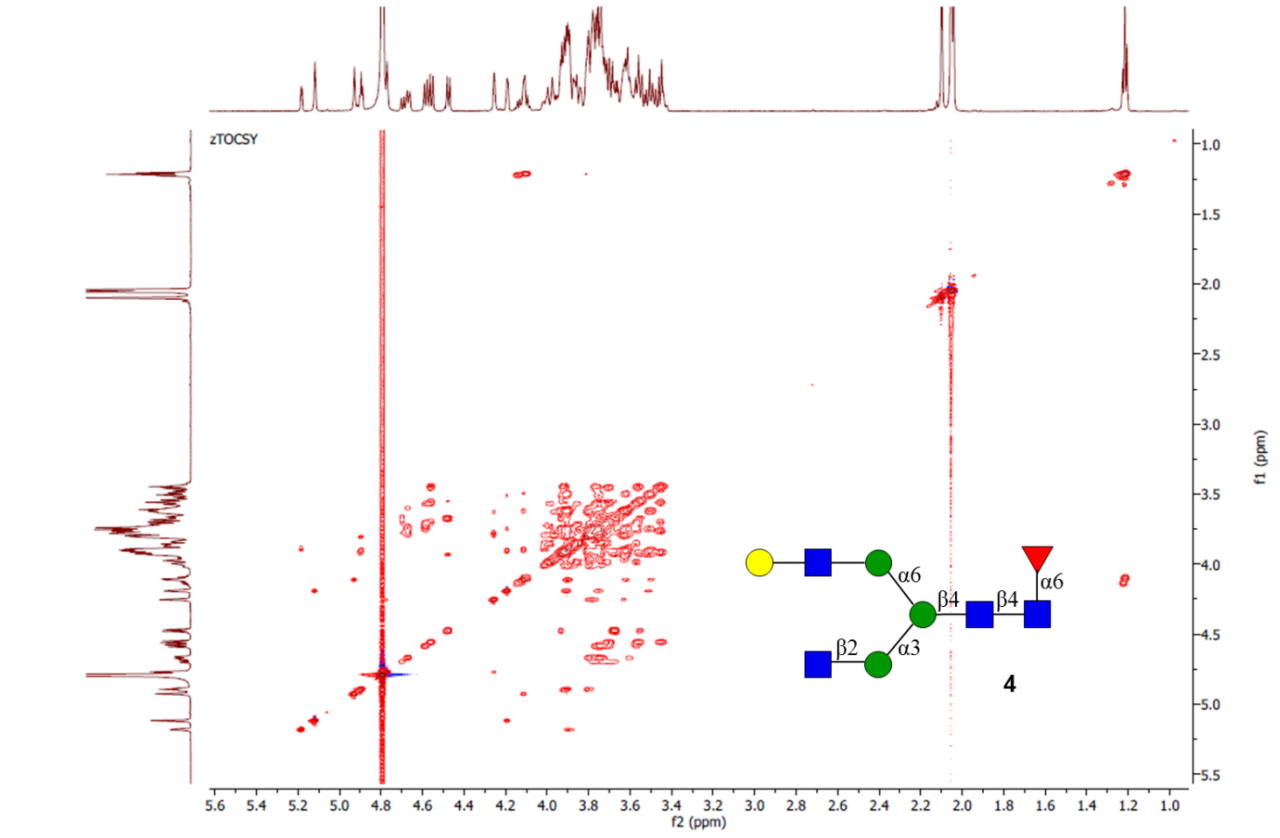

NMR spectra compound 4

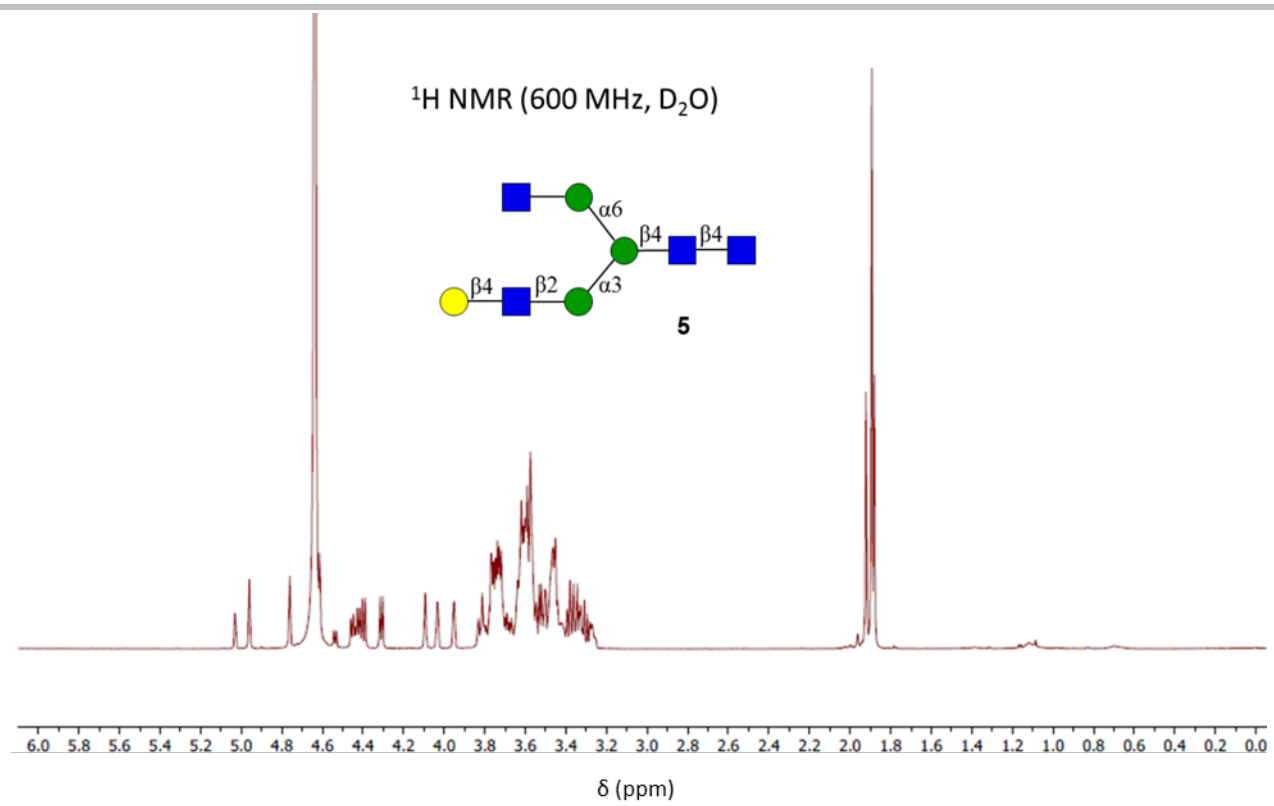
¹H NMR (600 MHz, D2O)
α6
β4
β4
β4
β2
α3
5
δ (ppm)

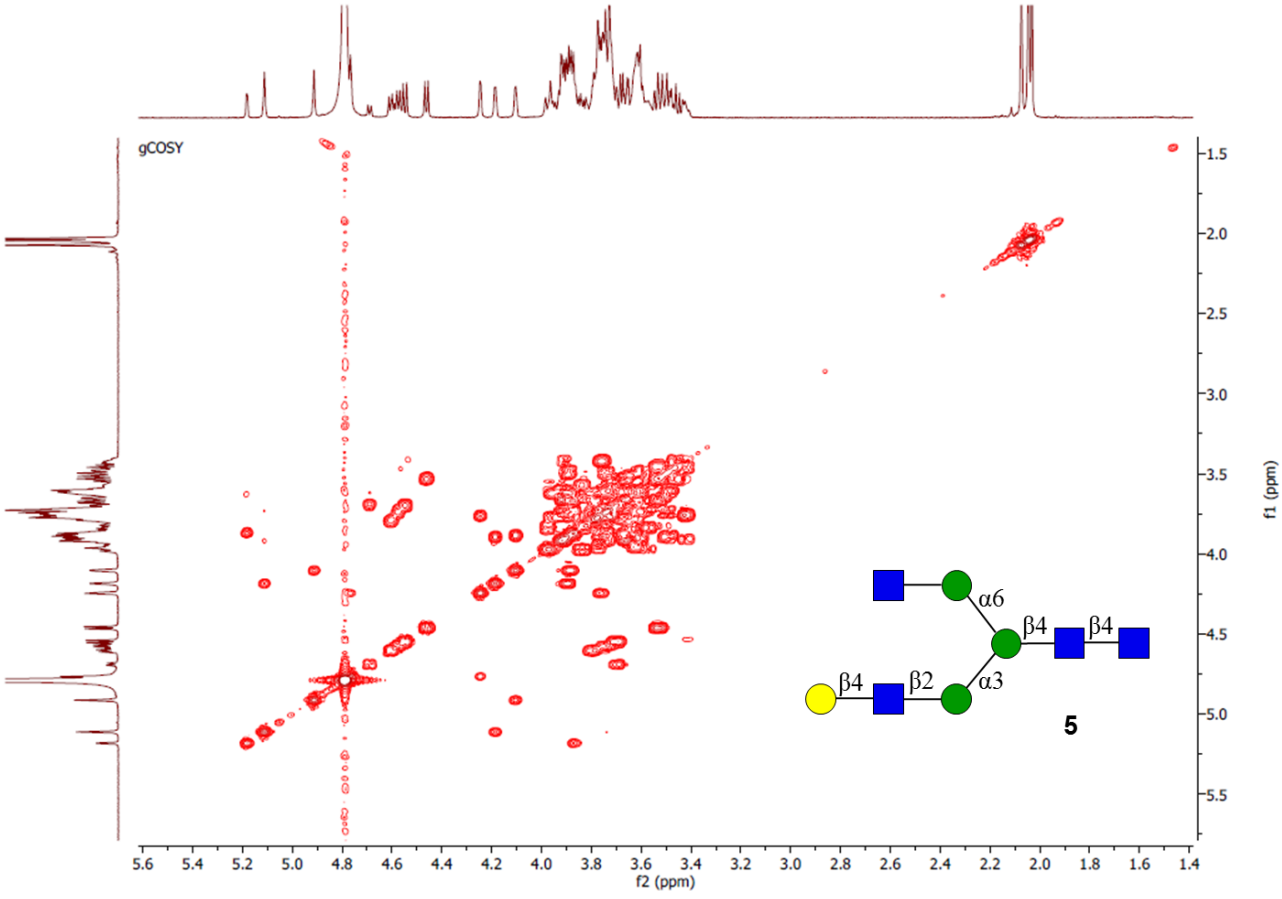
gCOSY
α6
β4
β4
β4
β2
α3
5
f2 (ppm)
f1 (ppm)

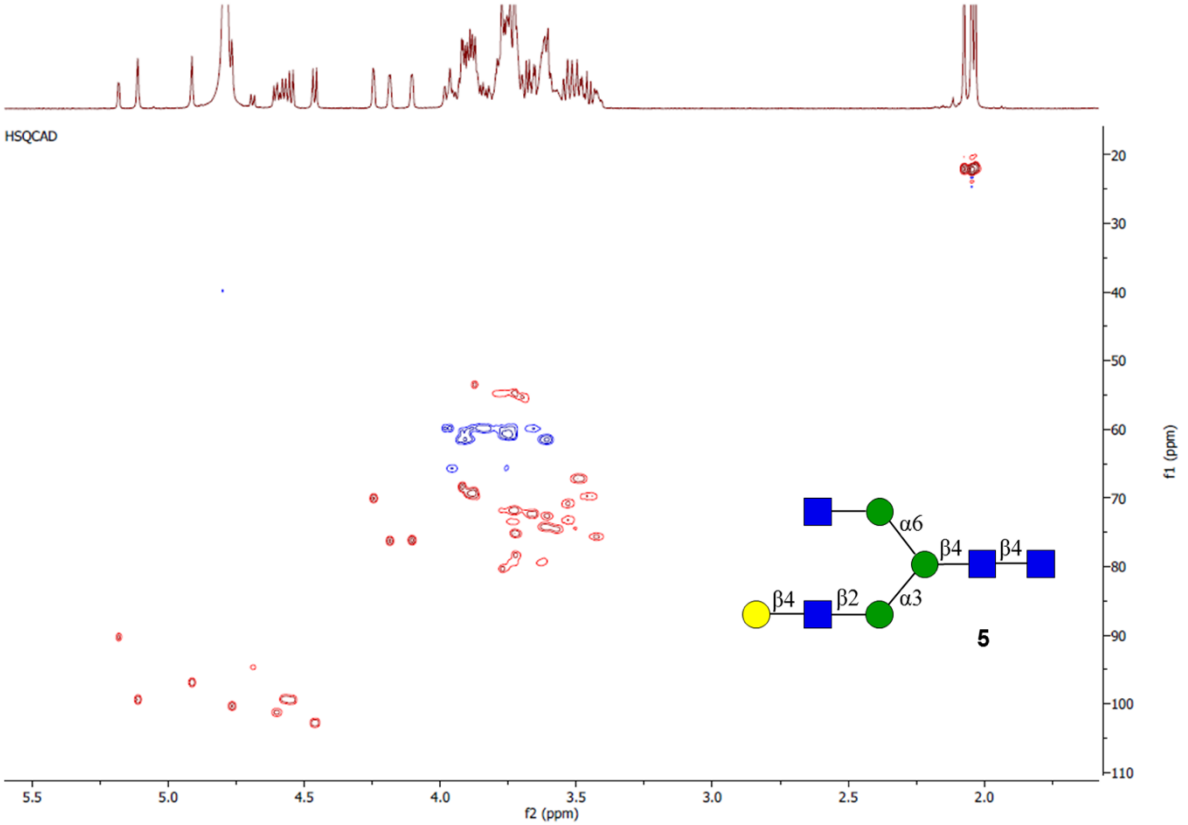

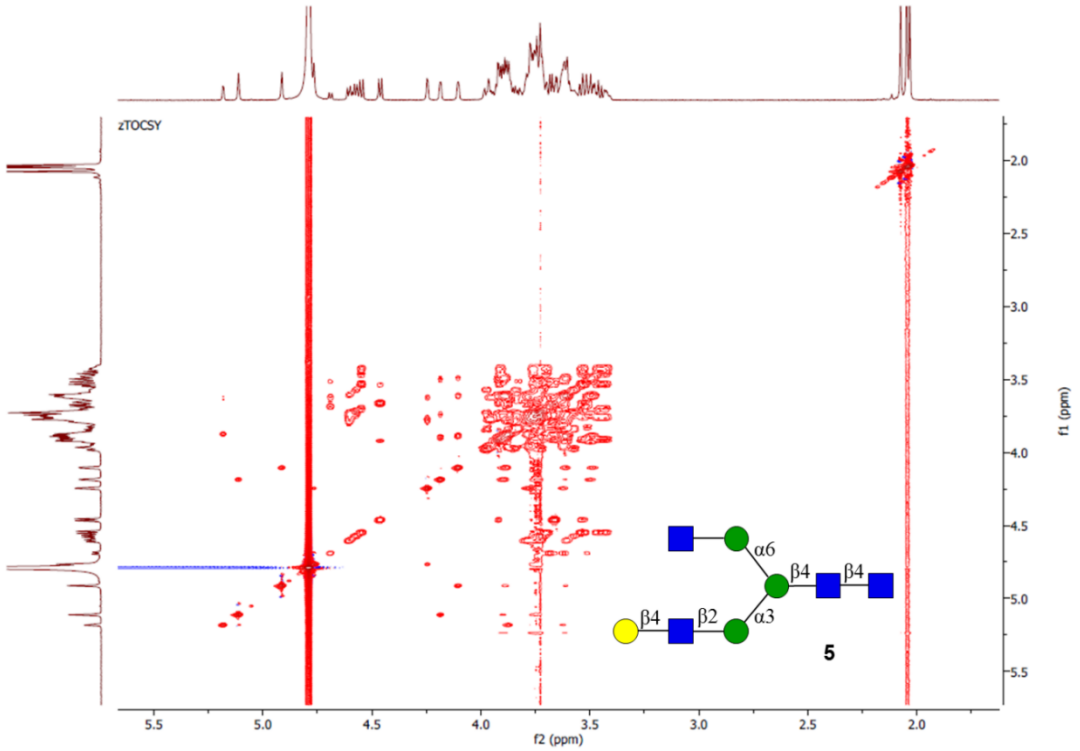

NMR spectra compound 5

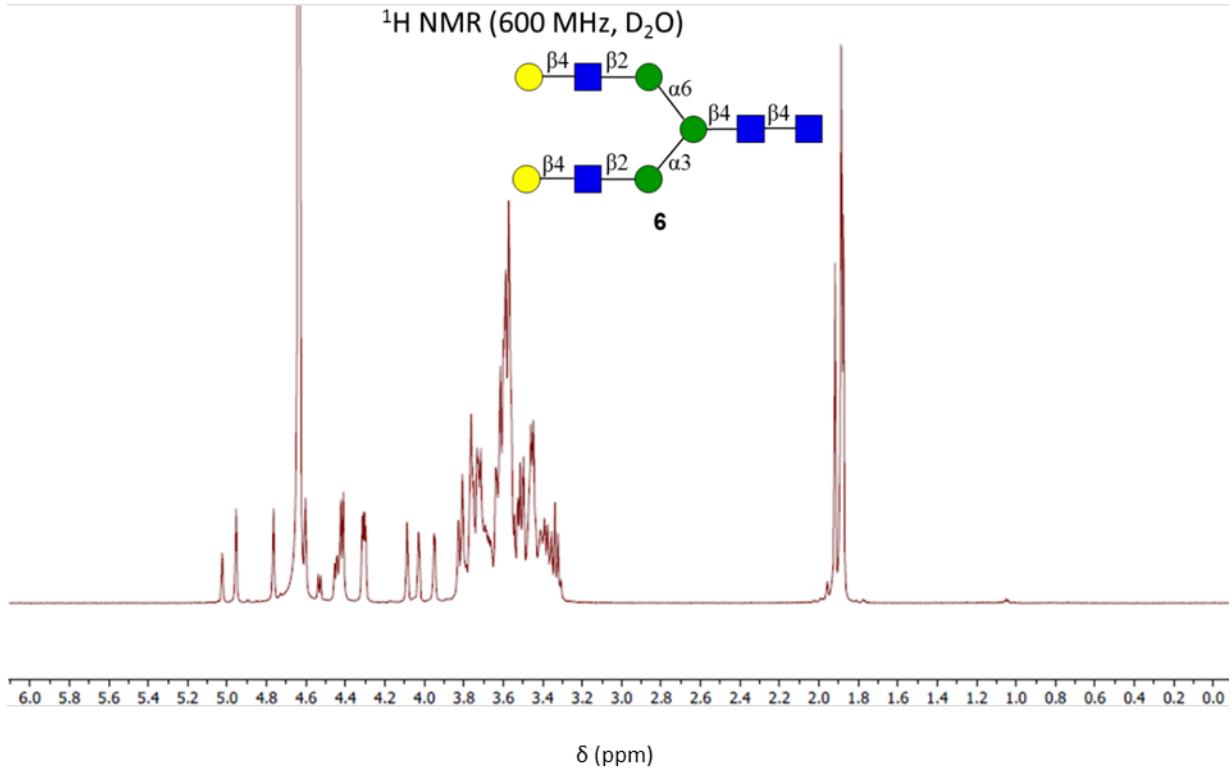
^{1}H NMR (600 MHz, D_2O)
β4
β2
α6
β4
β4
β4
β2
α3
6
δ (ppm)

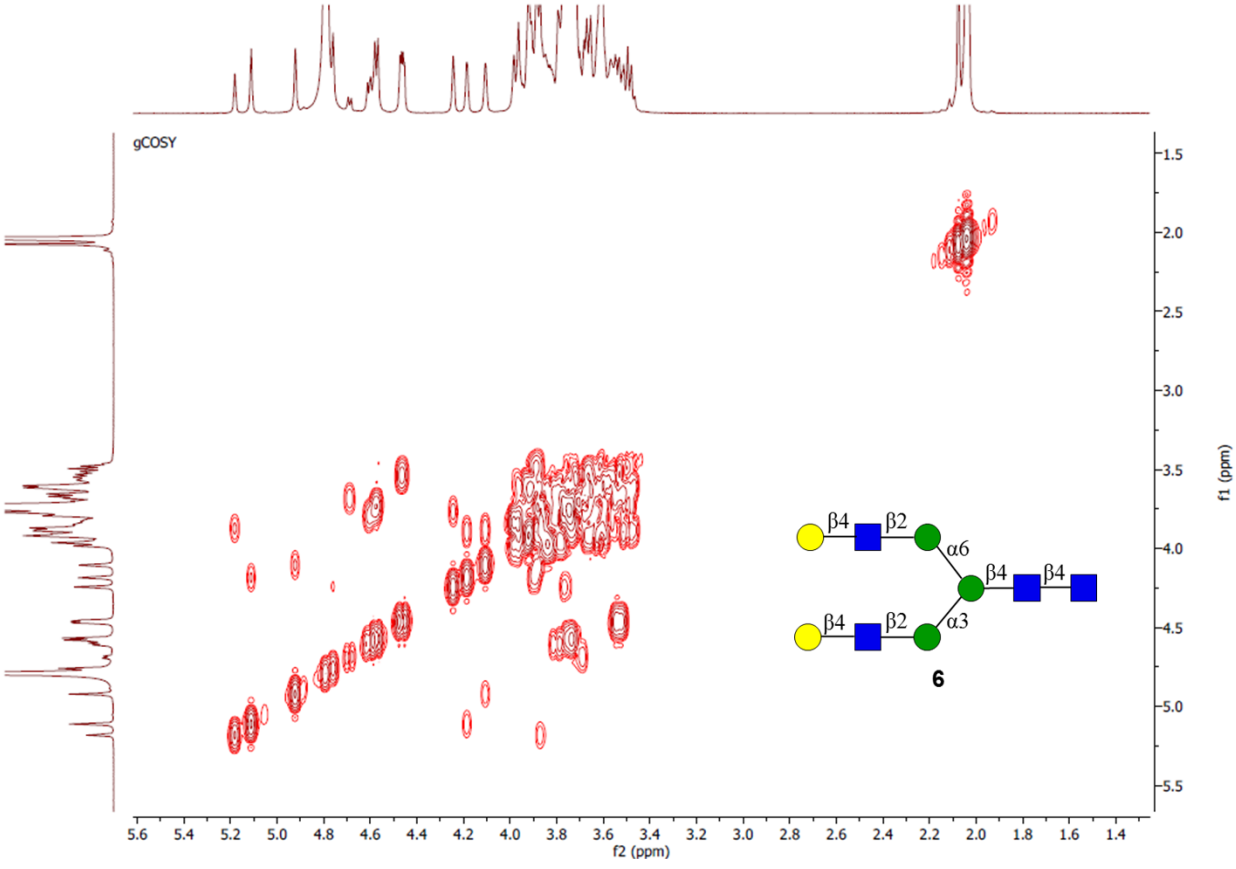
gCOSY
β4
β2
α6
β4
β4
β4
β2
α3
6
f2 (ppm)
f1 (ppm)

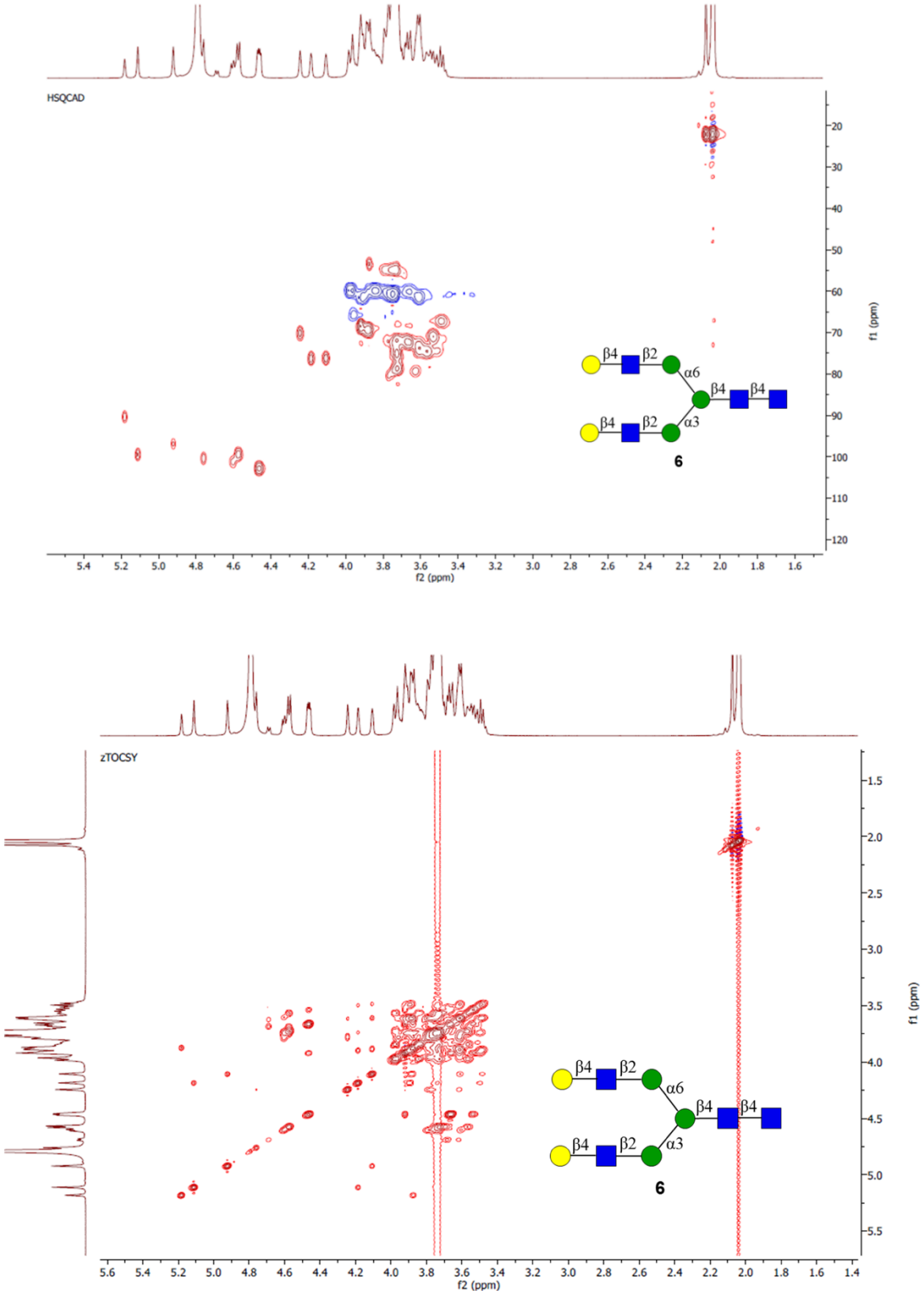

NMR spectra compound 6

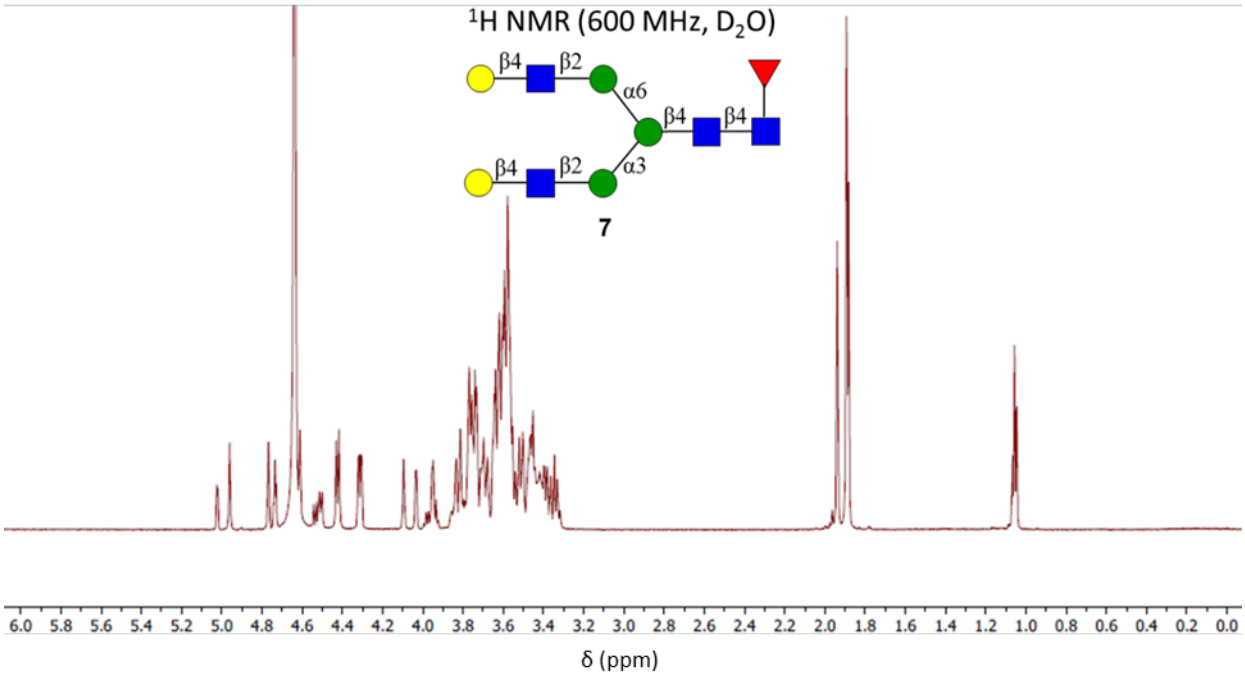
^{1}H NMR (600 MHz, D_2O)
β4
β2
α6
β4
β4
β4
β2
α3
7
δ (ppm)

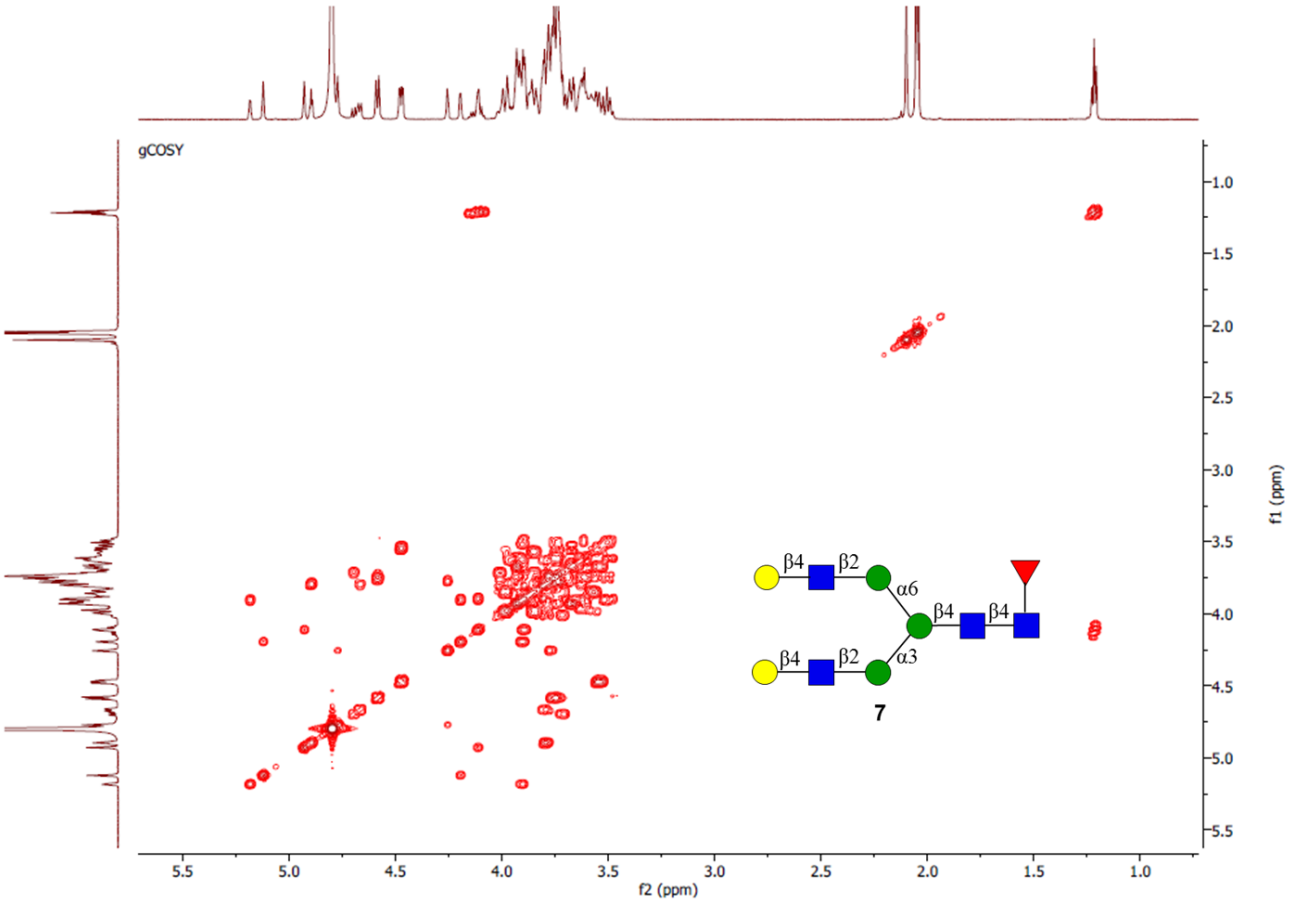
gCOSY
β4
β2
α6
β4
β4
β4
β2
α3
7
f2 (ppm)
f1 (ppm)

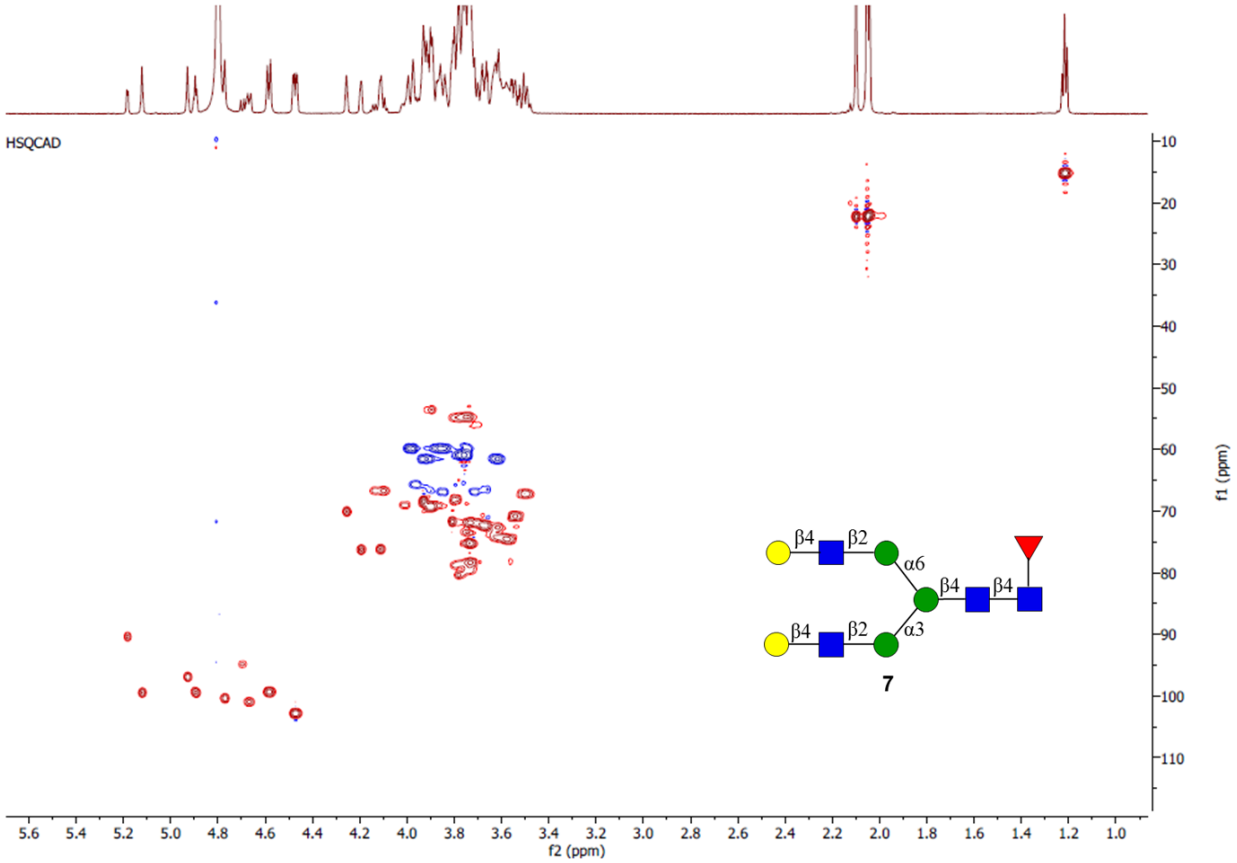

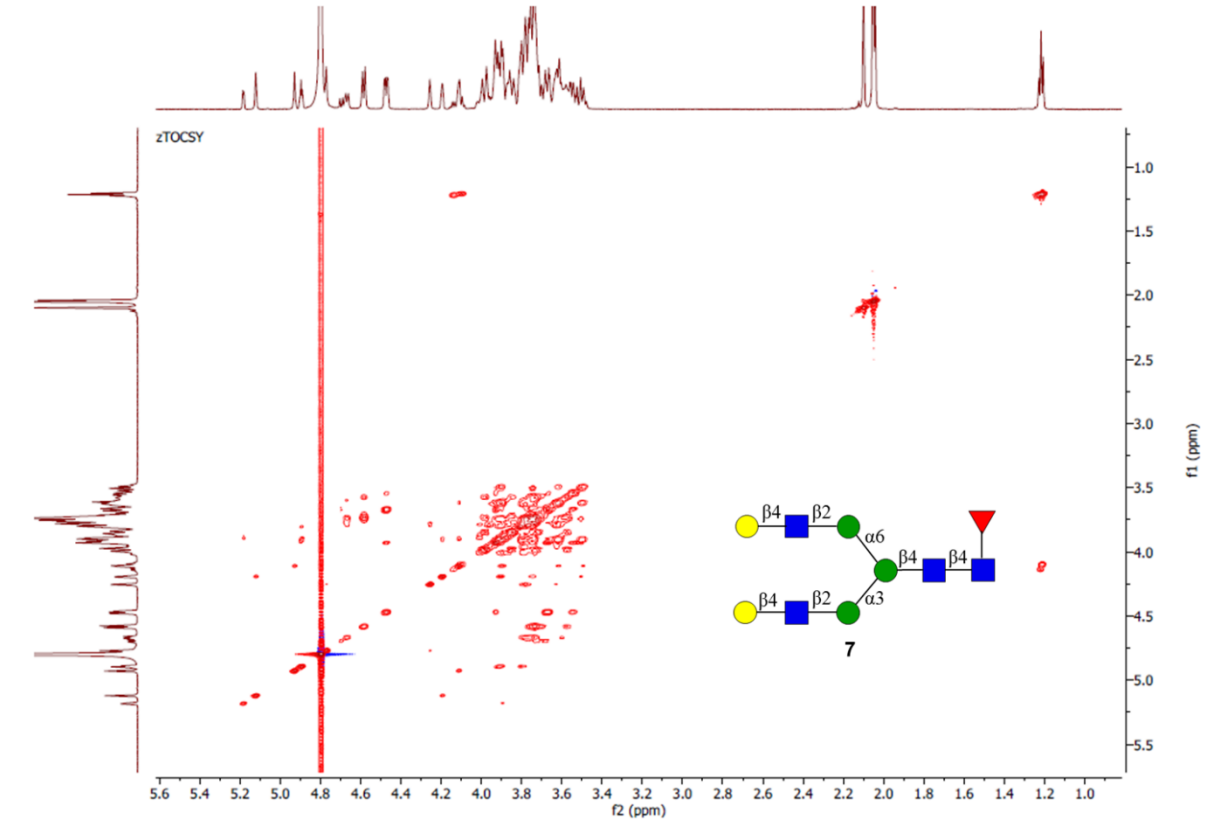

NMR spectra compound 7

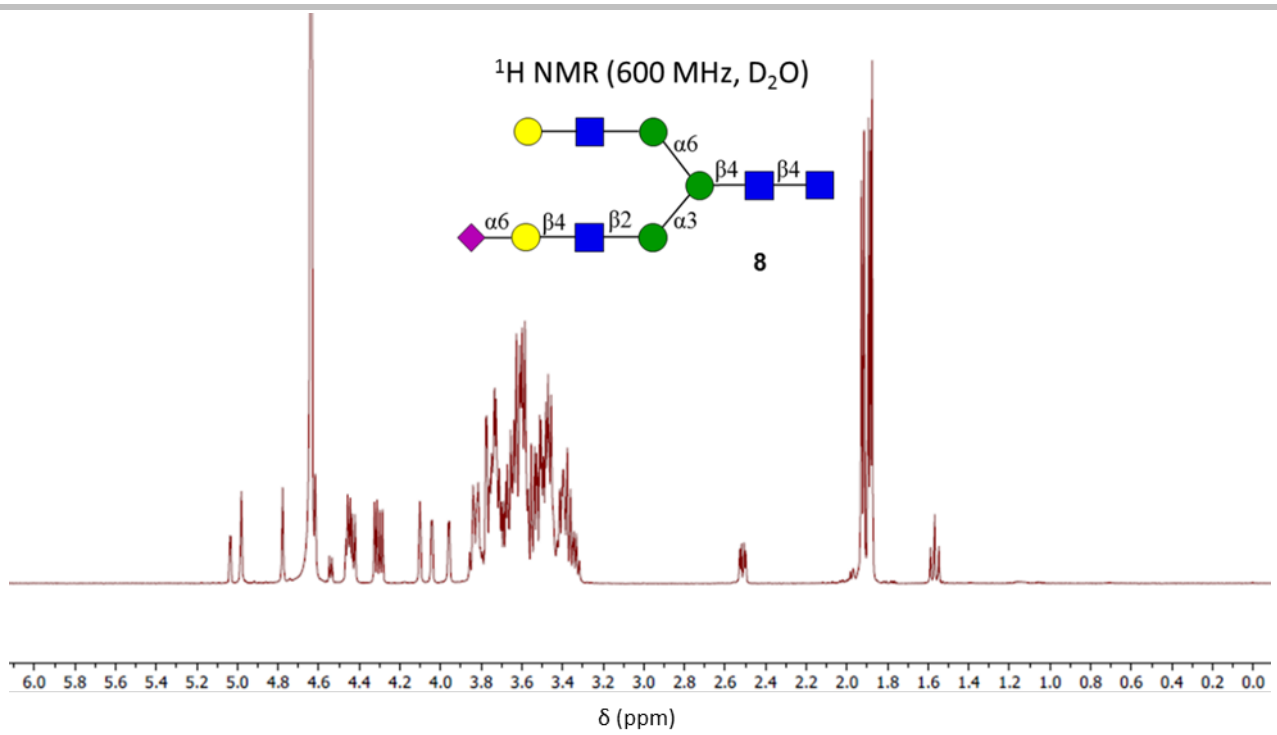
^{1}H NMR (600 MHz, D_2O)
α6
β4
β4
α6
β4
β2
α3
8
6.0 5.8 5.6 5.4 5.2 5.0 4.8 4.6 4.4 4.2 4.0 3.8 3.6 3.4 3.2 3.0 2.8 2.6 2.4 2.2 2.0 1.8 1.6 1.4 1.2 1.0 0.8 0.6 0.4 0.2 0.0
δ (ppm)

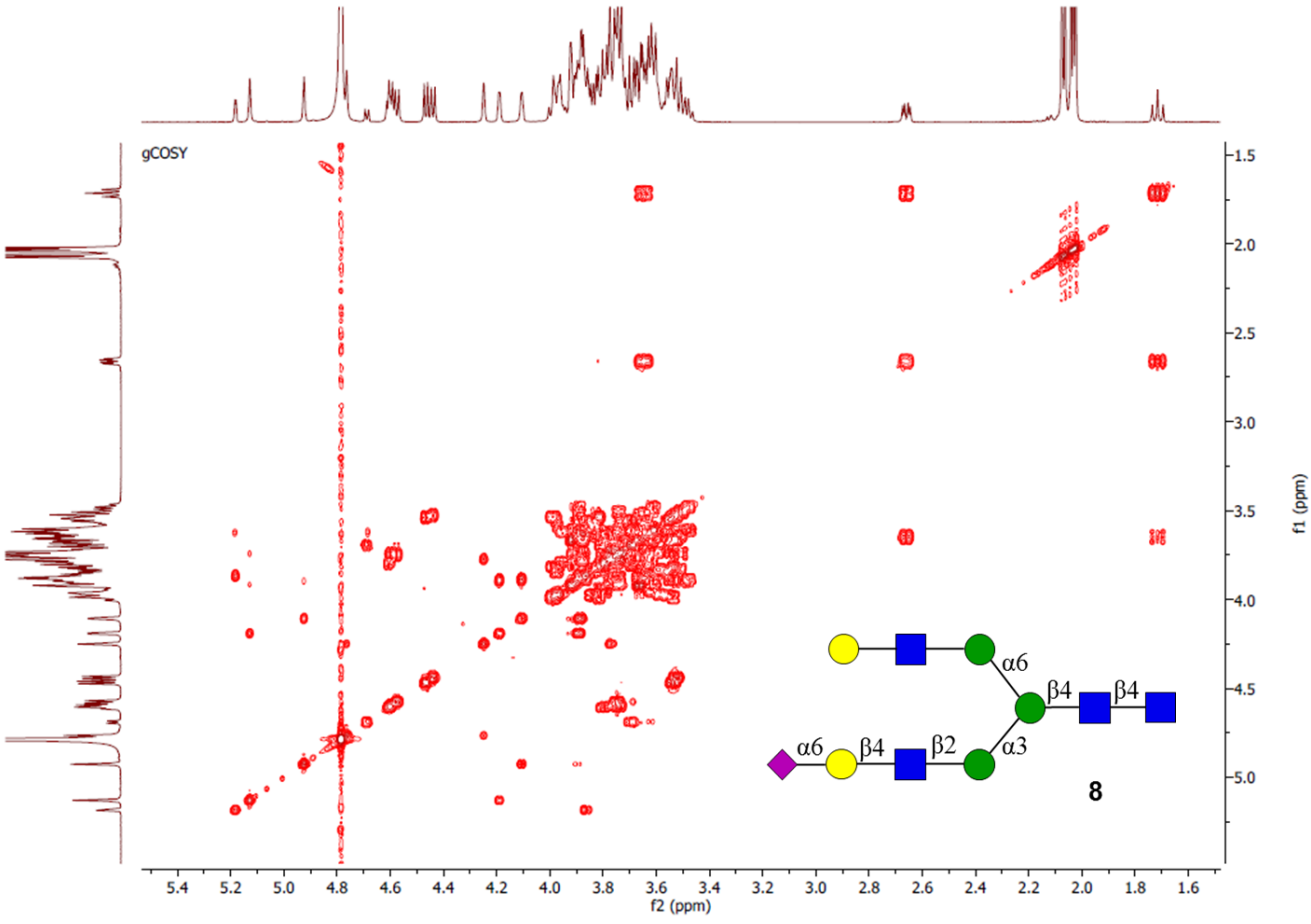
gCOSY
α6
β4
β4
α6
β4
β2
α3
8
5.4 5.2 5.0 4.8 4.6 4.4 4.2 4.0 3.8 3.6 3.4 3.2 3.0 2.8 2.6 2.4 2.2 2.0 1.8 1.6
f2 (ppm)
1.5 2.0 2.5 3.0 3.5 4.0 4.5 5.0
f1 (ppm)

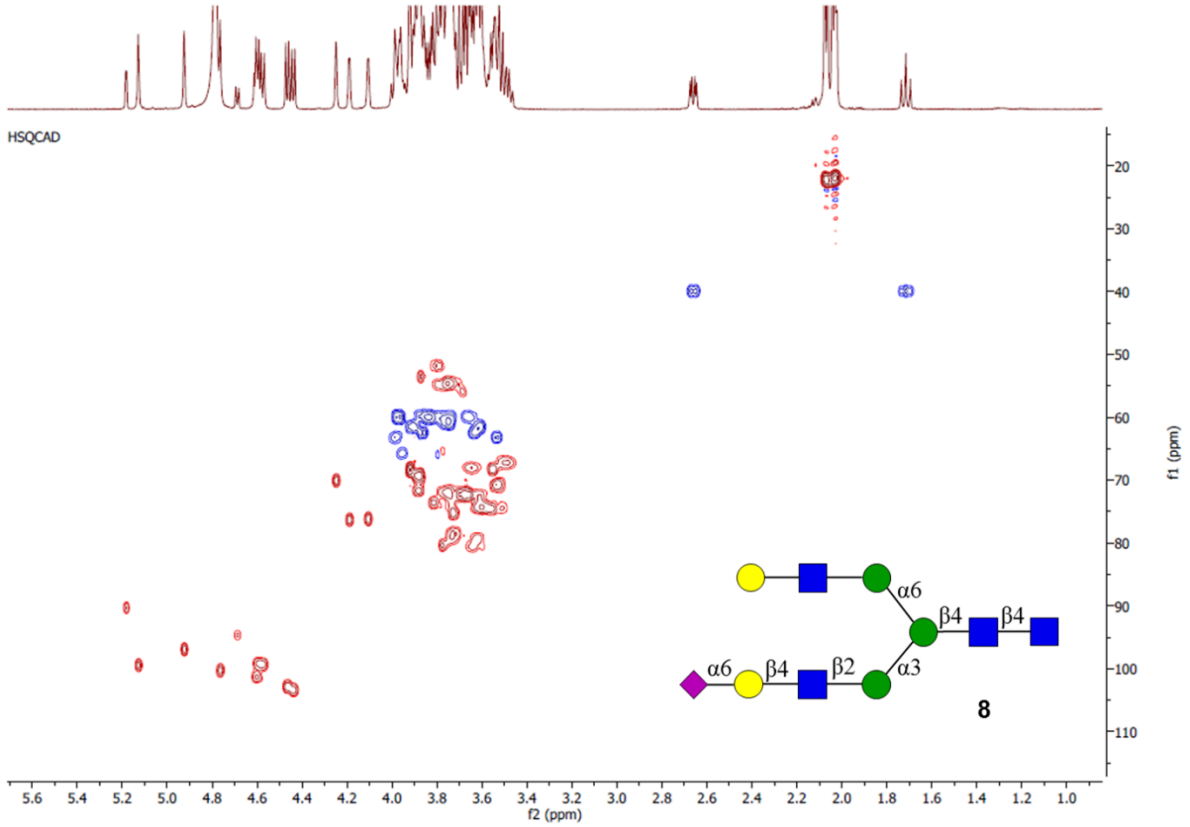

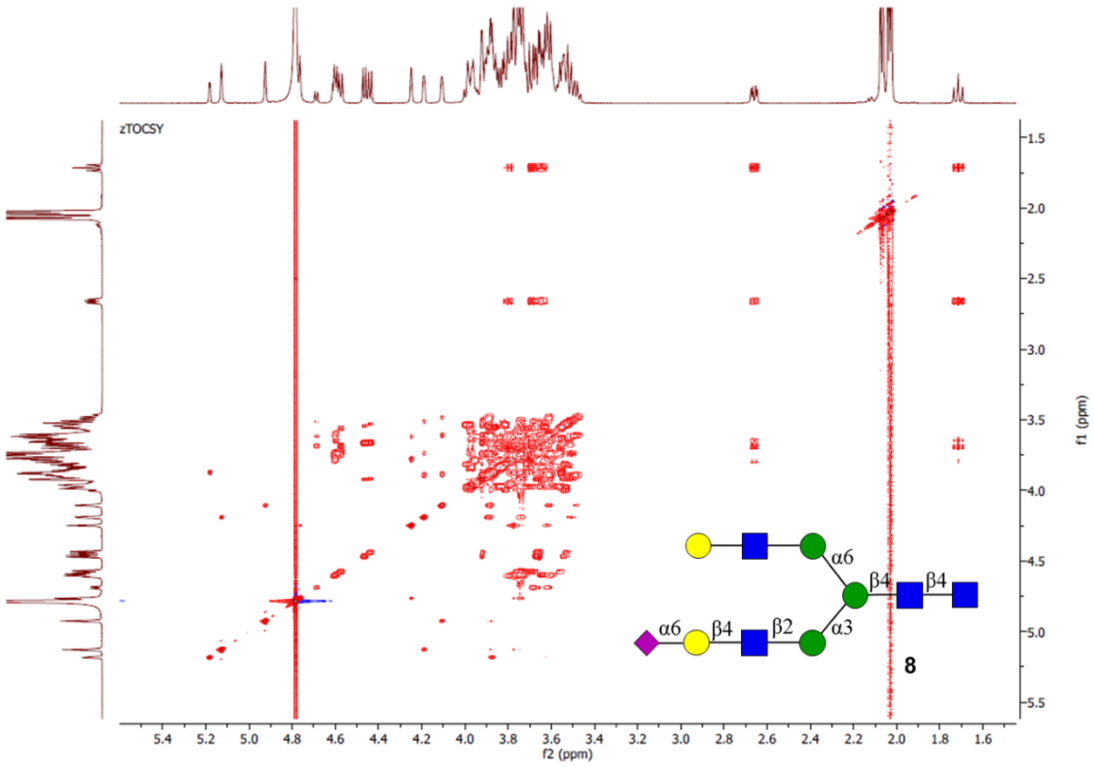

NMR spectra compound 8

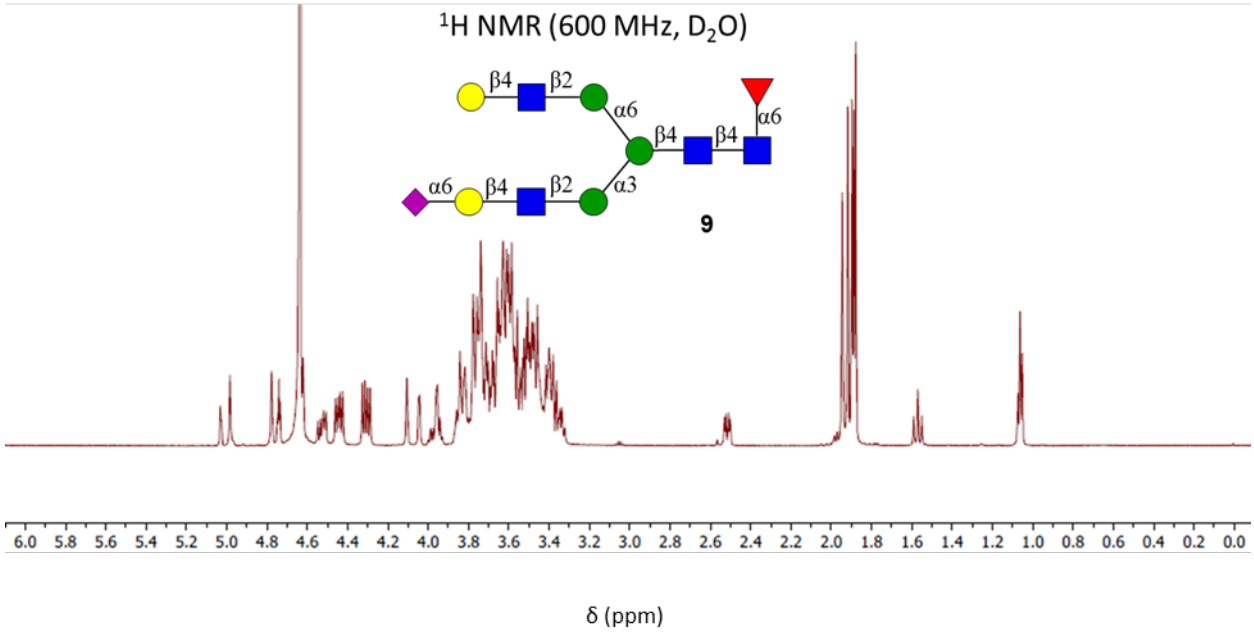
^{1}H NMR (600 MHz, D_2O)
β4
β2
α6
β4
β4
α6
α6
β4
β2
α3
9
6.0 5.8 5.6 5.4 5.2 5.0 4.8 4.6 4.4 4.2 4.0 3.8 3.6 3.4 3.2 3.0 2.8 2.6 2.4 2.2 2.0 1.8 1.6 1.4 1.2 1.0 0.8 0.6 0.4 0.2 0.0
δ (ppm)

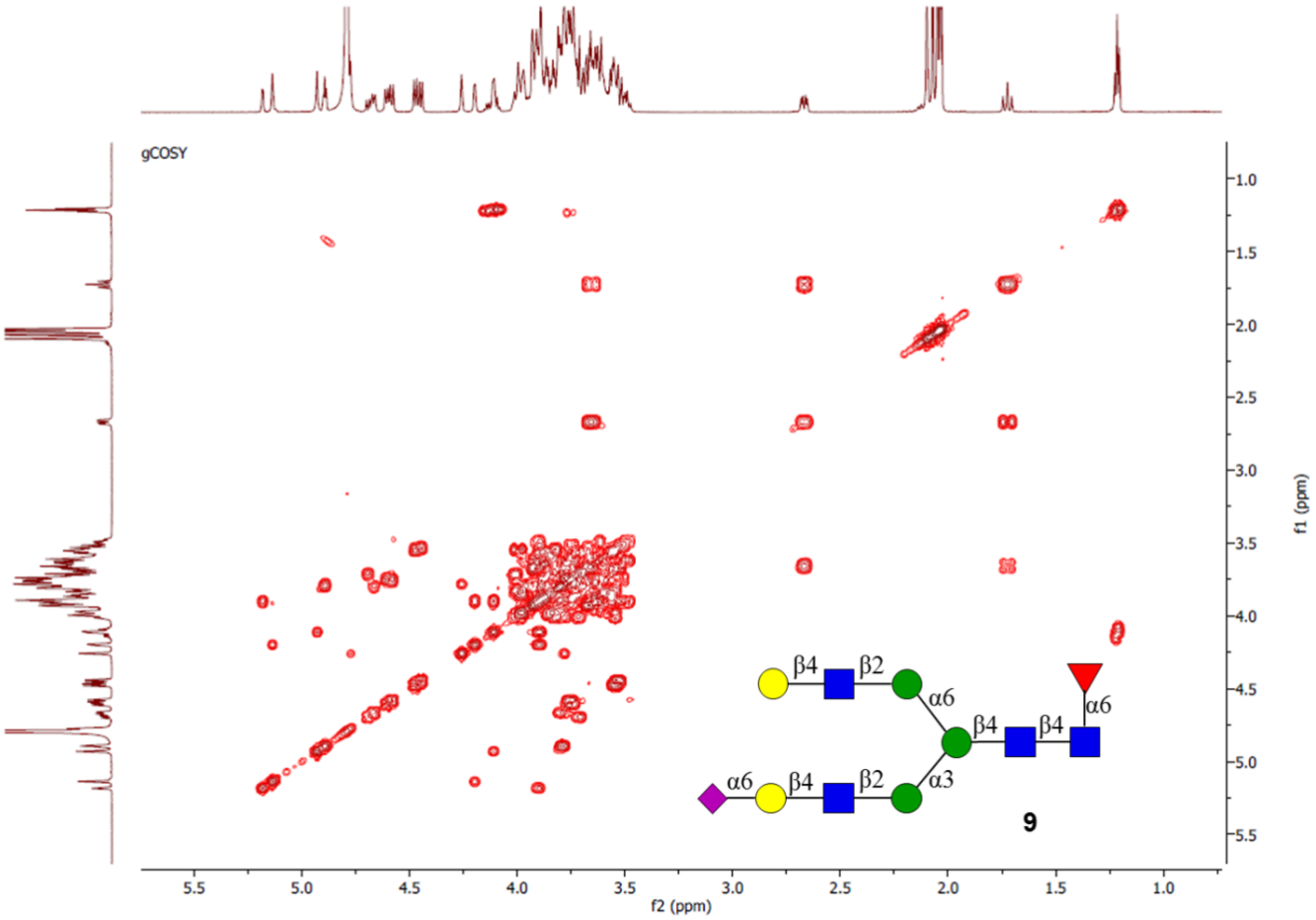
gCOSY
β4
β2
α6
β4
β4
α6
α6
β4
β2
α3
9
5.5 5.0 4.5 4.0 3.5 3.0 2.5 2.0 1.5 1.0
f2 (ppm)
1.0 1.5 2.0 2.5 3.0 3.5 4.0 4.5 5.0 5.5
f1 (ppm)

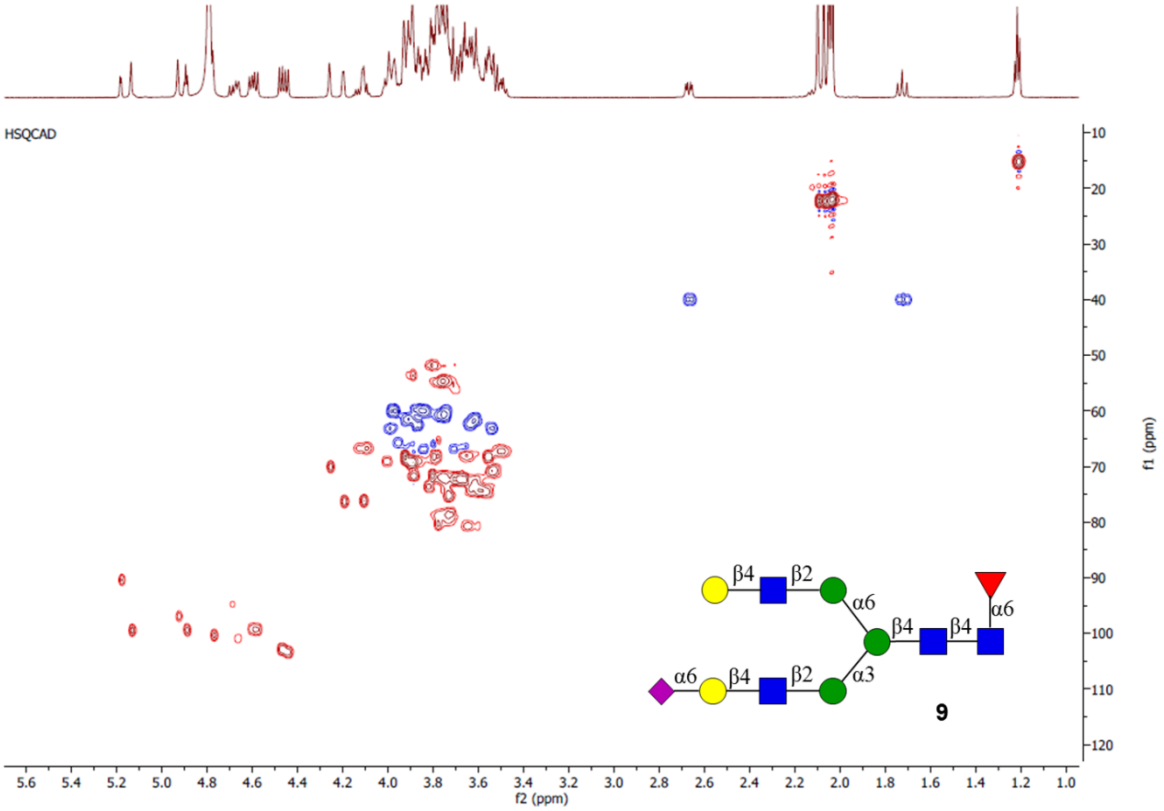

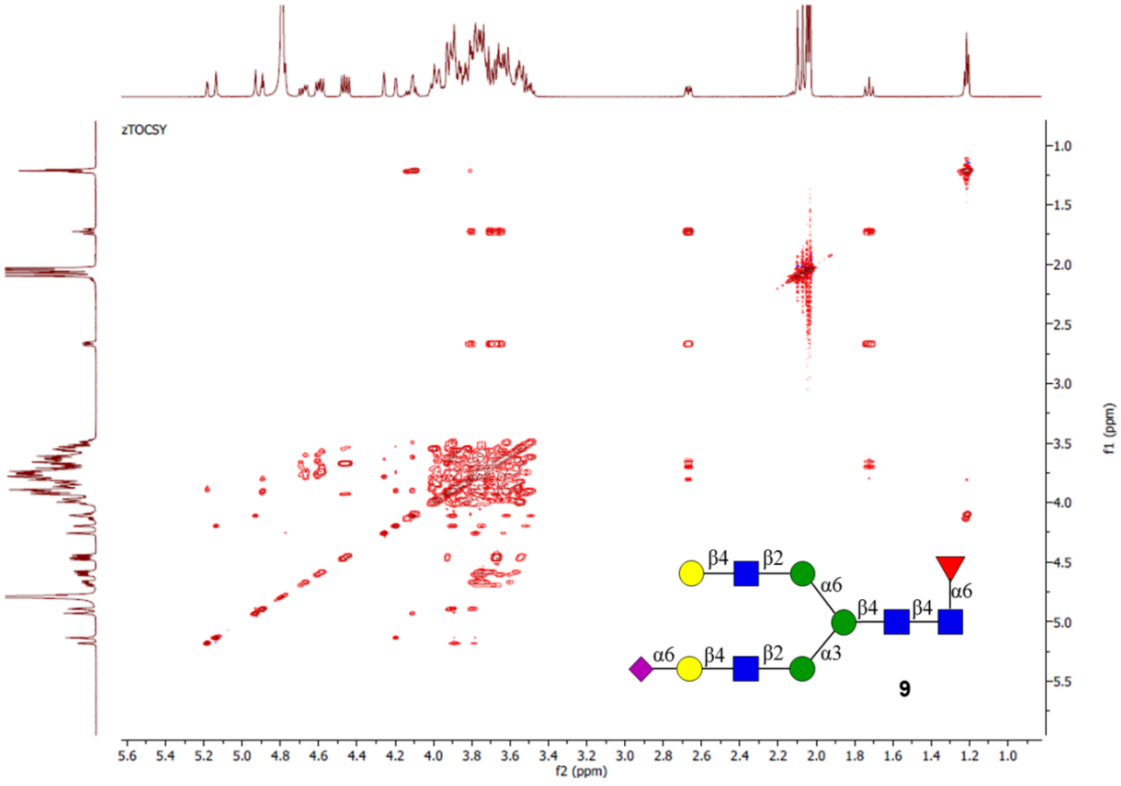

NMR spectra compound 9

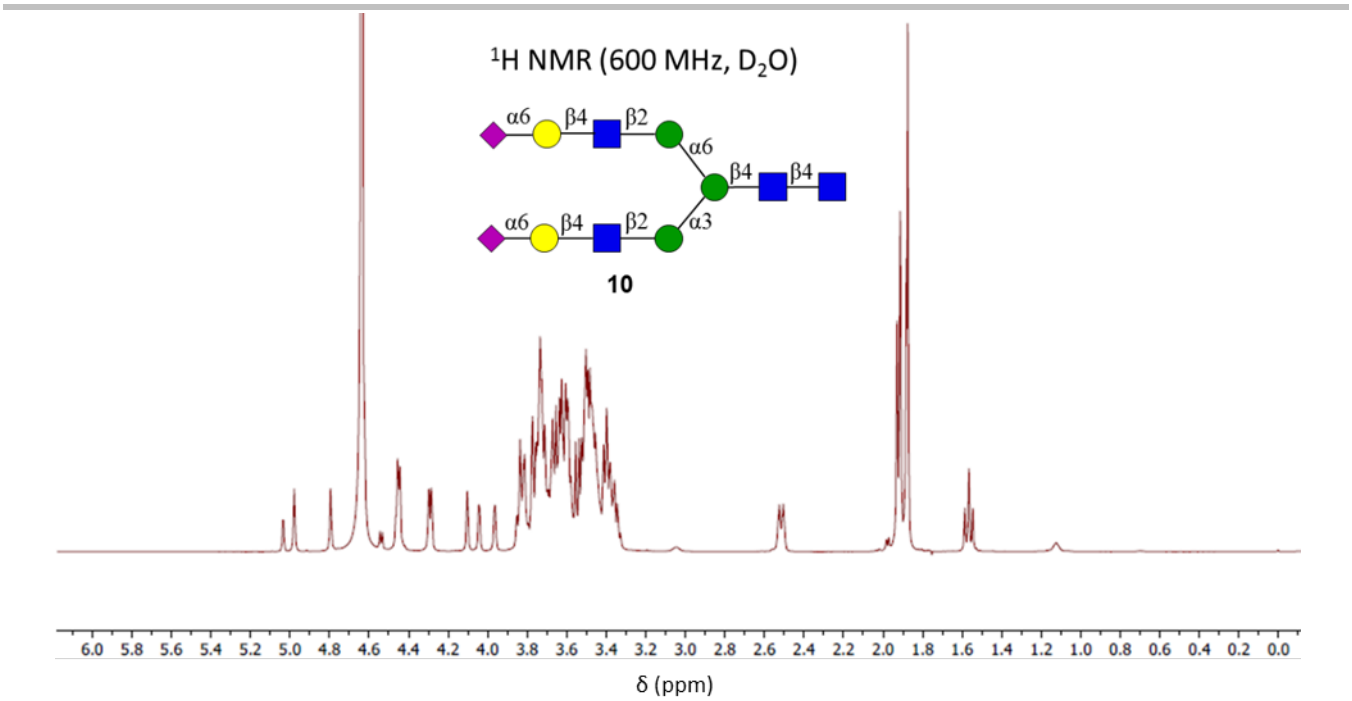
^{1}H NMR (600 MHz, D_2O)
α6 β4 β2 α6 β4 β4
α6 β4 β2 α3
10
δ (ppm)

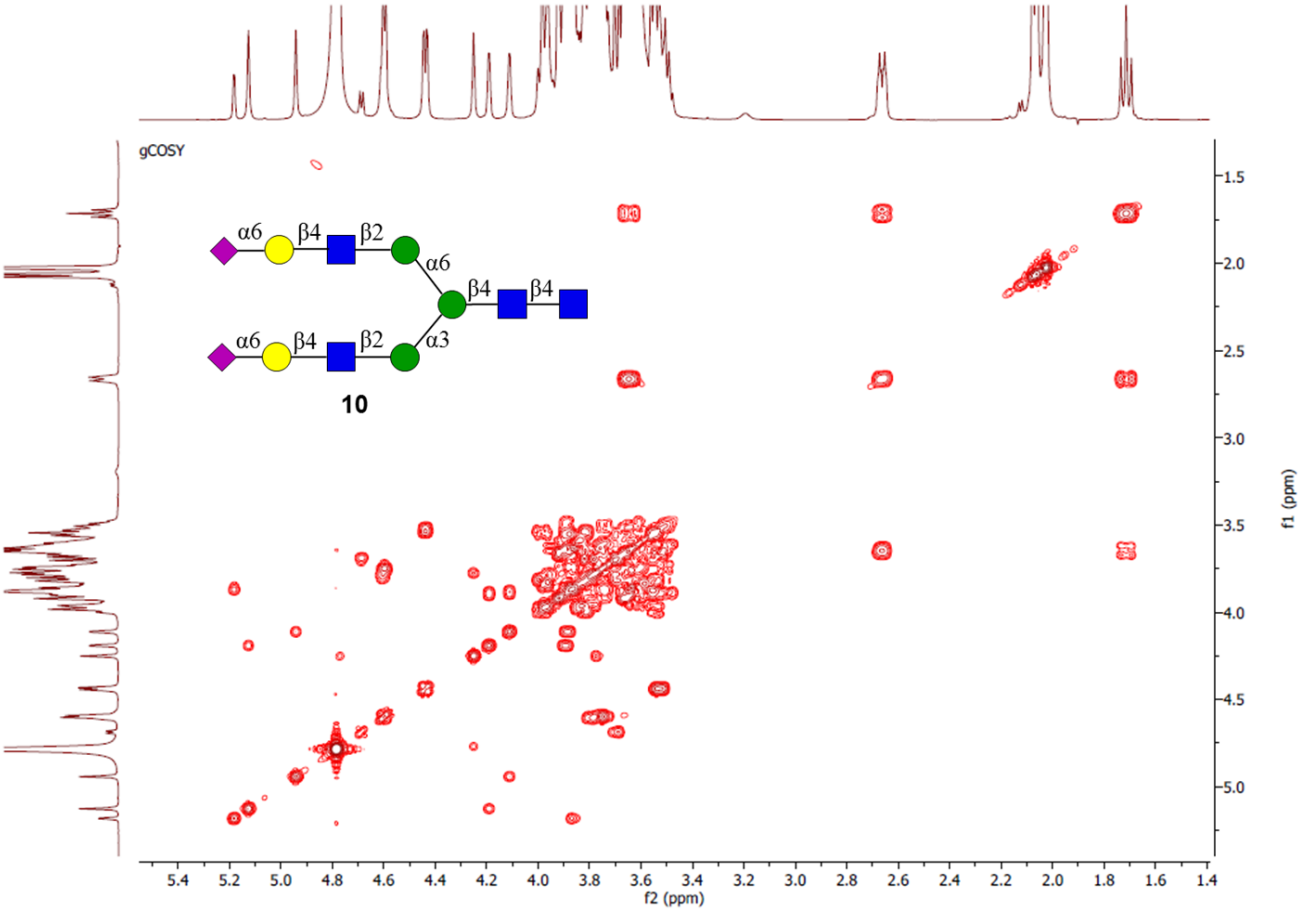
gCOSY
α6 β4 β2 α6 β4 β4
α6 β4 β2 α3
10
f2 (ppm)
f1 (ppm)

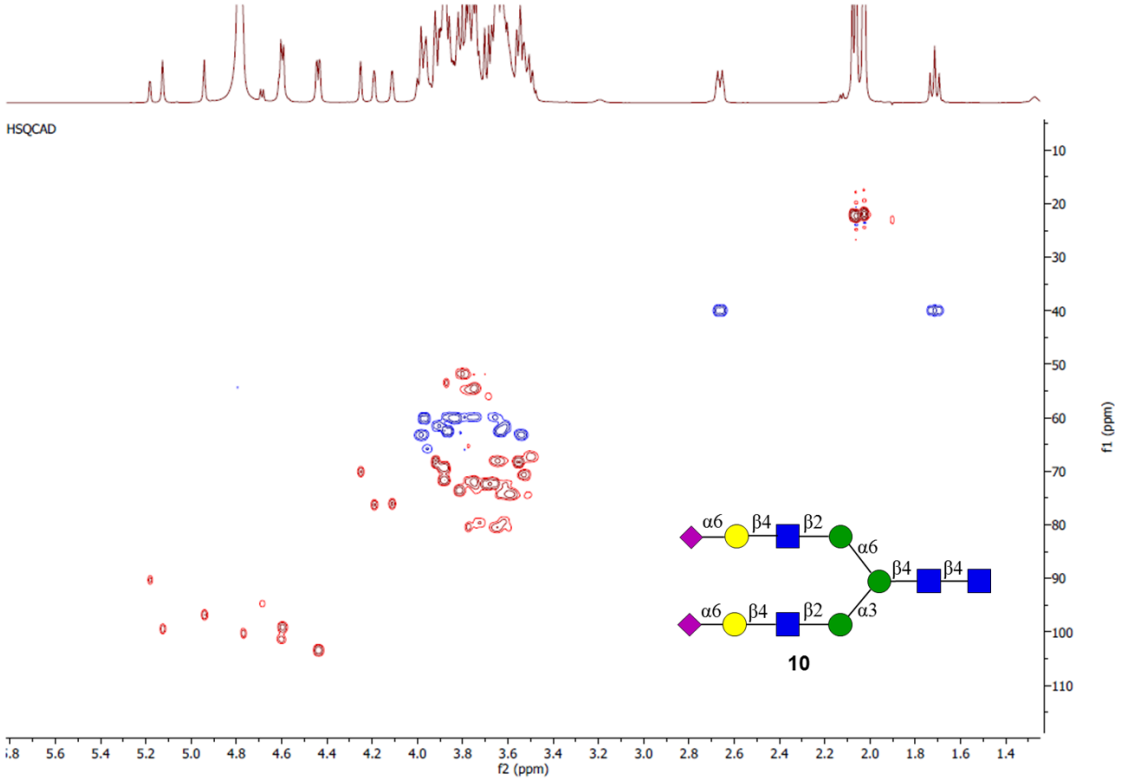

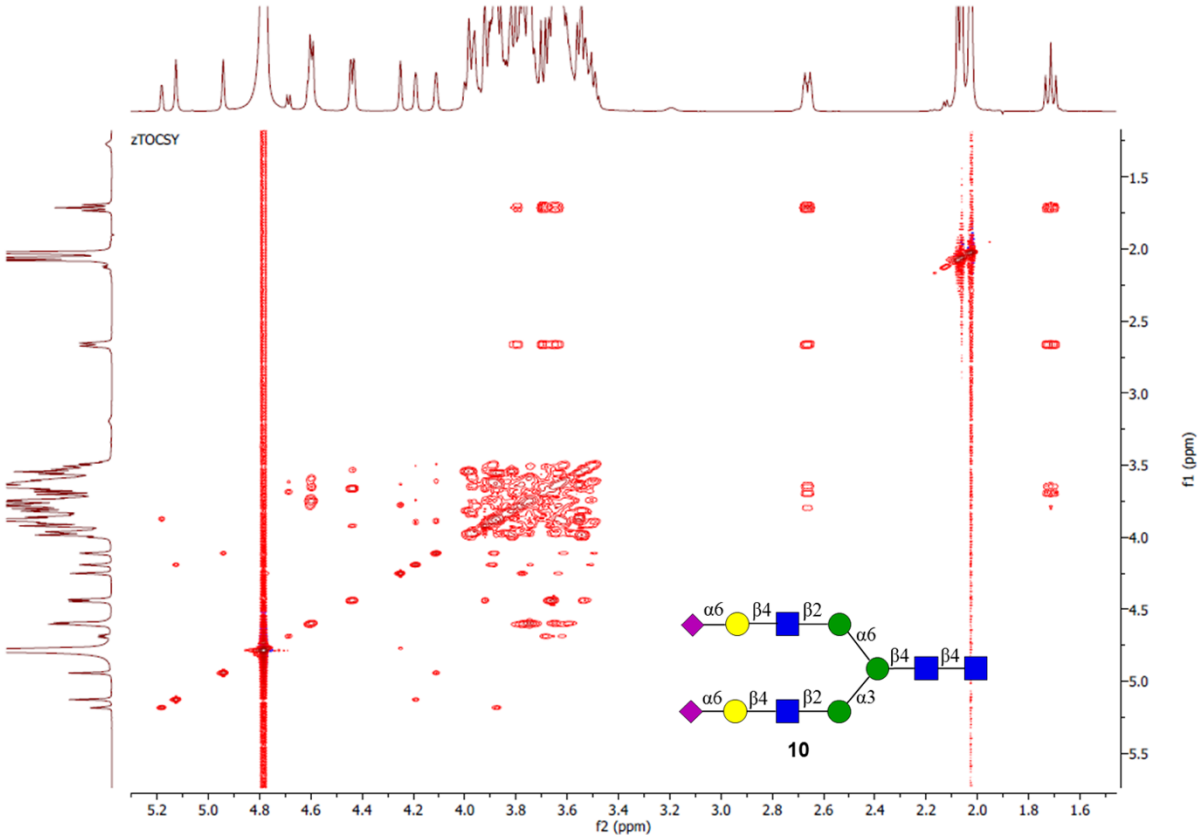

NMR spectra compound 10

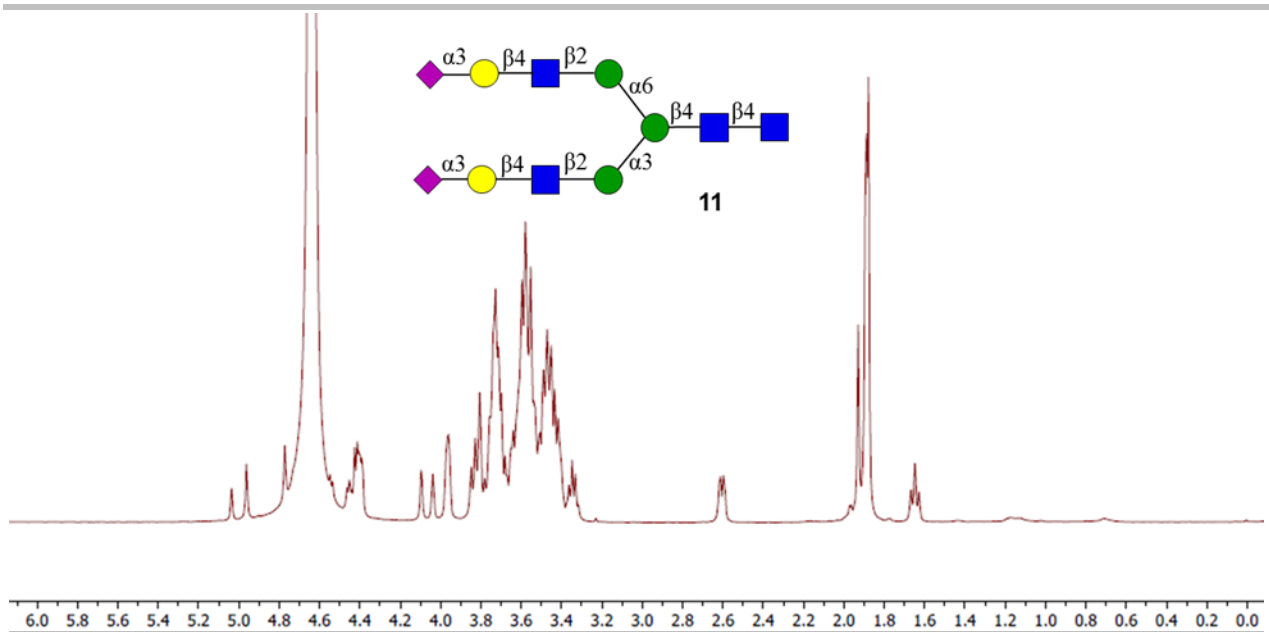
α3 β4 β2 α6 β4 β4
α3 β4 β2 α3
11
6.0 5.8 5.6 5.4 5.2 5.0 4.8 4.6 4.4 4.2 4.0 3.8 3.6 3.4 3.2 3.0 2.8 2.6 2.4 2.2 2.0 1.8 1.6 1.4 1.2 1.0 0.8 0.6 0.4 0.2 0.0
δ (ppm)

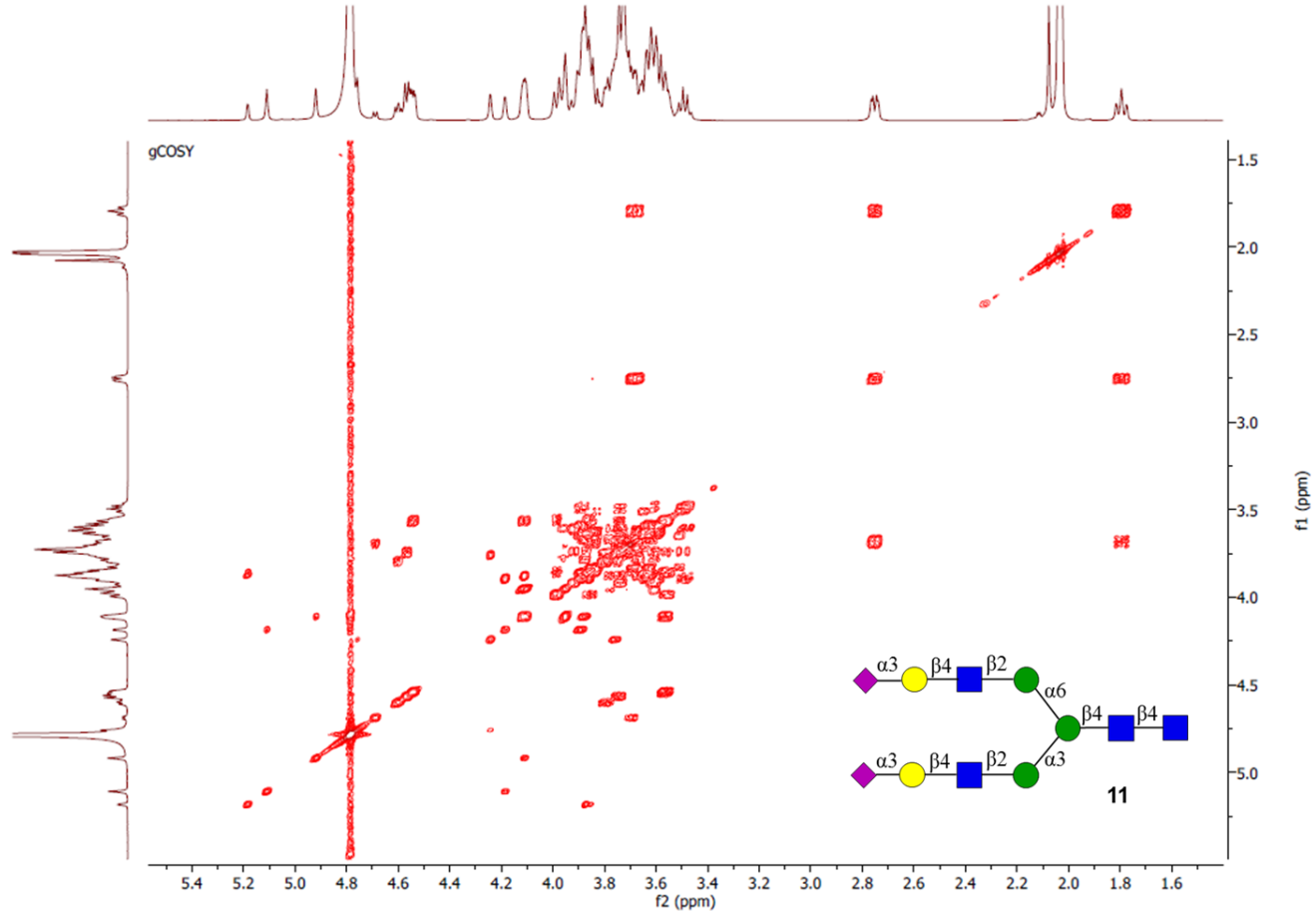
gCOSY
α3 β4 β2 α6 β4 β4
α3 β4 β2 α3
11
5.4 5.2 5.0 4.8 4.6 4.4 4.2 4.0 3.8 3.6 3.4 3.2 3.0 2.8 2.6 2.4 2.2 2.0 1.8 1.6
f2 (ppm)
1.5 2.0 2.5 3.0 3.5 4.0 4.5 5.0
f1 (ppm)

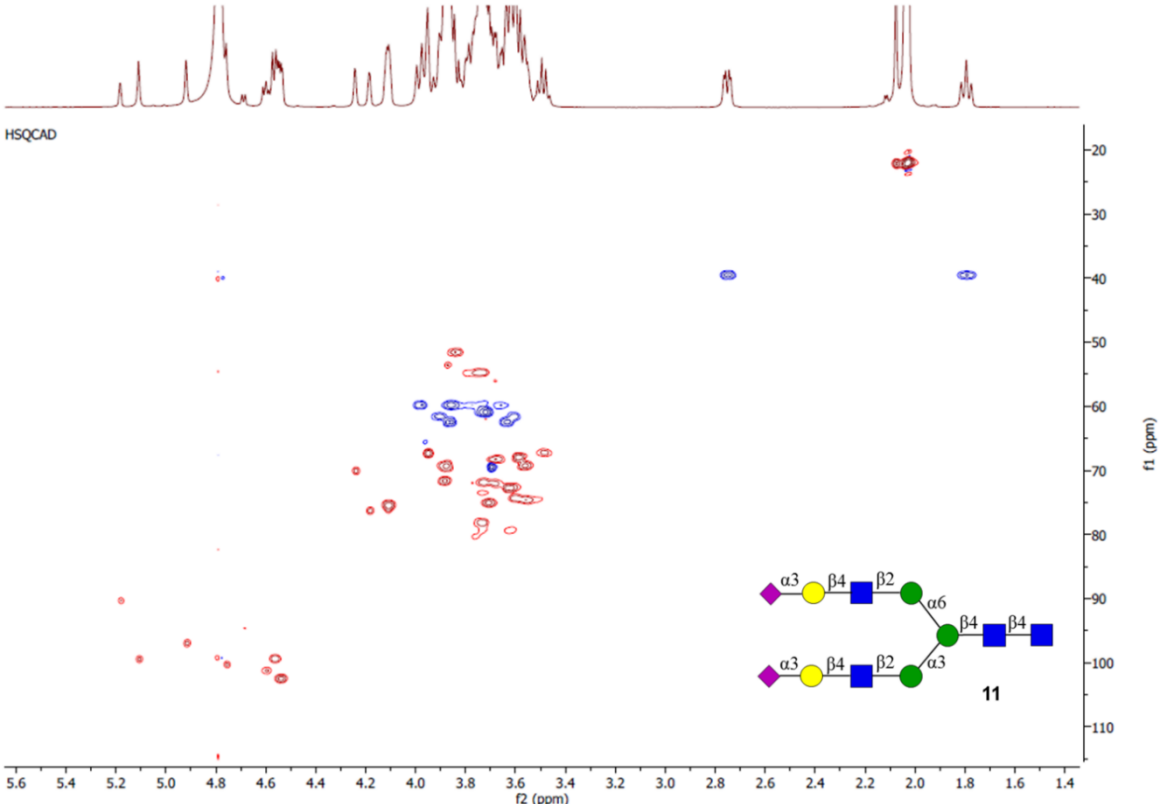

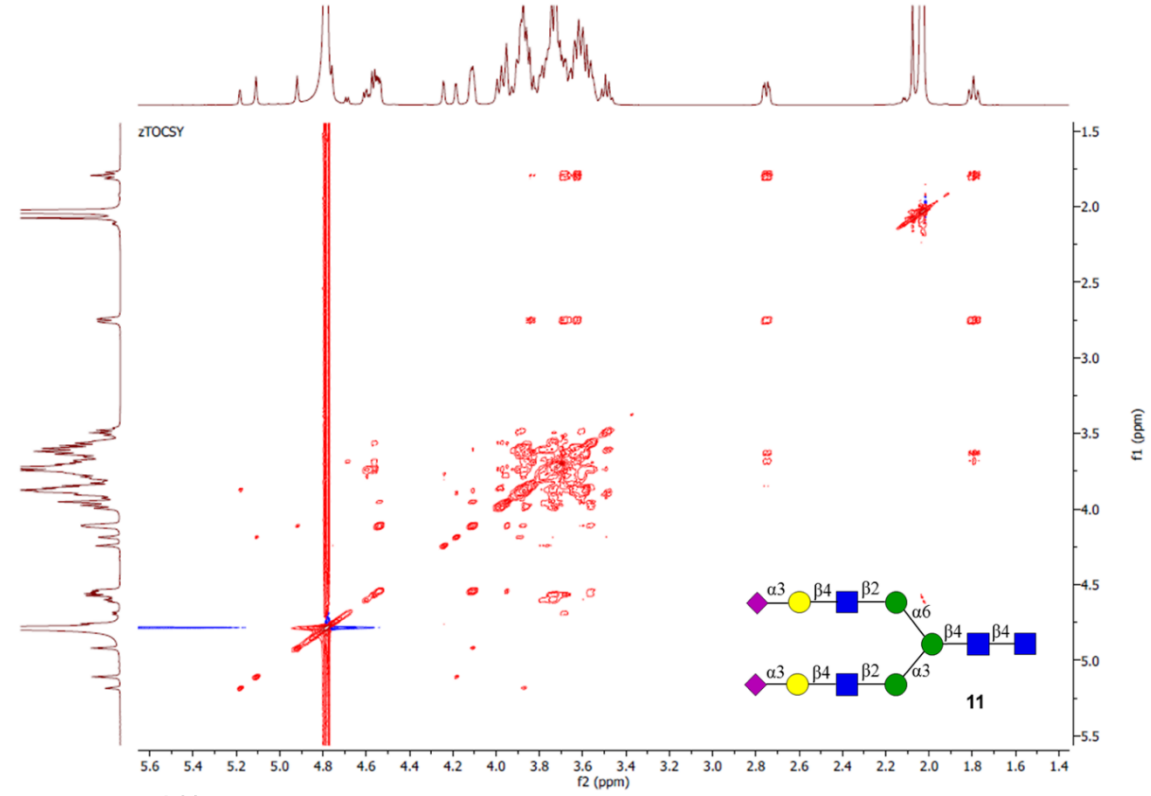

NMR spectra compound 11

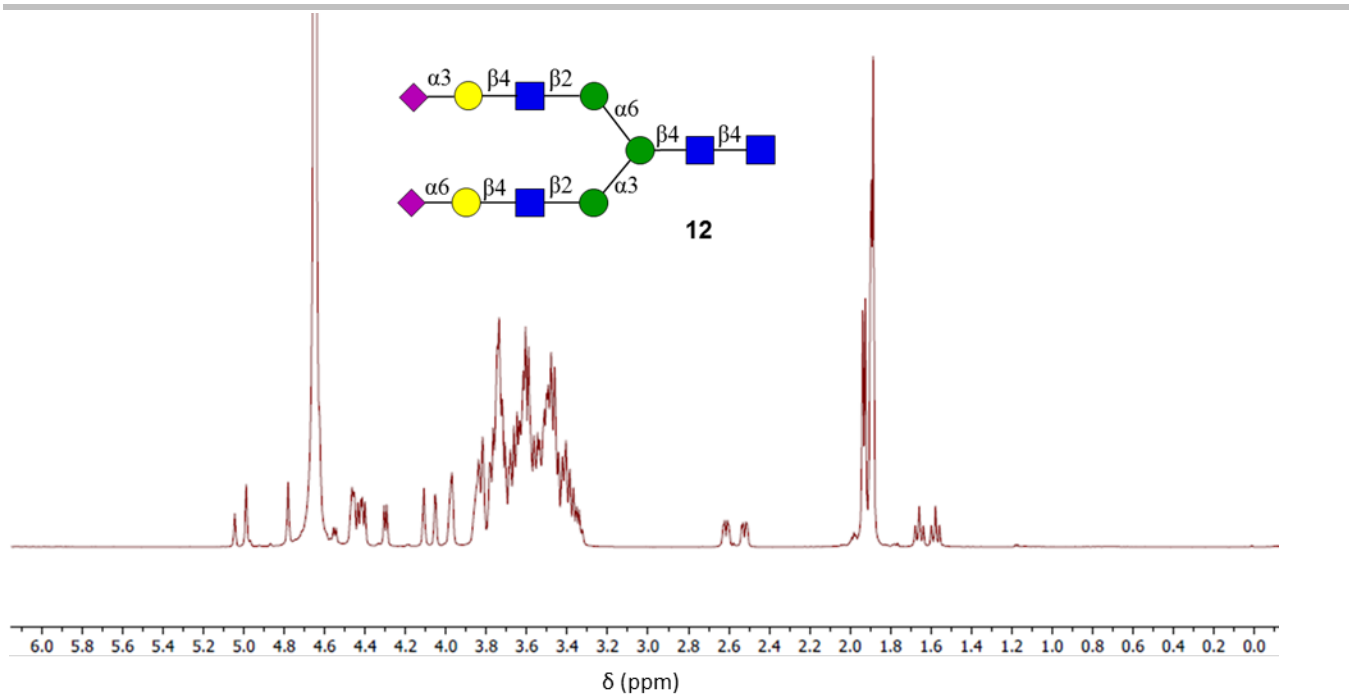
α3
β4
β2
α6
β4
β4
α6
β4
β2
α3
12
6.0 5.8 5.6 5.4 5.2 5.0 4.8 4.6 4.4 4.2 4.0 3.8 3.6 3.4 3.2 3.0 2.8 2.6 2.4 2.2 2.0 1.8 1.6 1.4 1.2 1.0 0.8 0.6 0.4 0.2 0.0
δ (ppm)

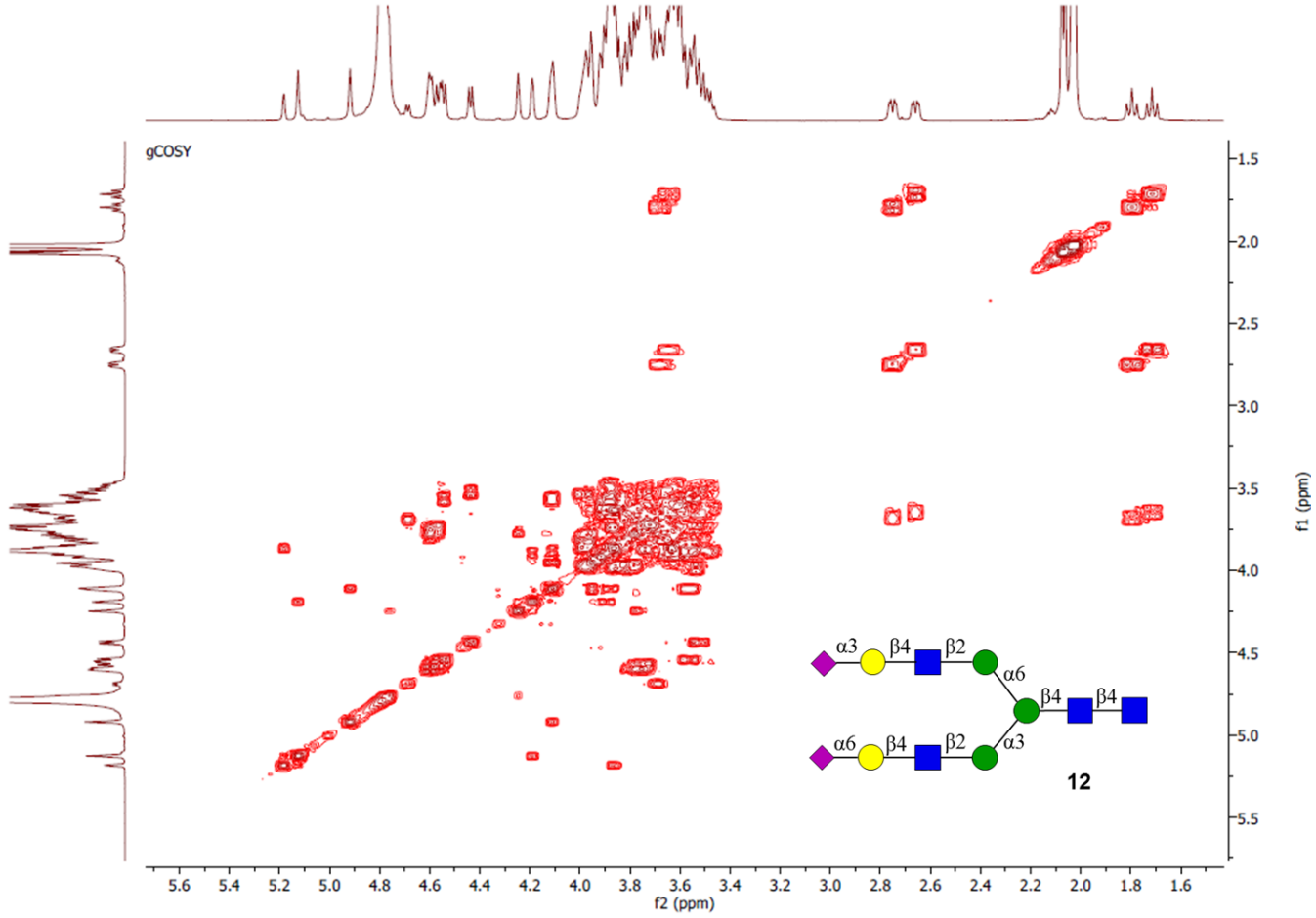
gCOSY
α3
β4
β2
α6
β4
β4
α6
β4
β2
α3
12
5.6 5.4 5.2 5.0 4.8 4.6 4.4 4.2 4.0 3.8 3.6 3.4 3.2 3.0 2.8 2.6 2.4 2.2 2.0 1.8 1.6
f2 (ppm)
1.5 2.0 2.5 3.0 3.5 4.0 4.5 5.0 5.5
f1 (ppm)

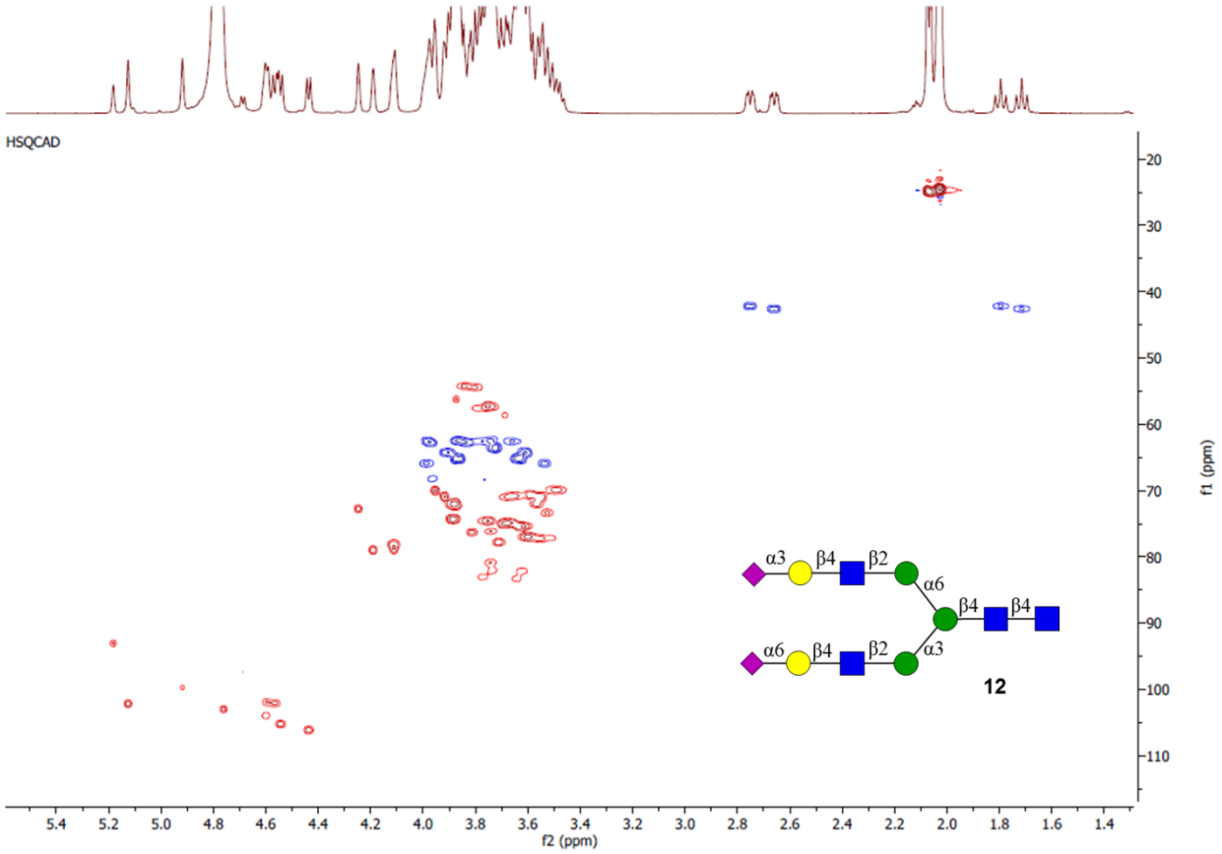

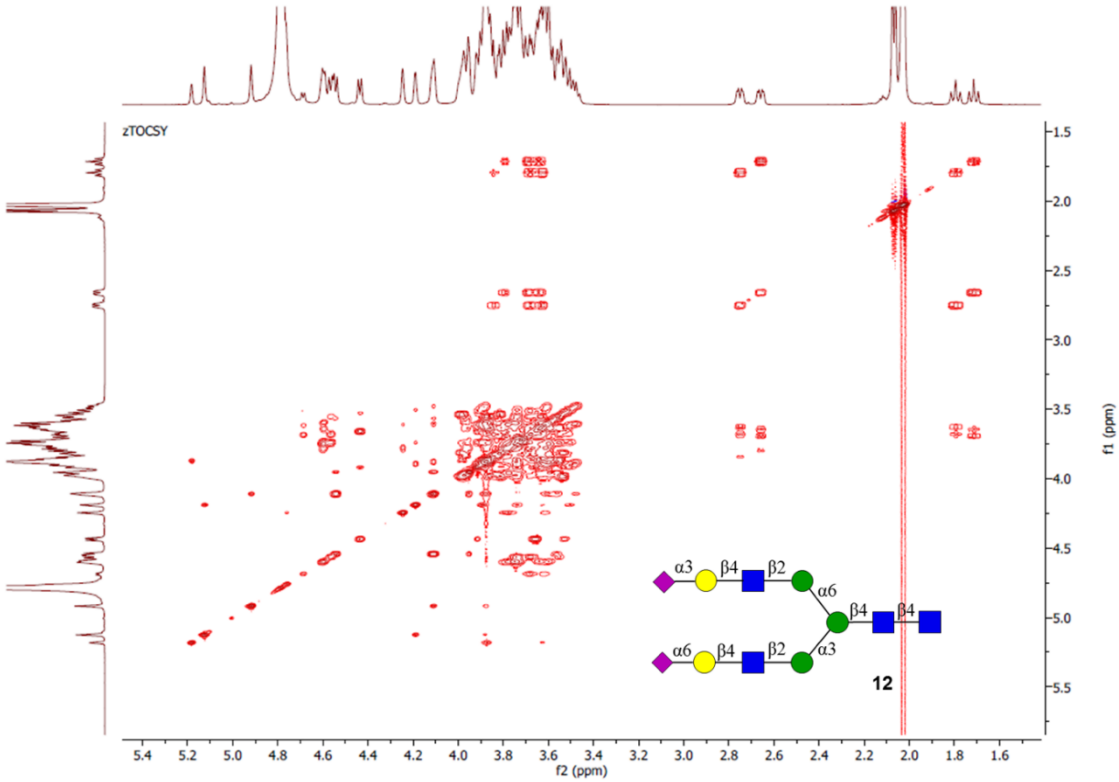

NMR spectra compound 12

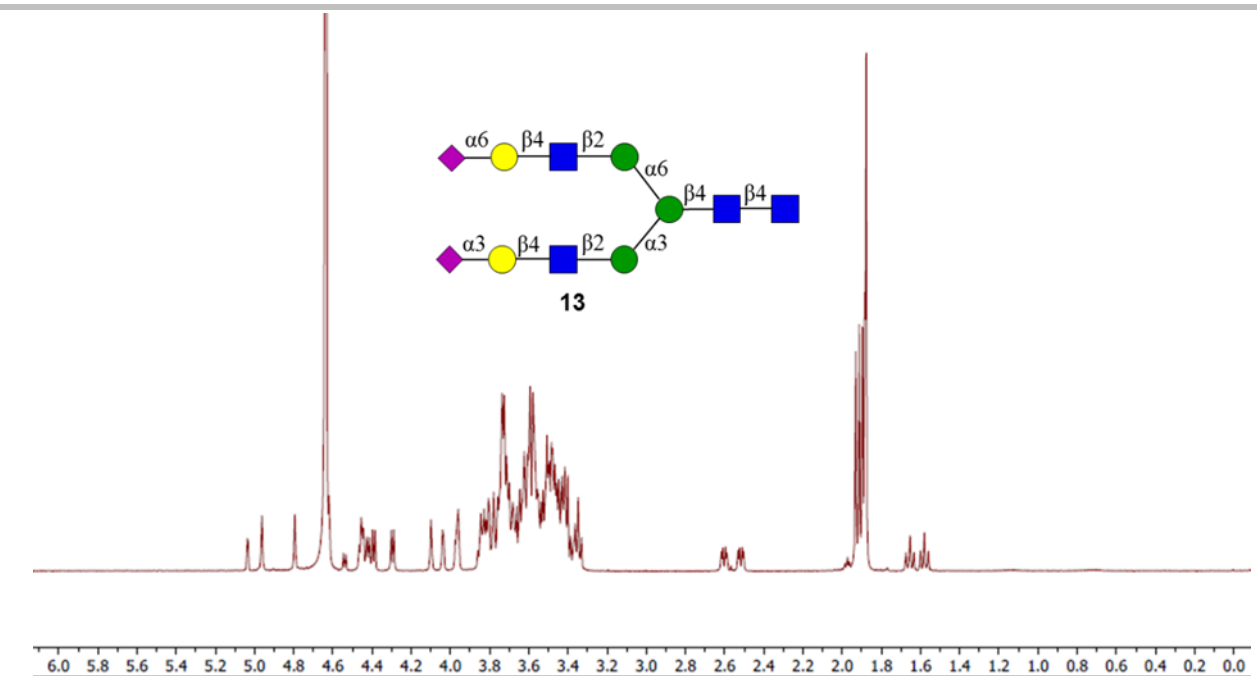
α6
β4
β2
α6
β4
β4
α3
β4
β2
α3
13
6.0 5.8 5.6 5.4 5.2 5.0 4.8 4.6 4.4 4.2 4.0 3.8 3.6 3.4 3.2 3.0 2.8 2.6 2.4 2.2 2.0 1.8 1.6 1.4 1.2 1.0 0.8 0.6 0.4 0.2 0.0
δ (ppm)

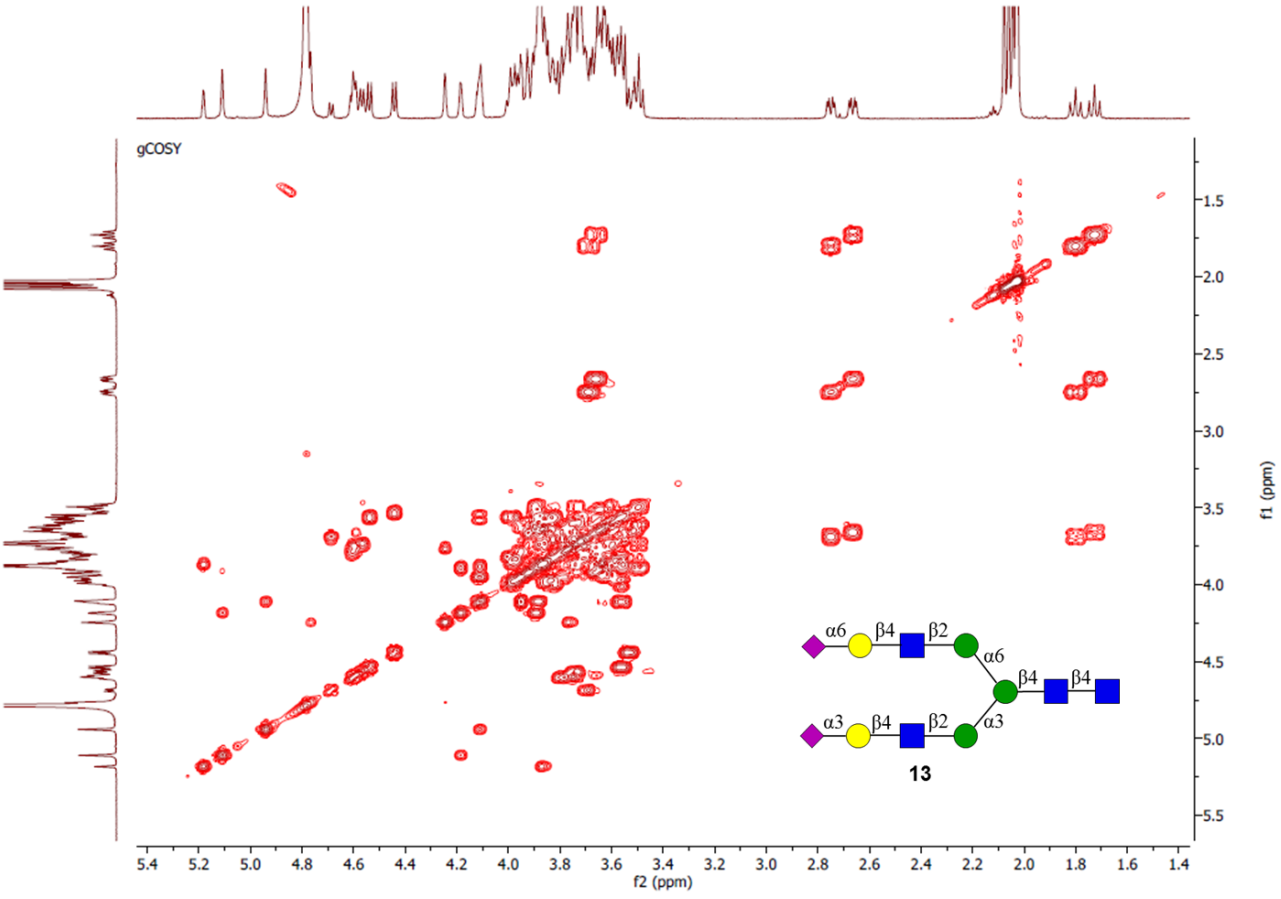
gCOSY
α6
β4
β2
α6
β4
β4
α3
β4
β2
α3
13
5.4 5.2 5.0 4.8 4.6 4.4 4.2 4.0 3.8 3.6 3.4 3.2 3.0 2.8 2.6 2.4 2.2 2.0 1.8 1.6 1.4
f2 (ppm)
1.5 2.0 2.5 3.0 3.5 4.0 4.5 5.0 5.5
f1 (ppm)

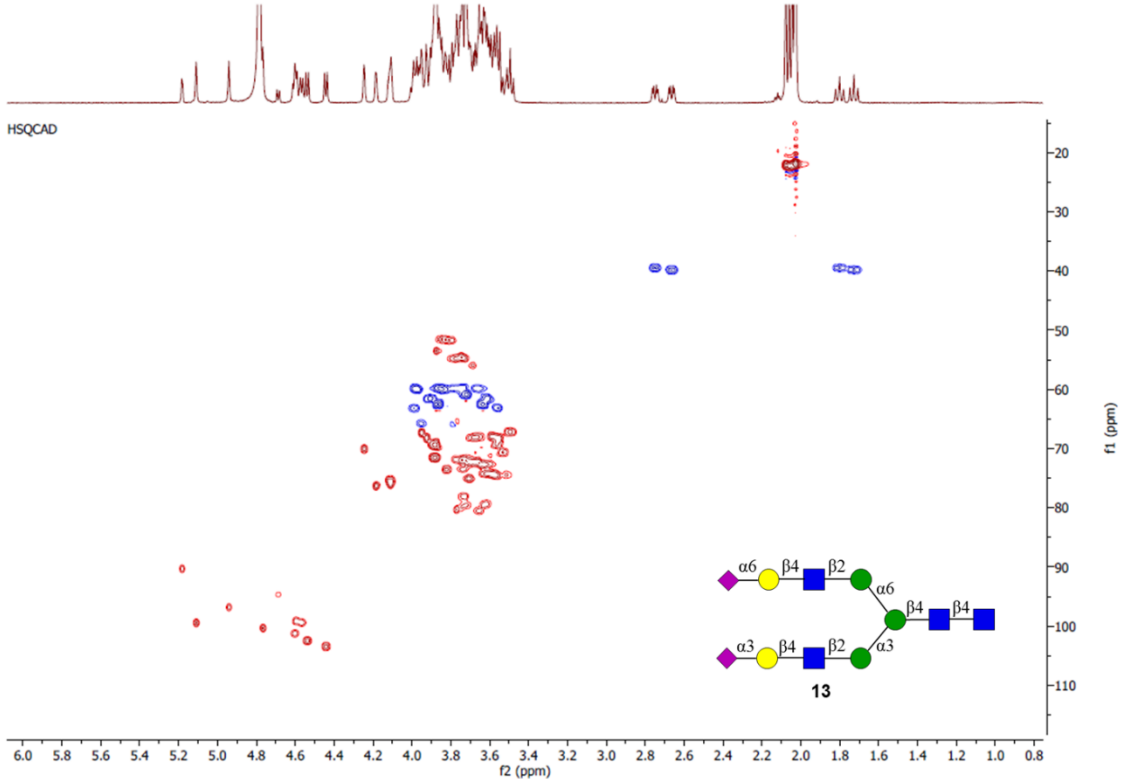

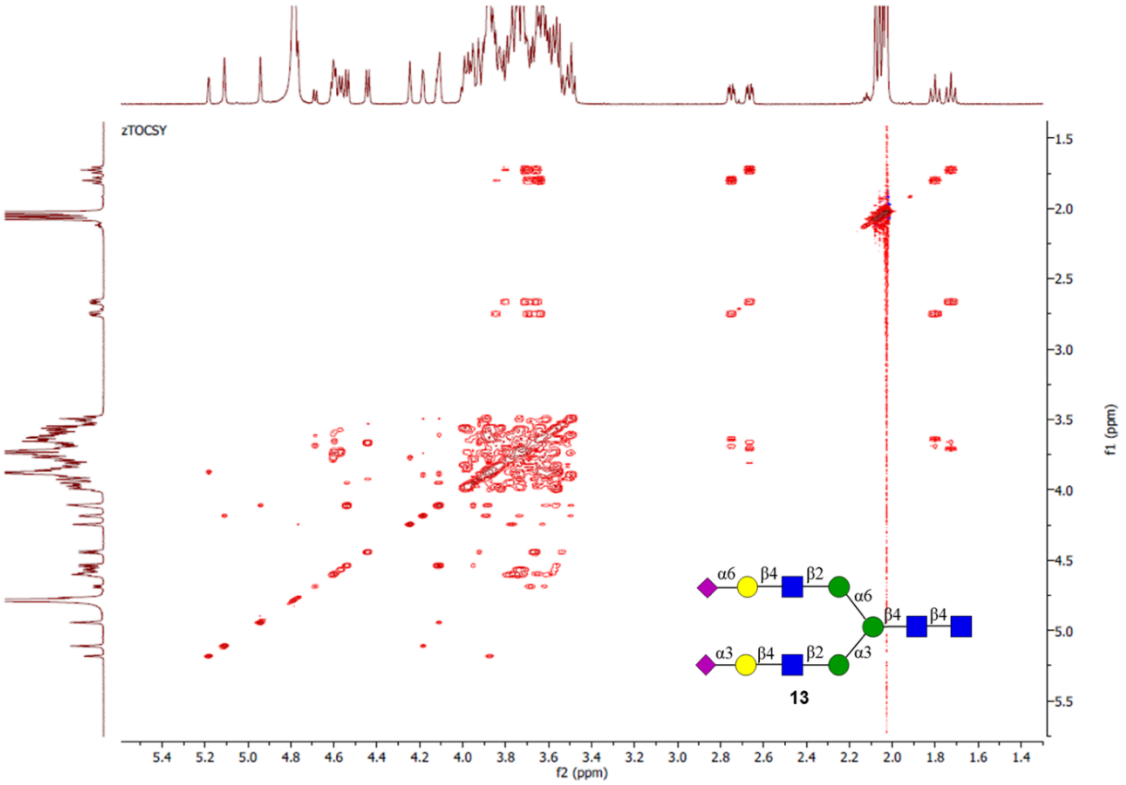

NMR spectra compound 13

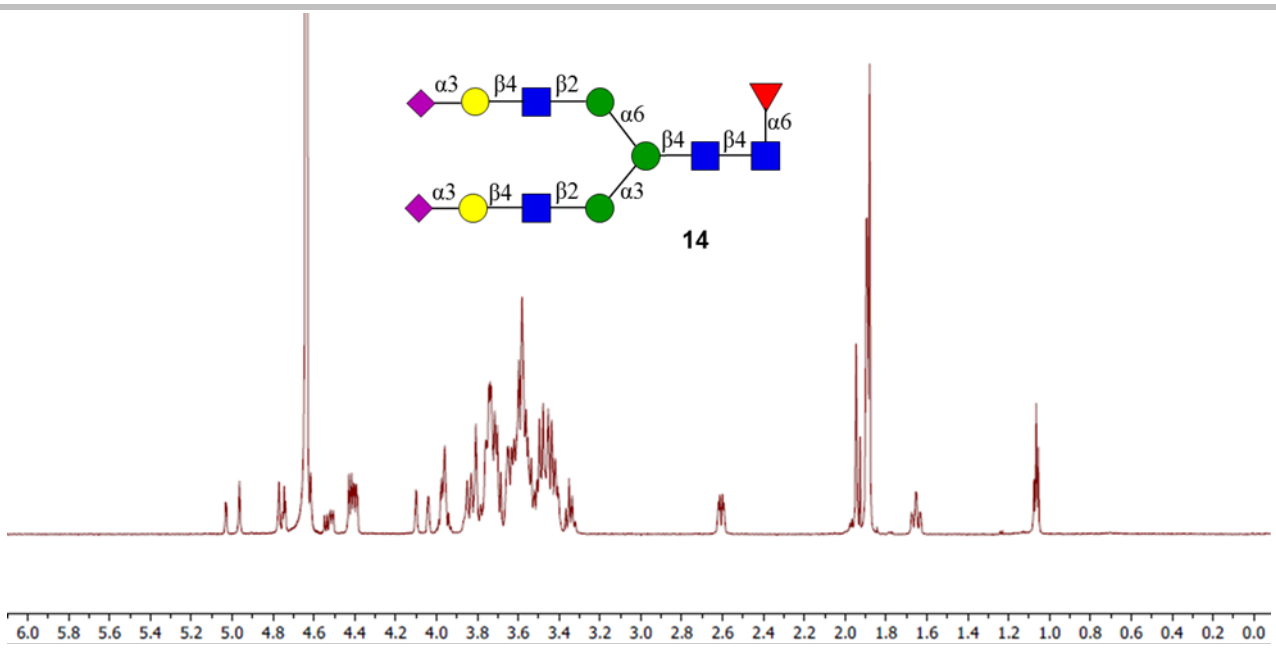
α3 β4 β2 α6 β4 β4 α6
α3 β4 β2 α3
14
6.0 5.8 5.6 5.4 5.2 5.0 4.8 4.6 4.4 4.2 4.0 3.8 3.6 3.4 3.2 3.0 2.8 2.6 2.4 2.2 2.0 1.8 1.6 1.4 1.2 1.0 0.8 0.6 0.4 0.2 0.0
δ (ppm)

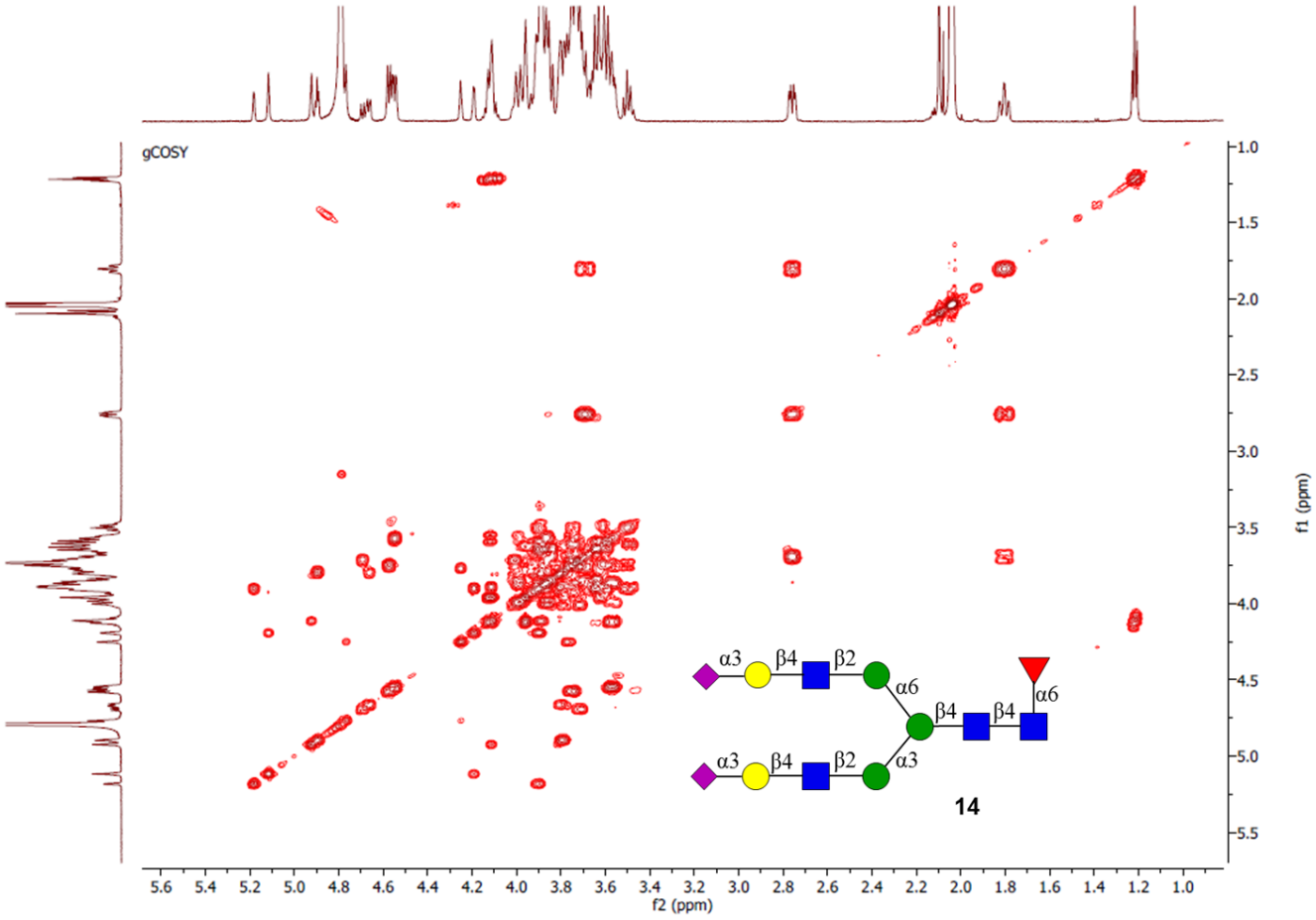
gCOSY
α3 β4 β2 α6 β4 β4 α6
α3 β4 β2 α3
14
5.6 5.4 5.2 5.0 4.8 4.6 4.4 4.2 4.0 3.8 3.6 3.4 3.2 3.0 2.8 2.6 2.4 2.2 2.0 1.8 1.6 1.4 1.2 1.0
f2 (ppm)
1.0 1.5 2.0 2.5 3.0 3.5 4.0 4.5 5.0 5.5
f1 (ppm)

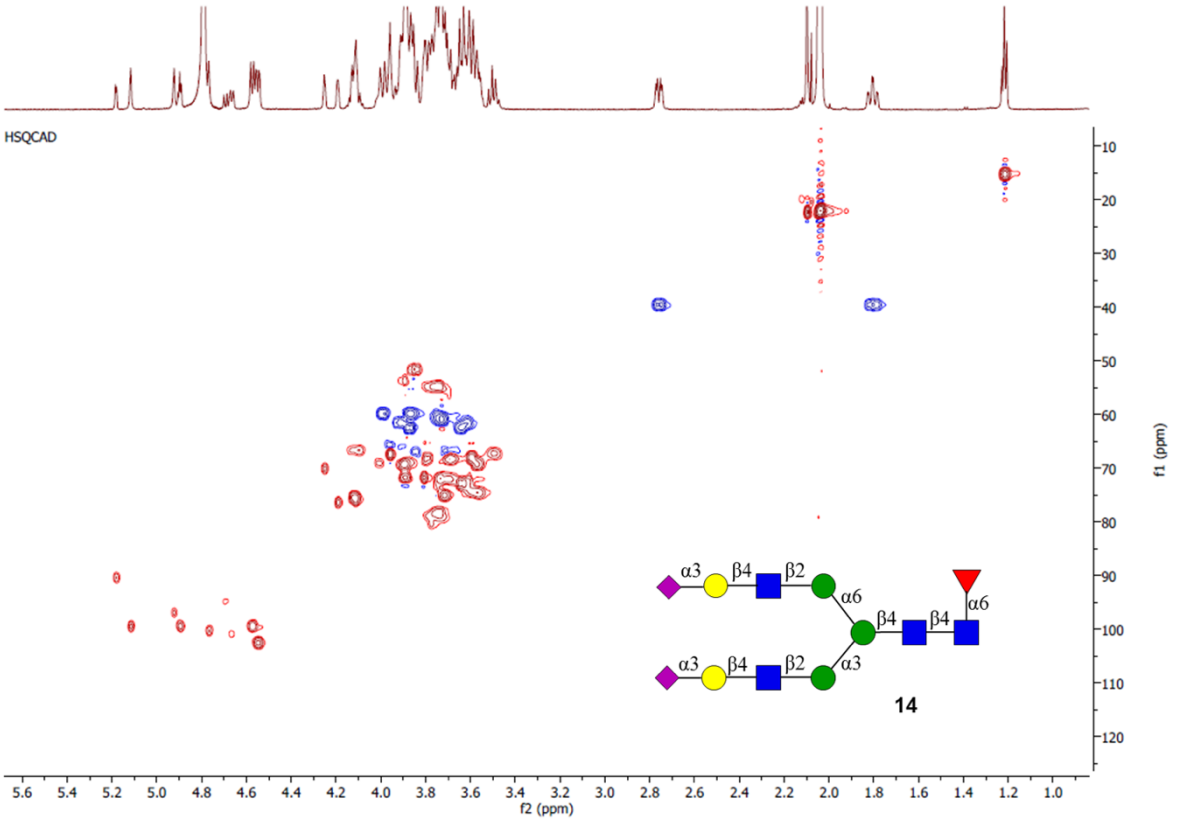

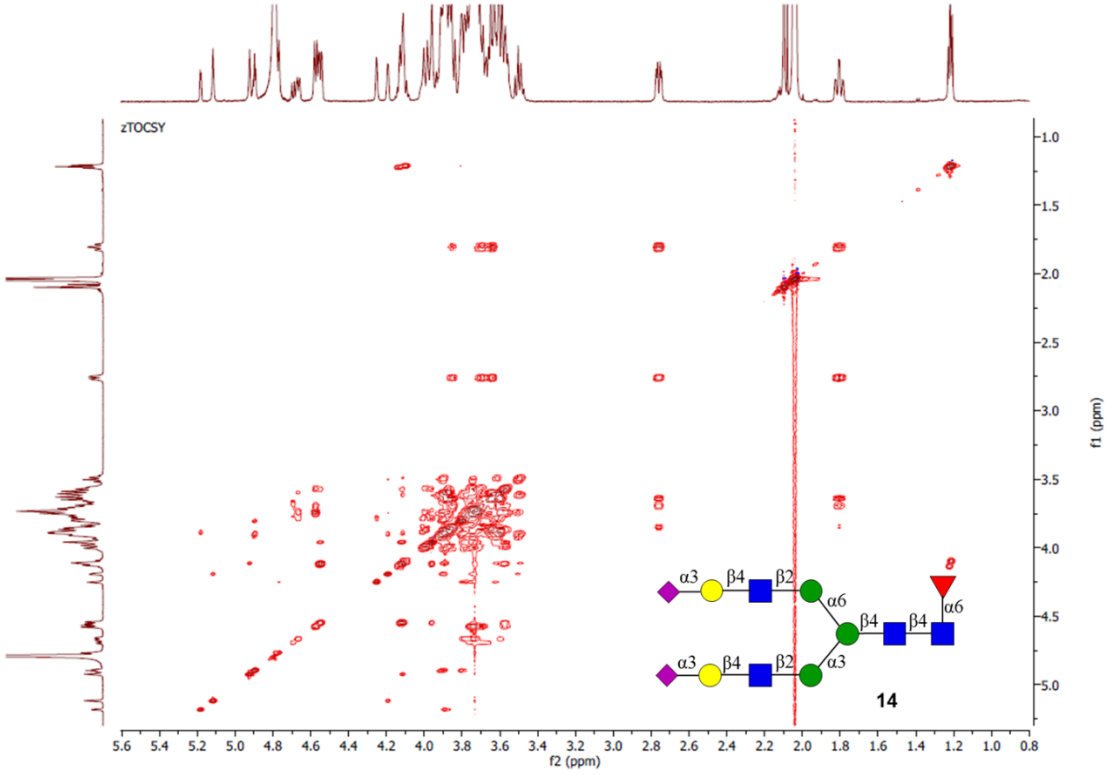

NMR spectra compound 14

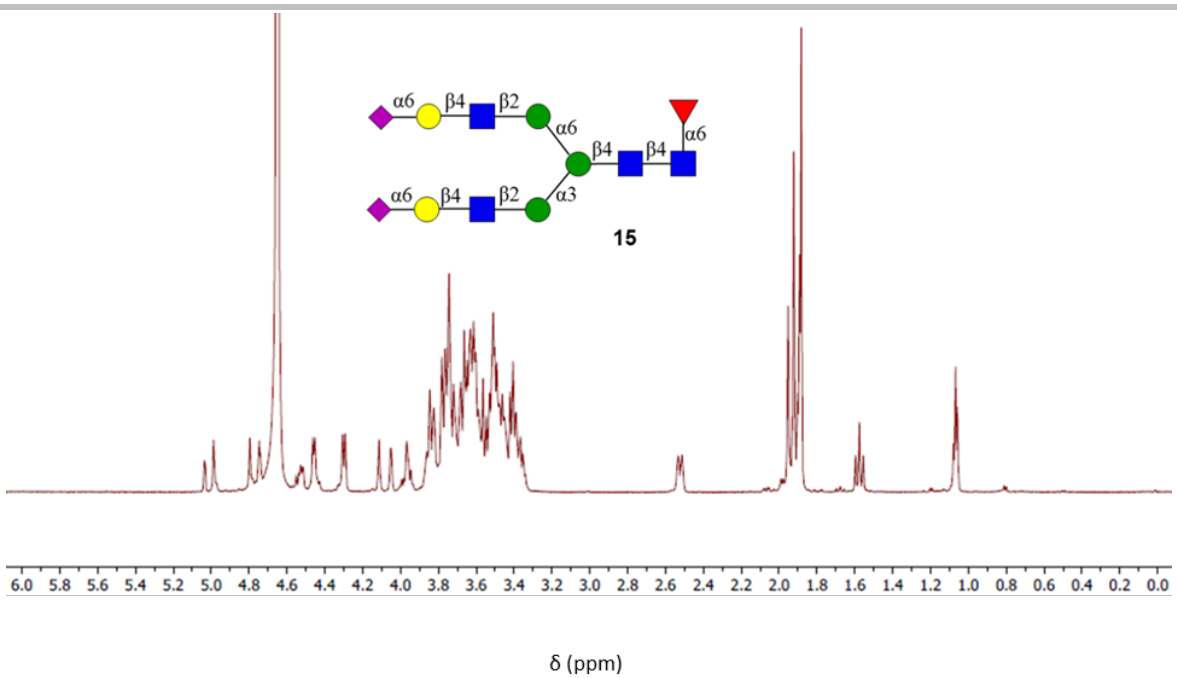
α6 β4 β2 α6 β4 β4 α6
α6 β4 β2 α3
15
6.0 5.8 5.6 5.4 5.2 5.0 4.8 4.6 4.4 4.2 4.0 3.8 3.6 3.4 3.2 3.0 2.8 2.6 2.4 2.2 2.0 1.8 1.6 1.4 1.2 1.0 0.8 0.6 0.4 0.2 0.0
δ (ppm)

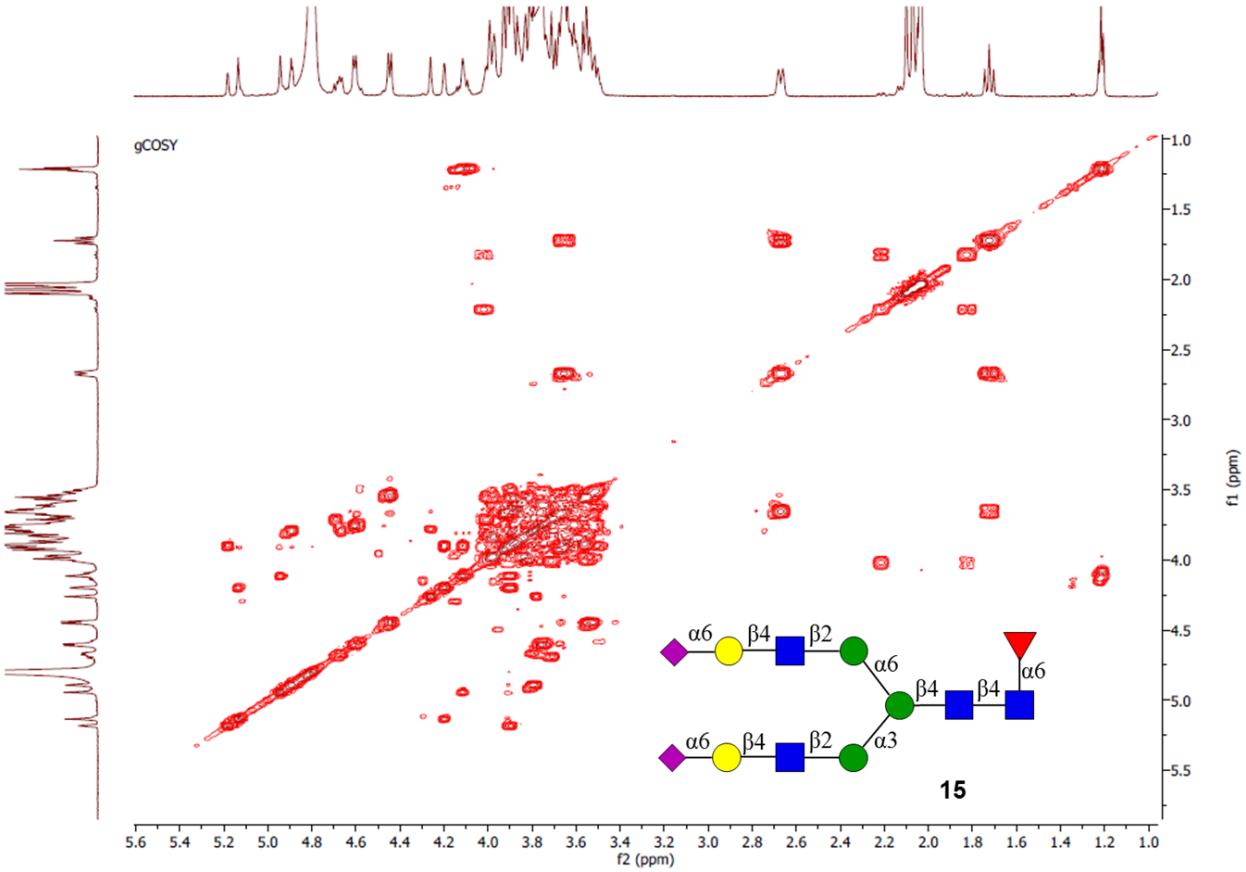
gCOSY
α6 β4 β2 α6 β4 β4 α6
α6 β4 β2 α3
15
5.6 5.4 5.2 5.0 4.8 4.6 4.4 4.2 4.0 3.8 3.6 3.4 3.2 3.0 2.8 2.6 2.4 2.2 2.0 1.8 1.6 1.4 1.2 1.0
f2 (ppm)
1.0 1.5 2.0 2.5 3.0 3.5 4.0 4.5 5.0 5.5
f1 (ppm)

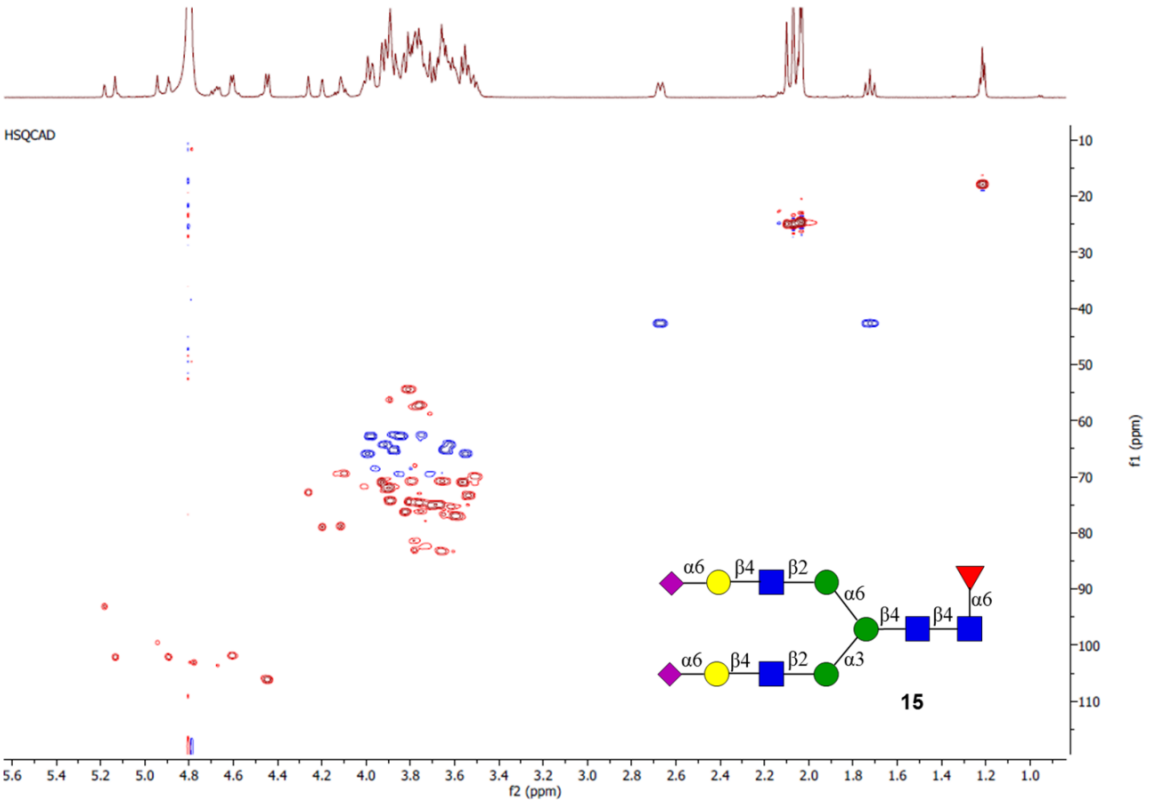

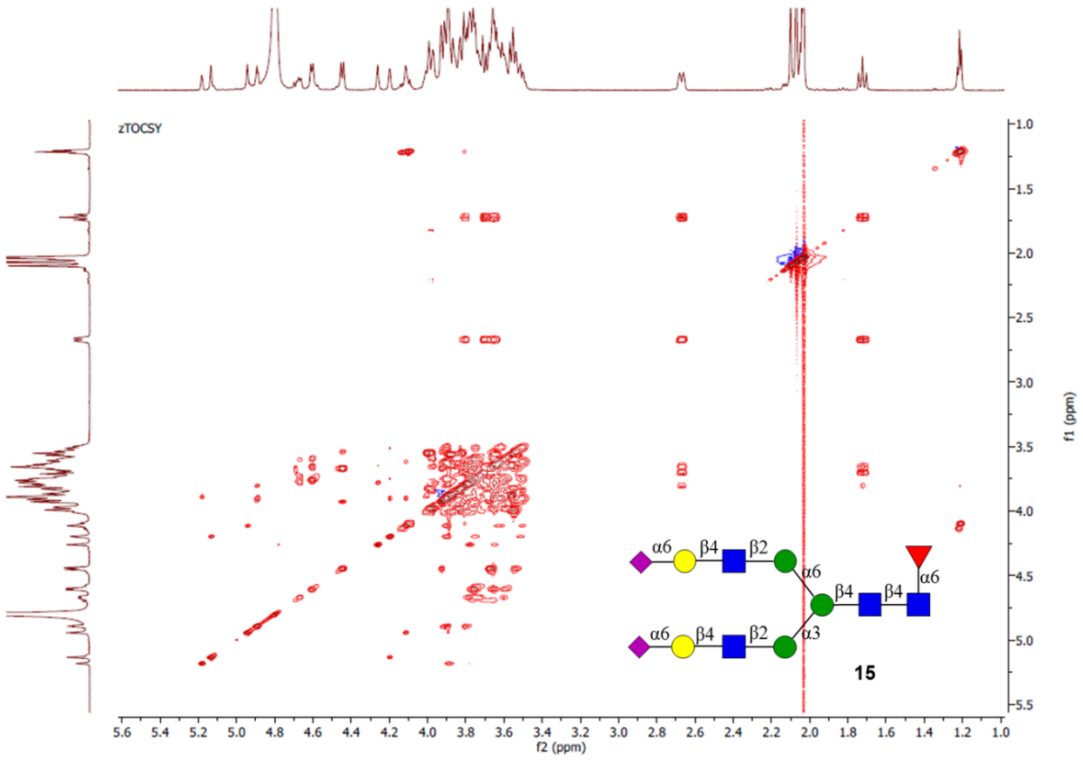

NMR spectra compound 15

1.4 N-glycan release, 2-AA labelling and purification

Bovine fetuin (100 µg) was dissolved in 75 µL of water with 12.5 µL of denaturing buffer and heated at 100 °C for 10 minutes. After cooling to room temperature, 12.5 µL of glycobuffer, 12.5 µL of NP-40 solution and 2.5 U of PNGase F were added and the mixture was incubated at 37 °C overnight. After incubation, the sample was first cleaned using a C_{18} solid phase extraction (SPE) cartridge, eluting the glycans with 1mL of 5% ACN:95% water with 0.05% TFA (% v/v) and then evaporated under a stream of nitrogen. The residue was dissolved in water and N-glycans were extracted by PGC SPE by first washing retained analytes with 1 mL of 0.05% TFA in water, then with 1 mL ACN:water 5:95 (%v/v) containing 0.05% TFA (%v/v) and finally eluting with 1 mL of ACN/H_2O 1:1 (v/v) containing 0.1% TFA. The sample was then evaporated under a stream of nitrogen and labelled by adding 10 µL of water and 10 µL of the labelling mixture containing 48 mg/mL 2-AA and 63 mg/mL of sodium cyanoborohydride in 10:3 (v/v) DMSO/acetic acid and incubation at 65 °C for 2 hours. This labelling procedure was also applied for pure standards. Labelled N-glycans were purified by Minitrap G-10 size exclusion SPE. Labelled sample was diluted to 100 µL with water and loaded onto an equilibrated column, washed with 700 µL of water and then eluted with 600 µL of water. Collected samples were evaporated under a stream of nitrogen and reconstituted in 30:70 water/ACN (%v/v) before analysis.

1.5 HILIC-IMS-QTOF analysis of glycans

N-glycan standards, both 2-AA labelled and unlabeled, were analyzed by direct infusion into an IMS-QTOF as well as by HILIC-QIMS-QTOF, and CCS values and ATDs were obtained. The instrument featured an Agilent 1260 Infinity LC system coupled to a 6560 IM-QTOF mass spectrometer through a jet stream electrospray ionization interface (Agilent Technologies, Santa Clara, CA). A ZIC-HILIC column (3µm, 100Å, 150 mm x 2.1 mm) with a guard column of 20 mm x 2.1 mm (Merck, Darmstadt, Germany), maintained at a temperature of 60 ºC, was used for the LC separation. Gradient elution was applied using 50 mM ammonium formate, adjusted to pH 4.4 with formic acid, (eluent A) and 100% ACN (eluent B). The starting composition was 30 % A, increasing linearly to 50 % A in 20 minutes at a flow rate of 0.2 mL/min. Direct infusion experiments with standards were performed without a column with the starting eluent composition.

IMS separation was performed in the drift tube operated at an entrance voltage of -1700 V and exiting voltage of -250 V, using nitrogen as a drift gas. For stepped field CCS calculation, the drift tube entrance voltages were varied in the 1074-1674 V range with 100 V increment between steps. Trap funnel pressure was maintained at 5.07 mbar and the drift tube pressure at 5.27 mbar. The maximum drift time was set at 60 ms, with a trapping time of 20000 µs and a release time of 150 µs. Trapping funnel RF and rear funnel RF were set at 150 V. The MS settings were: a drying gas temperature of 300 °C at a flow rate of 8 L/min, a nebulizer pressure of 2.8 bar, a sheath gas flow of 11 L/min at a temperature of 350 °C and a capillary voltage of 3500 V.

1.6 Data treatment

Mass calibration was performed with the IMS-MS reprocessor software of Agilent Technologies. Bovine fetuin data files were chromatographically smoothed (3 points) with the PNNL preprocessor. After smoothing, CCS single field and multi-field calibration were performed with Mass Hunter IM-MS software. In order to check for glycan structures, the feature finding option of the IM-MS browser was used, setting the glycans mode as isotope model, limiting charge states to 5 and ion intensities to ≥50. In this way, CCS values of glycans were automatically calculated by the software. Glycan masses that were found were assigned to possible compositions with the online GlycoMod software.

2. Results and Discussion

2.1 Arrival time distributions of standards as $[M-H]^-$ and $[M-2H]^{2-}$ ions

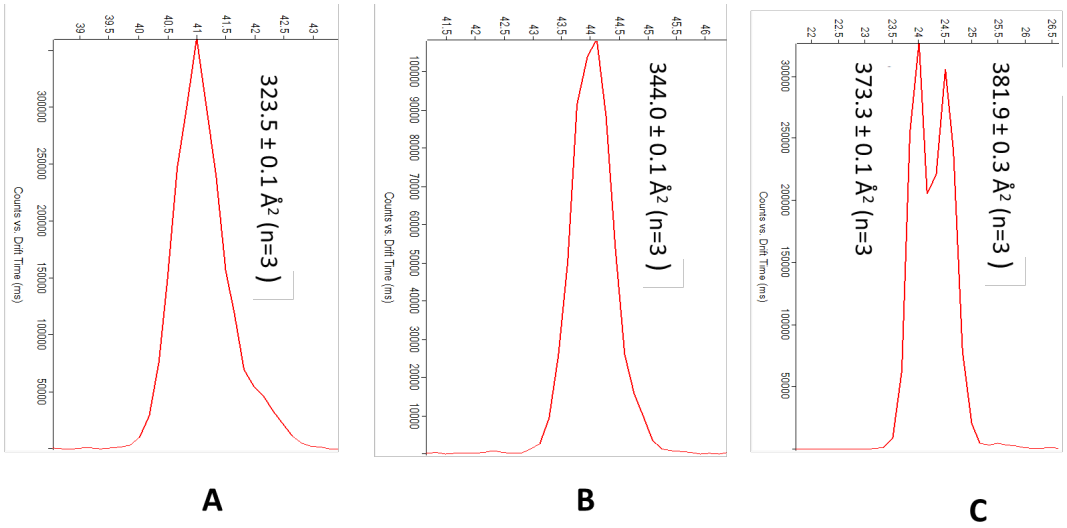

Fig. S1: ATDs and CCSs of standard **1** as unlabeled $[M-H]^-$ ions (A), 2-AA labeled $[M-1H]^-$ ions (B) and 2-AA labeled $[M-2H]^{2-}$ ions (C).

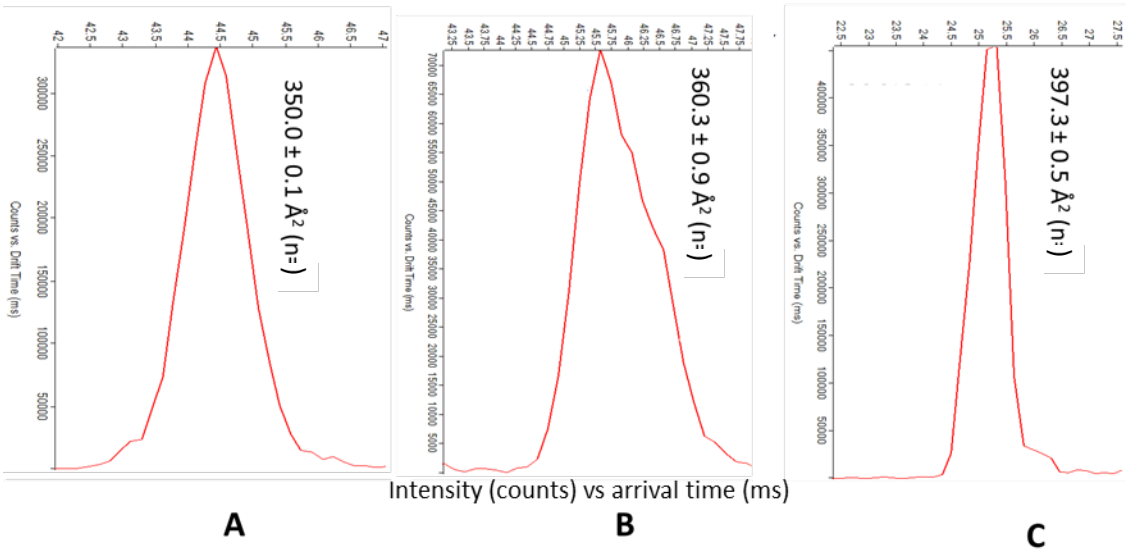

Fig. S2: ATDs and CCSs of standard **2** as unlabeled $[M-H]^-$ ions (A), 2-AA labeled $[M-1H]^-$ ions (B) and 2-AA labeled $[M-2H]^{2-}$ ions (C).

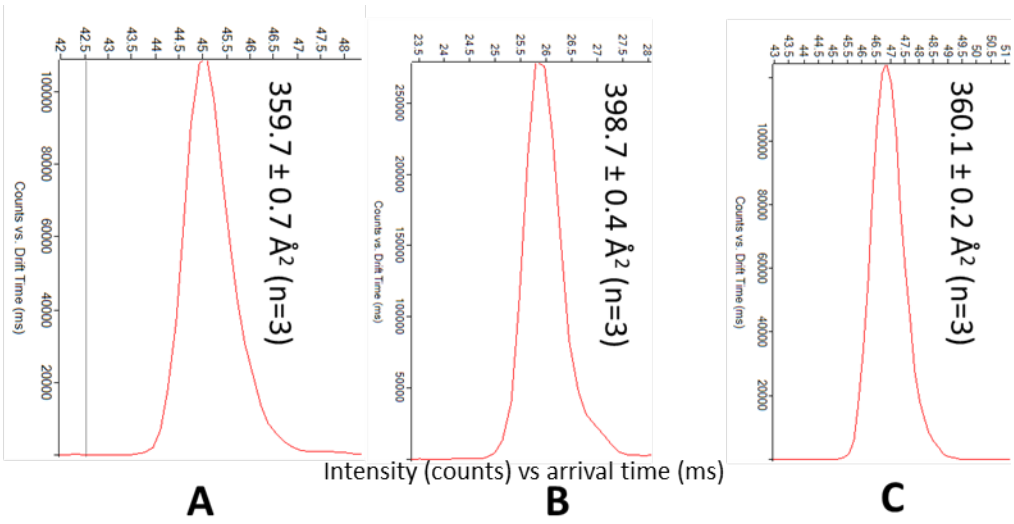

Fig. S3: ATDs and CCSs of standard **3** as unlabeled $[M-H]^-$ ions (A), 2-AA labeled $[M-1H]^-$ ions (B) and 2-AA labeled $[M-2H]^{2-}$ ions (C).

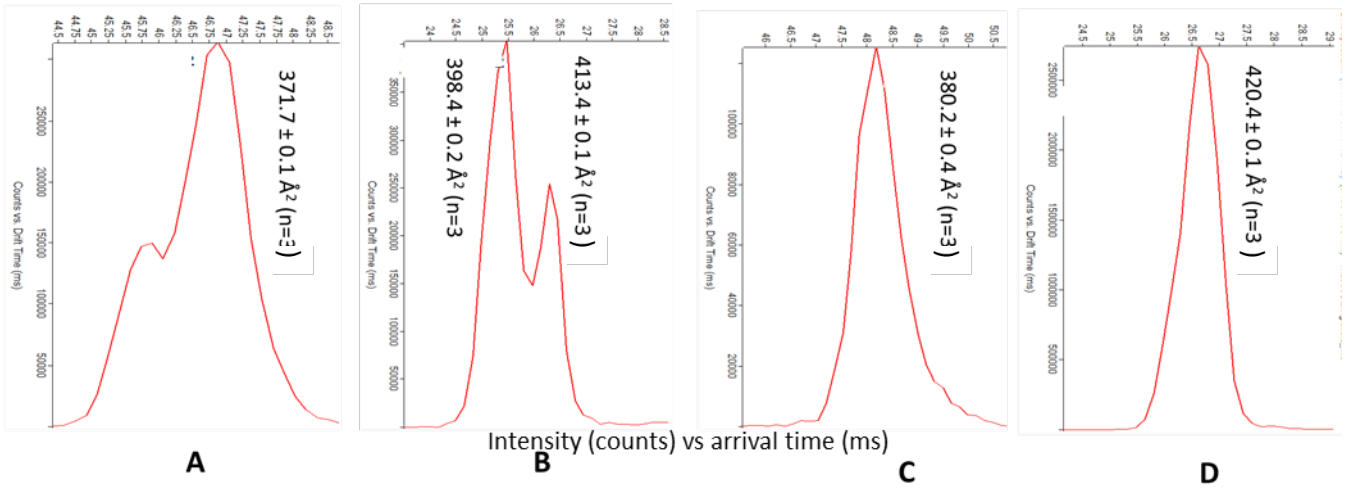

Fig. S4: ATDs and CCSs of standard **4** as unlabeled $[M-H]^-$ ions (A), unlabeled $[M-2H]^{2-}$ ions (B), 2-AA labeled $[M-1H]^-$ ions (C) and 2-AA labeled $[M-2H]^{2-}$ ions (D).

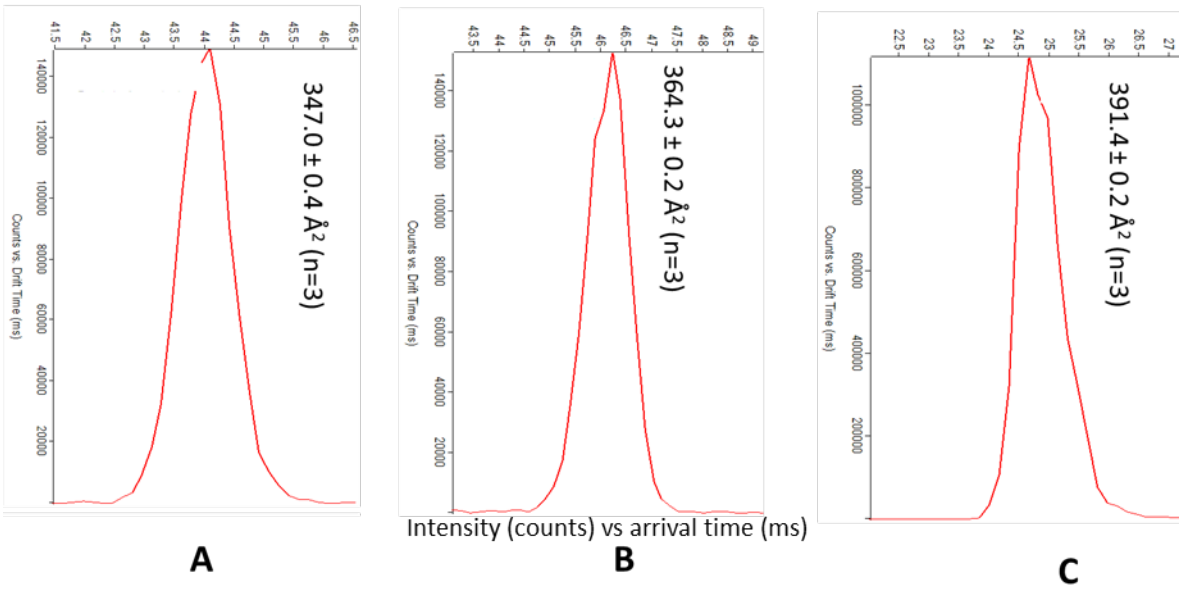

Fig. S5: ATDs and CCSs of standard **5** as unlabeled $[M-H]^-$ ions (A), 2-AA labeled $[M-H]^-$ ions (B) and 2-AA labeled $[M-2H]^{2-}$ ions (C).

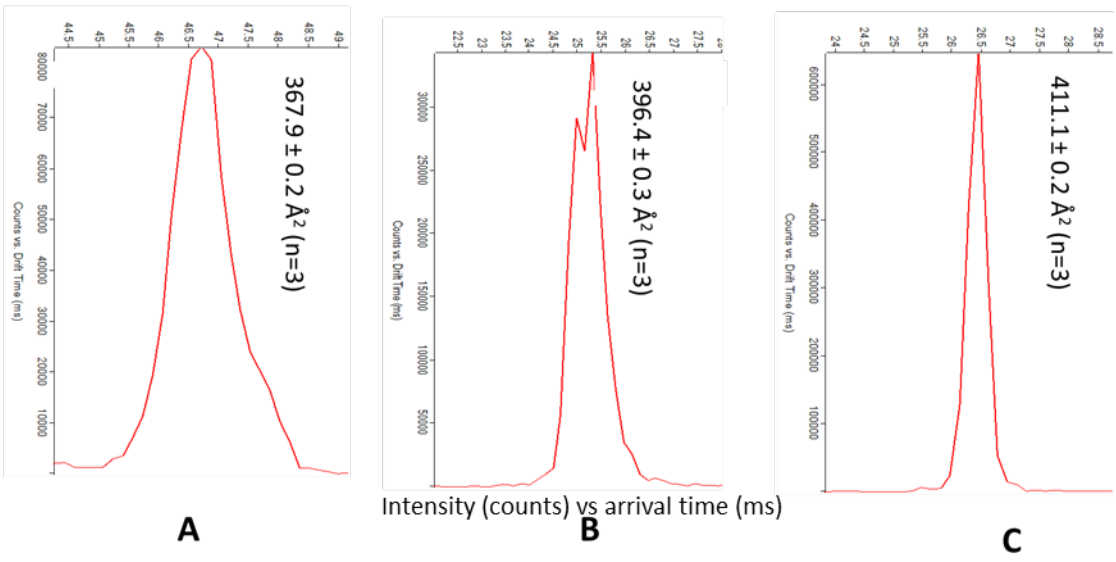

Fig. S6: ATDs and CCSs of standard **6** as unlabeled $[M-H]^-$ ions (A), 2-AA labeled $[M-1H]^-$ ions (B) and 2-AA labeled $[M-2H]^{2-}$ ions (C).

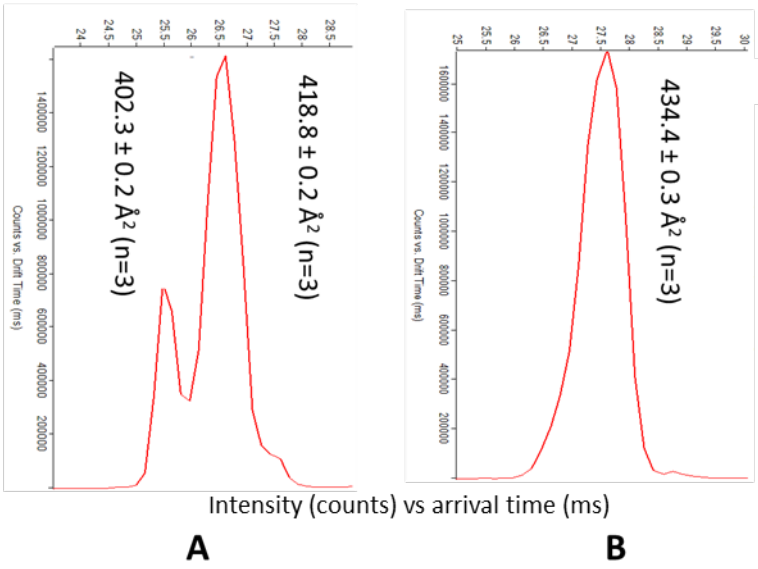

Fig. S7: ATDs and CCSs of standard **7** as unlabeled $[M-2H]2^-$ ions (A) and 2-AA labeled $[M-2H]2^-$ ions (B).

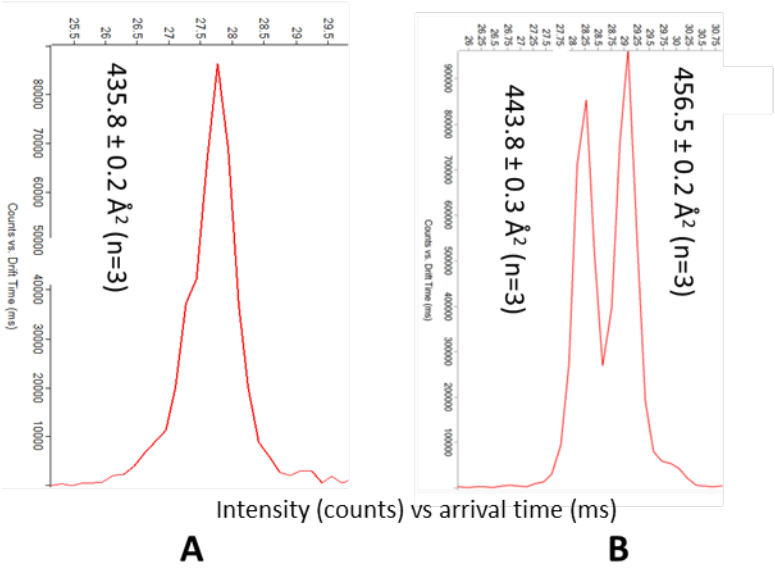

Fig. S8: ATDs and CCSs of standard **8** as unlabeled $[M-2H]2^-$ ions (A) and 2-AA labeled $[M-2H]2^-$ ions (B).

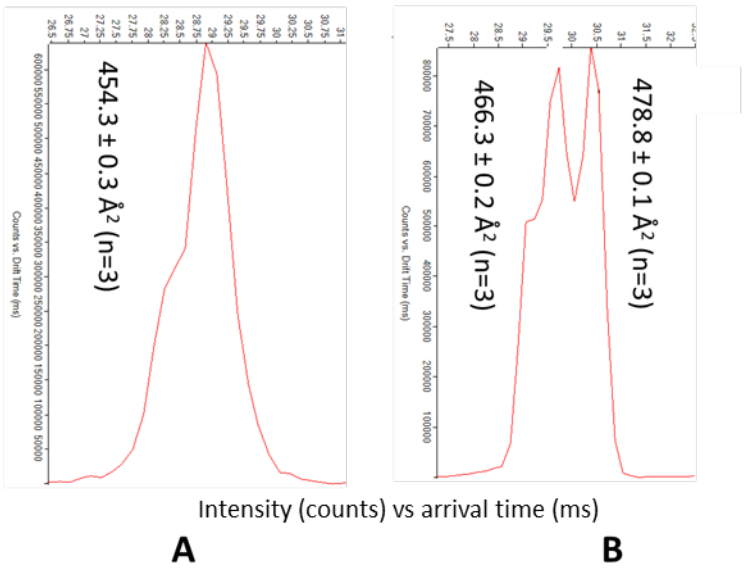

Fig. S9: ATDs and CCSs of standard **9** as unlabeled $[M-2H]2^-$ ions (A) and 2-AA labeled $[M-2H]2^-$ ions (B).

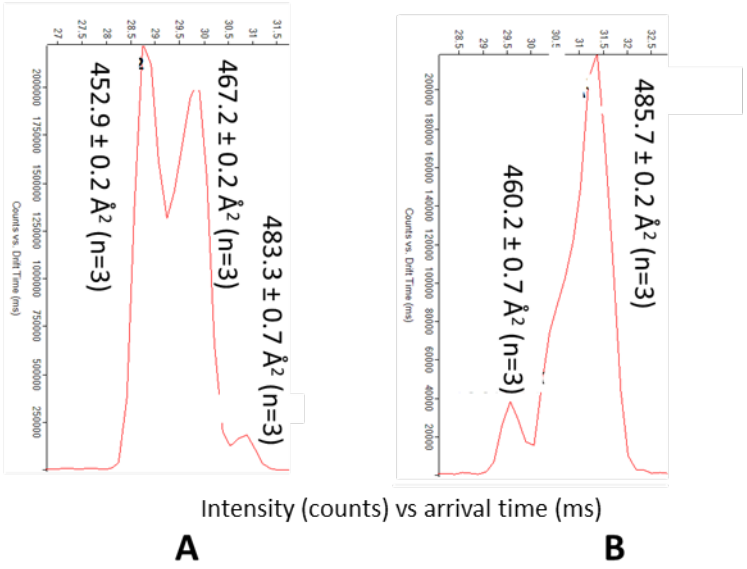

Fig. S10: ATDs and CCSs of standard **10** as unlabeled $[M-2H]2^-$ ions (A) and 2-AA labeled $[M-2H]2^-$ ions (B).

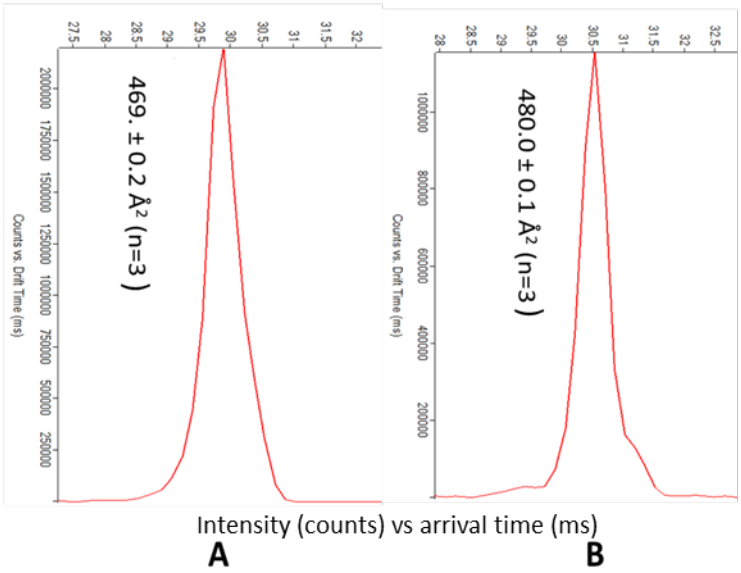

Fig. S11: ATDs and CCSs of standard **11** as unlabeled [M-2H]2^{-} ions (A) and 2-AA labeled [M-2H]2^{-} ions (B).

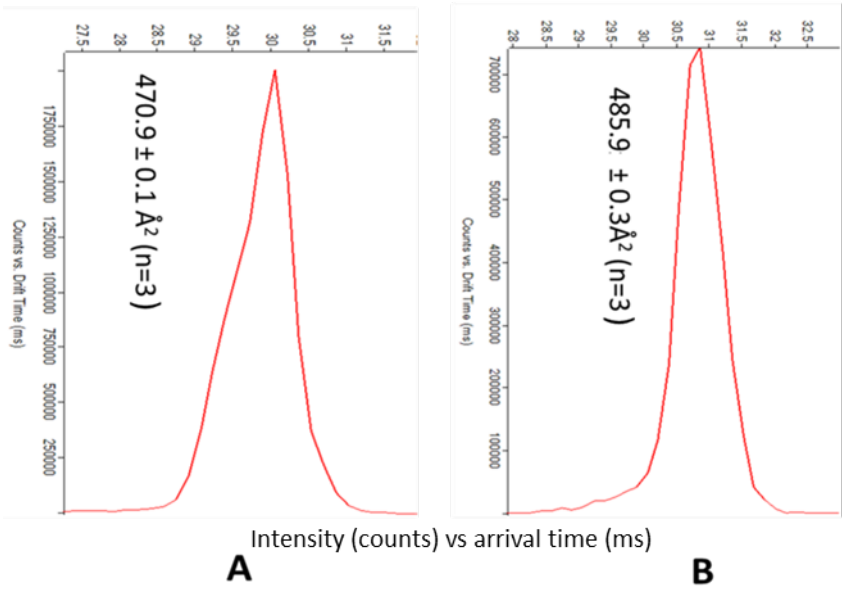

Fig. S12: ATDs and CCSs of standard **12** as unlabeled [M-2H]2^{-} ions (A) and 2-AA labeled [M-2H]2^{-} ions (B).

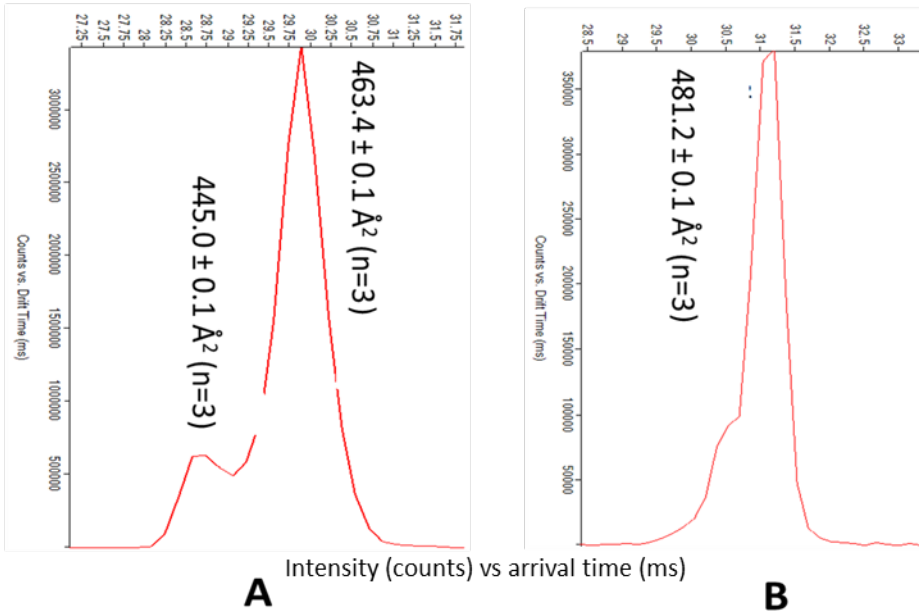

Fig. S13: ATDs and CCSs of standard **13** as unlabeled $[M-2H]2^-$ ions (A) and 2-AA labeled $[M-2H]2^-$ ions (B).

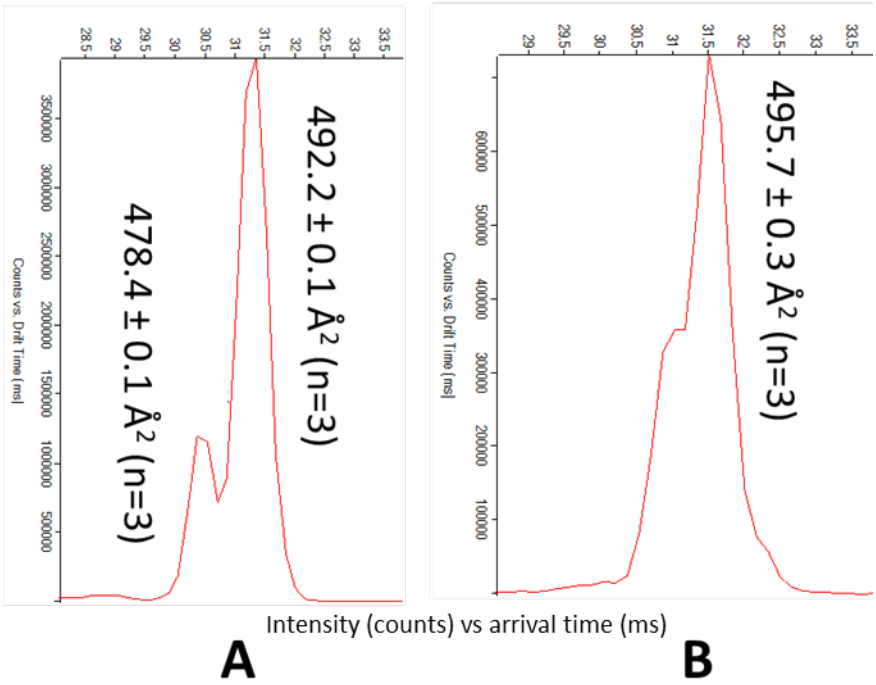

Fig. S14: ATDs and CCSs of standard **14** as unlabeled $[M-2H]2^-$ ions (A) and 2-AA labeled $[M-2H]2^-$ ions (B).

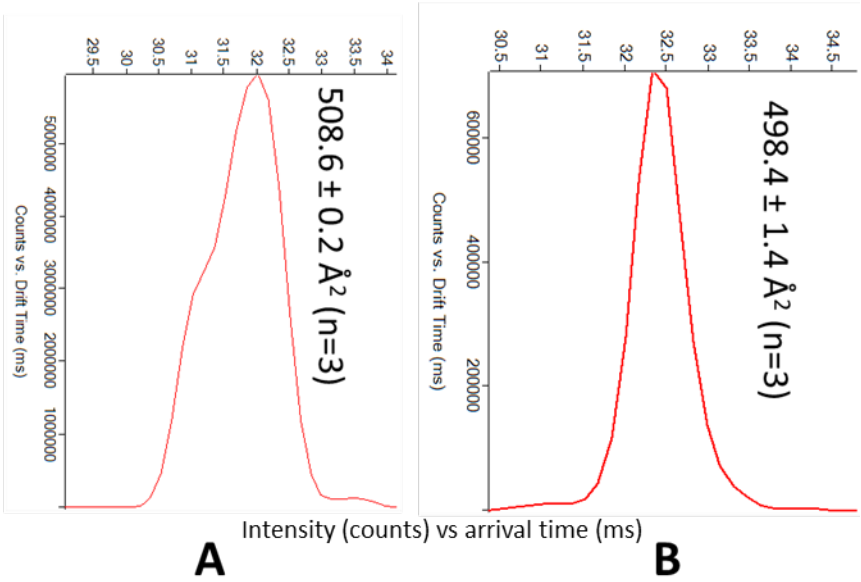

Fig. S15: ATDs and CCSs of standard **15** as unlabeled $[M-2H]2^-$ ions (A) and 2-AA labeled $[M-2H]2^-$ ions (B).

2.2 ATDs of standards obtained with different trapping RF values

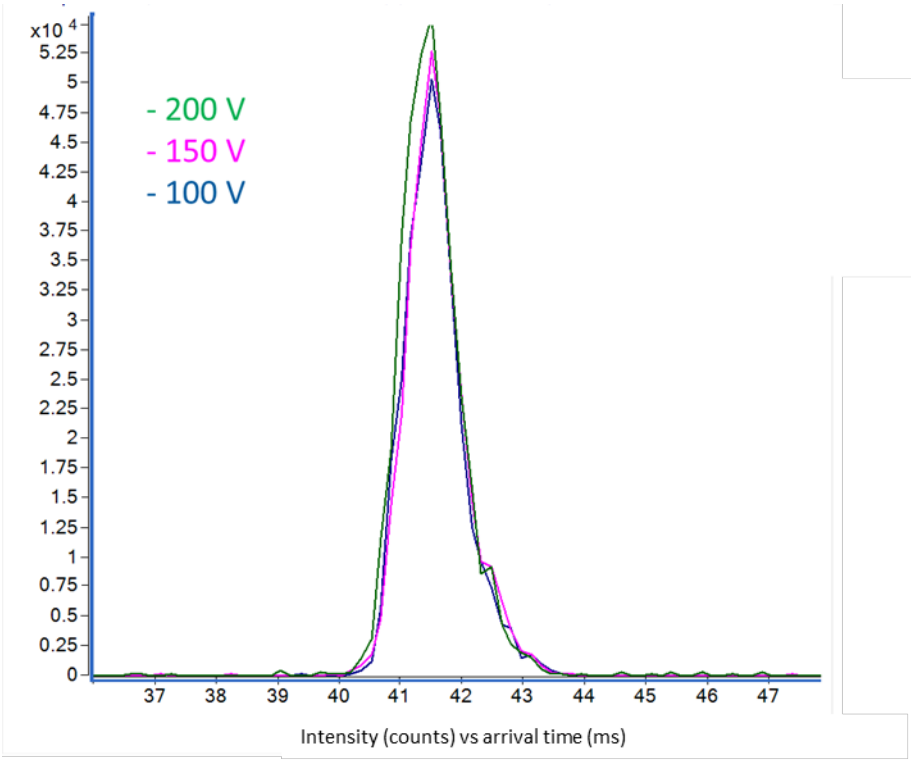

Fig. S16: overlaid ATDs of unlabeled standard **1** as $[M-H]^-$ ions, obtained at different RF voltages (100V pictured in blue, 150V in pink, and 200V in green)

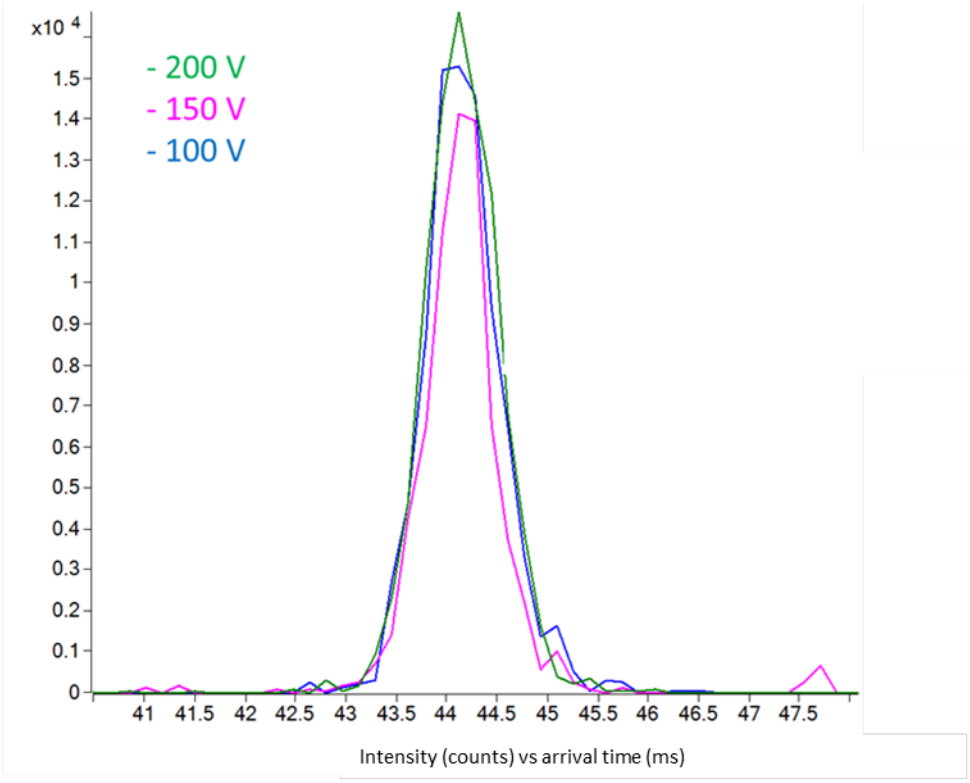

Fig. S17: overlaid IMS ATDs of 2-AA labelled standard **1 as** $[M-H]^-$ ions, obtained at different RF voltages (100V pictured in blue, 150V in pink, and 200V in green)

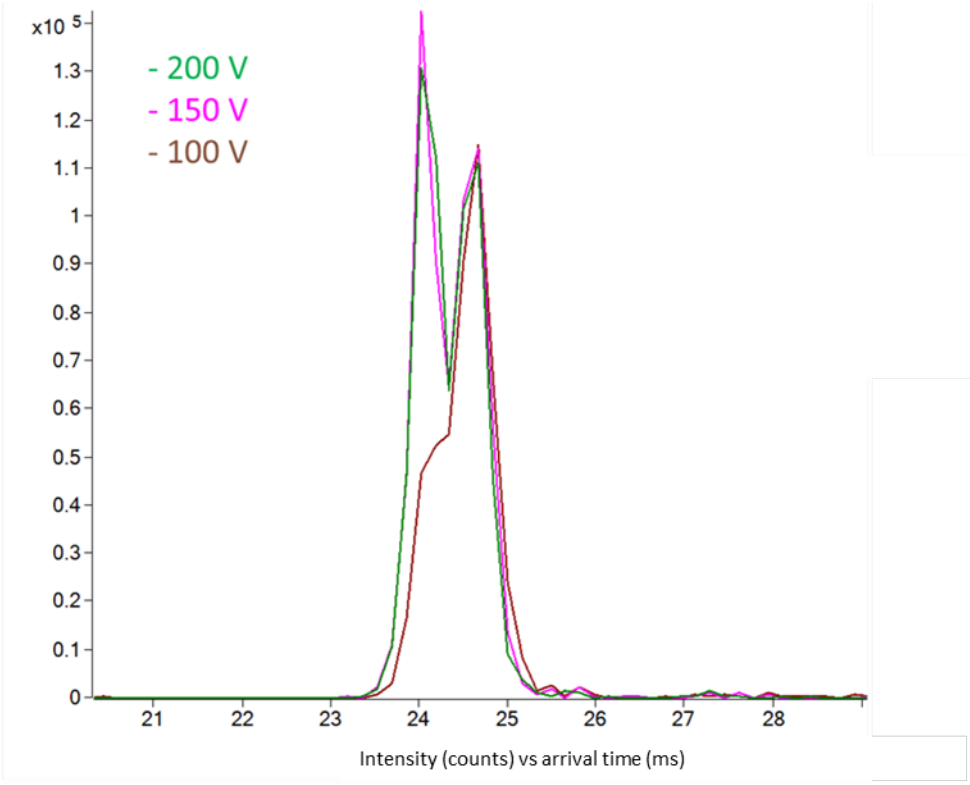

Fig. S18: overlaid IMS ATDs of 2-AA labelled standard **1** as $[M-2H]^{2-}$ ions, obtained at different RF voltages (100V pictured in brown, 150V in pink, and 200V in green)

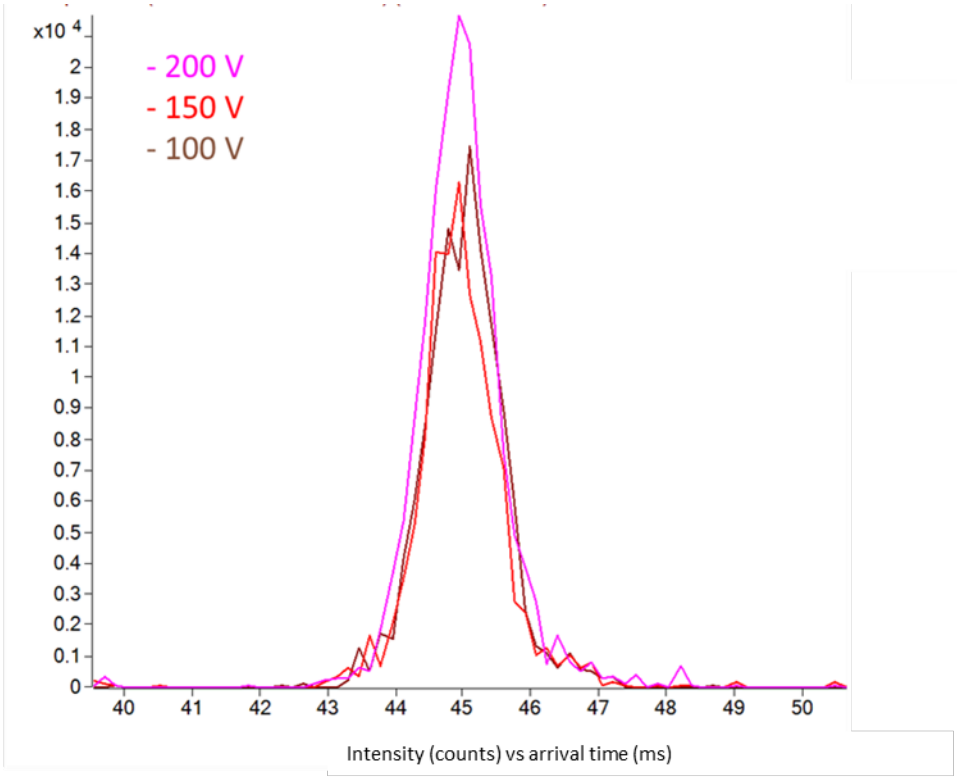

Fig. S19: overlaid IMS ATDs of unlabeled standard **2** as $[M-H]^{-}$ ions, obtained at different RF voltages (100V pictured in brown, 150V in red, and 200V in pink)

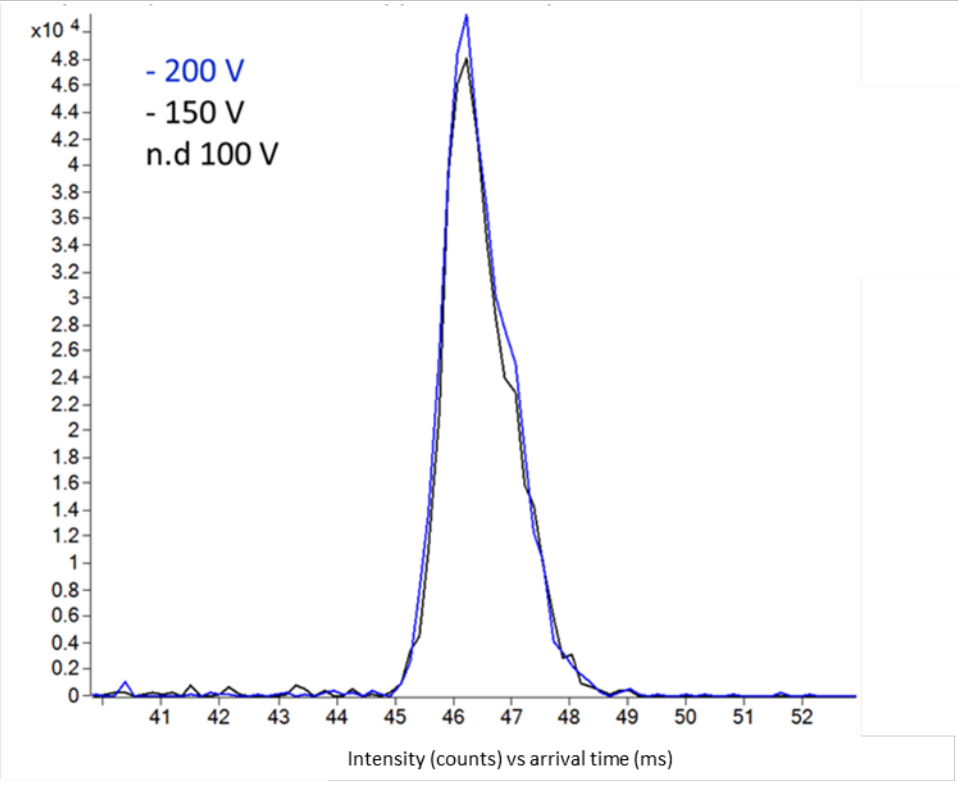

Fig. S20: overlaid IMS ATDs of 2-AA labeled standard **2** as $[M-H]^-$ ions, obtained at different RF voltages (100V was not detected, 150V in black, and 200V in blue)

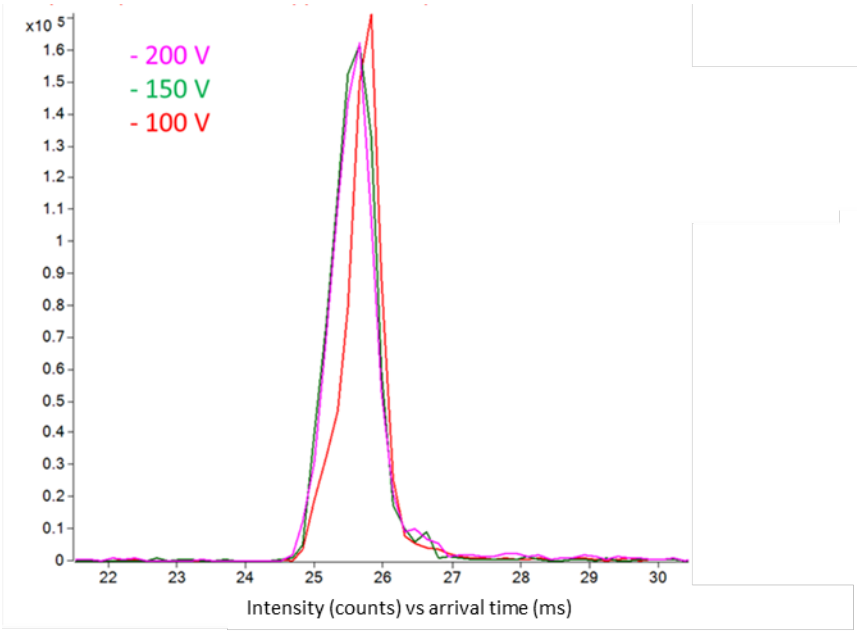

Fig. S21: overlaid IMS ATDs of 2-AA labelled standard **2** as $[M-2H]^{2-}$ ions, obtained at different RF voltages (100V was not detected, 150V in black, and 200V in blue)

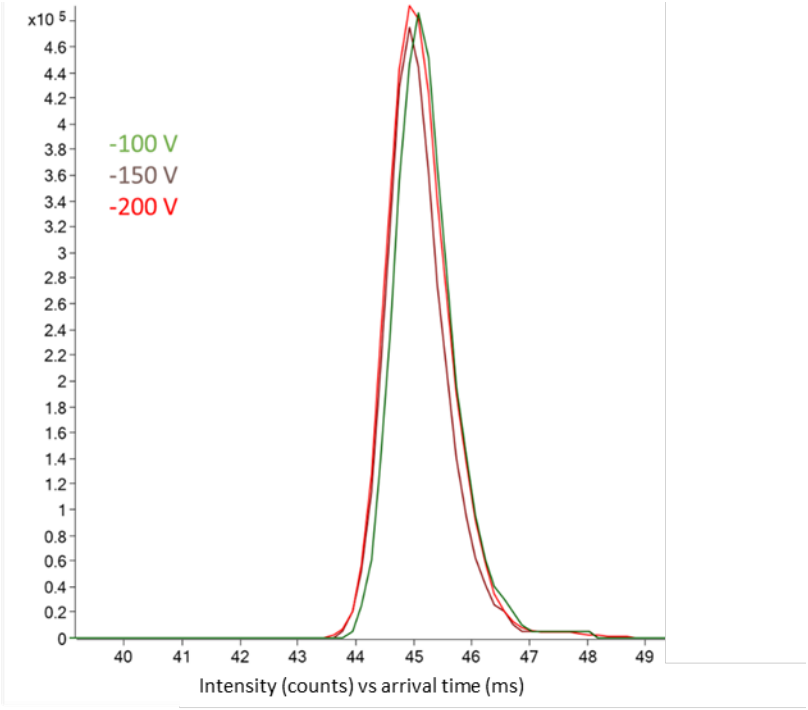

Fig. S22: overlaid IMS ATDs of unlabeled standard **3** as $[M-H]^-$ ions, obtained at different RF voltages (100V in green, 150V in brown, and 200V in red)

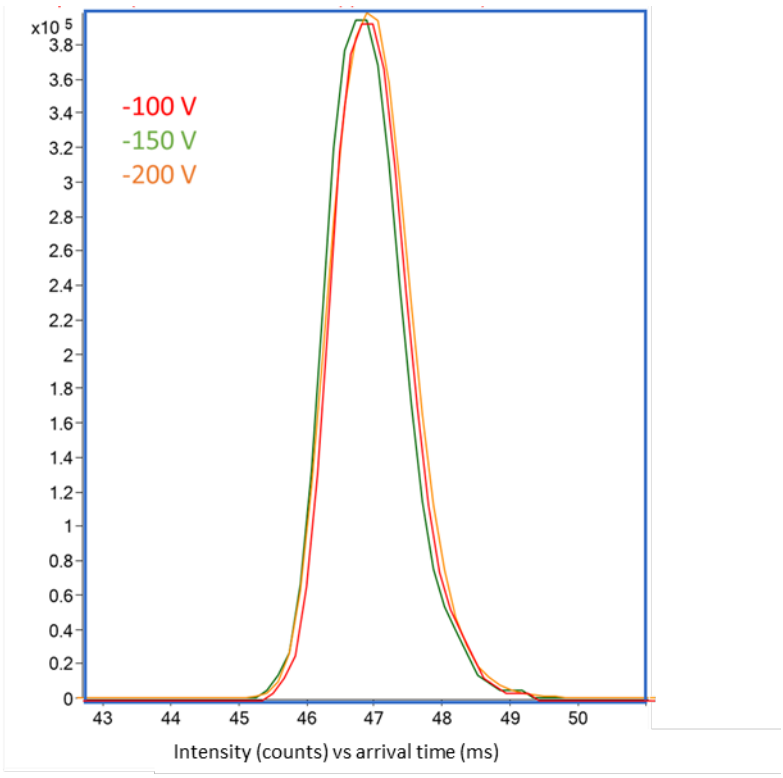

Fig. S23: overlaid IMS ATDs of 2-AA labelled standard **3** as $[M-H]^-$ ions obtained, at different RF voltages (100V in red, 150V in green, and 200V in orange)

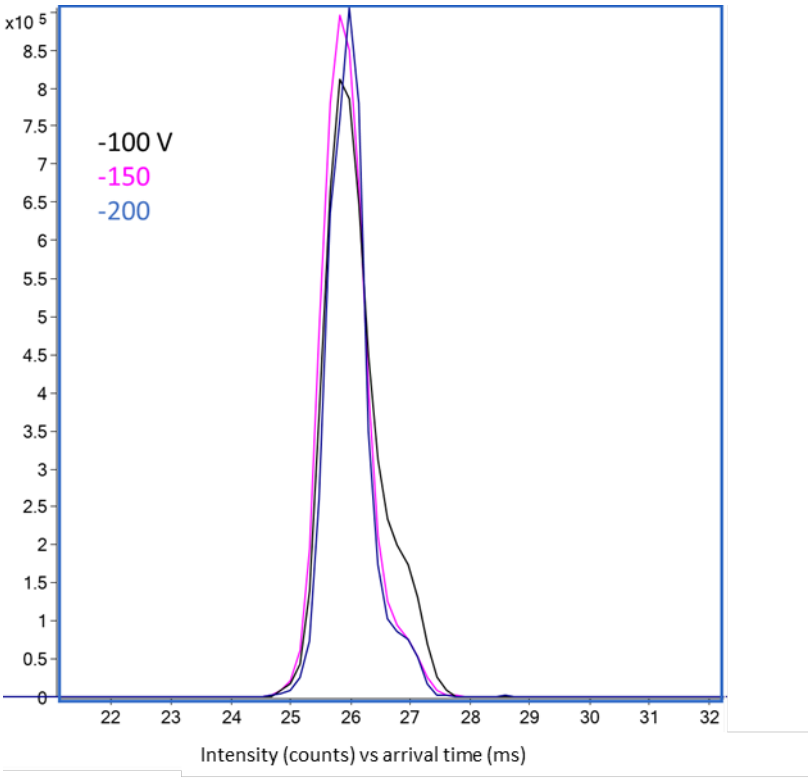

Fig. S24: overlaid IMS ATDs of 2-AA labelled standard **3** as $[M-2H]^{2-}$ ions, obtained at different RF voltages (100V in red, 150V in green, and 200V in orange)

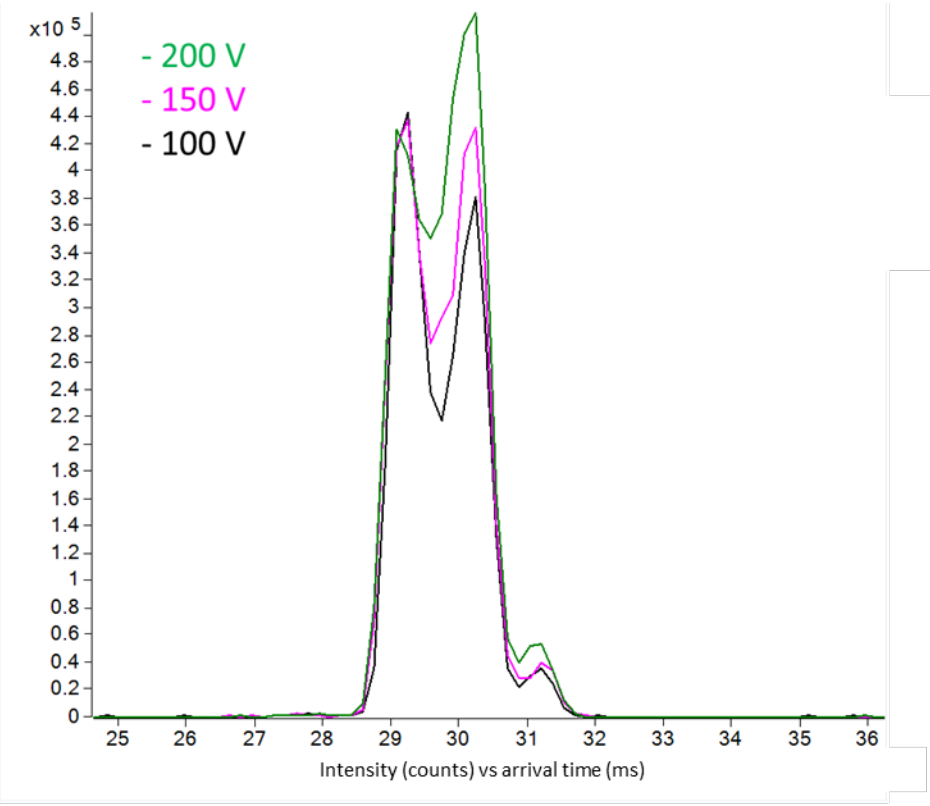

Fig. S25: overlaid IMS ATDs of unlabeled standard **4** as $[M-2H]^{2-}$ ions, obtained at different RF voltages (100V pictured in black, 150V in pink, and 200V in green)

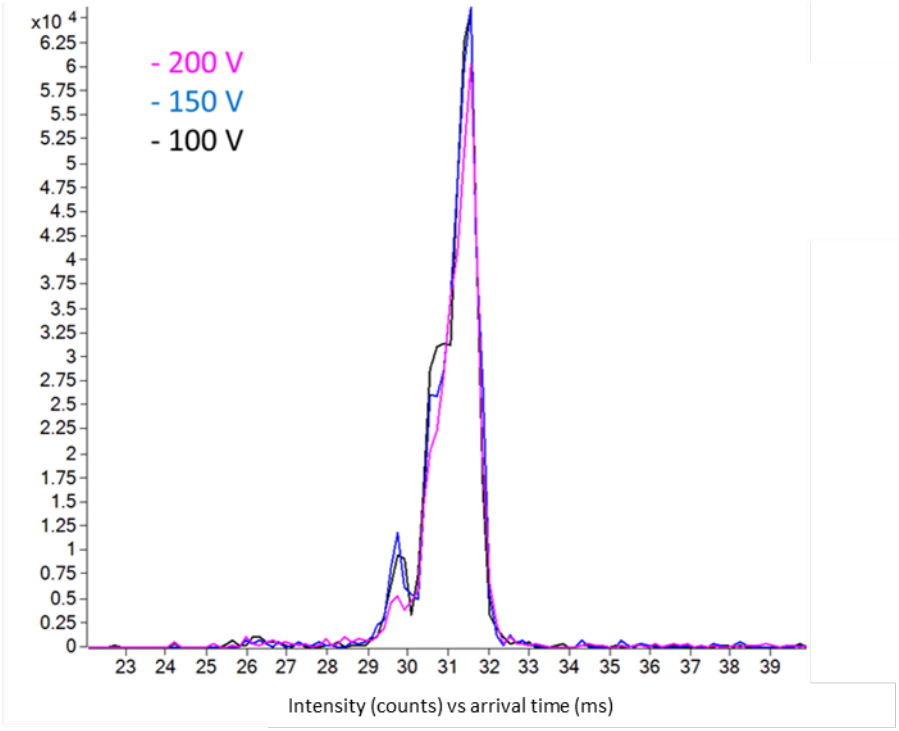

Fig. S26: overlaid IMS ATDs of 2-AA labelled standard **4** as $[M-2H]^{2-}$ ions, obtained at different RF voltages (100V in black, 150V in blue, and 200V in pink)

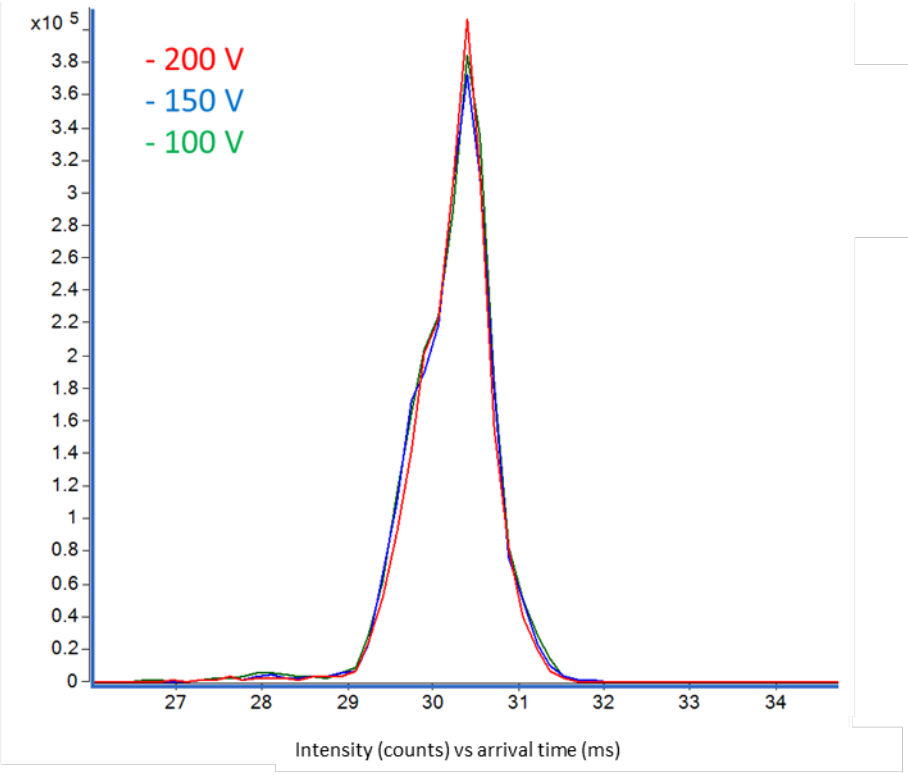

Fig. S27: overlaid IMS ATDs of unlabeled standard **5** as $[M-2H]^{2-}$ ions, obtained at different RF voltages (100V pictured in black, 150V in blue, and 200V in pink)

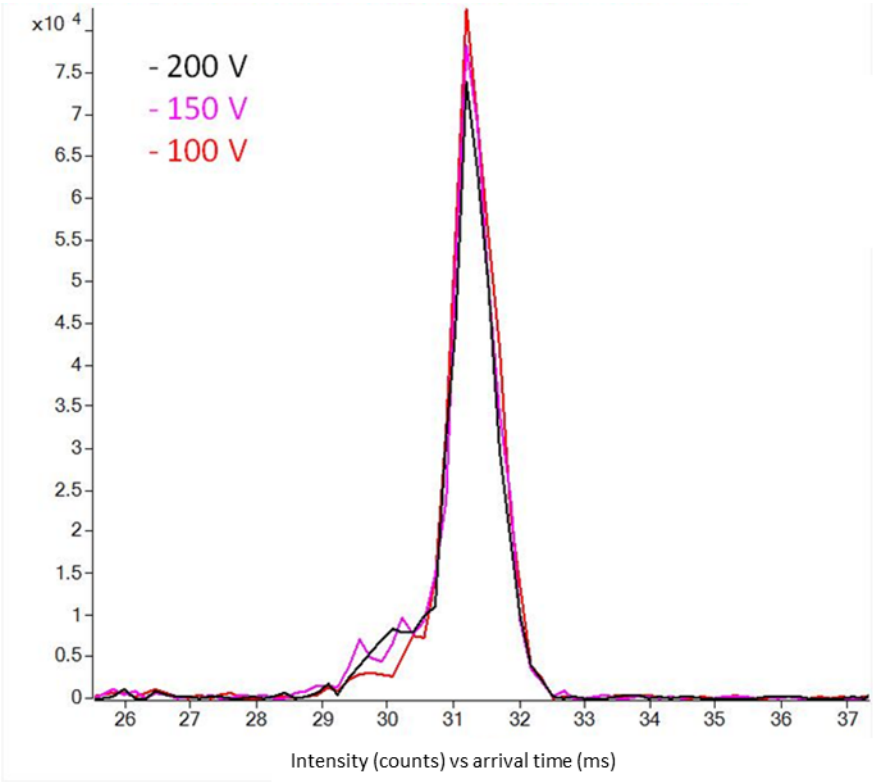

Fig. S28: overlaid IMS ATDs of 2-AA labelled standard **5** as $[M-2H]^{2-}$ ions, obtained at different RF voltages (100V pictured in red, 150V in pink, and 200V in black)

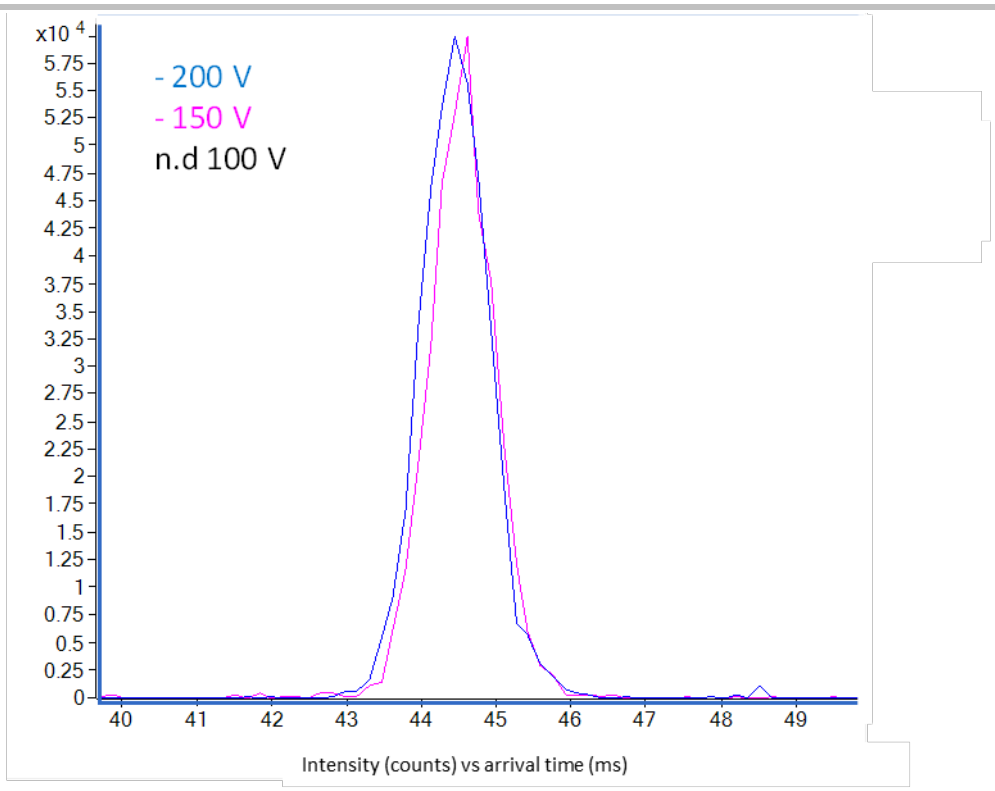

Fig. S29: Overlaid IMS ATDs of unlabeled standard **6** as $[M-H]^-$ ions, obtained at different RF voltages (100V was not detected, 150V in pink, and 200V in blue)

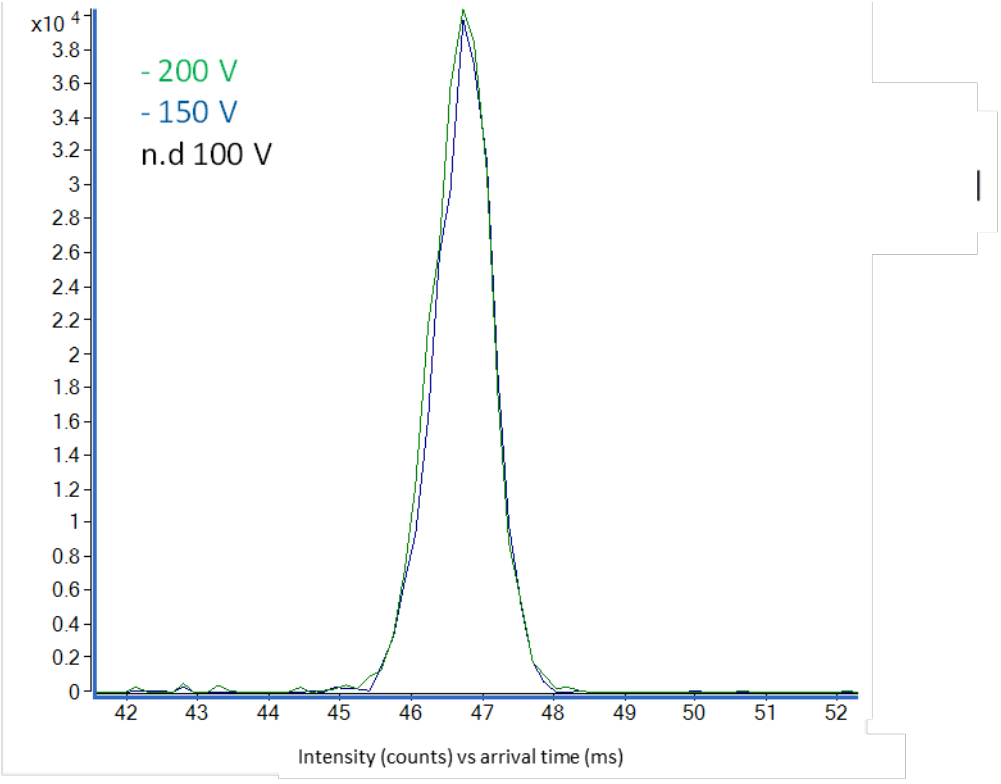

Fig. S30: Overlaid IMS ATDs of 2-AA labelled standard **6** as $[M-H]^-$ ions, obtained at different RF voltages (100V was not detected, 150V in blue, and 200V in green)

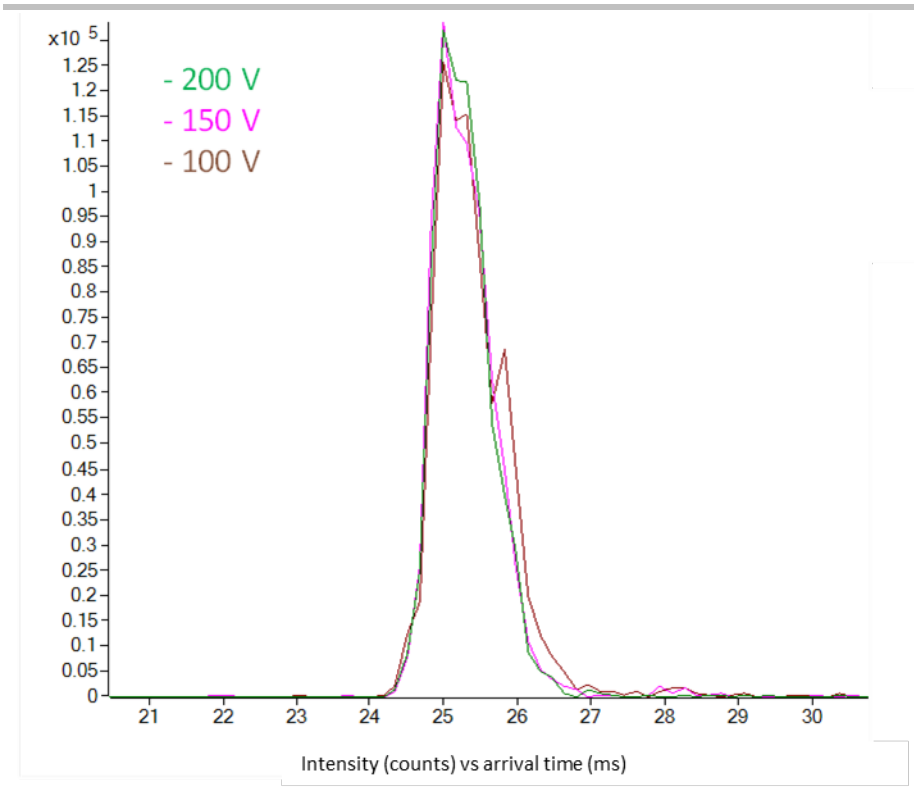

Fig. S31: Overlaid IMS ATDs of 2-AA labelled standard **6** as $[M-2H]^{2-}$ ions, obtained at different RF voltages (100V in brown, 150V in pink and 200V in green)

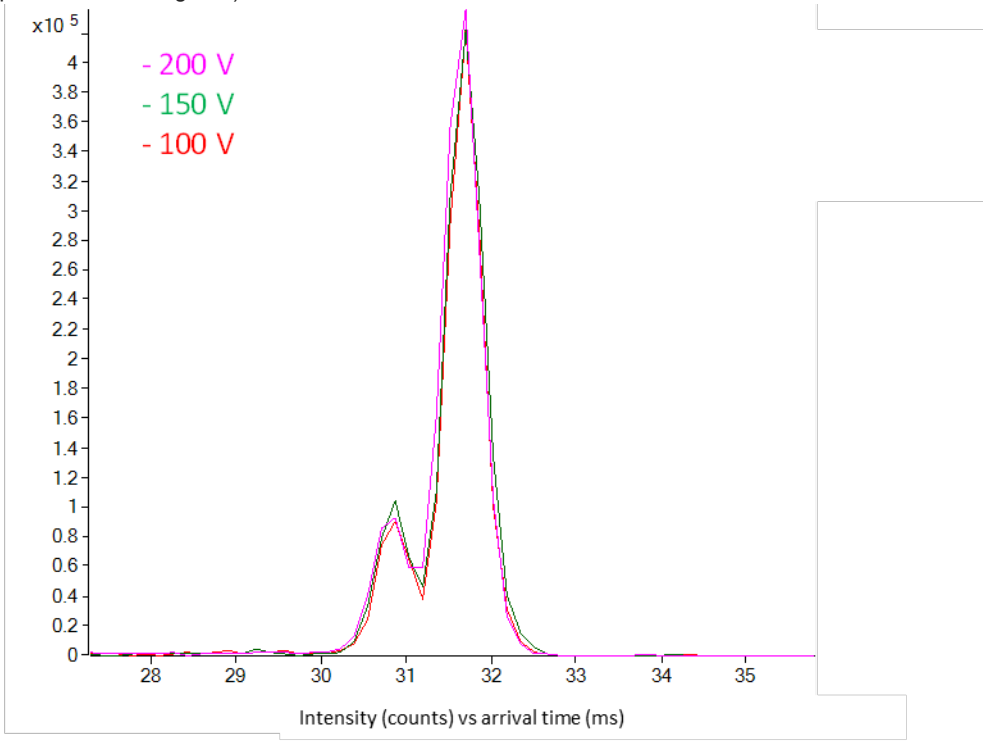

Fig. S32: Overlaid IMS ATDs of unlabeled standard **7** as $[M-2H]^{2-}$ ions, obtained at different RF voltages (100V in red, 150V in green and 200V in pink)

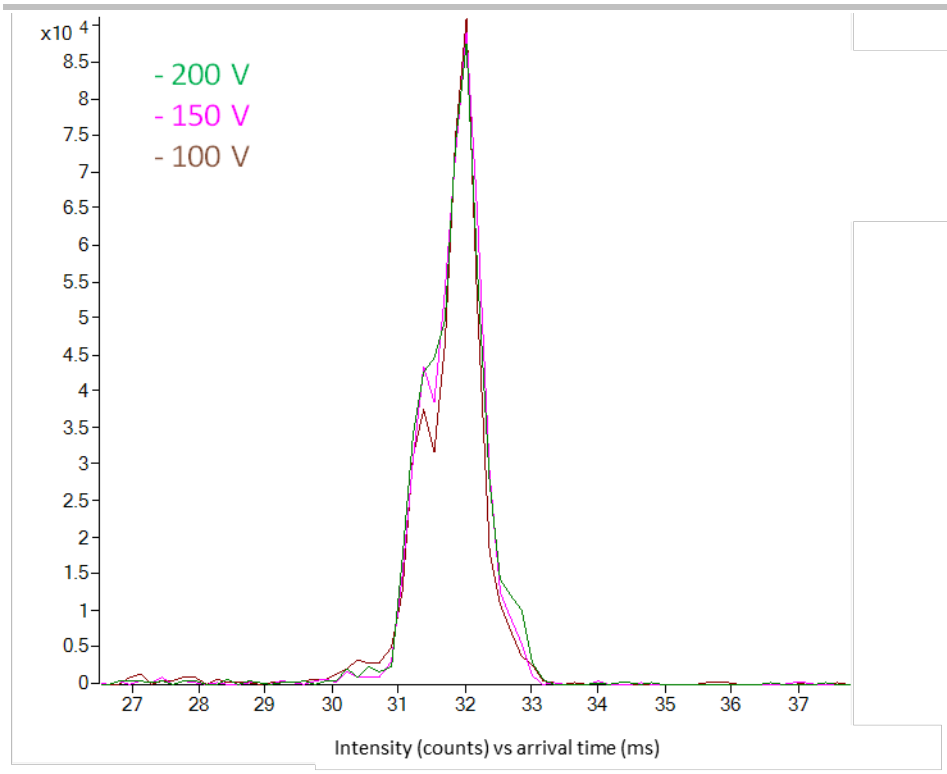

Fig. S33: Overlaid IMS ATDs of 2-AA labelled standard **7** as $[M-2H]^{2-}$ ions, obtained at different RF voltages (100V in brown, 150V in pink and 200V in green)

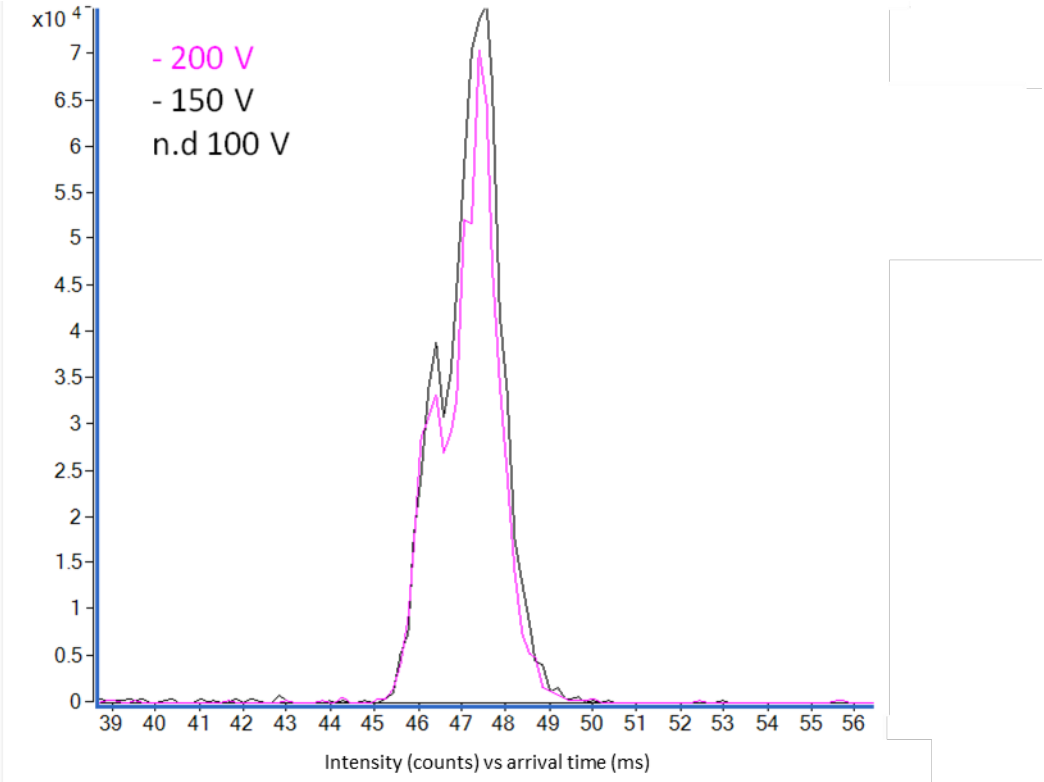

Fig. S34: Overlaid IMS ATDs of unlabeled standard **8** as $[M-H]^{-}$ ions, obtained at different RF voltages (100V was not detected, 150V in black, and 200V in pink)

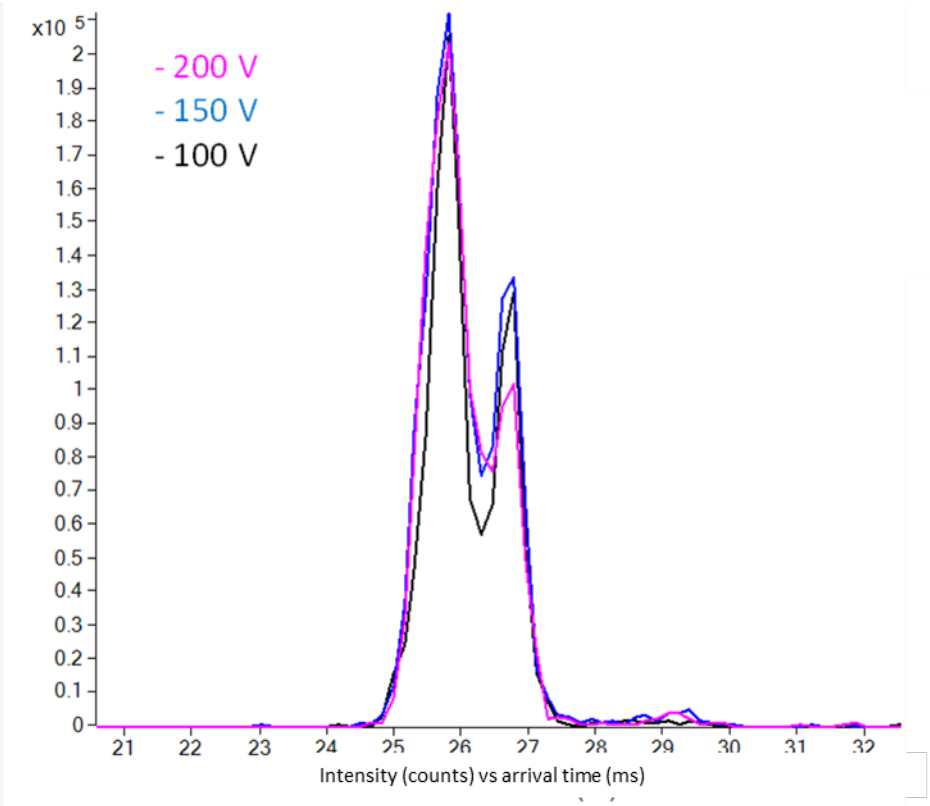

Fig. S35: Overlaid IMS ATDs of unlabeled standard **8** as $[M-2H]^{2-}$ ions, obtained at different RF voltages (100V is pictured in black, 150V in blue, and 200V in pink)

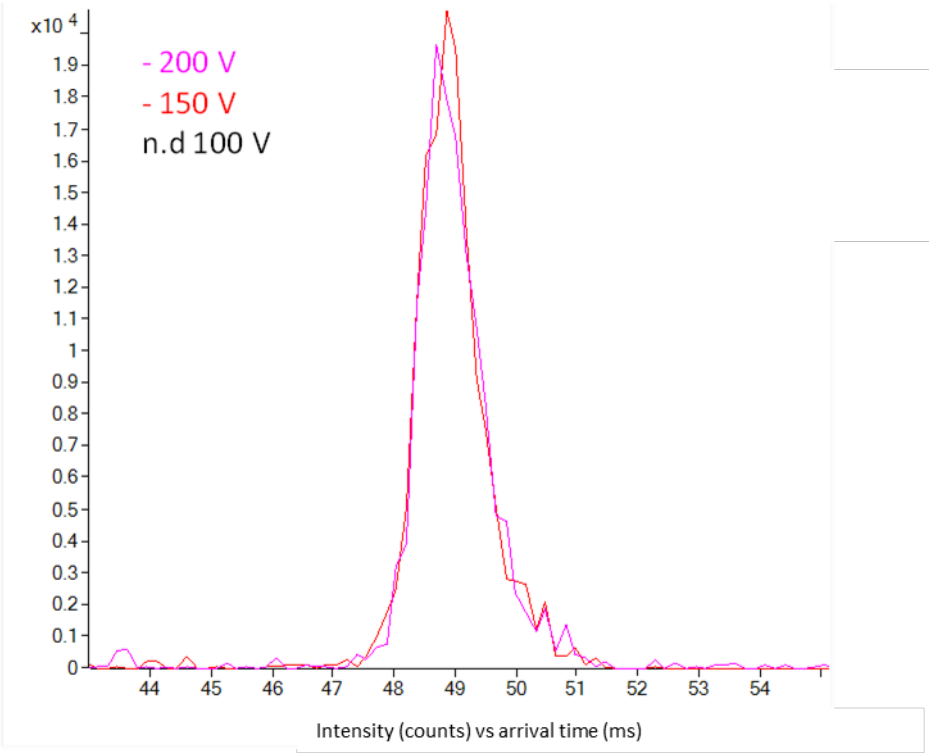

Fig. S36: Overlaid IMS ATDs of 2-AA labelled standard **8** as $[M-H]^{-}$ ions, obtained at different RF voltages (100V was not detected, 150V in red and 200V in pink)

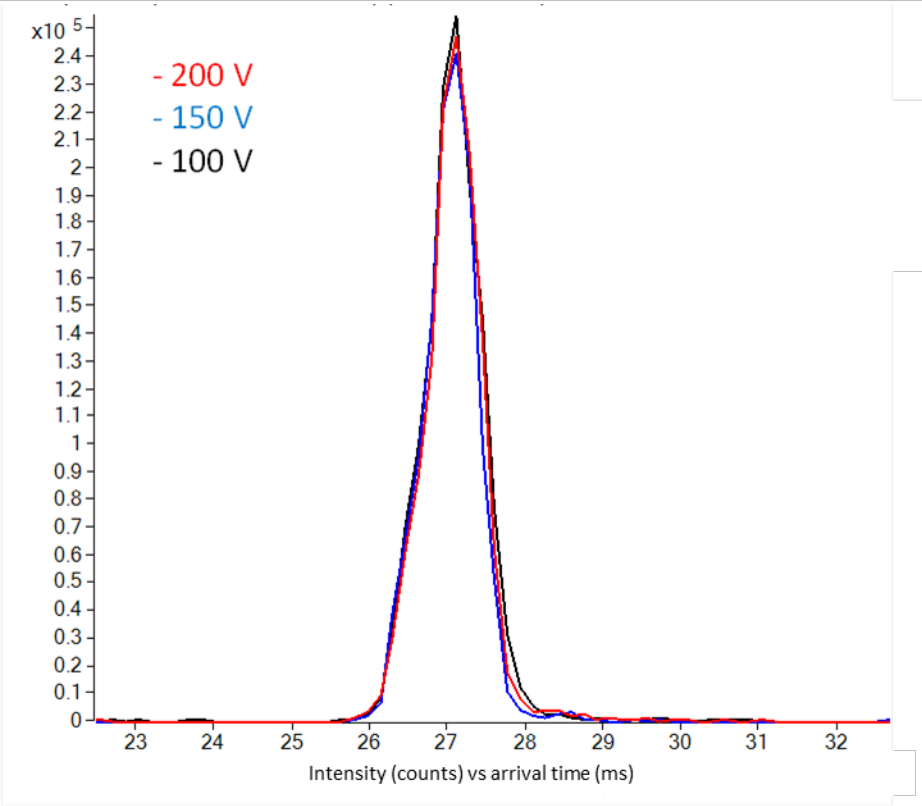

Fig. S37: Overlaid IMS ATDs of 2-AA labelled standard **8** as $[M-2H]^{2-}$ ions, obtained at different RF voltages (100V in black, 150V in blue and 200V in red)

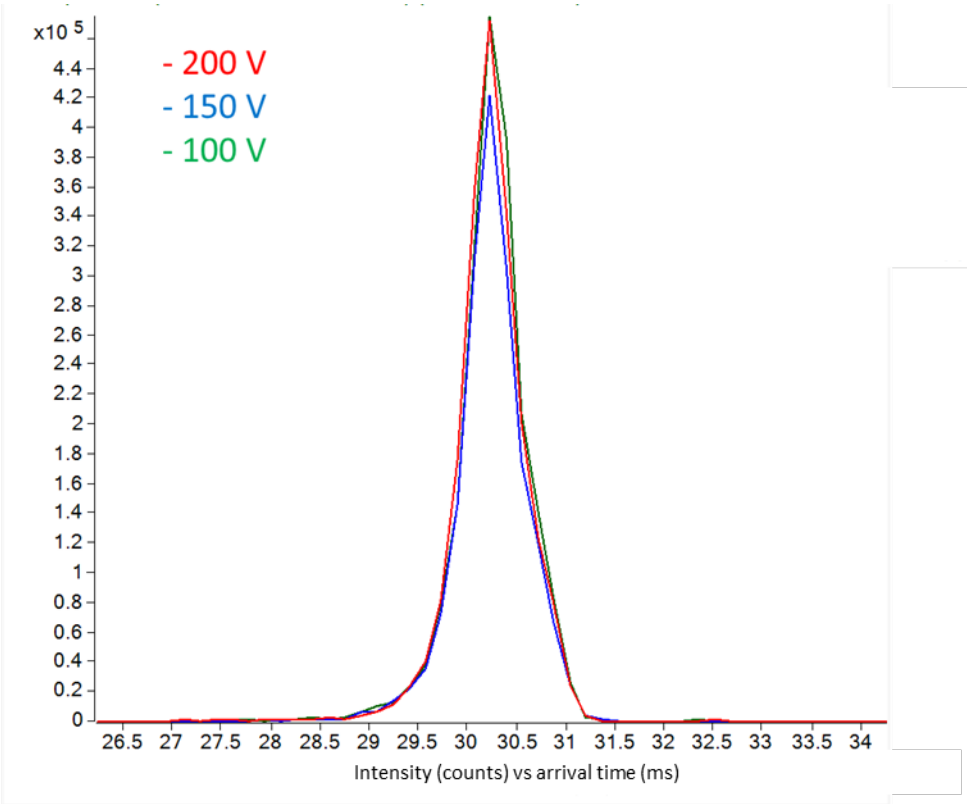

Fig. S38: overlaid IMS ATDs of unlabeled standard **9** as $[M-2H]^{2-}$ ions, obtained at different RF voltages (100V pictured in green, 150V in blue, and 200V in red)

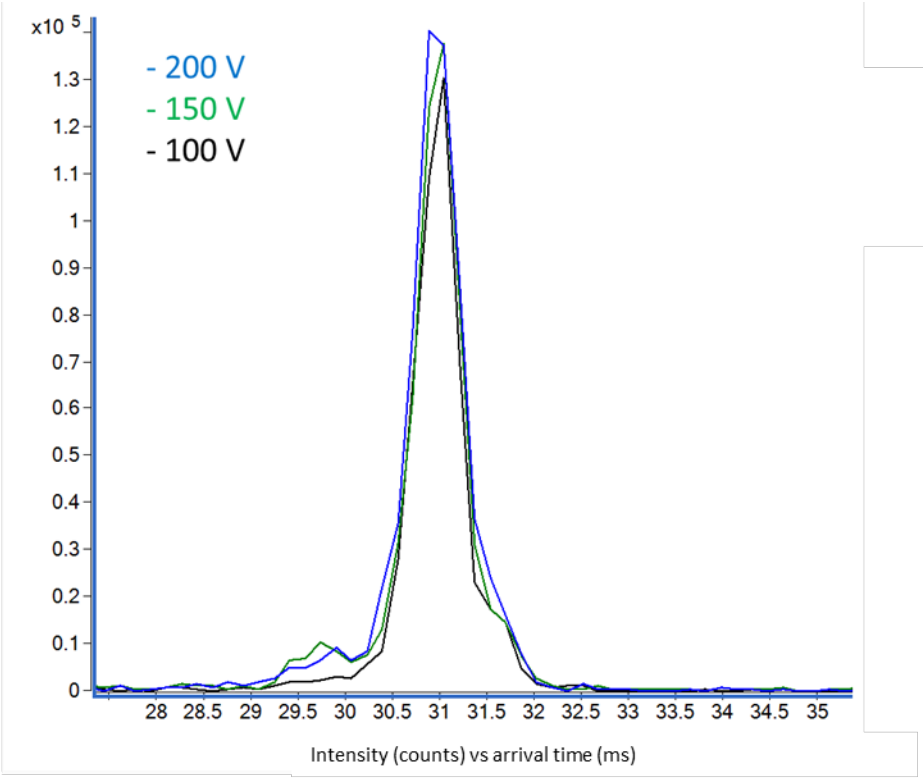

Fig. S39: overlaid IMS ATDs of 2-AA labelled standard **9** as $[M-2H]^{2-}$ ions, obtained at different RF voltages (100V pictured in green, 150V in blue, and 200V in red)

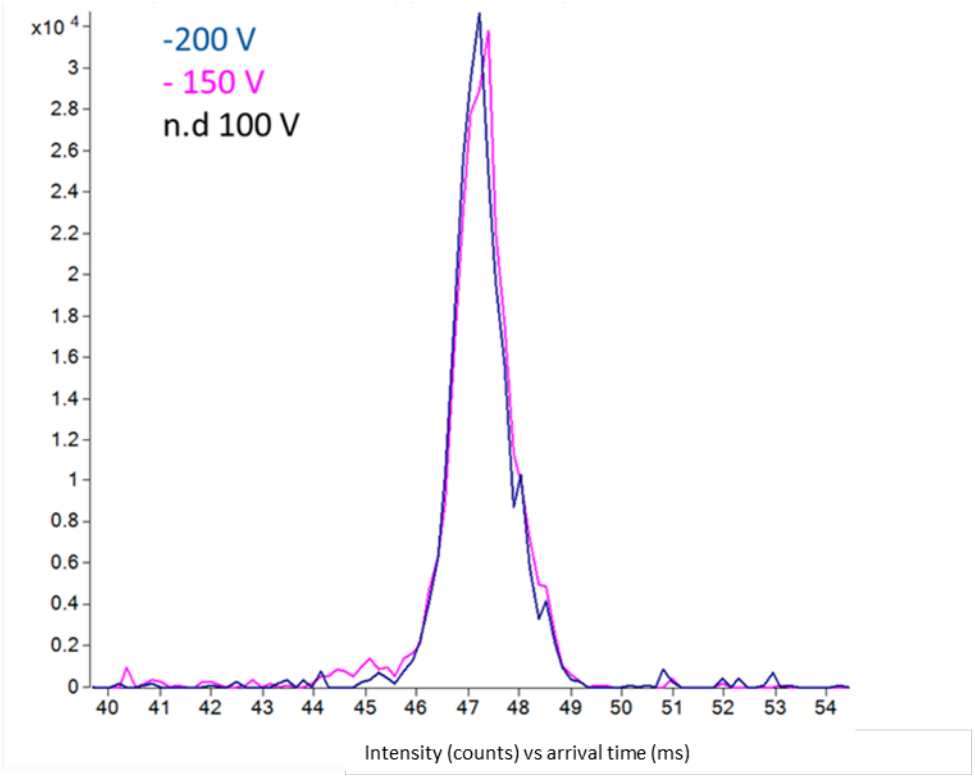

Fig. S40: overlaid IMS ATDs of unlabeled standard **10** as $[M-H]^{-}$ ions, obtained at different RF voltages (100V was not detected, 150V in pink, and 200V in blue)

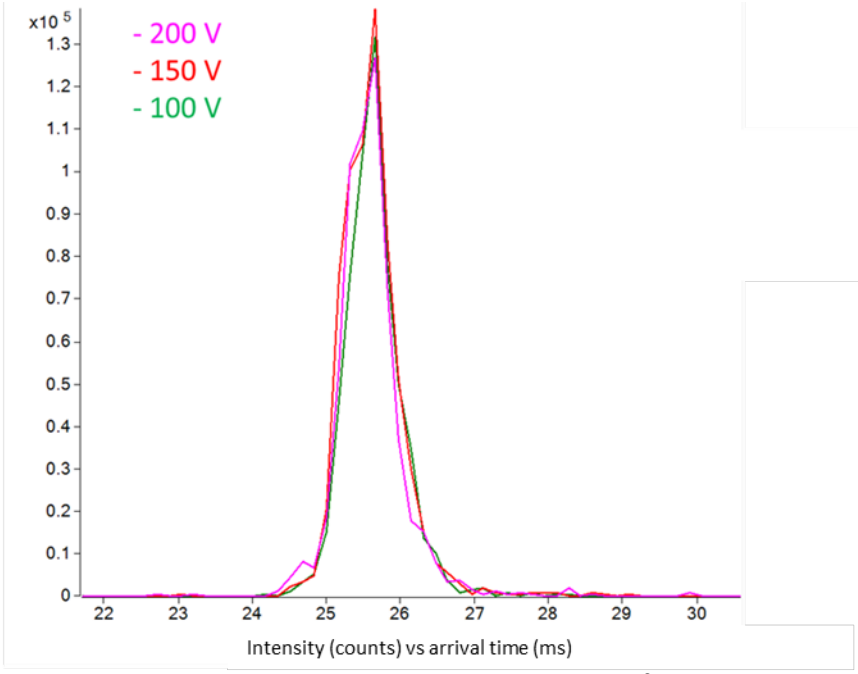

Fig. S41: overlaid IMS ATDs of unlabeled standard **10** as $[M-2H]^{2-}$ ions, obtained at different RF voltages (100V pictured in green, 150V in red, and 200V in pink)

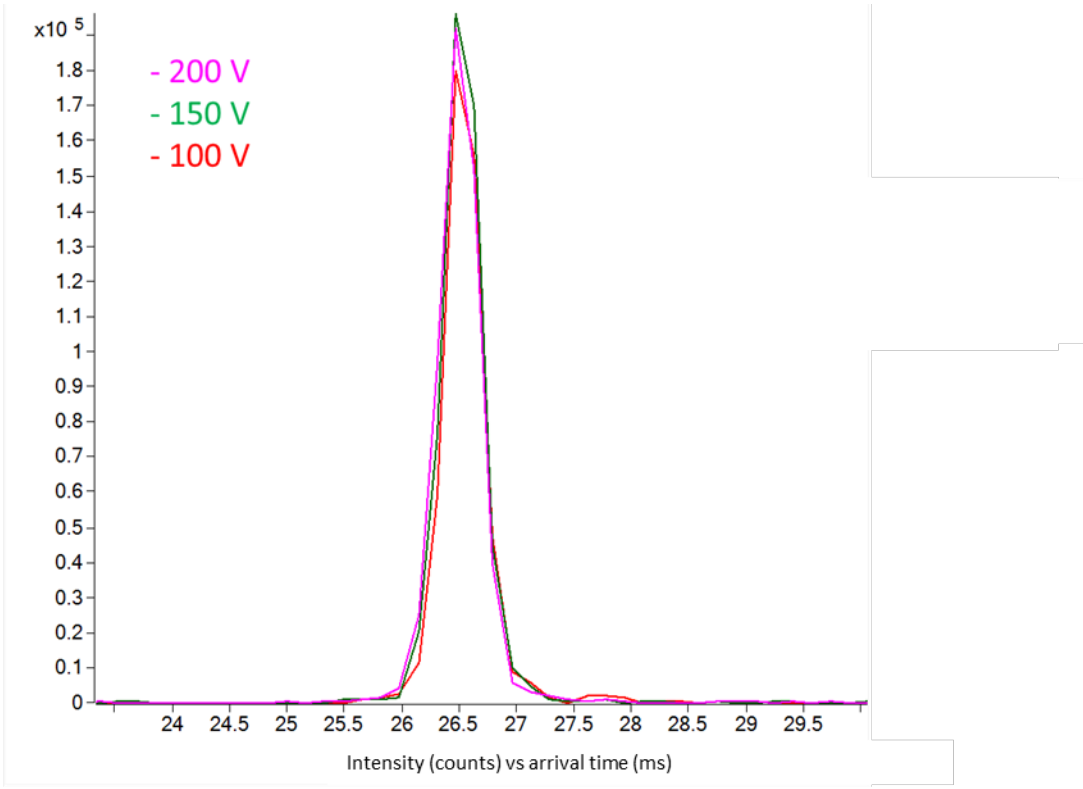

Fig. S42: overlaid IMS ATDs of 2-AA labelled standard **10** as $[M-2H]^{2-}$ ions, obtained at different RF voltages (100V pictured in red, 150V in green, and 200V in pink)

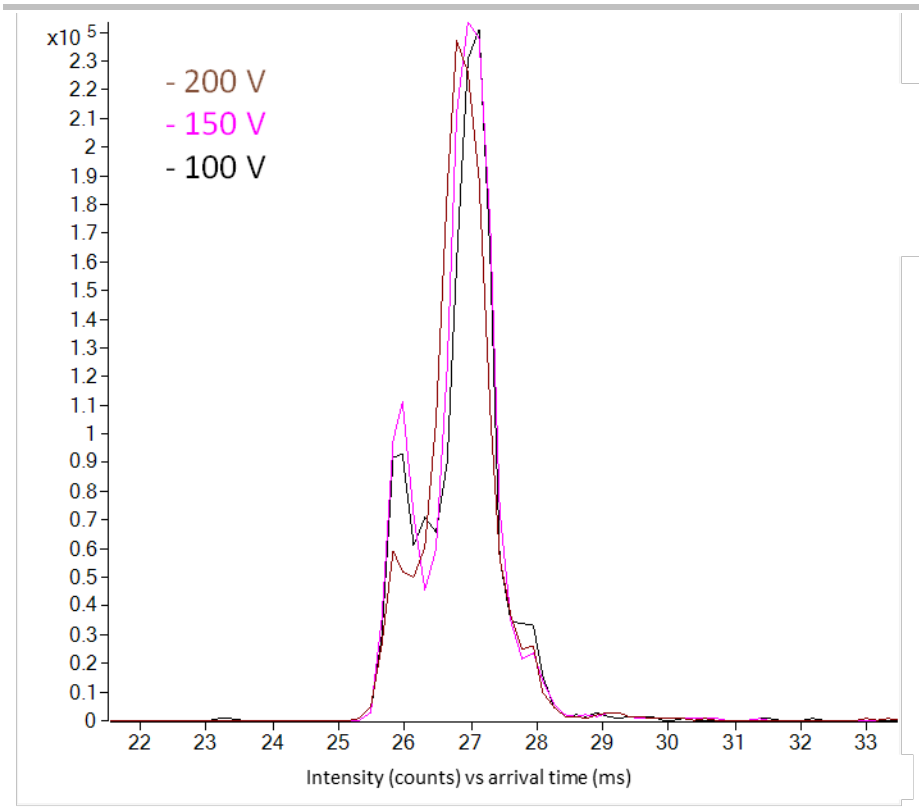

Fig. S43: Overlaid IMS ATDs of unlabeled standard **11** as $[M-2H]^{2-}$ ions, obtained at different RF voltages (100V in black, 150V in pink and 200V in brown)

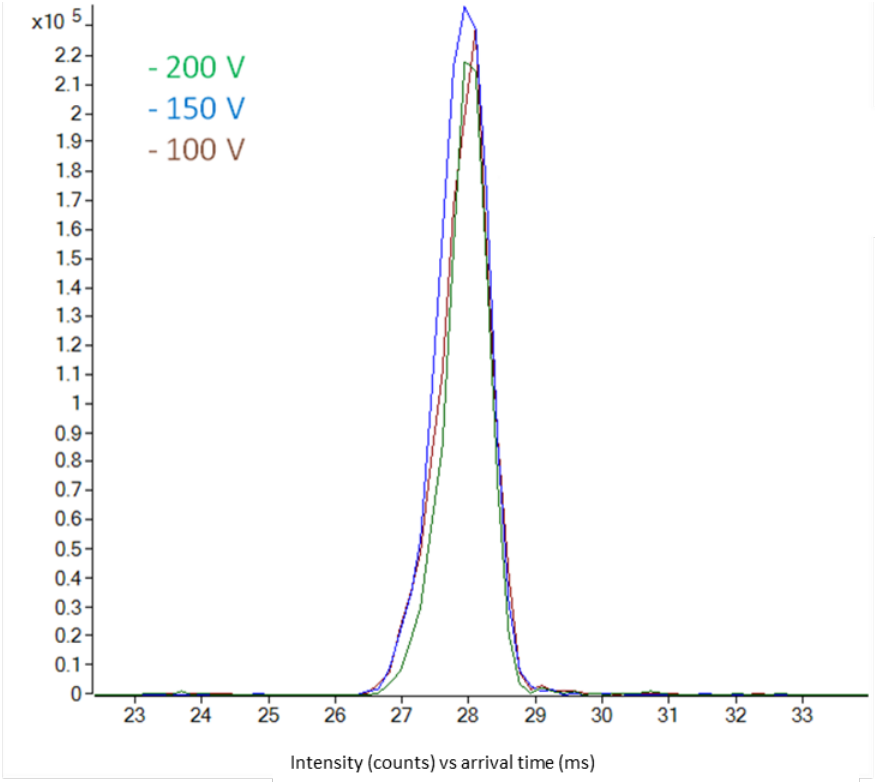

Fig. S44: Overlaid IMS ATDs of 2-AA labelled standard **11** as $[M-2H]^{2-}$ ions, obtained at different RF voltages (100V in brown, 150V in blue and 200V in green)

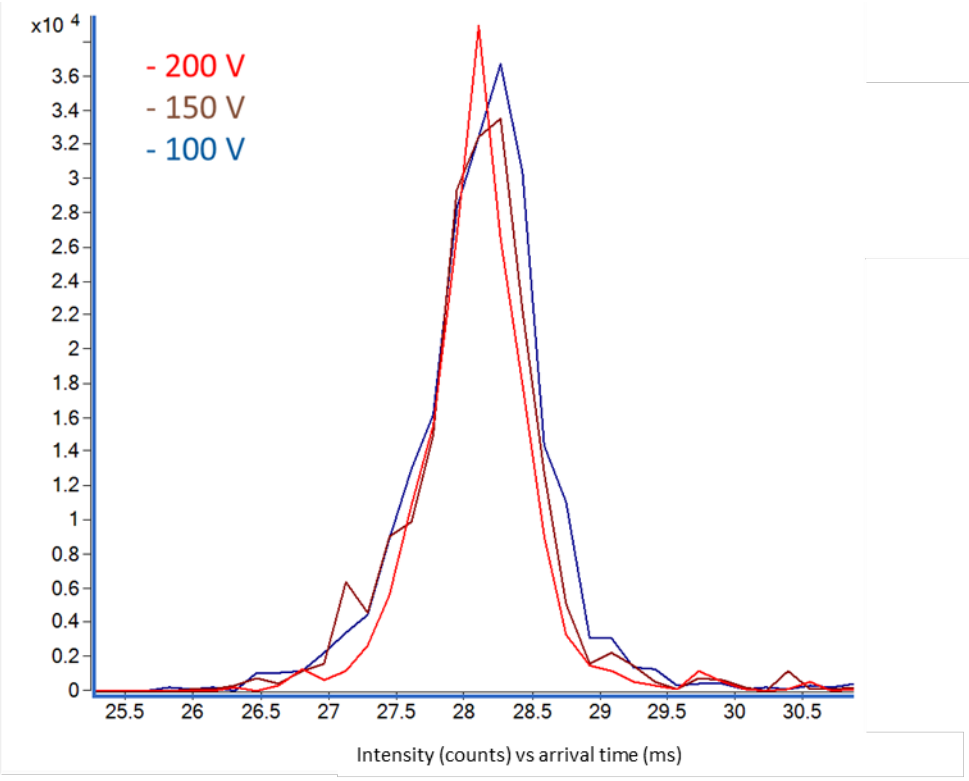

Fig. S45: overlaid IMS ATDs of unlabeled standard **12** as $[M-2H]^{2-}$ ions, obtained at different RF voltages (100V in blue, 150V in brown, and 200V in red)

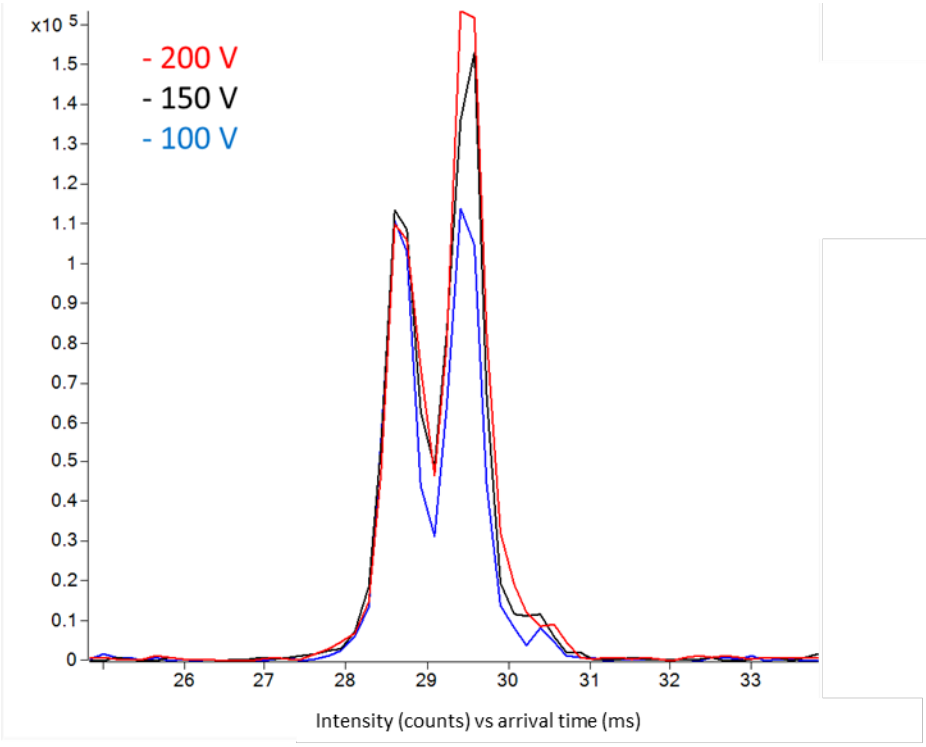

Fig. S46: overlaid IMS ATDs of 2-AA labelled standard **12** as $[M-2H]^{2-}$ ions, obtained at different RF voltages (100V pictured in blue, 150V in black, and 200V in red)

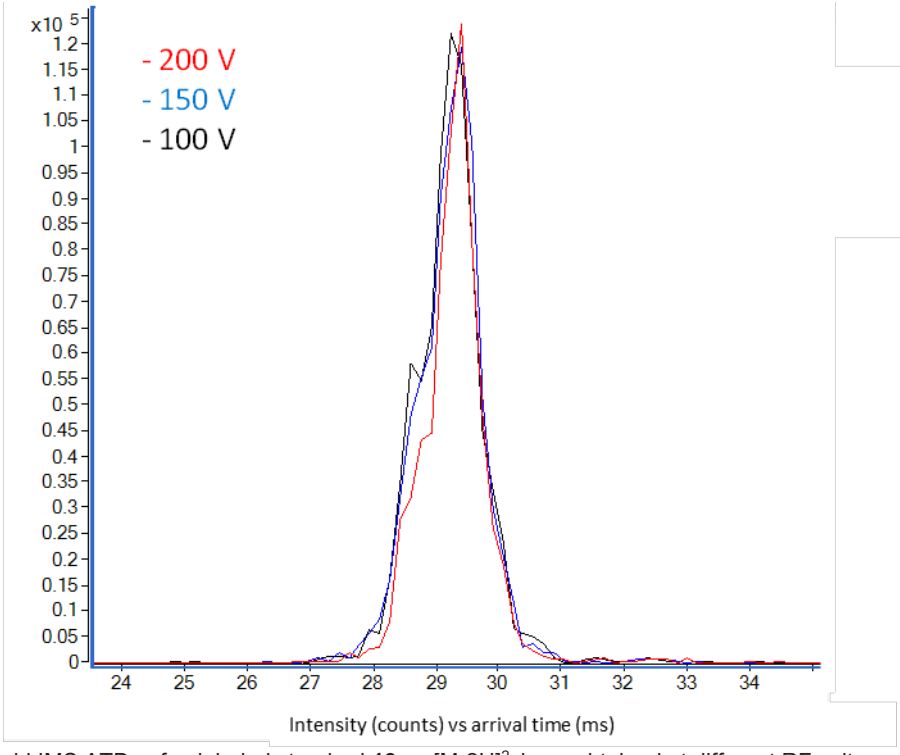

Fig. S47: Overlaid IMS ATDs of unlabeled standard **13** as $[M-2H]^{2-}$ ions, obtained at different RF voltages (100V in black, 150V in blue and 200V in red)

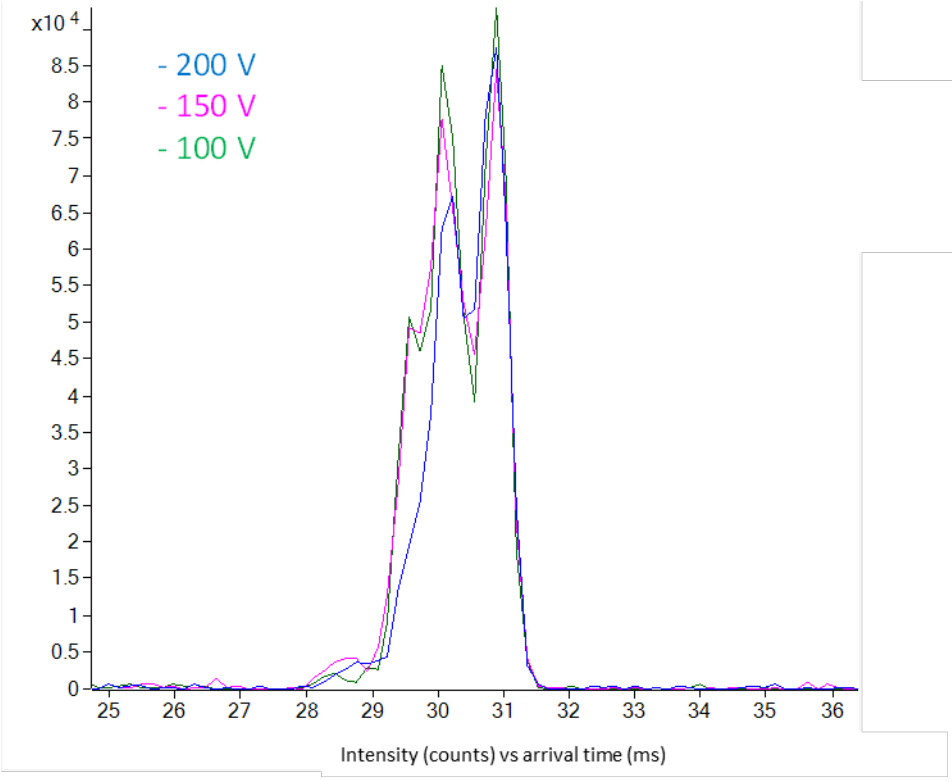

Fig. S48: Overlaid IMS ATDs of 2-AA labelled standard **13** as $[M-2H]^{2-}$ ions, obtained at different RF voltages (100V in green, 150V in pink and 200V in blue)

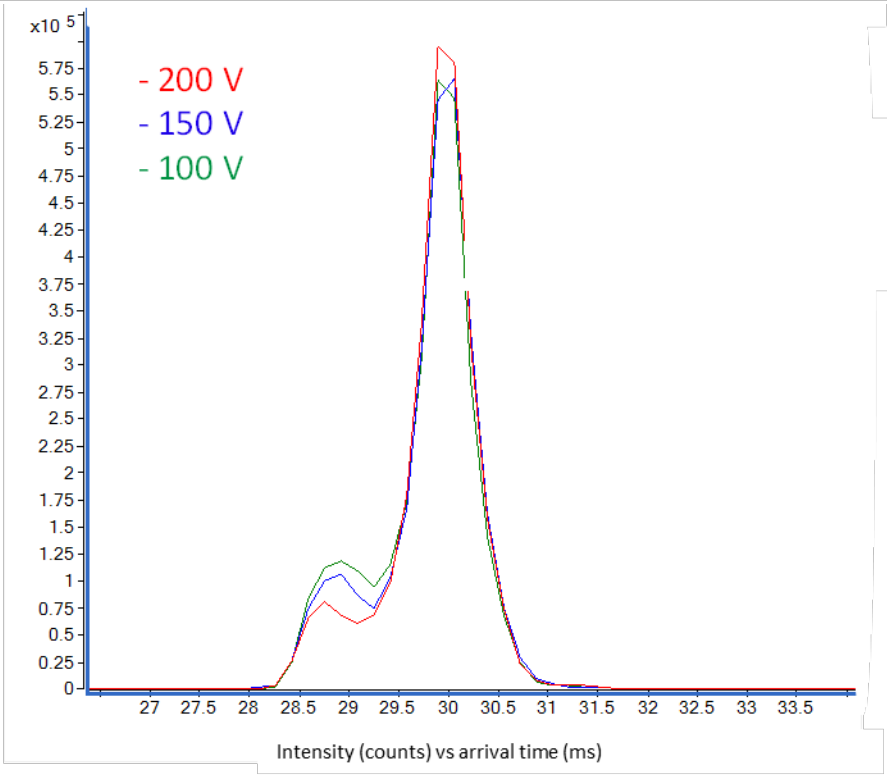

Fig. S49: Overlaid IMS ATDs of unlabeled standard **14** as $[M-2H]^{2-}$ ions, obtained at different RF voltages (100V pictured in green, 150V in blue, and 200V in red)

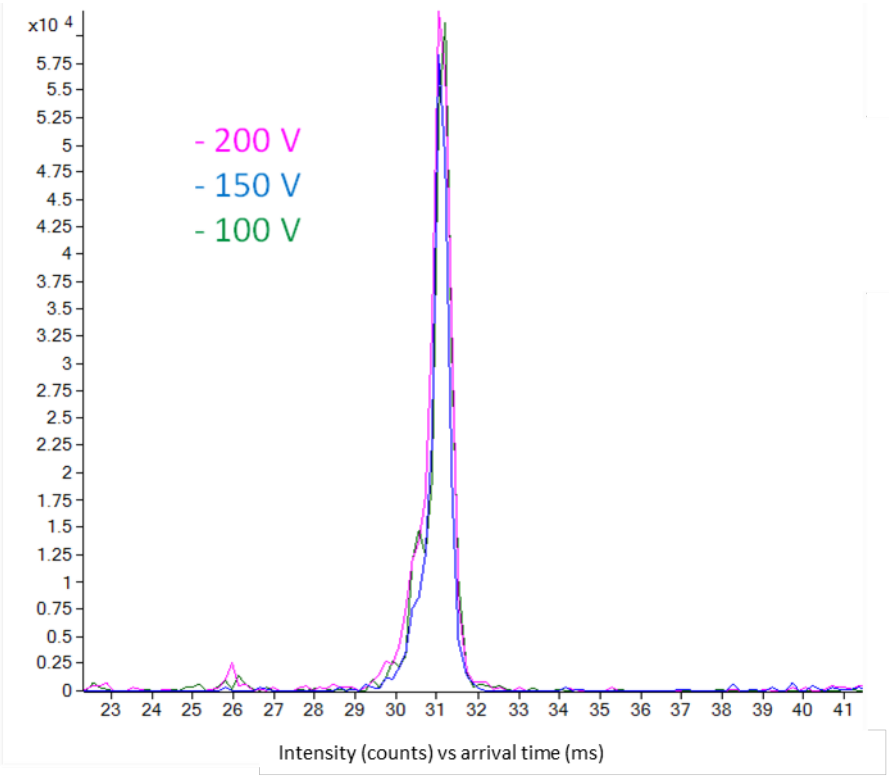

Fig. S50: Overlaid IMS ATDs of 2-AA labelled standard **14** as $[M-2H]^{2-}$ ions, obtained at different RF voltages (100V pictured in green, 150V in blue, and 200V in pink)

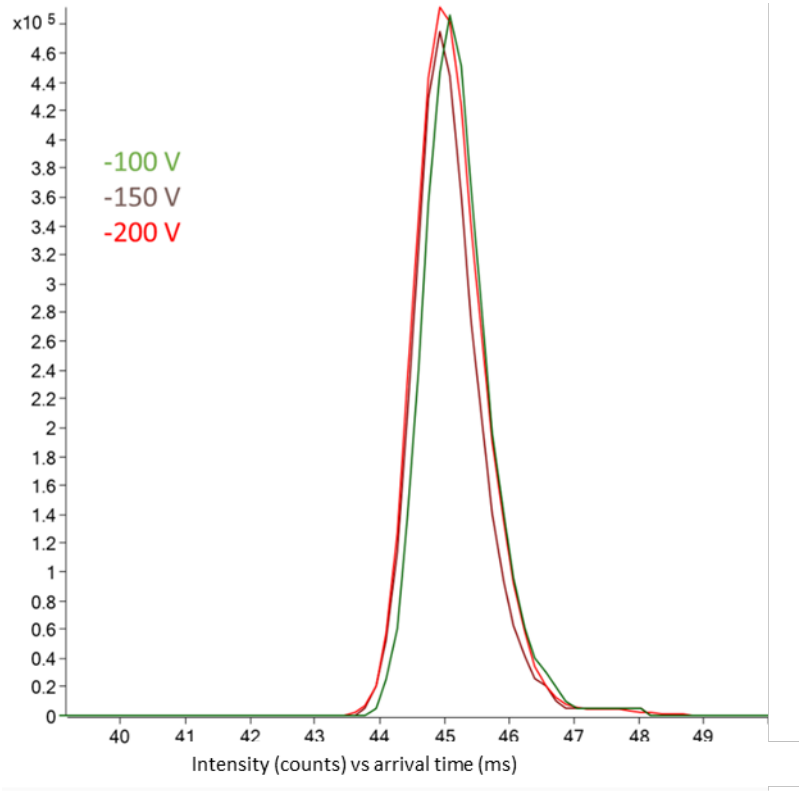

Fig. S51: Overlaid IMS ATDs of 2-AA labelled standard **15** as $[M-2H]^{2-}$ ions, obtained at different RF voltages (100V pictured in green, 150V in brown, and 200V in red)

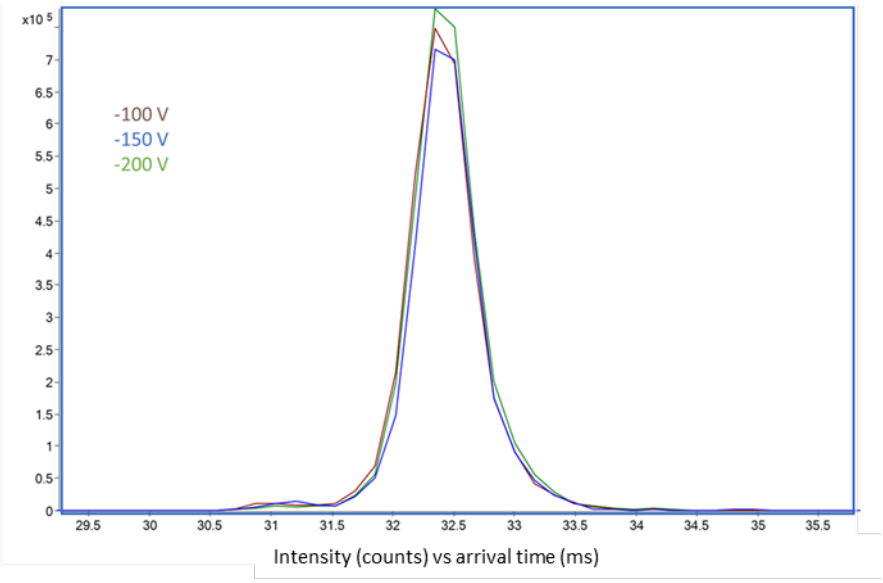

Fig. S52: Overlaid IMS ATDs of 2-AA labelled standard **15** as $[M-2H]^{2-}$ ions, obtained at different RF voltages (100V pictured in brown, 150V in blue, and 200V in green)

2.3 ATDs of standards at different concentrations

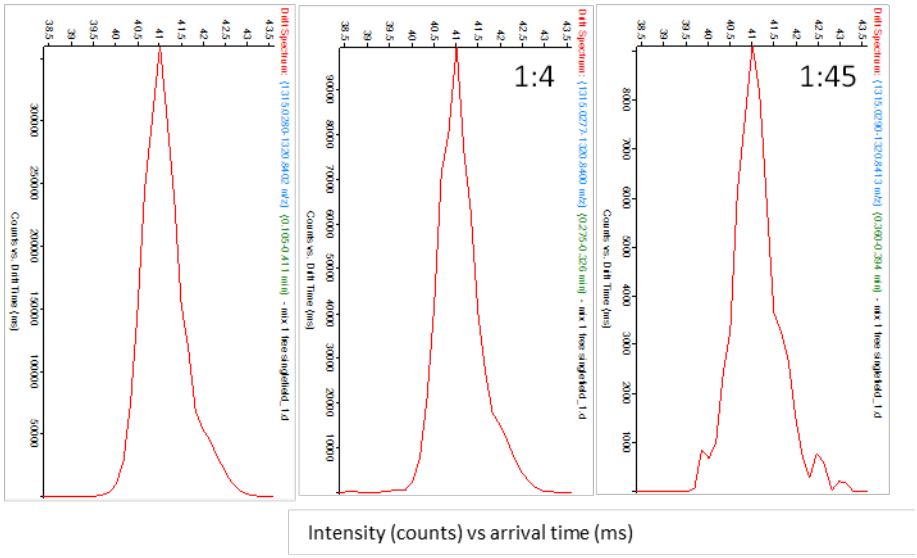

Fig. S53: ATDs of $[M-H]^-$ ions of unlabeled standard **1** at different dilutions (relatively 1, 1:4 and 1:45)

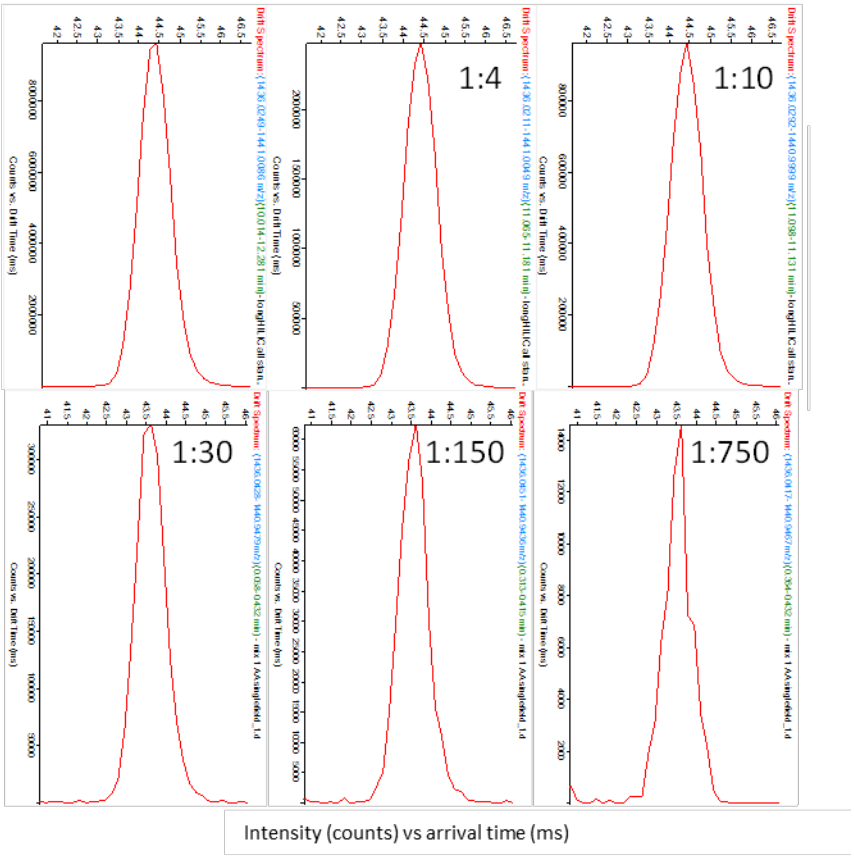

Fig. S54: ATDs of $[M-H]^-$ ions of 2-AA labelled standard **1** at different dilutions (relatively 1, 1:4, 1:10, 1:30, 1:50 and 1:750)

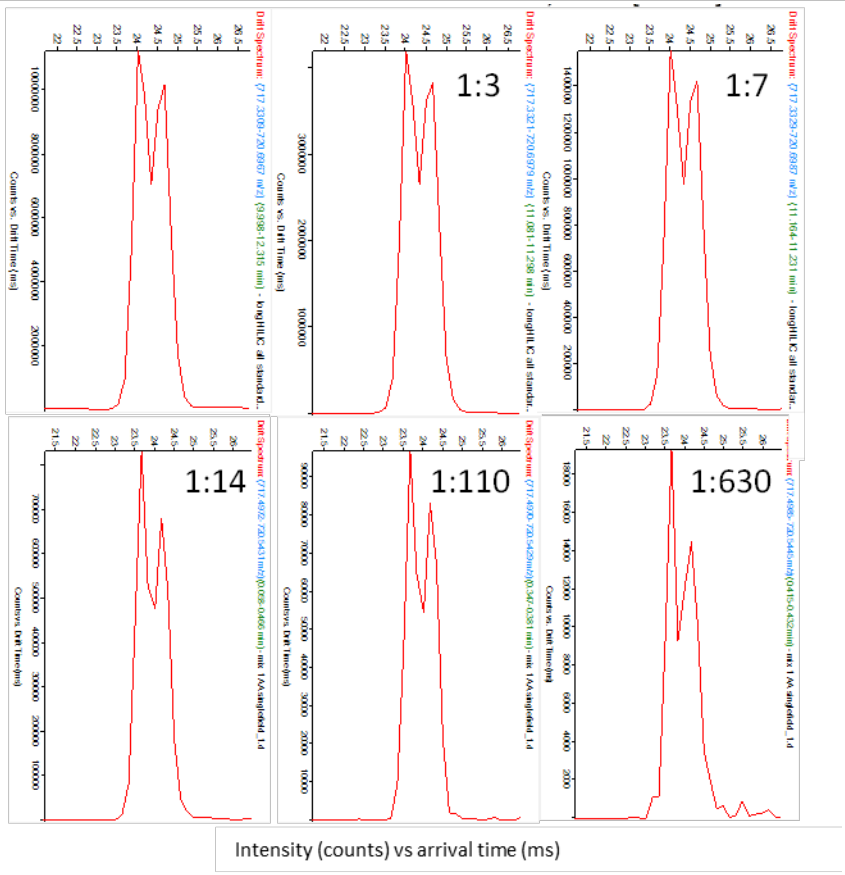

Fig. S55: ATDs of $[M-2H]^{2-}$ ions of 2-AA labeled standard **1** at different dilutions (relatively 1, 1:3, 1:7, 1:14, 1:110 and 1:630)

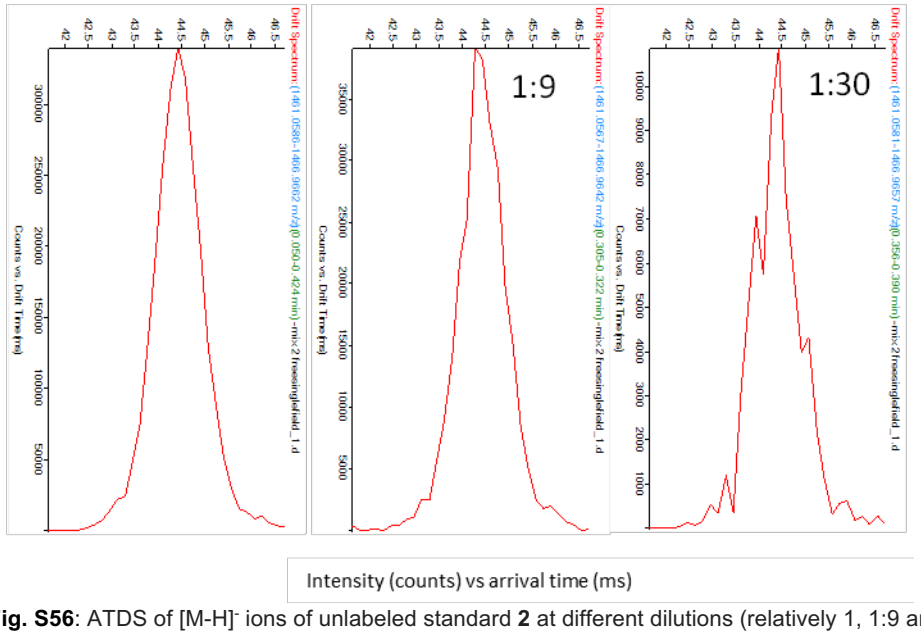

Fig. S56: ATDS of $[M-H]^{-}$ ions of unlabeled standard **2** at different dilutions (relatively 1, 1:9 and 1:30)

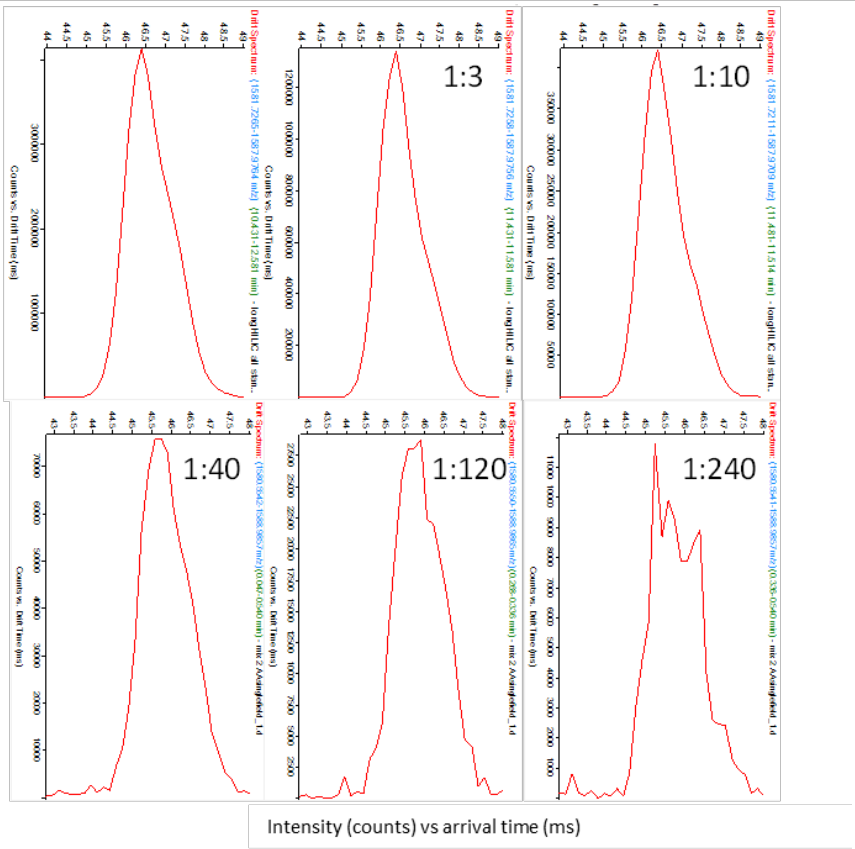

Fig. S57: ATDs of $[M-H]^-$ ions of 2-AA labelled standard **2** at different dilutions (relatively 1, 1:3 and 1:10, 1:40, 1:120 and 1:240)

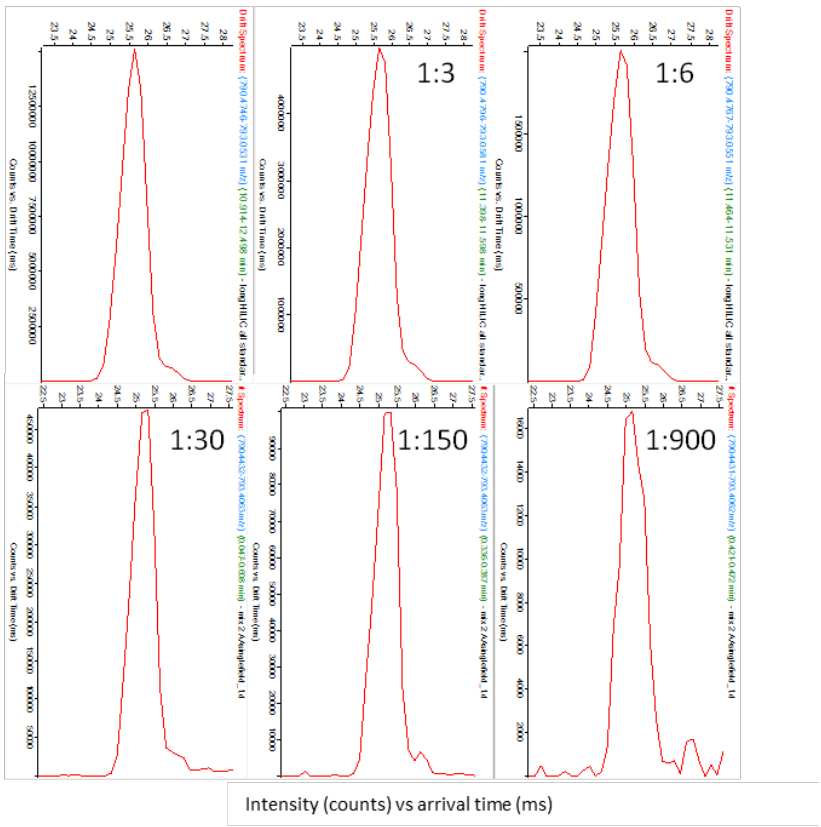

Fig. S58: ATDs of $[M-2H]^{2-}$ ions of 2-AA labelled standard **2** at different dilutions (relatively 1, 1:3, 1:6, 1:30, 1:150 and 1:900)

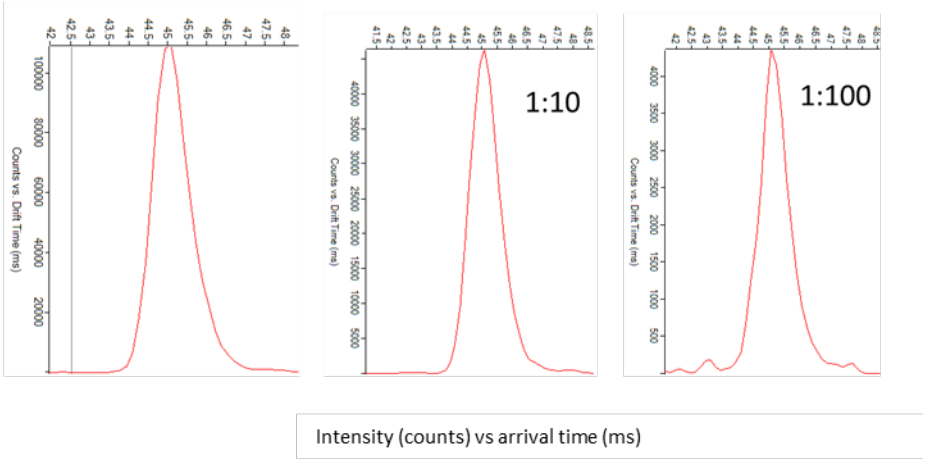

Fig. S59: ATDs of $[M-H]^-$ ions of unlabeled standard **3** at different dilutions (relatively 1, 1:10 and 1:100)

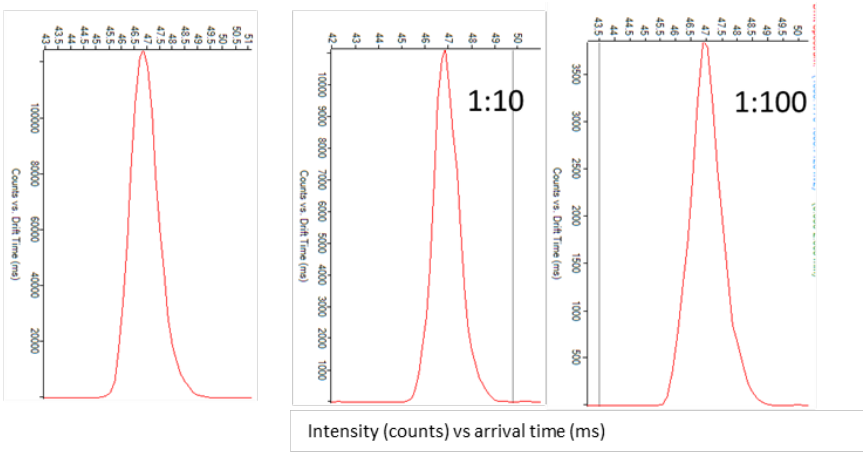

Fig. S60: ATDs of $[M-H]^-$ ions of 2-AA labelled standard **3** at different dilutions (relatively 1, 1:10 and 1:100)

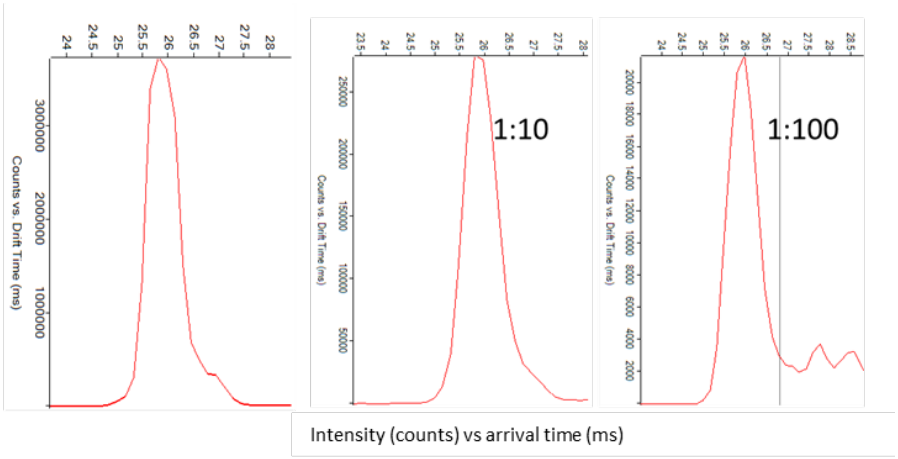

Fig. S61: ATDs of $[M-2H]^{2-}$ ions of 2-AA labelled standard **3** at different dilutions (relatively 1, 1:10 and 1:100)

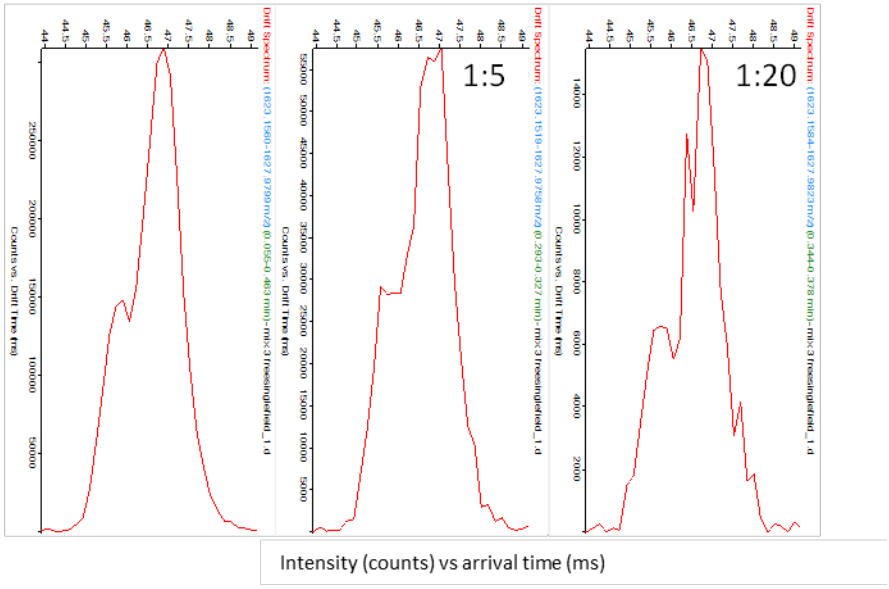

Fig. S62: ATDs of $[M-H]^-$ ions of unlabeled standard **4** at different dilutions (relatively 1, 1:5 and 1:20)

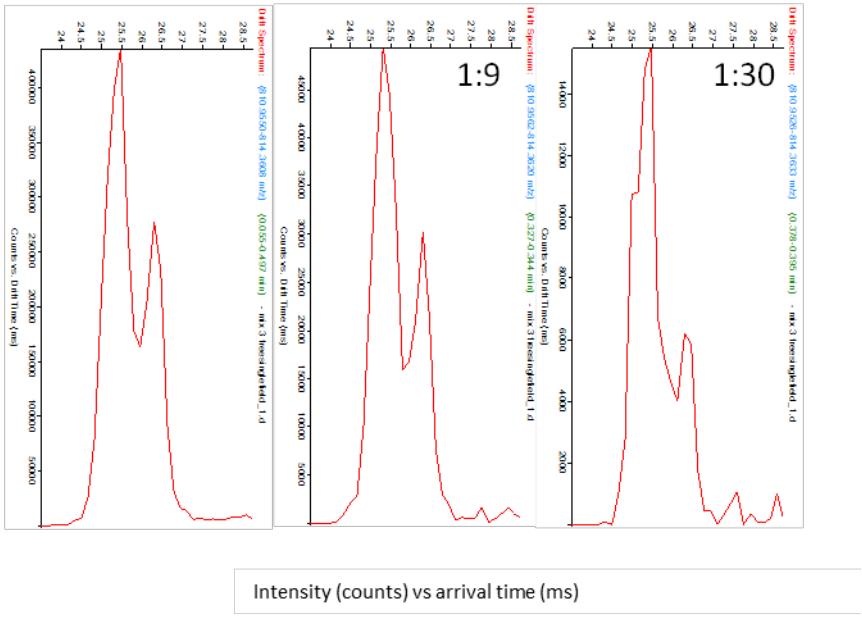

Fig. S63: IMS spectra obtained from $[M-2H]^{2-}$ ions of unlabeled standard **4** at different abundances (relatively 1, 1:9 and 1:30)

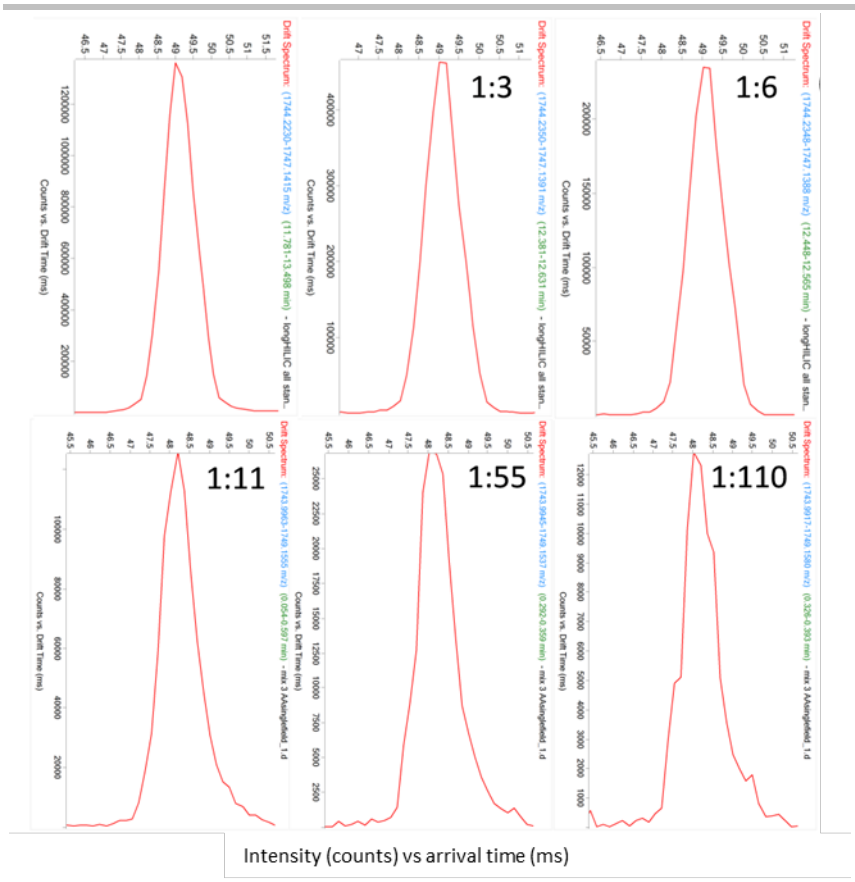

Fig. S64: IMS spectra obtained from $[M-H]^-$ ion of 2-AA standard **4** at different abundances (relatively 1, 1:3, 1:6, 1:11, 1:55 and 1:110)

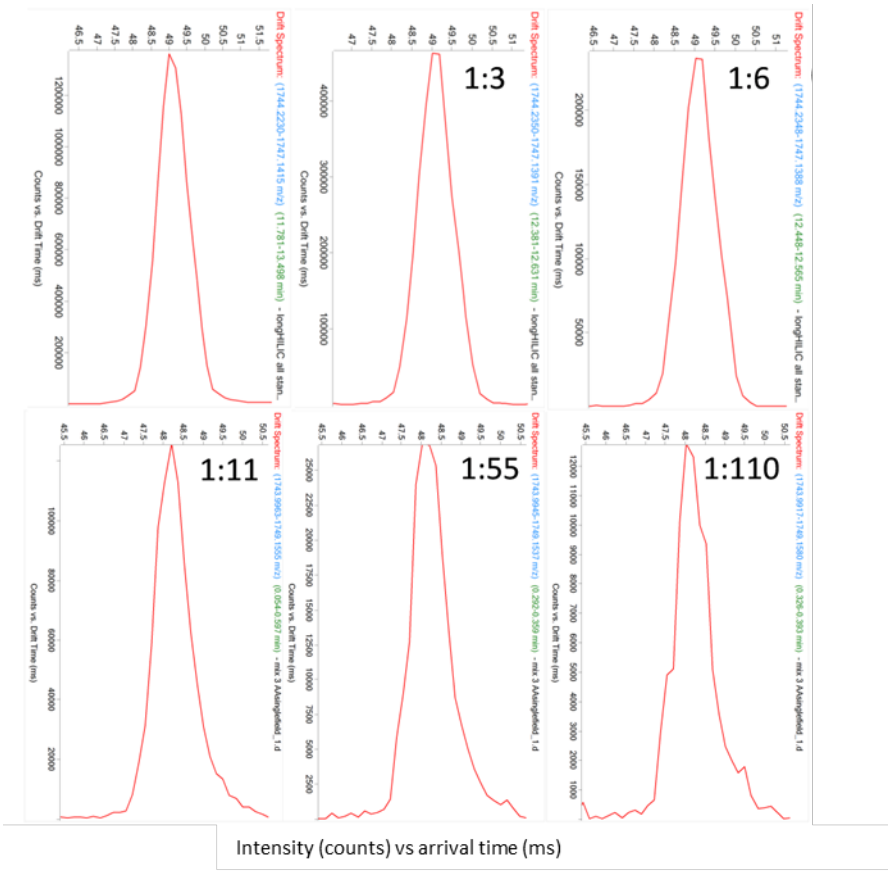

Fig. S65: IMS spectra obtained from $[M-2H]^{2-}$ ion of 2-AA standard **4** at different abundances (relatively 1, 1:2, 1:4, 1:8, 1:240 and 1:1500)

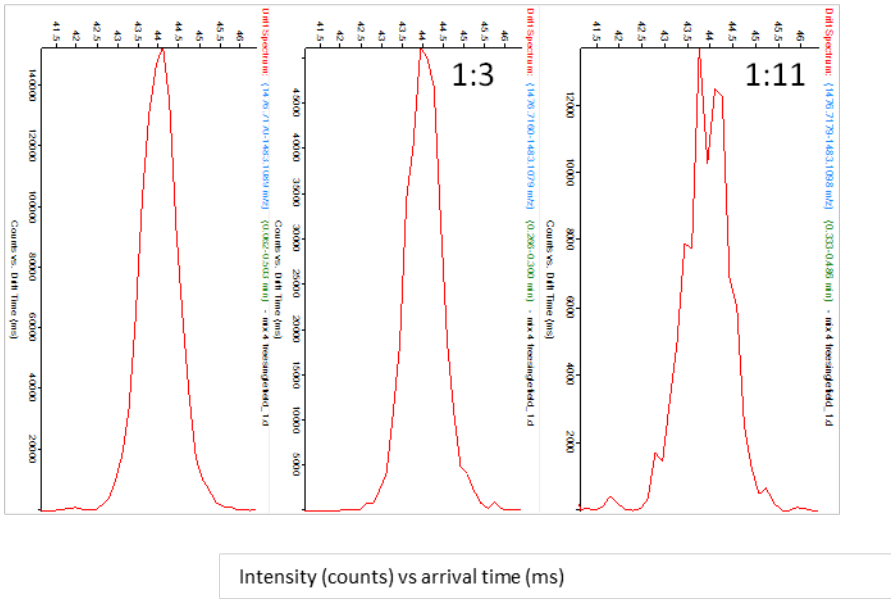

Fig. S66: IMS spectra obtained from $[M-H]^{-}$ ions of unlabeled standard **5** at different abundances (relatively 1, 1:3 and 1:11)

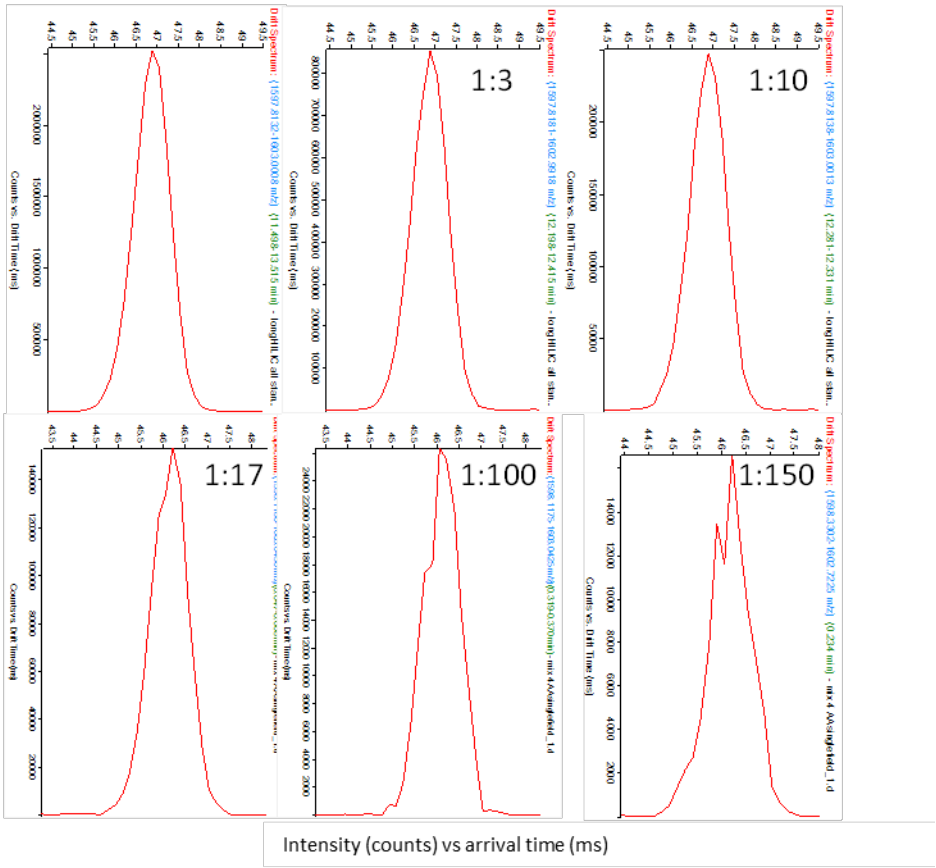

Fig. S67: IMS spectra obtained from $[M-H]^{-}$ ion of 2-AA standard **5** at different abundances (relatively 1, 1:3, 1:10, 1:17, 1:100 and 1:150)

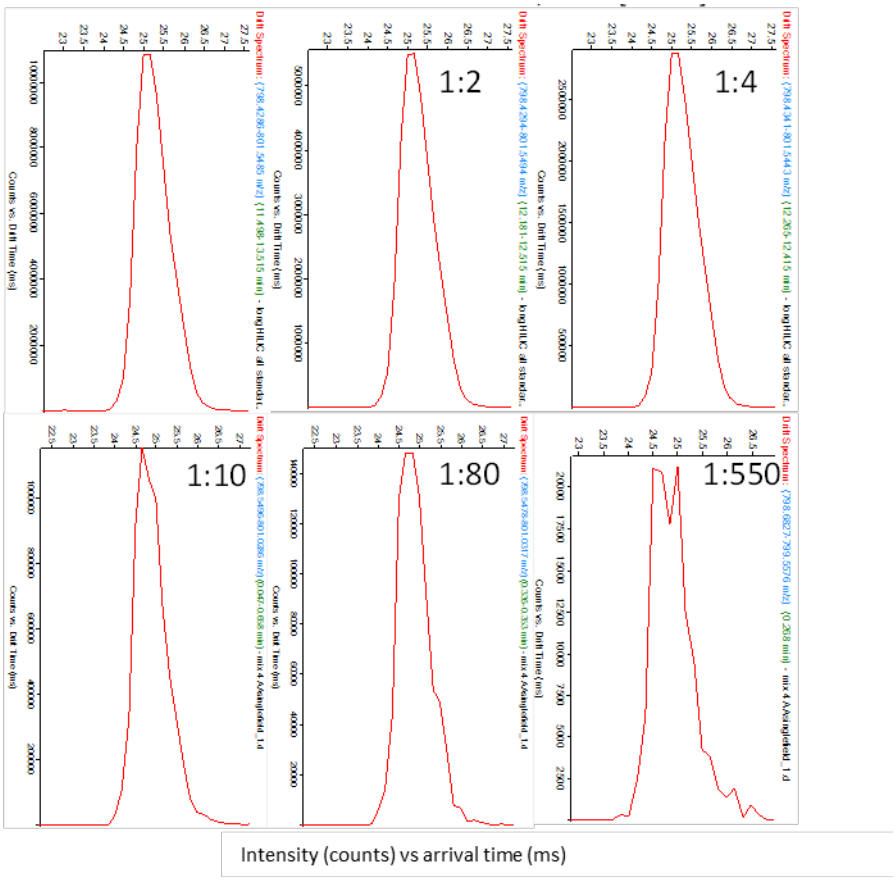

Fig. S68: IMS spectra obtained from $[M-2H]^{2-}$ ion of 2-AA standard **5** at different abundances (relatively 1, 1:2, 1:4, 1:10, 1:80 and 1:550)

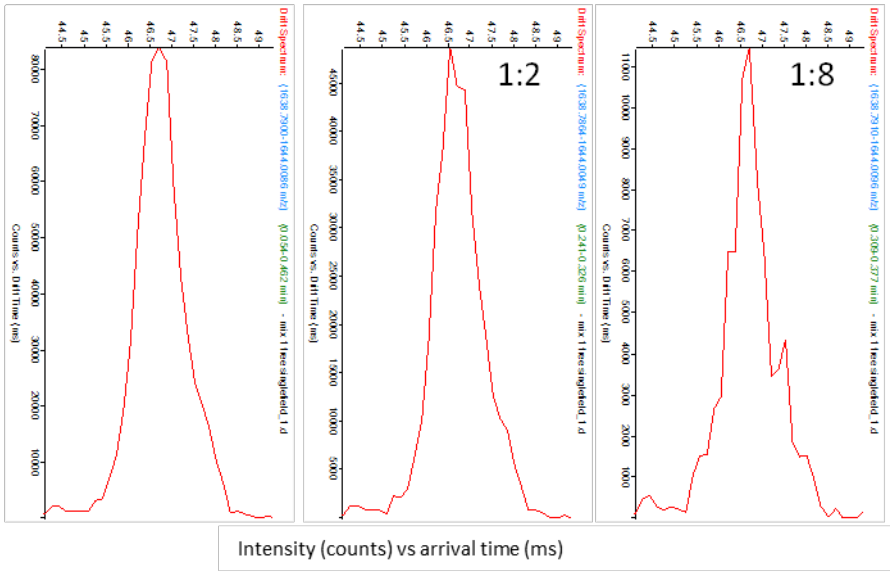

Fig. S69: ATDs of $[M-H]^{-}$ ions of unlabeled standard **6** at different dilutions (relatively 1, 1:2 and 1:8)

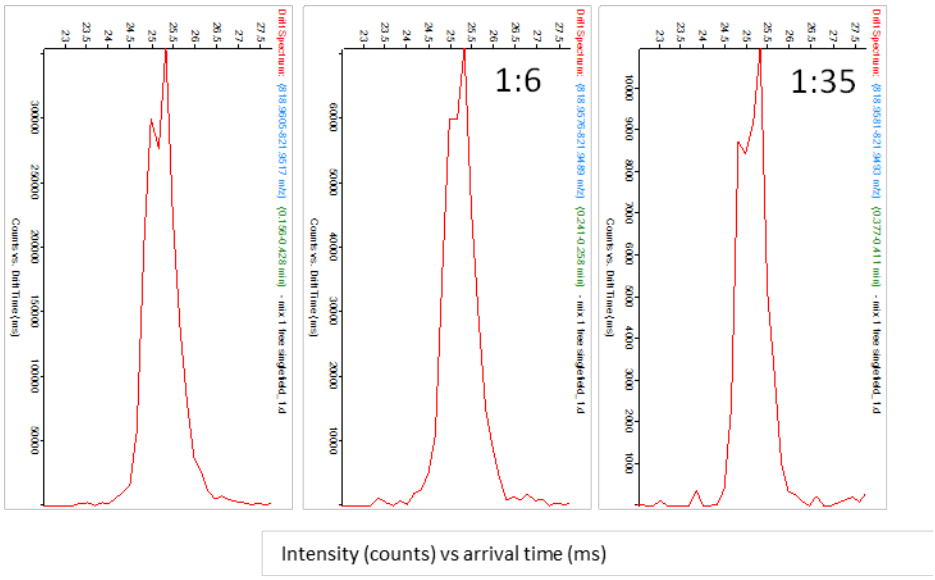

Fig. S70: ATDs of $[M-2H]^{2-}$ ions of unlabeled standard **6** at different dilutions (relatively 1, 1:6 and 1:35)

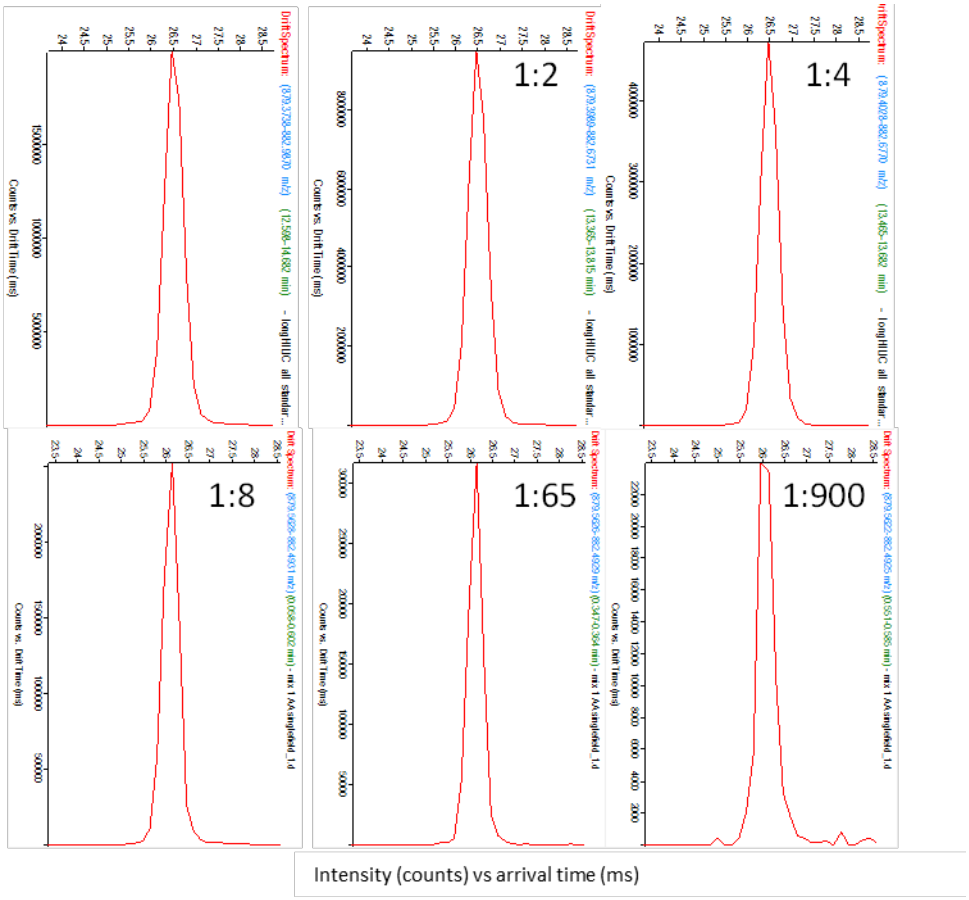

Fig. S71: ATDs of $[M-2H]^{2-}$ ion of 2-AA standard **6** at different dilutions (relatively 1, 1:2, 1:4, 1:8, 1:65 and 1:900)

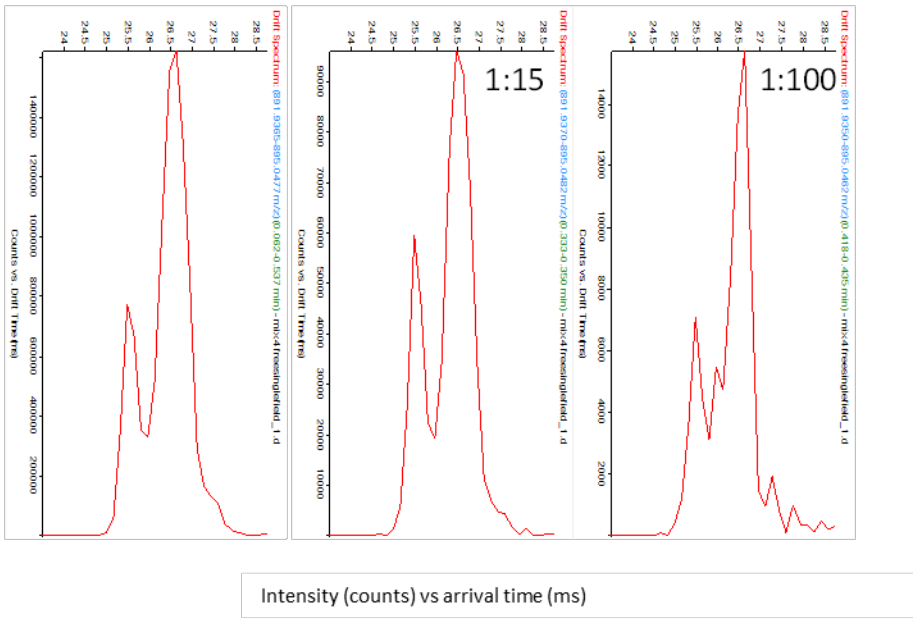

Fig. S72: IMS spectra obtained from $[M-2H]^{2-}$ ions of unlabeled standard **7** at different abundances (relatively 1, 1:15 and 1:100)

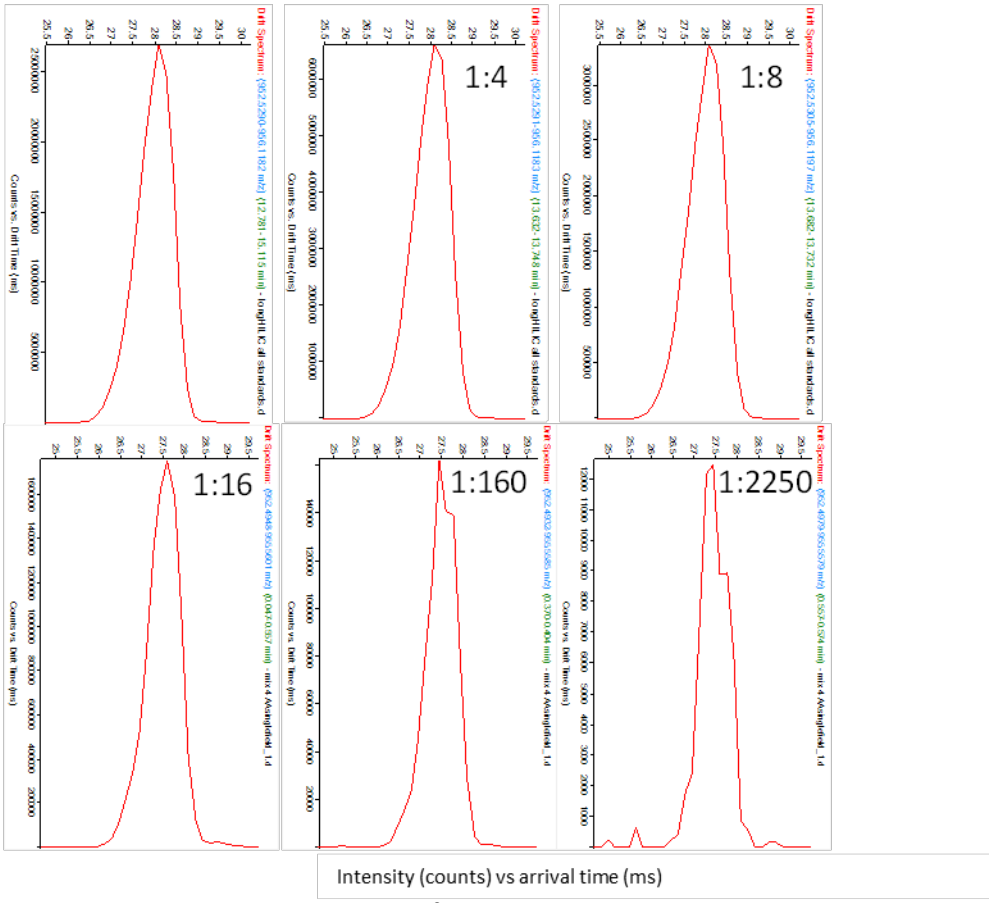

Fig. S73: IMS spectra obtained from $[M-2H]^{2-}$ ion of 2-AA standard **7** at different abundances (relatively 1, 1:14, 1:8, 1:16, 1:160 and 1:2250)

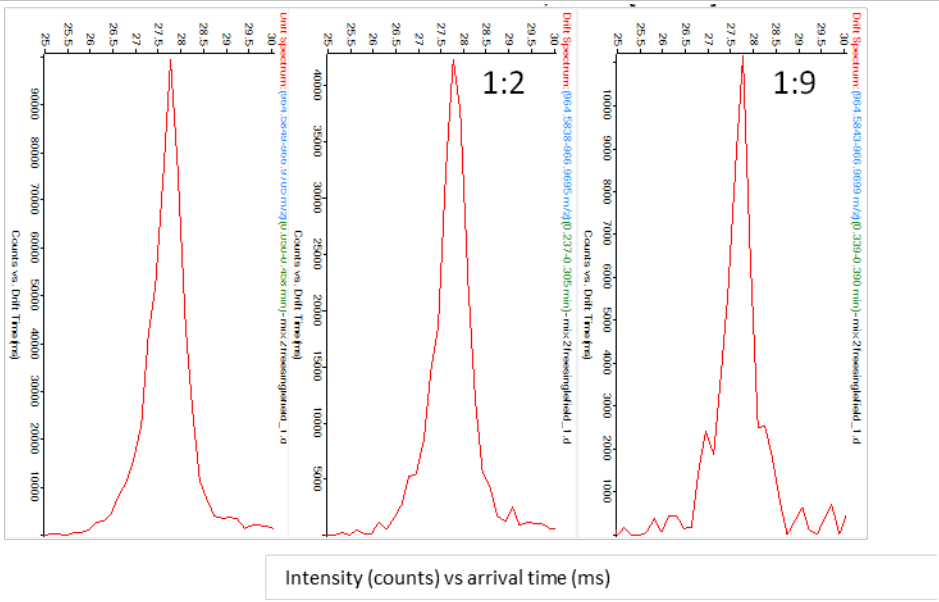

Fig. S74: ATDs of $[M-2H]^{2-}$ ions of free standard **8** at different dilutions (relatively 1, 1:2 and 1:9)

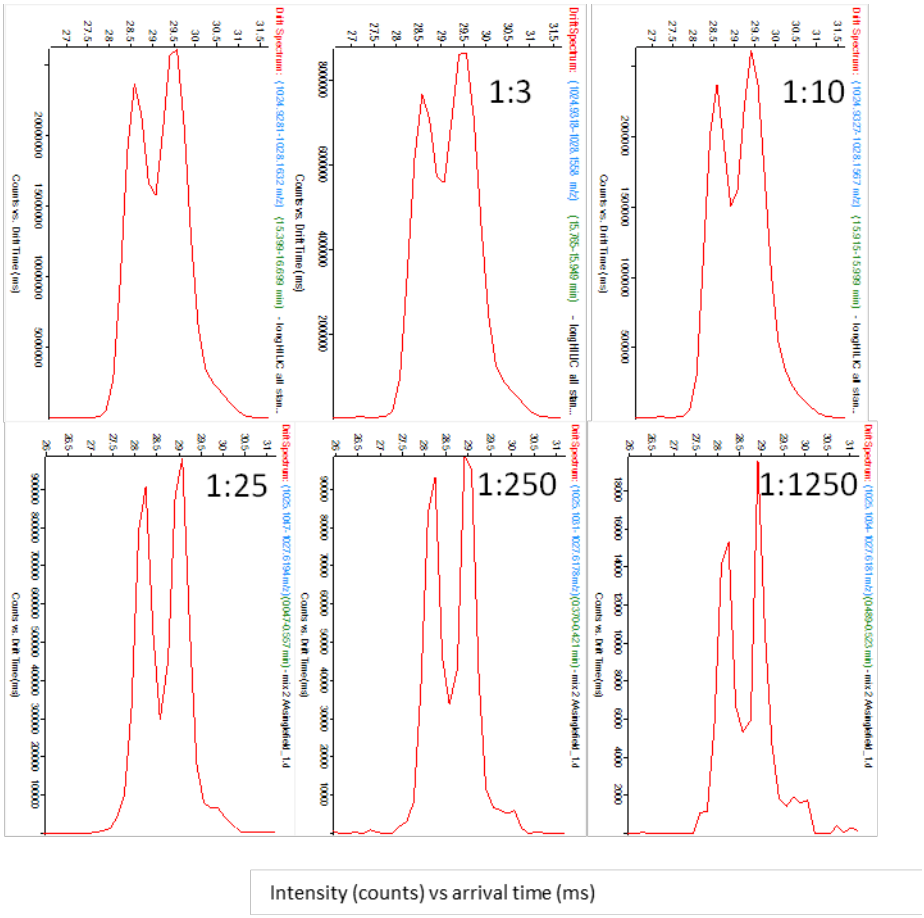

Fig. S75: ATDs of $[M-2H]^{2-}$ ions of 2-AA labelled standard **8** at different dilutions (relatively 1, 1:3, 1:10, 1:25, 1:250 and 1:1250)

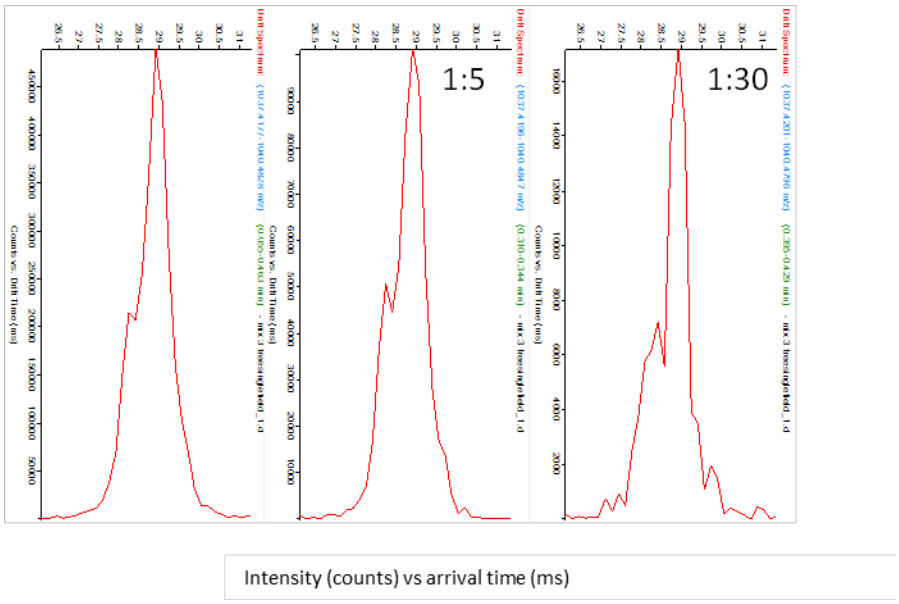

Fig. S76: IMS spectra obtained from $[M-2H]^{2-}$ ions of unlabeled standard **9** at different abundances (relatively 1, 1:5 and 1:30)

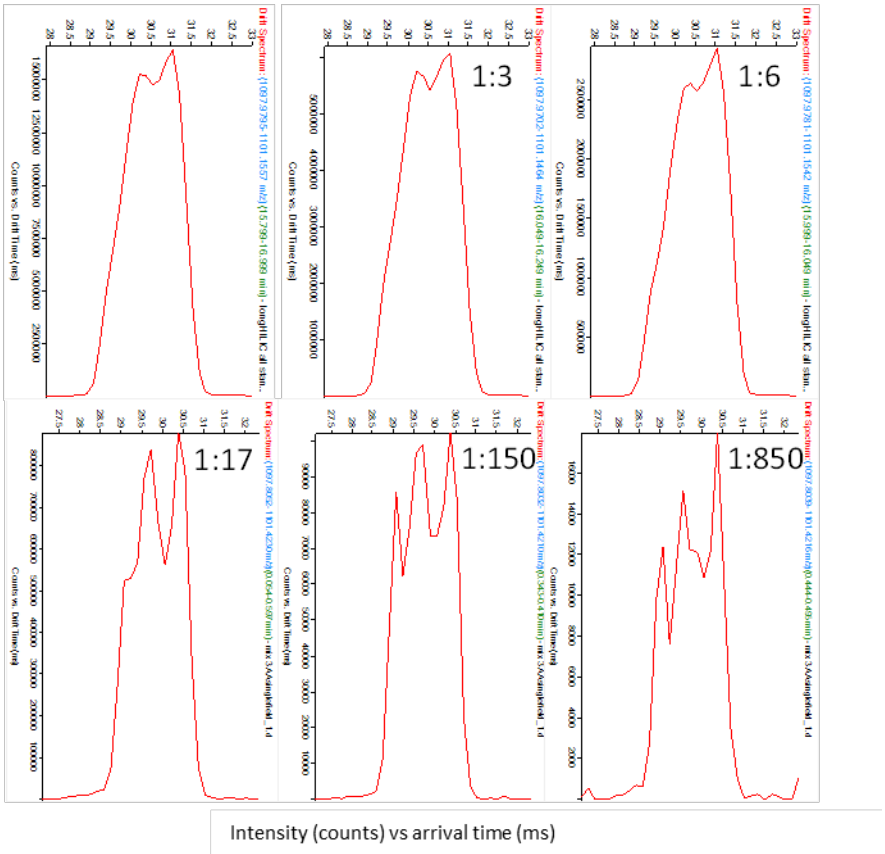

Fig. S77: IMS spectra obtained from $[M-2H]^{2-}$ ion of 2-AA standard **9** at different abundances (relatively 1, 1:3, 1:6, 1:17, 1:150 and 1:850)

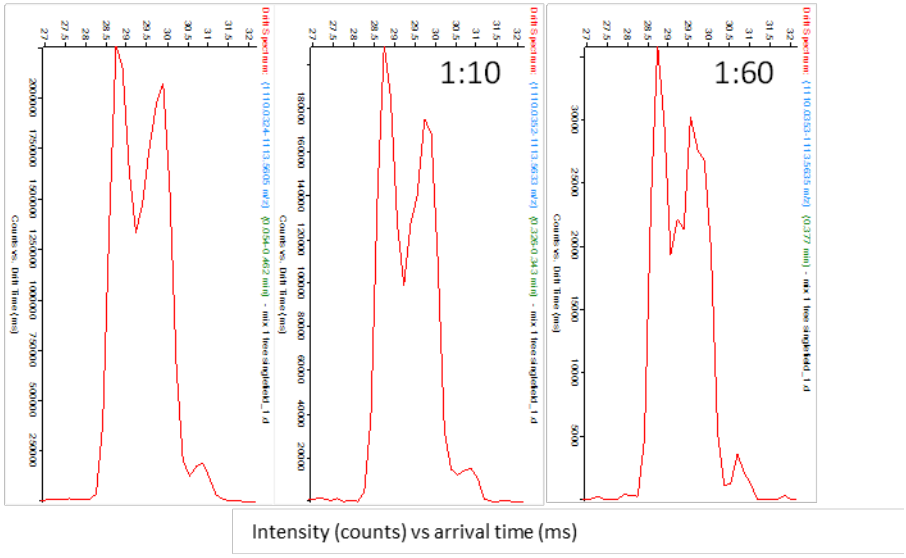

Fig. S78: ATDs of $[M-2H]^{2-}$ ions of unlabeled standard **10** at different dilutions (relatively 1, 1:10 and 1:60)

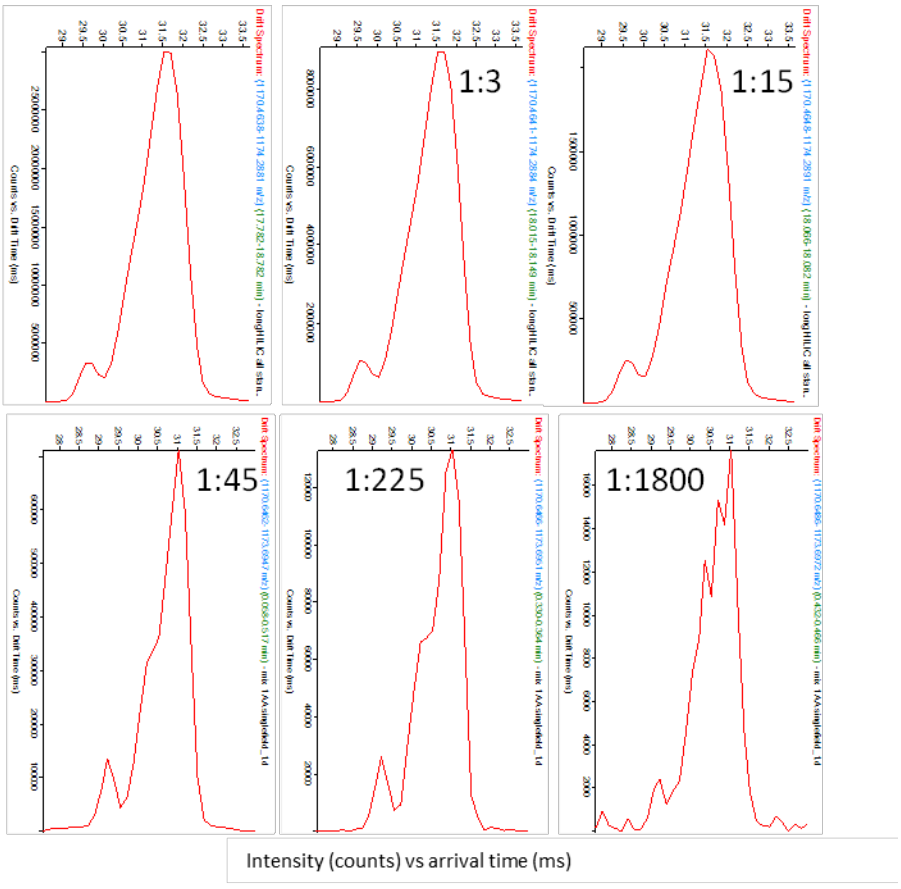

Fig. S79: ATDs of $[M-2H]^{2-}$ ions of 2-AA labelled standard **10** at different dilutions (relatively 1, 1:3, 1:15, 1:45, 1:225 and 1:1800)

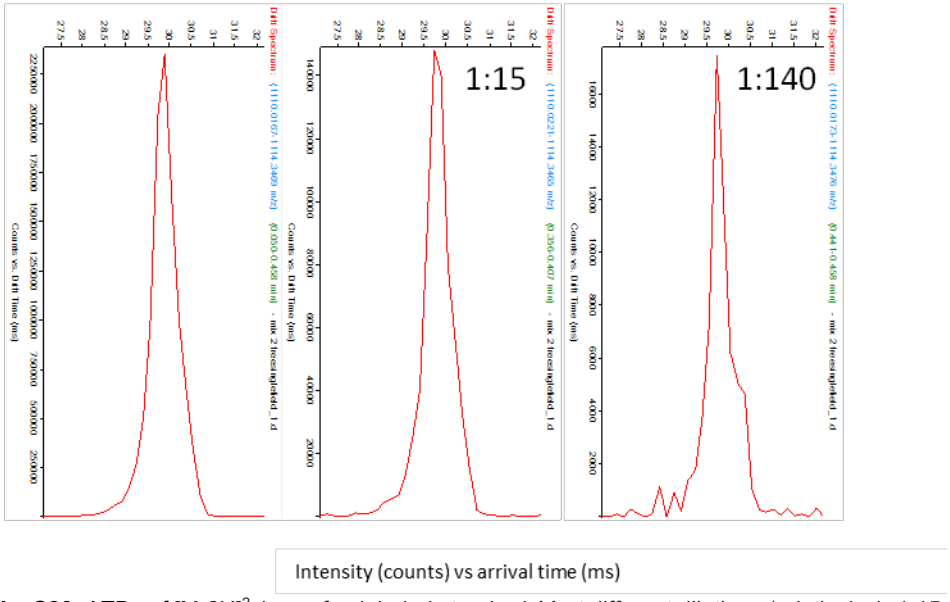

Fig. S80: ATDs of $[M-2H]^{2-}$ ions of unlabeled standard **11** at different dilutions (relatively 1, 1:15 and 1:140)

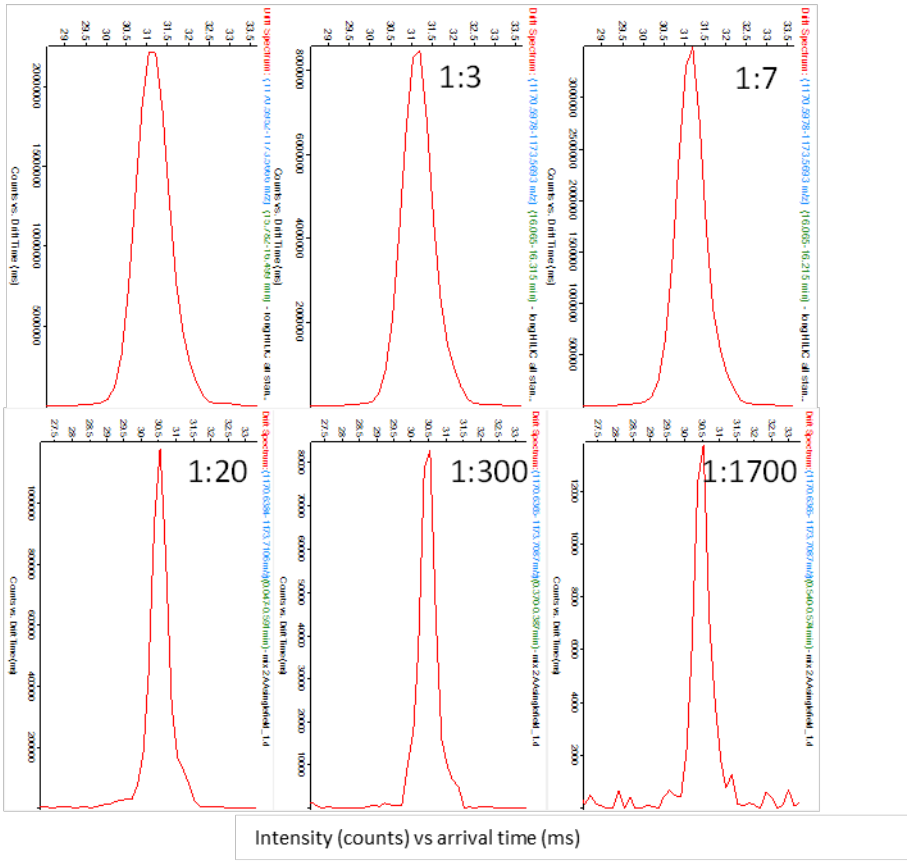

Fig. S81: ATDs of $[M-2H]^{2-}$ ions of 2-AA labelled standard **11** at different dilutions (relatively 1, 1:3, 1:7, 1:20, 1:300 and 1:1700)

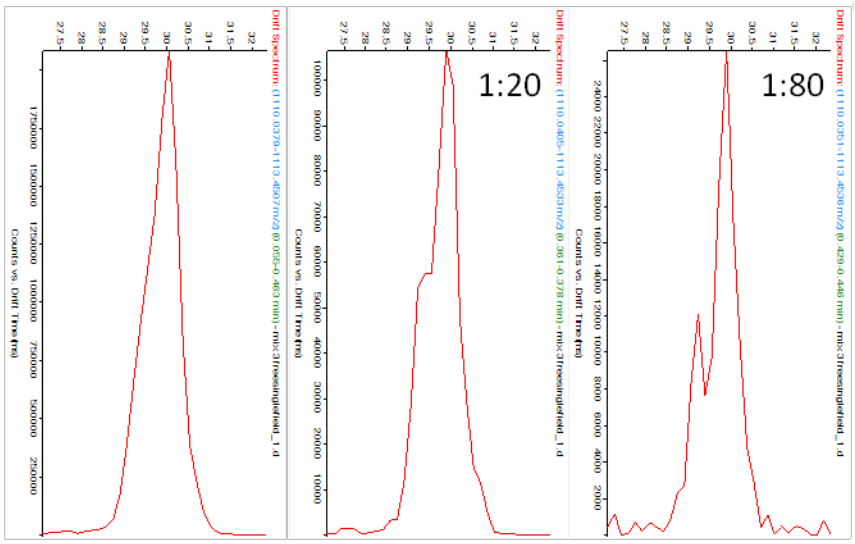

Fig. S82: ATDs of $[M-2H]^{2-}$ ions of unlabeled standard **12** at different dilutions (relatively 1, 1:20 and 1:80)

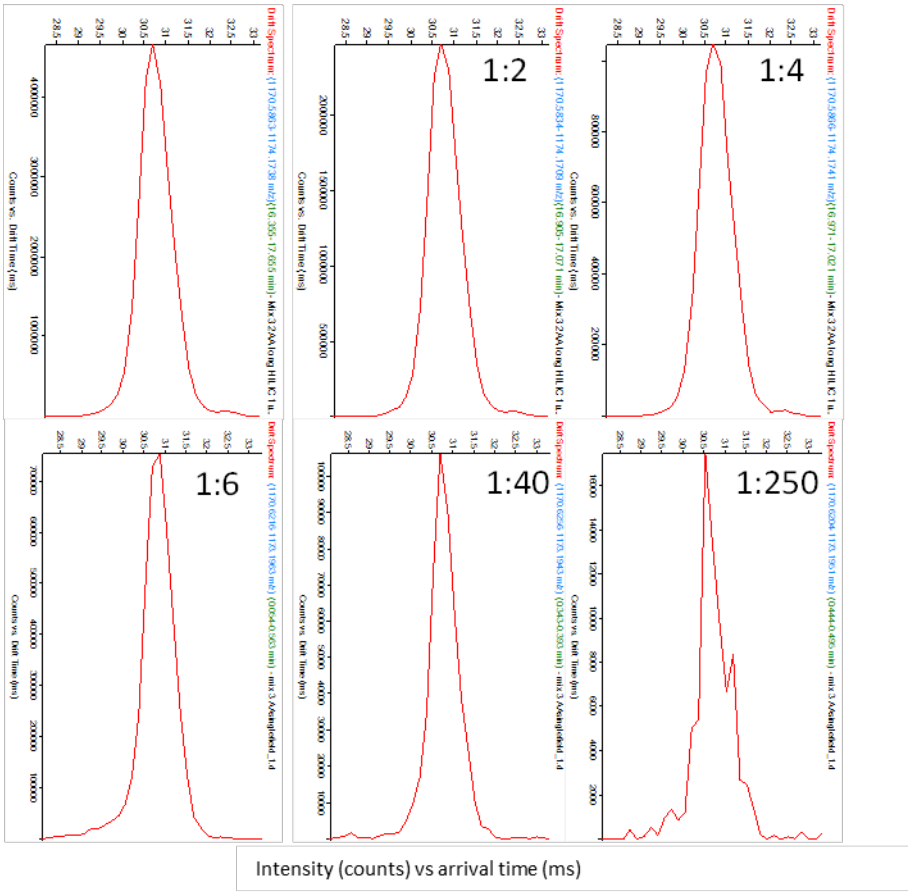

Fig. S83: ATDs of $[M-2H]^{2-}$ ions of 2-AA labelled standard **12** at different dilutions (relatively 1, 1:2, 1:4, 1:6, 1:40 and 1:250)

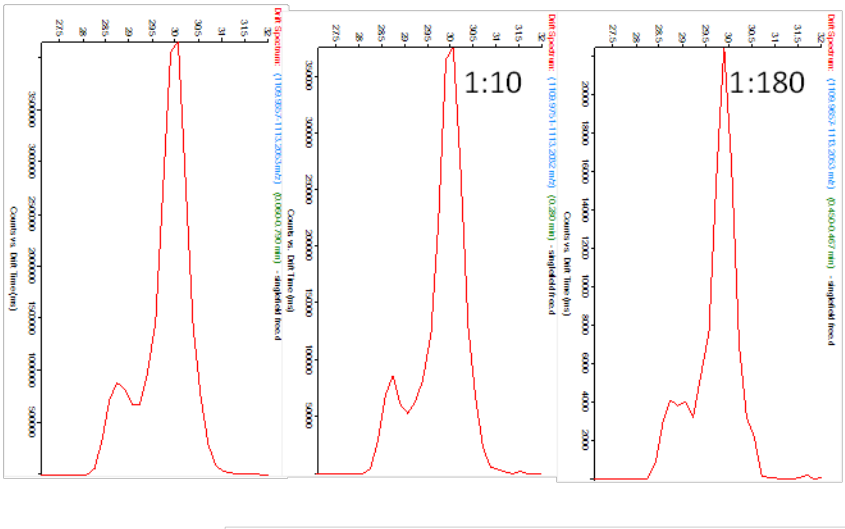

Fig. S84: ATDs of $[M-2H]^{2-}$ ions of unlabeled standard **13** at different dilutions (relatively 1, 1:10 and 1:180)

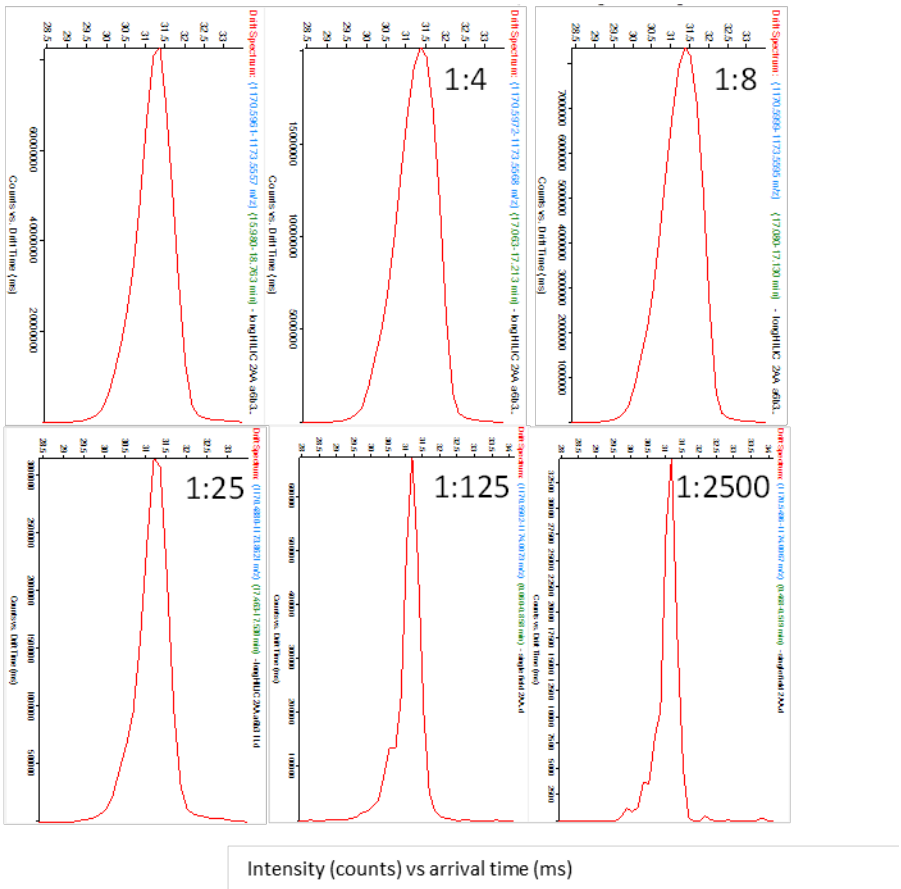

Fig. S85: ATDs of $[M-2H]^{2-}$ ions of 2-AA labelled standard **13** at different dilutions (relatively 1, 1:4, 1:8, 1:25, 1:125 and 1:2500)

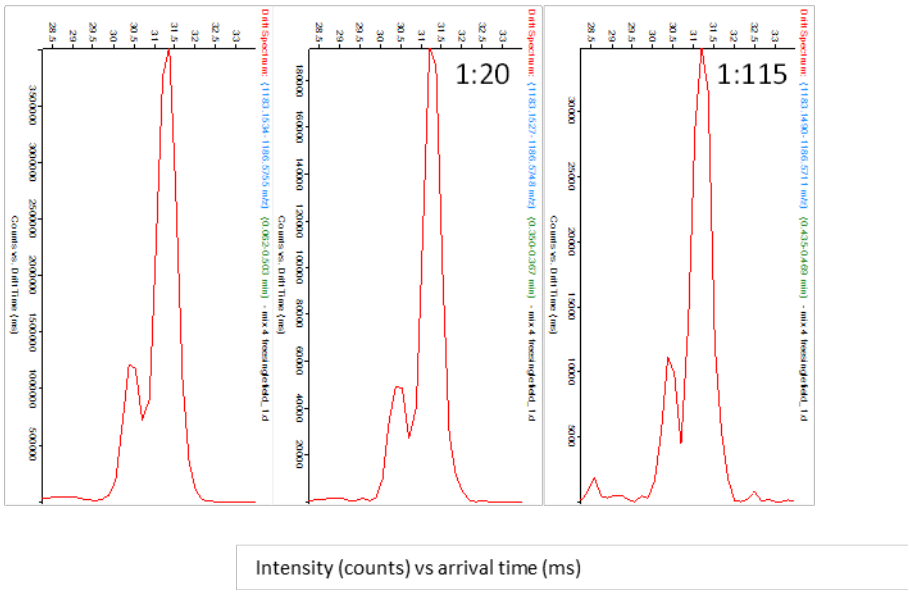

Fig. S86: IMS spectra obtained from $[M-2H]^{2-}$ ions of unlabeled standard **14** at different abundances (relatively 1, 1:20 and 1:115)

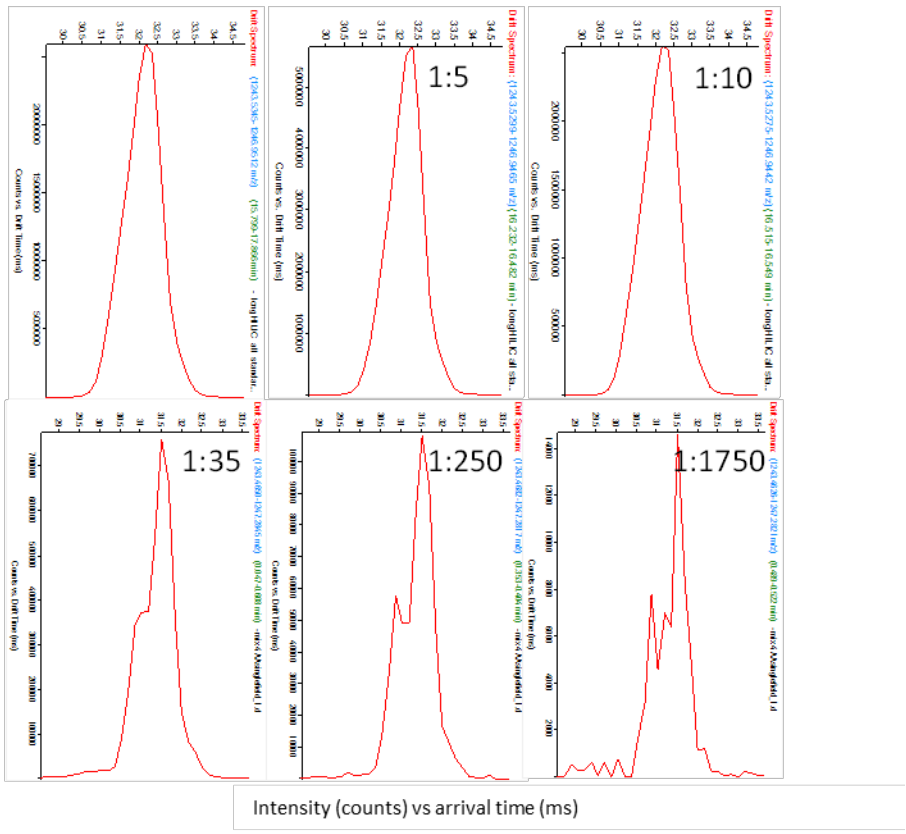

Fig. S87: IMS spectra obtained from $[M-2H]^{2-}$ ion of 2-AA standard **14** at different abundances (relatively 1, 1:7 and 1:50)

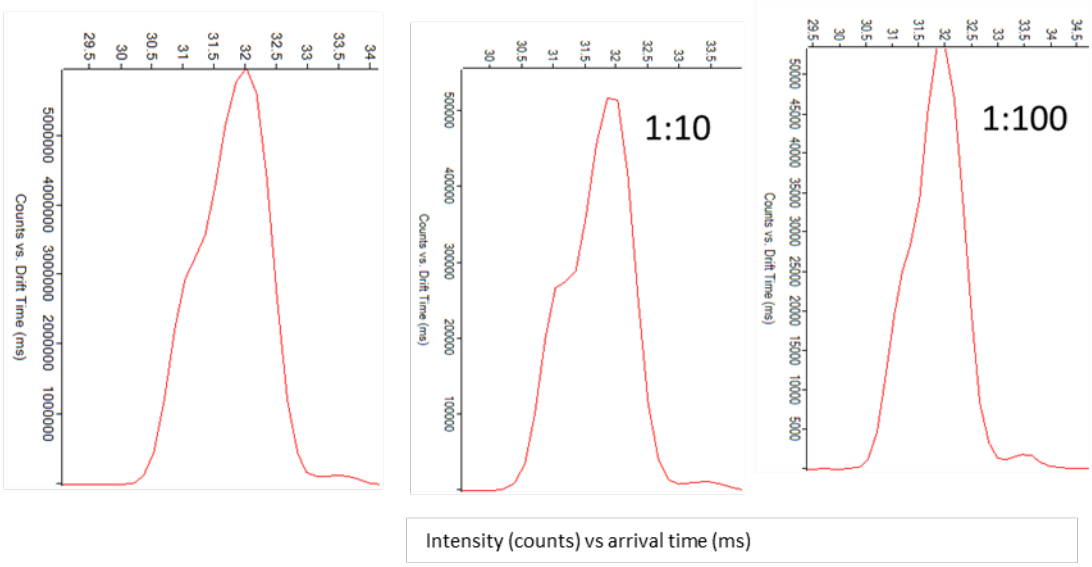

Fig. S88: IMS spectra obtained from $[M-2H]^{2-}$ ion of unlabeled standard **15** at different abundances (relatively 1, 1:7 and 1:50)

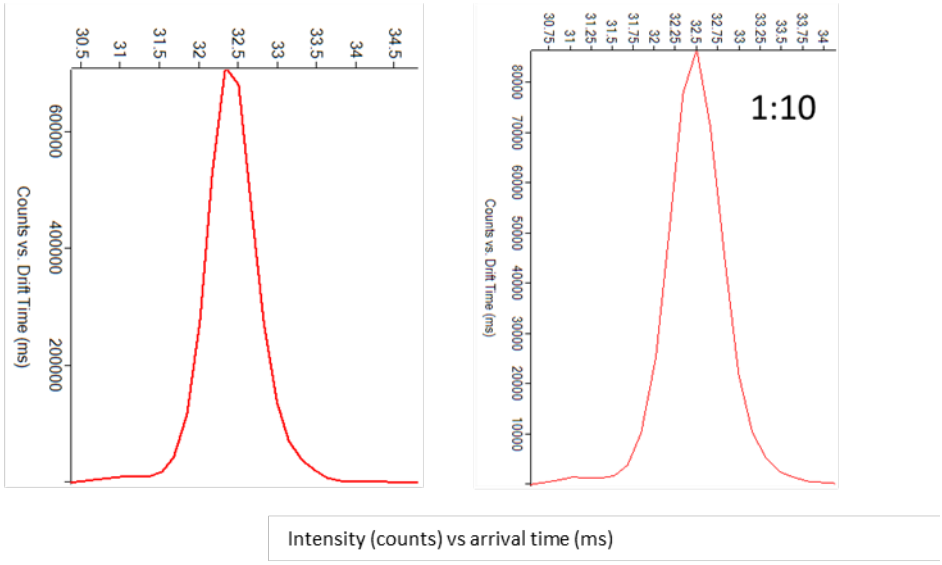

Fig. S89: IMS spectra obtained from $[M-2H]^{2-}$ ion of 2-AA labelled standard **15** at different abundances (relatively 1, 1:7 and 1:50)

2.4 Effect of solvent composition (ACN:water ratio) on gas phase conformation of unlabeled standards

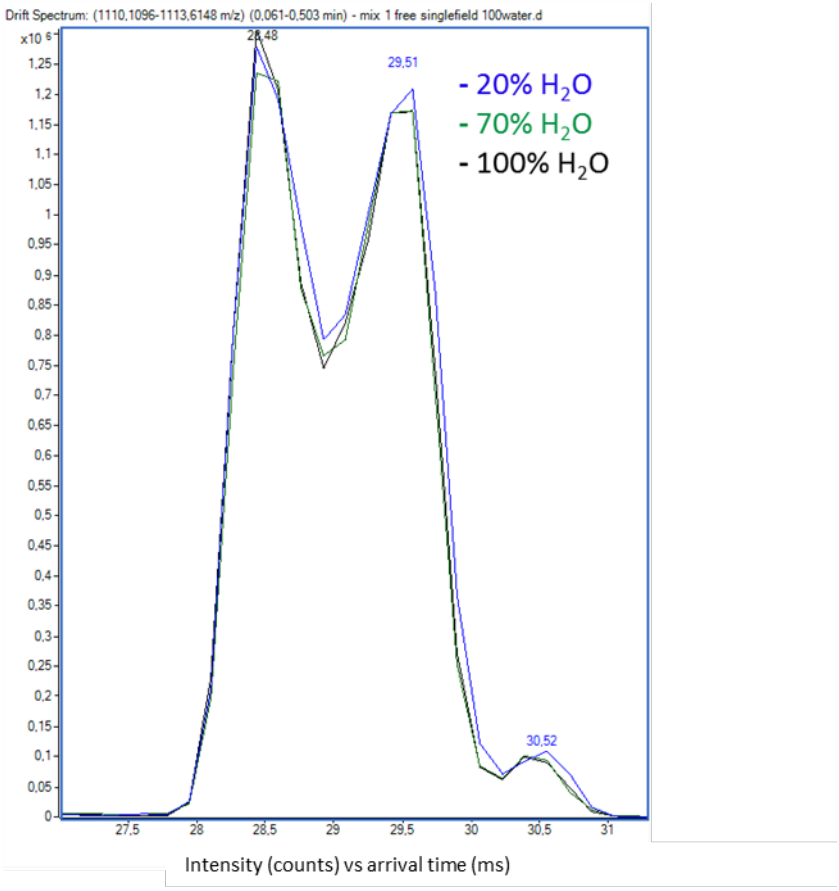

Fig. S90: ATD obtained from $[M-2H]^{2-}$ ions of unlabeled standard **10** at different ACN:H_2O solvent ratios (20% H_2O in blue, 70% H_2O in green and 100% H_2O in black)

2.5 ATDs of HILIC-separated anomers of standards

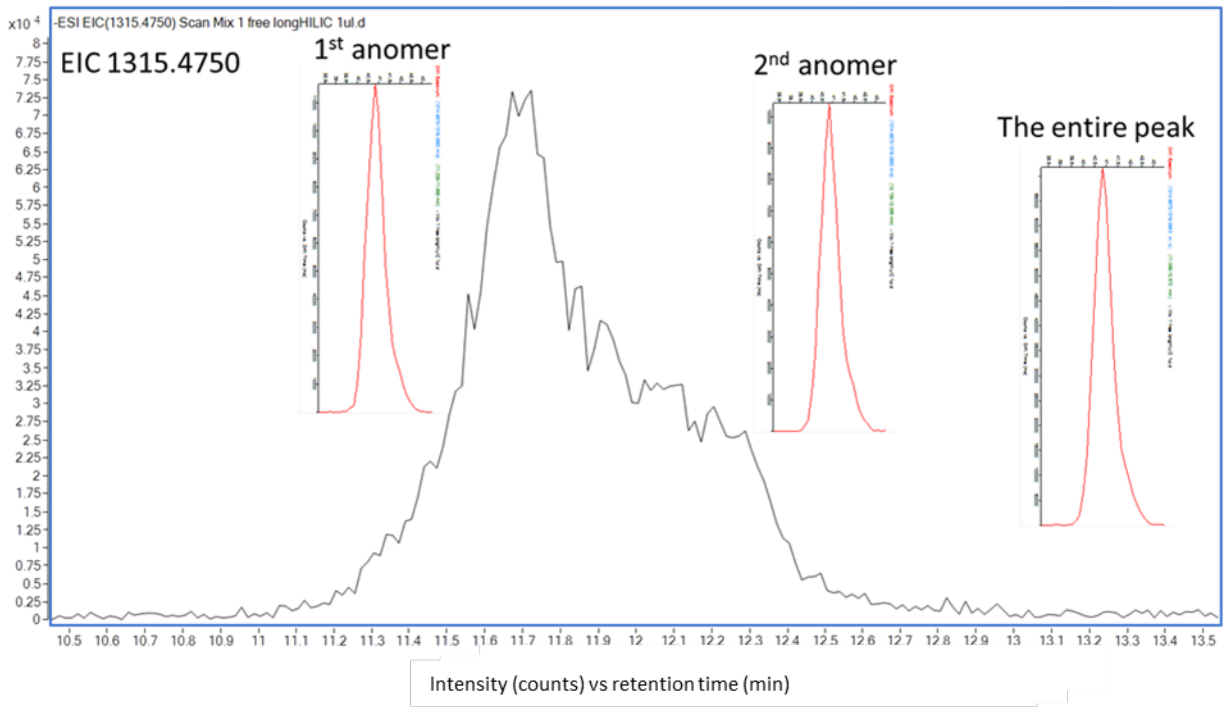

Fig. S91: ATDs (in red) from $[M-H]^-$ ions of unlabeled standard **1** anomers separated by HILIC (in black). (in black). A summed ATD of both anomers is shown on the right

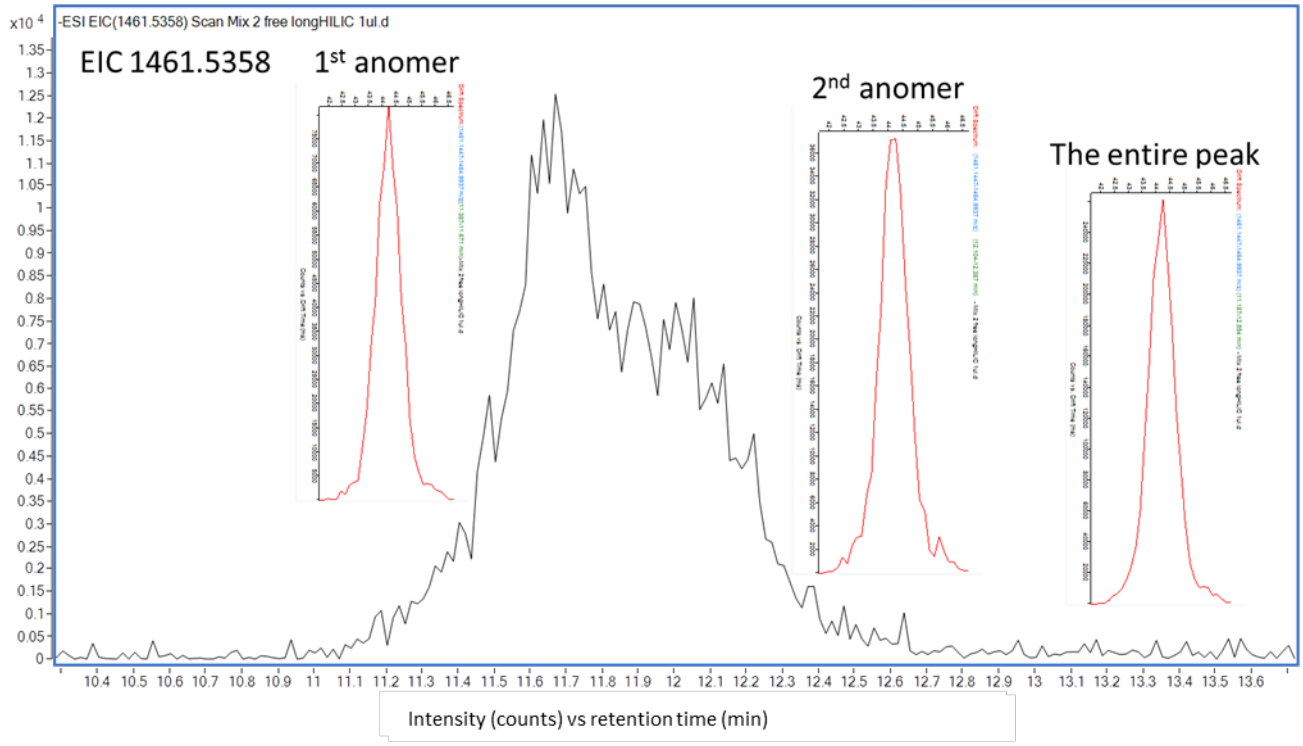

Fig. S92: ATD from $[M-H]^-$ ions of unlabeled standard **2** anomers separated by HILIC (in black). A summed ATD of both anomers is shown on the right

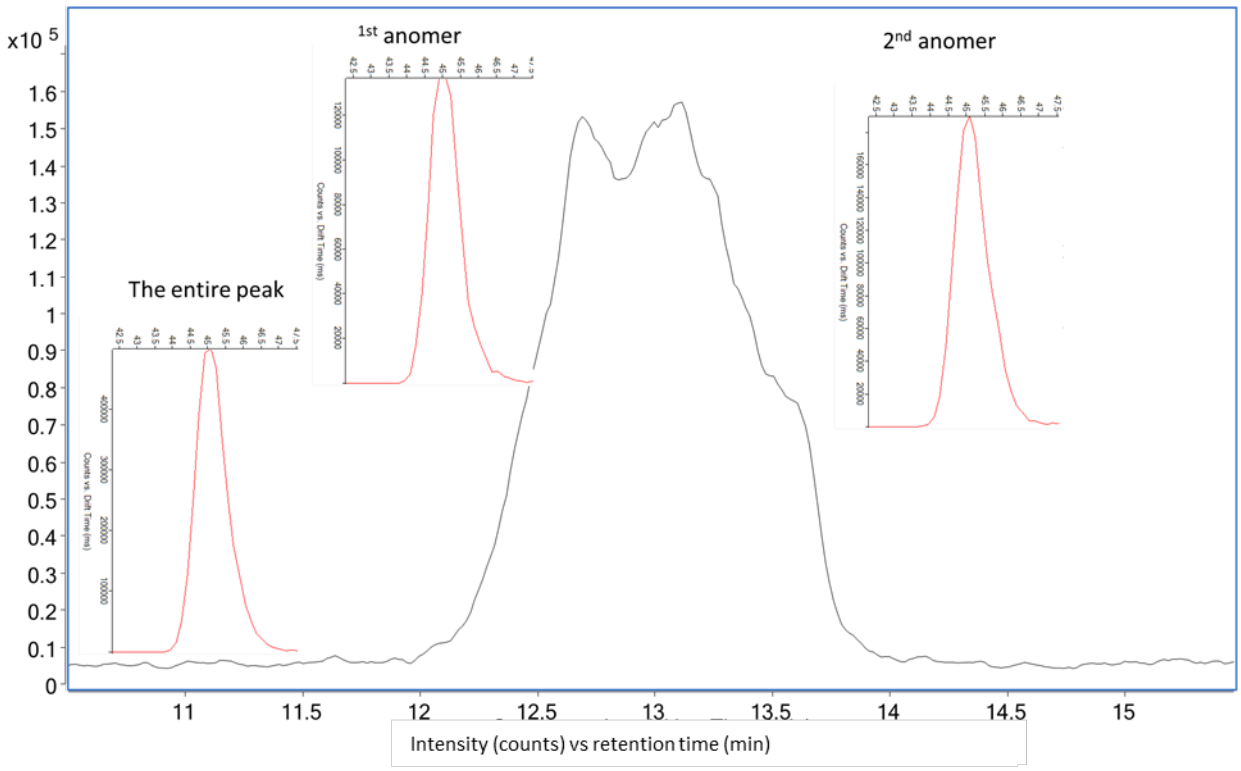

Fig. S93: ATD from [M-H]$^-$ ions of unlabeled standard **3** anomers separated by HILIC (in black). A summed ATD of both anomers is shown on the right

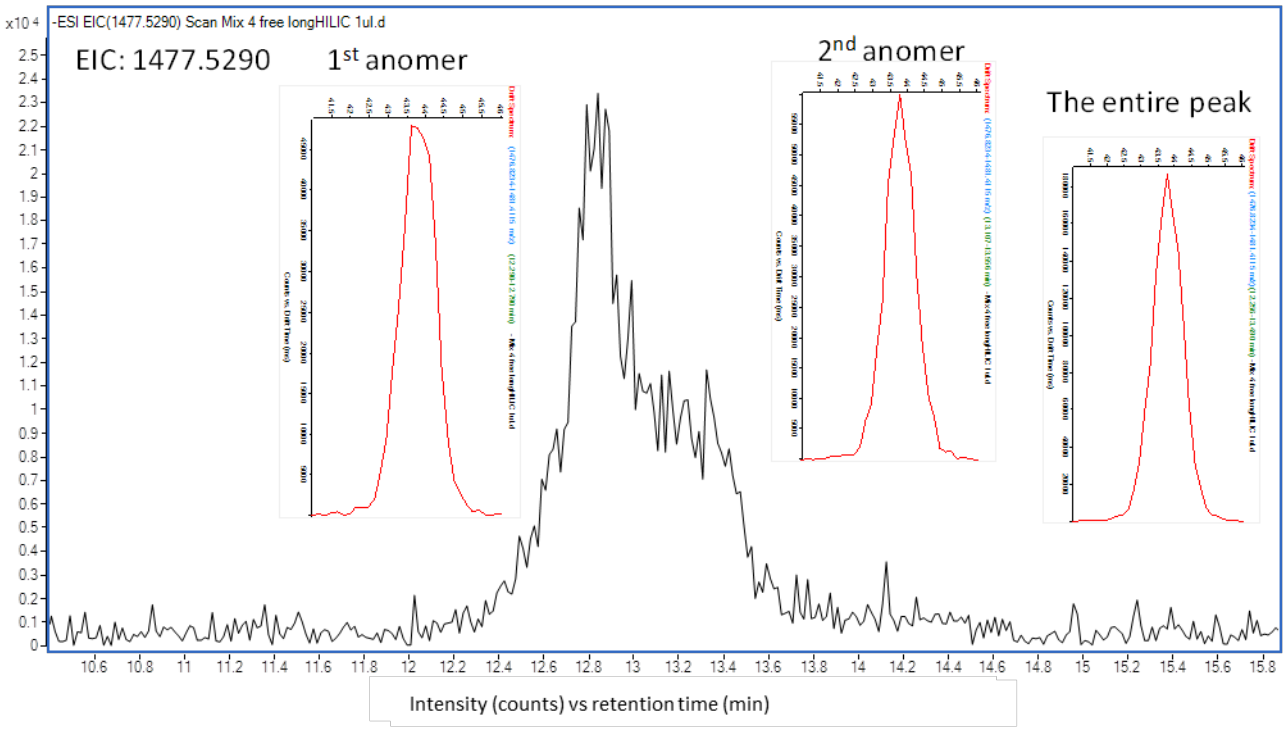

Fig. S94: ATDs (in red) from[M-H]$^-$ ions of unlabeled standard **4** anomers separated by HILIC (in black). A summed ATD of both anomers is shown on the right

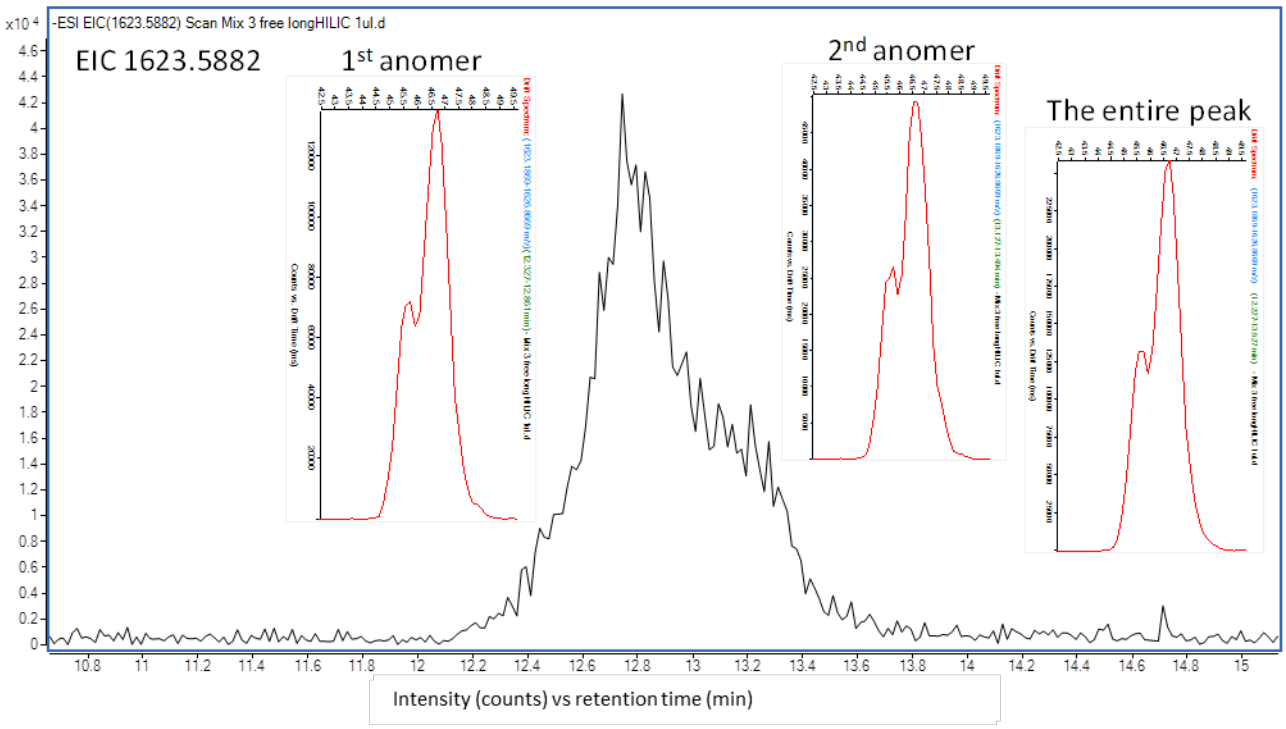

Fig. S95: ATDs (in red) from[M-H]$^{-}$ ions of unlabeled standard **5** anomers separated by HILIC (in black). A summed ATD of both anomers is shown on the right

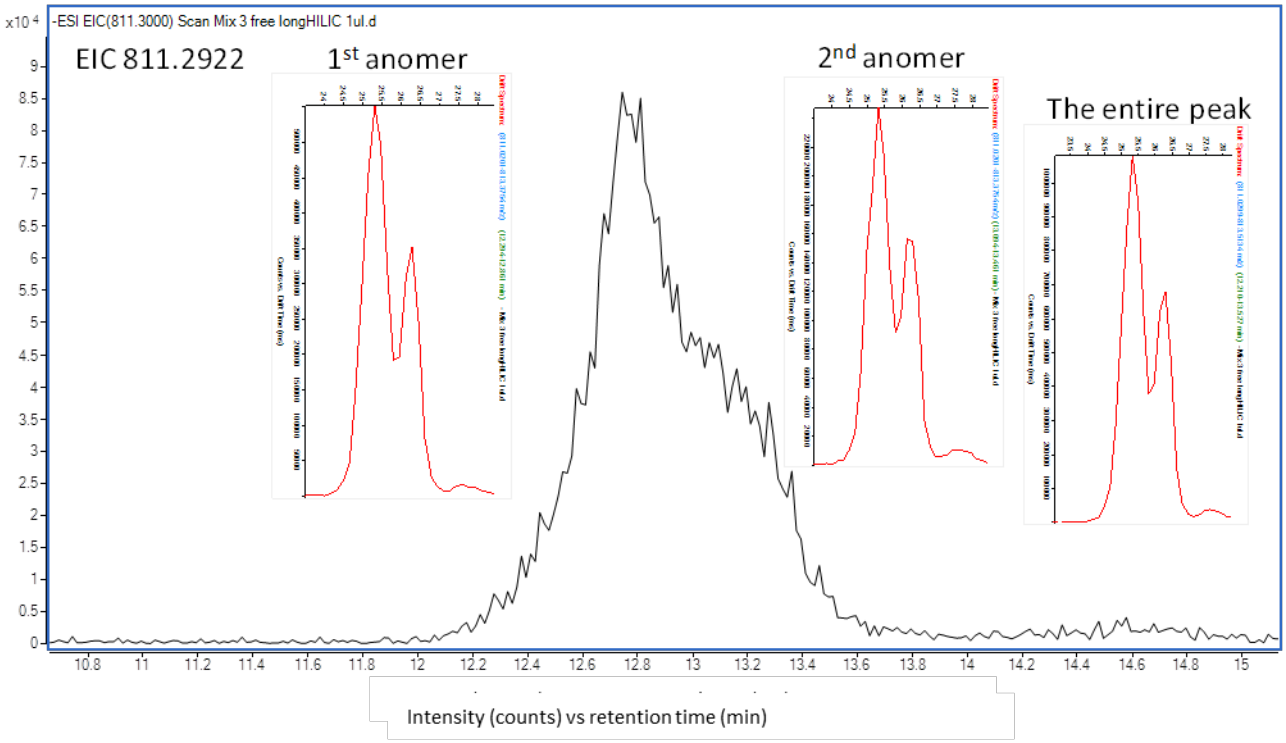

Fig. S96: ATDs (in red) from[M-2H]$^{2-}$ ions of unlabeled standard **5** anomers separated by HILIC (in black). A summed ATD of both anomers is shown on the right

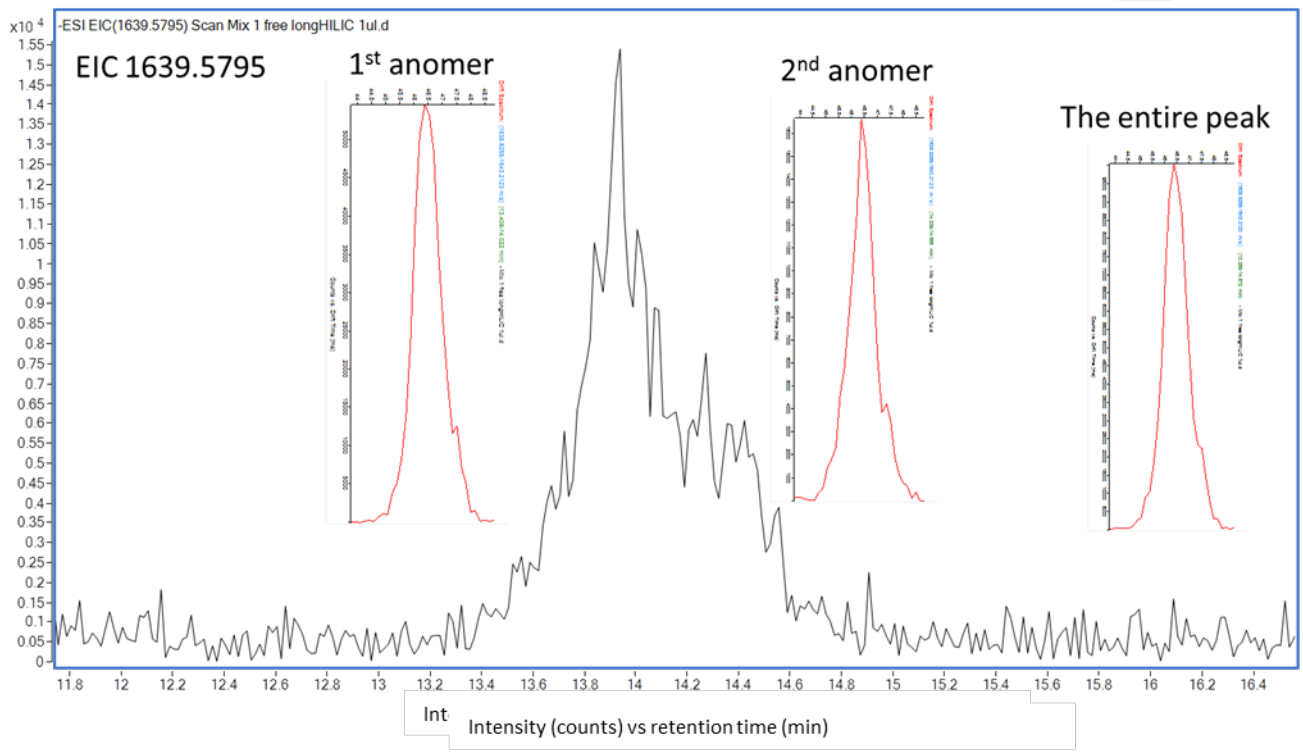

Fig. S97: ATDs (in red) from[M-H]$^-$ ions of unlabeled standard **6** anomers separated by HILIC (in black). A summed ATD of both anomers is shown on the right

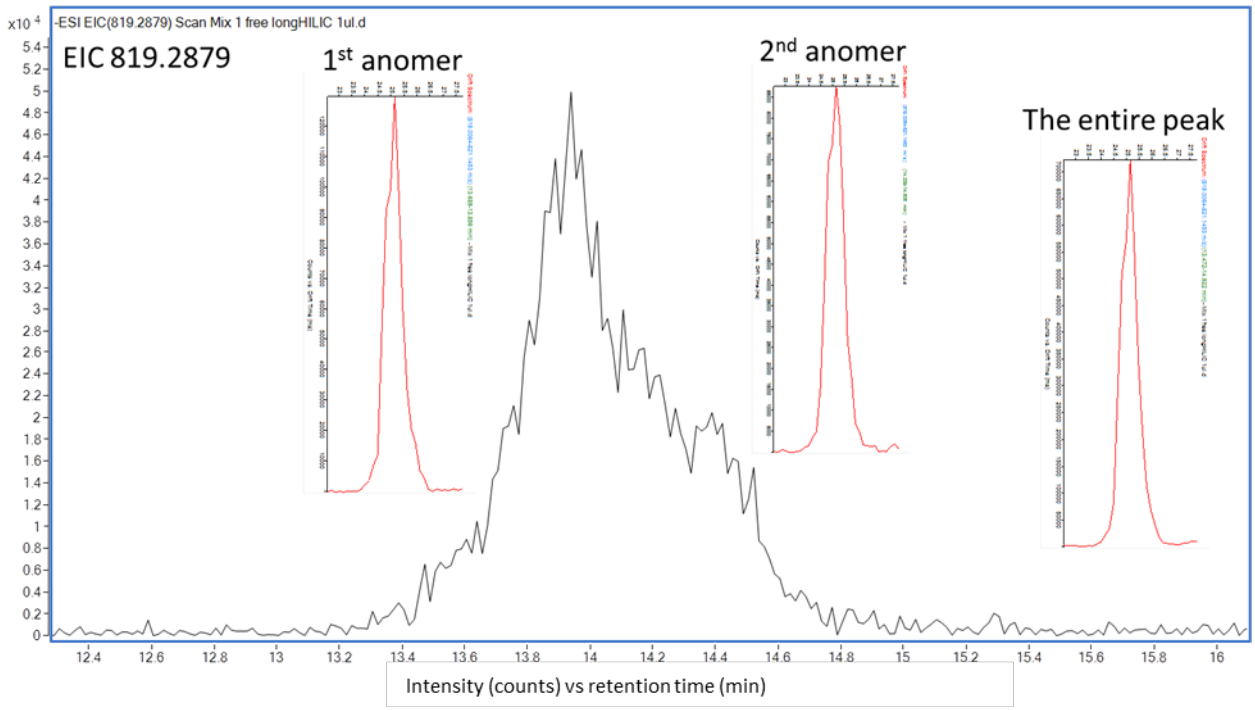

Fig. S98: ATDs (in red) from[M-2H]2- ions of unlabeled standard **6** anomers separated by HILIC (in black). A summed ATD of both anomers is shown on the right

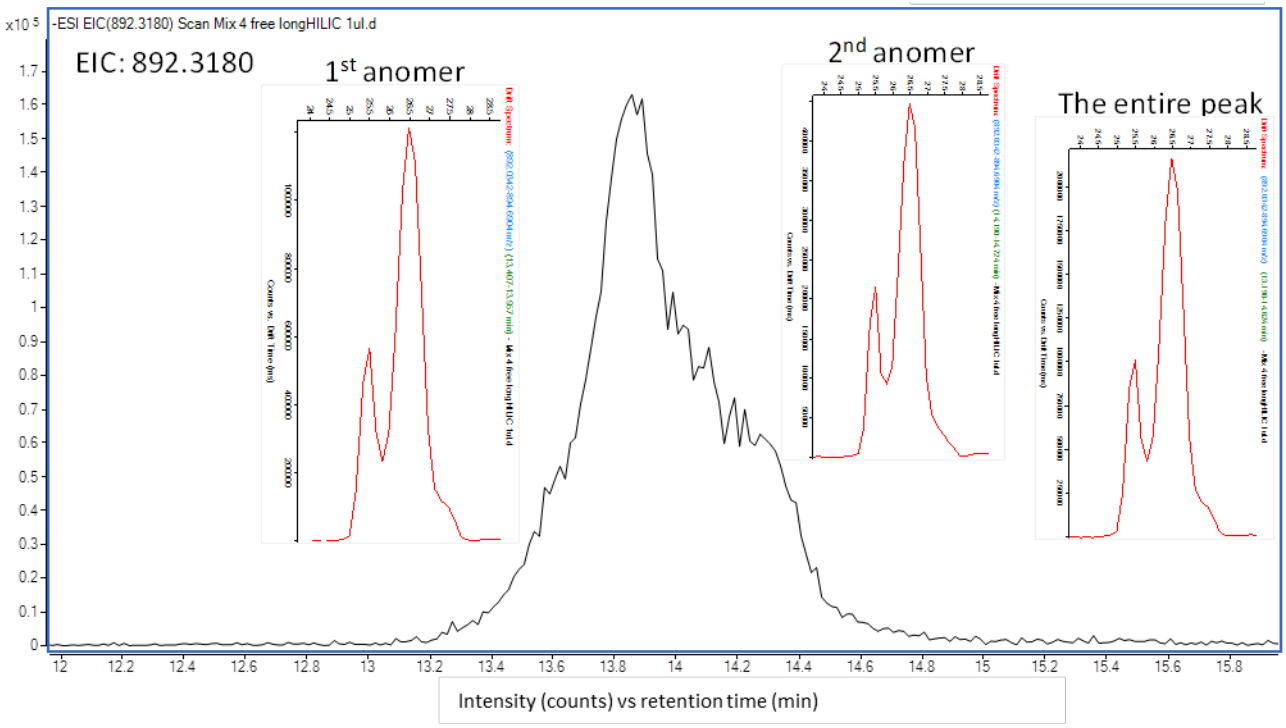

Fig. S99: ATDs (in red) from[M-2H]2- ions of unlabeled standard **7** anomers separated by HILIC (in black). A summed ATD of both anomers is shown on the right

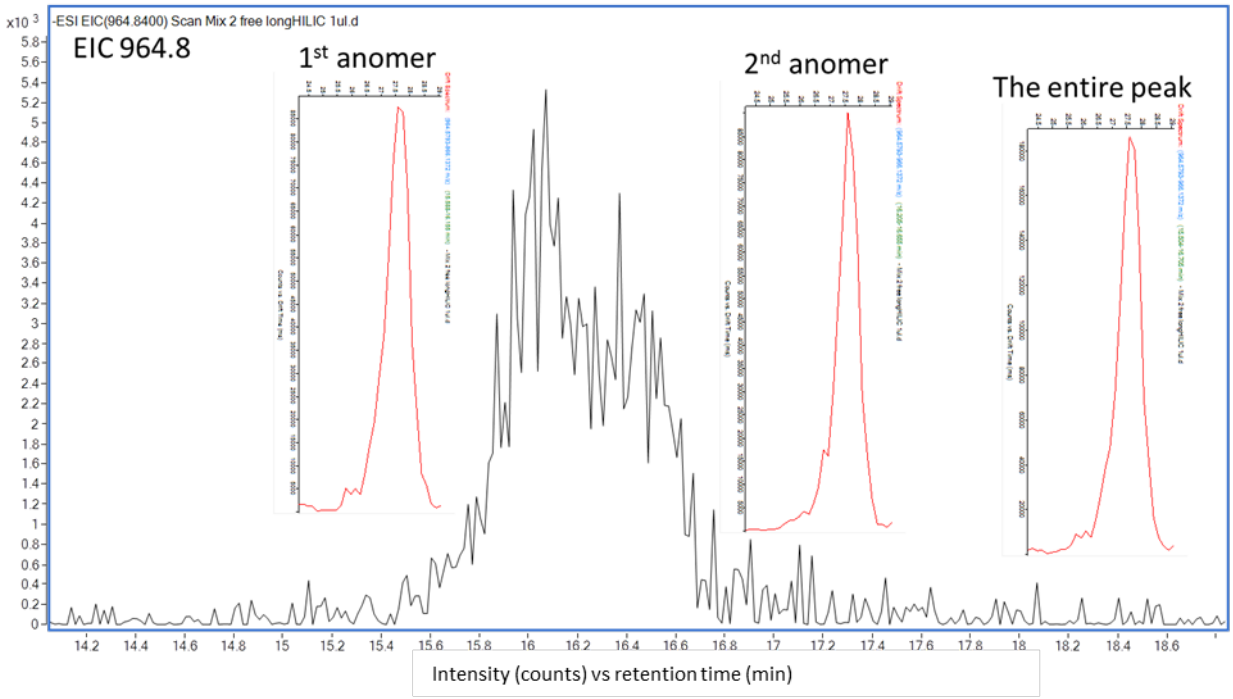

Fig. S100: ATDs (in red) from[M-2H]2- ions of unlabeled standard **8** anomers separated by HILIC (in black). A summed ATD of both anomers is shown on the right

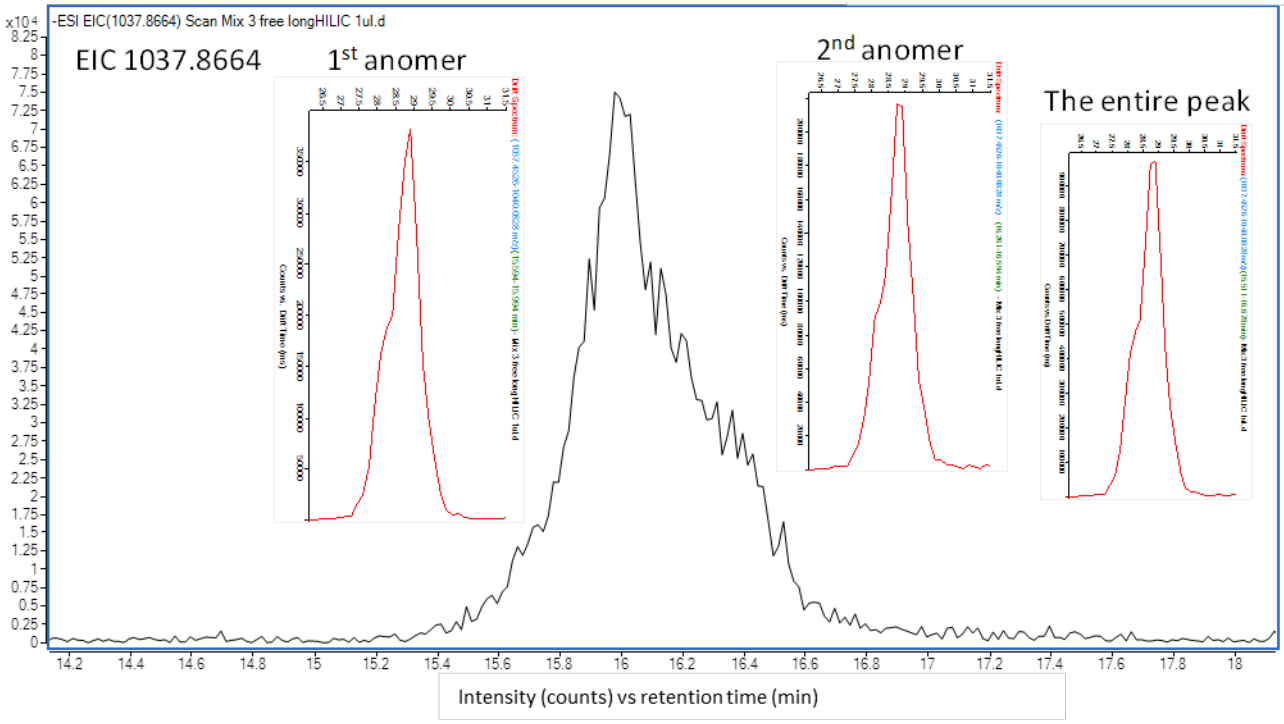

Fig. S101: ATDs (in red) from[M-2H]2- ions of unlabeled standard **9** anomers separated by HILIC (in black). A summed ATD of both anomers is shown on the right

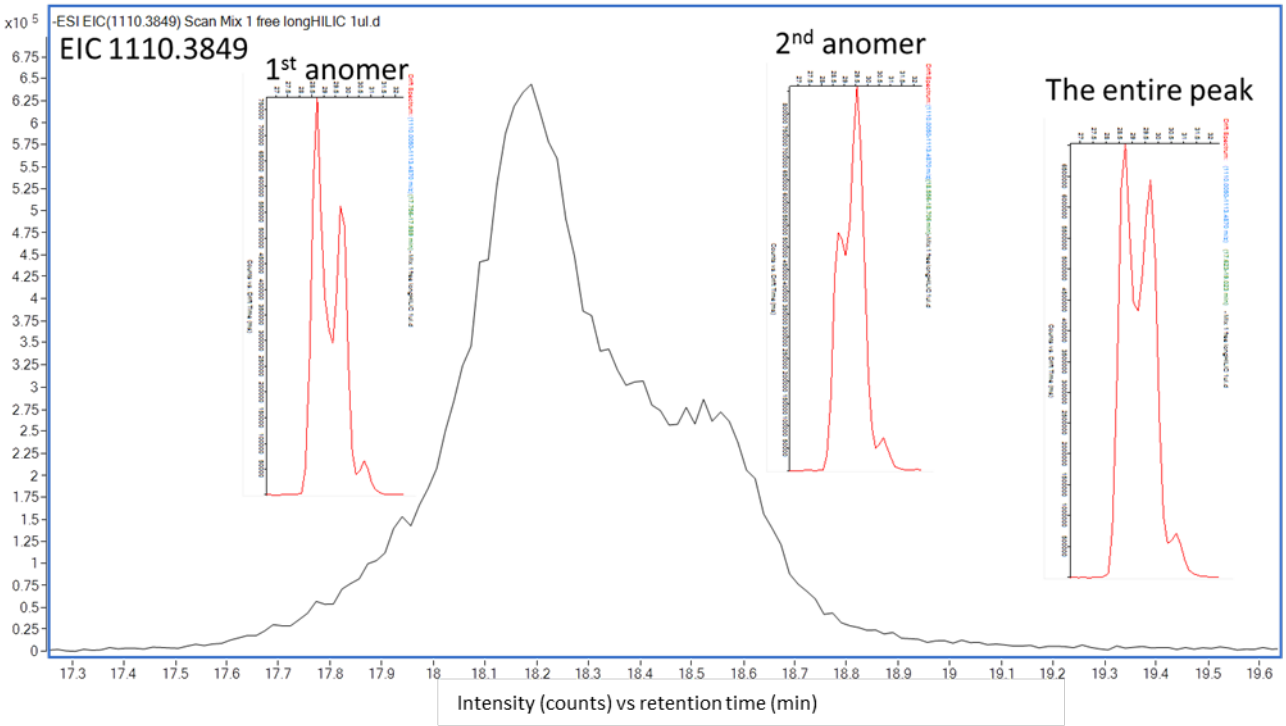

Fig. S102: ATDs (in red) from[M-2H]2- ions of unlabeled standard **10** anomers separated by HILIC (in black). A summed ATD of both anomers is shown on the right

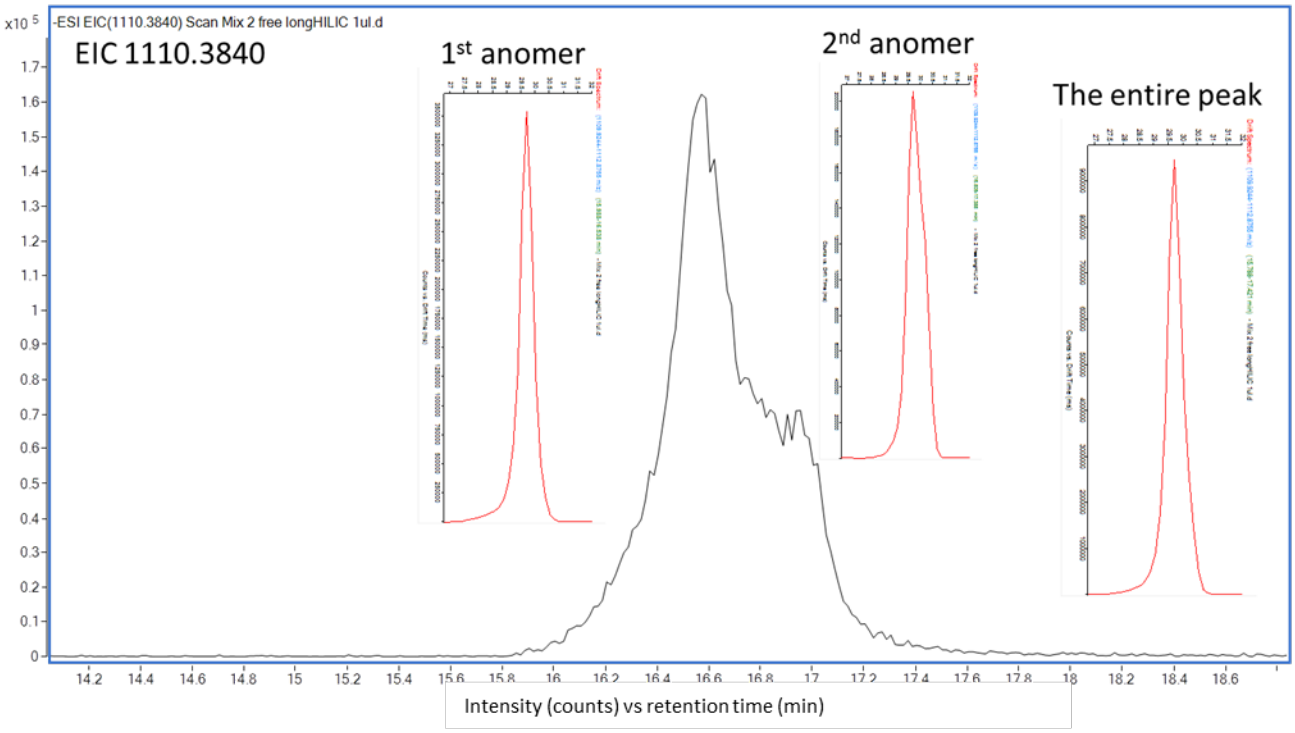

Fig. S103: ATDs (in red) from[M-2H]2- ions of unlabeled standard **11** anomers separated by HILIC (in black). A summed ATD of both anomers is shown on the right

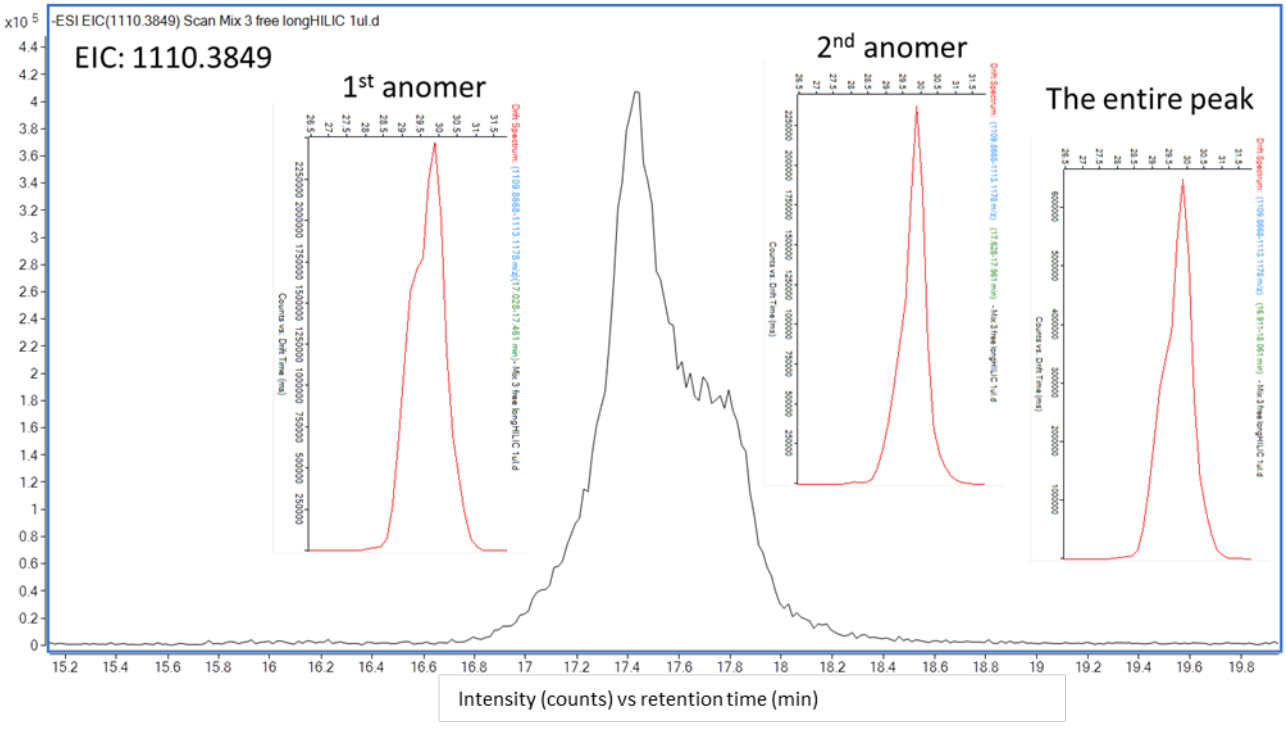

Fig. S104: ATDs (in red) from[M-2H]2- ions of unlabeled standard **12** anomers separated by HILIC (in black). A summed ATD of both anomers is shown on the right

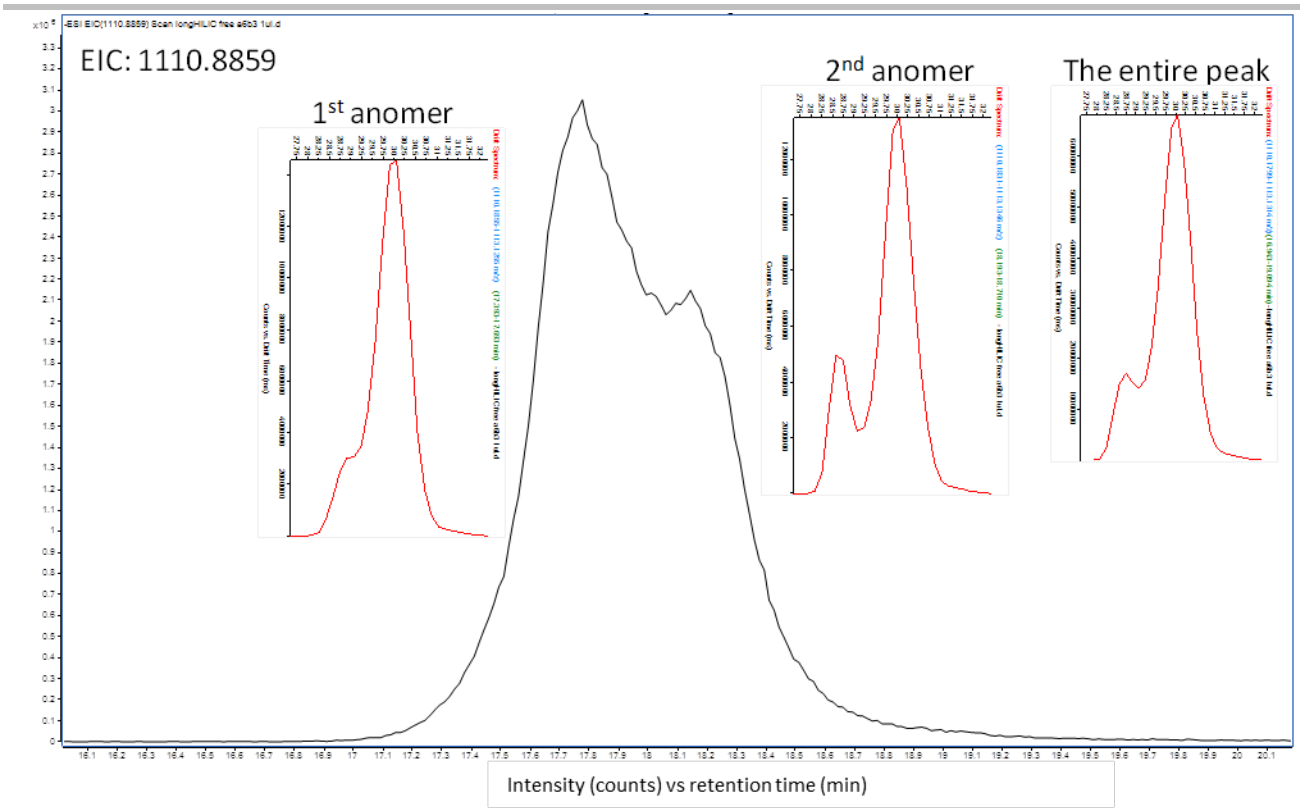

Fig. S105: ATDs (in red) from[M-2H]2- ions of unlabeled standard **13** anomers separated by HILIC (in black). A summed ATD of both anomers is shown on the right

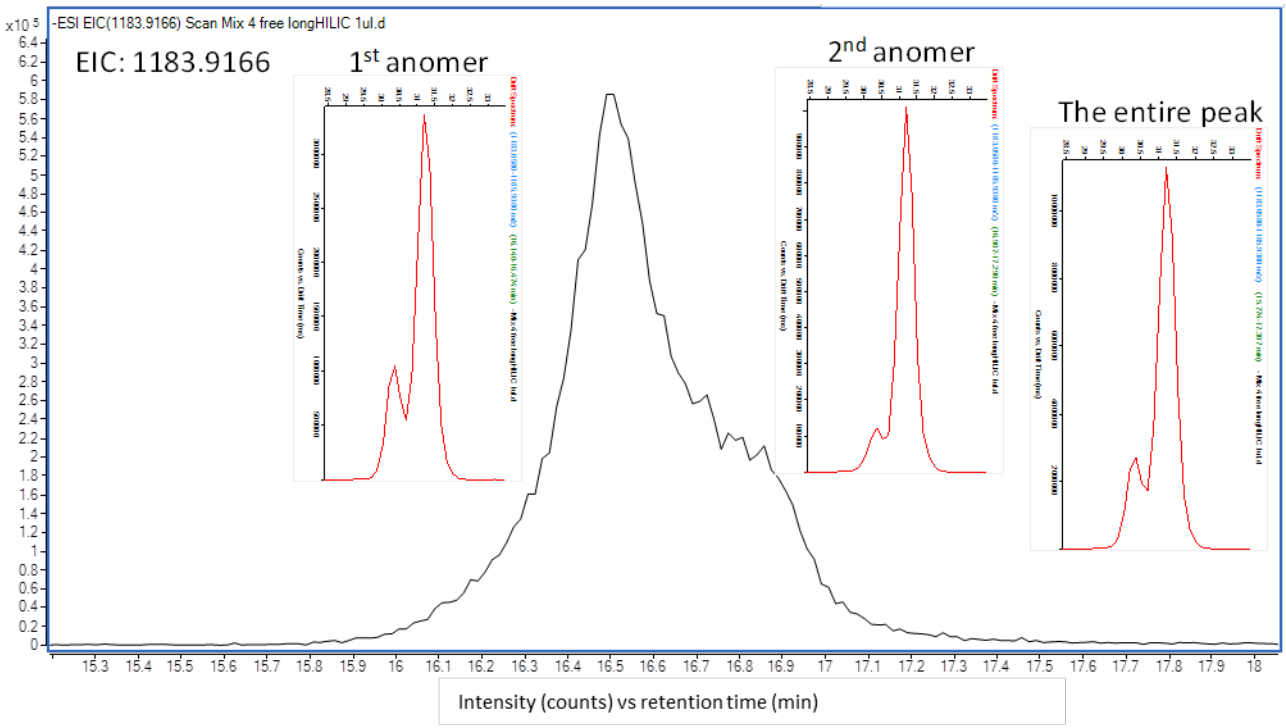

Fig. S106: ATDs (in red) from[M-2H]2- ions of unlabeled standard **14** anomers separated by HILIC (in black). A summed ATD of both anomers is shown on the right

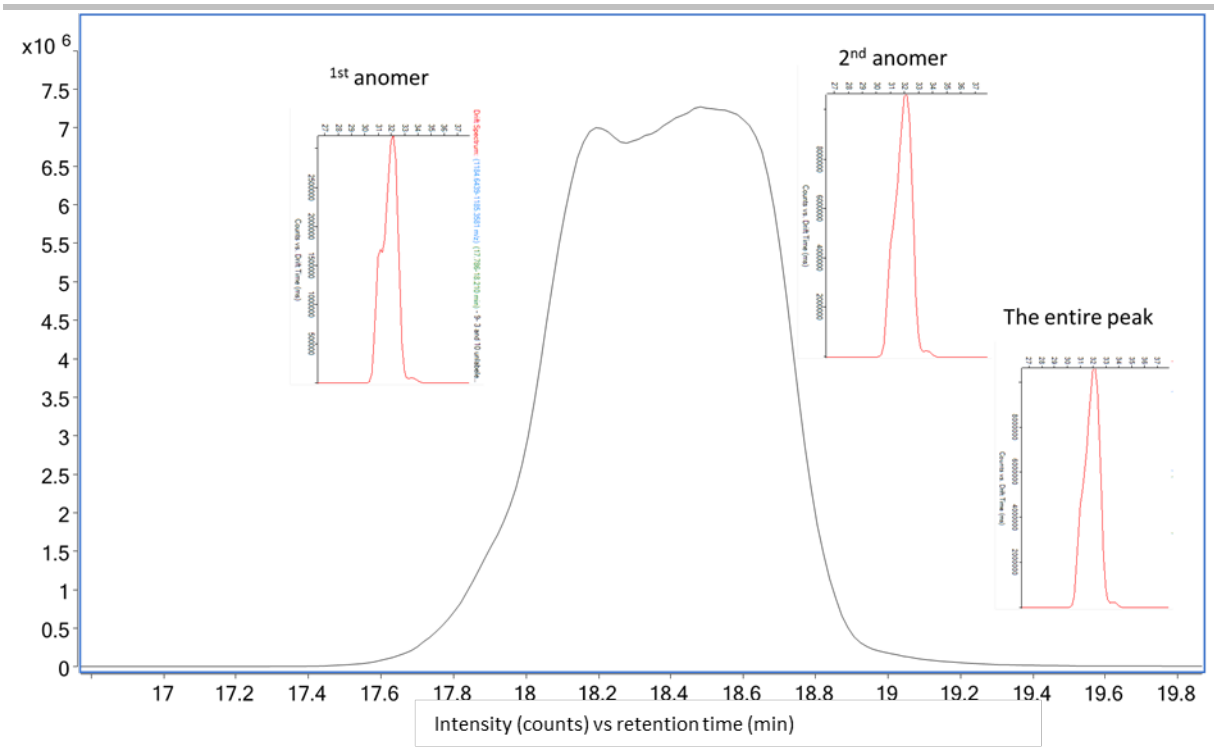

Fig. S107: ATDs (in red) from[M-2H]2- ions of unlabeled standard **15** anomers separated by HILIC (in black). A summed ATD of both anomers is shown on the right

2.6 HILIC-IMS-MS of fetuin released glycans

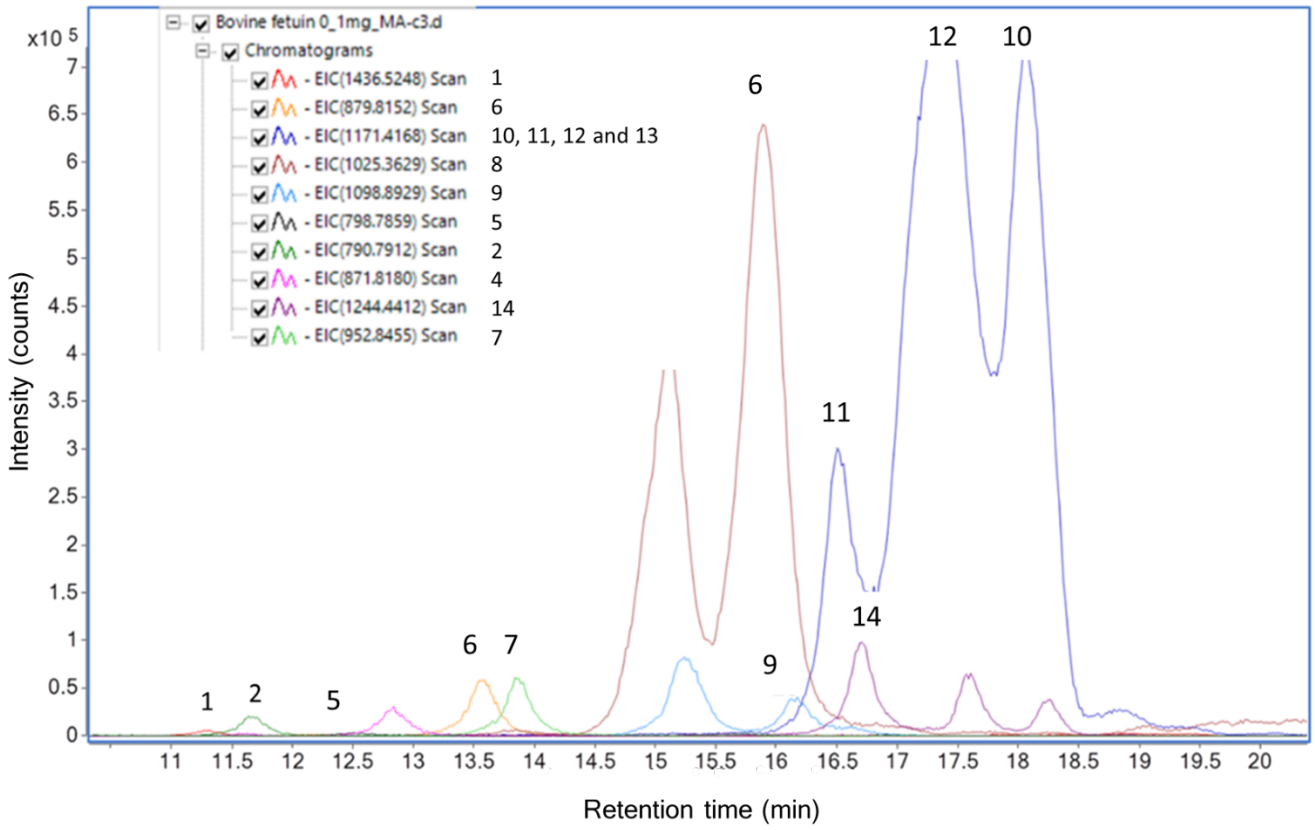

Fig. S108: Extracted ion chromatogram of the most abundant ions of fetuin realeased glycans. Peaks corresponding to identified glycans (by m/z, ATD and CCS values) are indicated by the number of the respective standard.

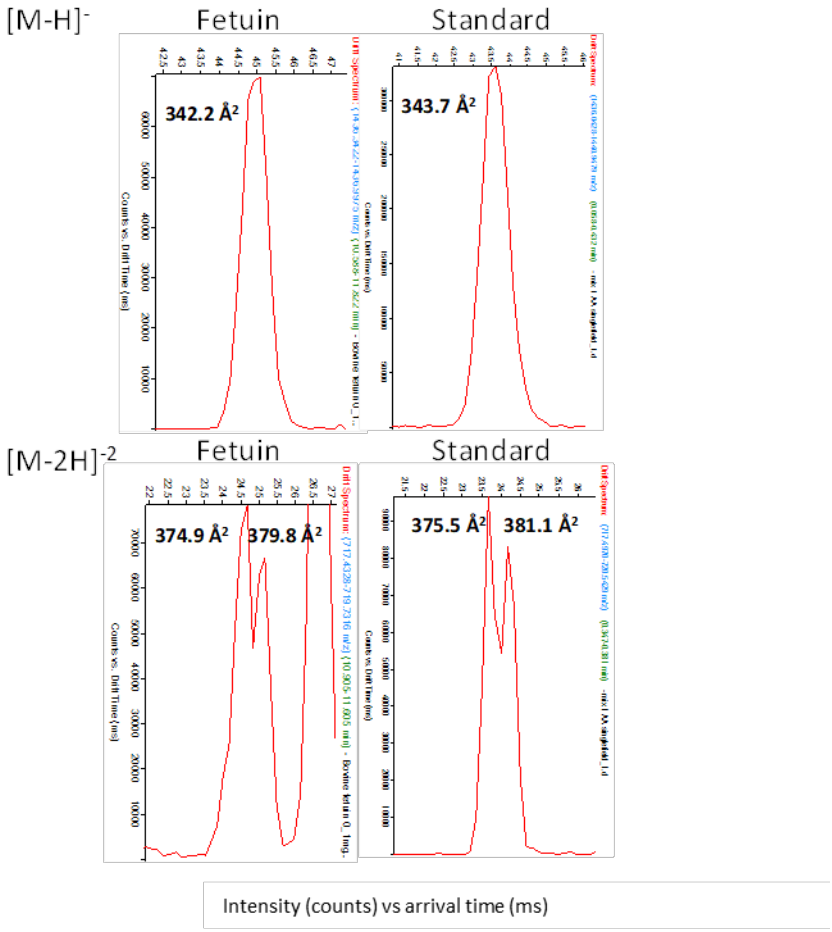

Fig. S109: ATDs of $[M-H]^-$ and $[M-2H]^{2-}$ ions from standard **1,** compared to the corresponding data from bovine fetuin glycans. For the $[M-2H]^{2-}$ ions of the standard, averaged CCS values are obtained by stepped field experiments and for $[M-H]^-$ ions by a single field experiment. The peak without CCS value from the fetuin released glycan sample is a non-related peak with a close m/z value.

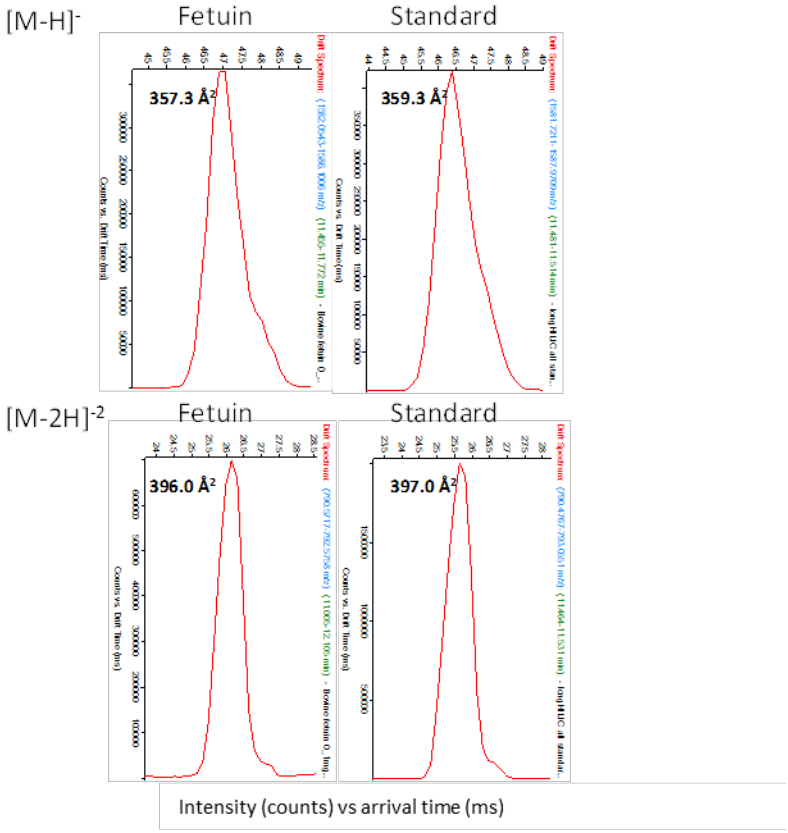

Fig. S110: ATDs of $[M-H]^-$ and $[M-2H]^{2-}$ ions from standard **2** compared to the corresponding data from bovine fetuin glycans. Averaged CCS values from interday stepped field experiments are used for the standard.

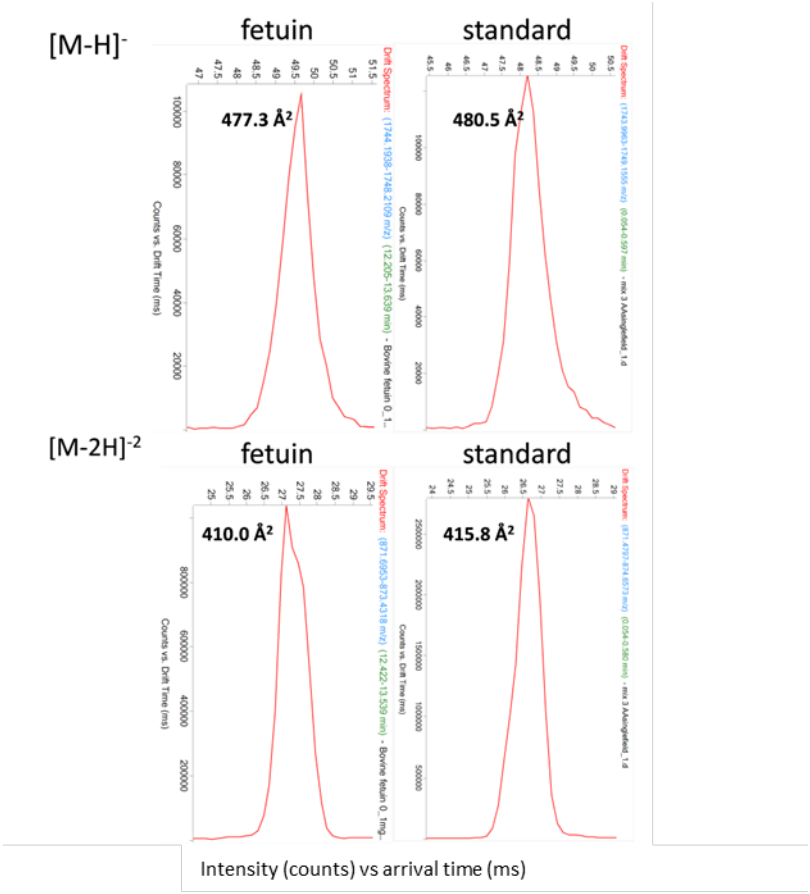

Fig. S111: ATDs of $[M-H]^-$ and $[M-2H]^{2-}$ ions from standard **4** compared to the corresponding data from bovine fetuin released glycans. Averaged CCS values for standards are obtained from interday stepped field experiments. The CCS deviation of standard and fetuin released glycan is too high and a shoulder in the $[M-2H]^{2-}$ ion ATD confirms the presence of a different compound.

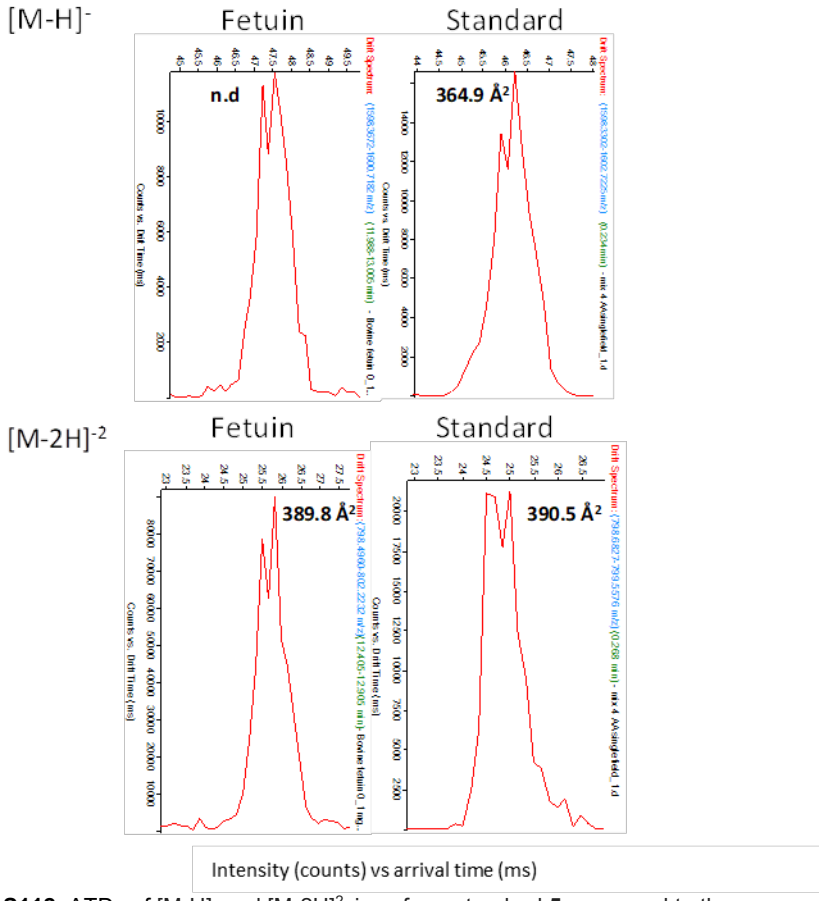

Fig. S112: ATDs of $[M-H]^-$ and $[M-2H]^{2-}$ ions from standard **5** compared to the corresponding data from bovine fetuin released glycans. For the $[M-2H]^{2-}$ ions of the standard, averaged CCS values are obtained by stepped field experiments and for $[M-H]^-$ ions by a single field experiment..

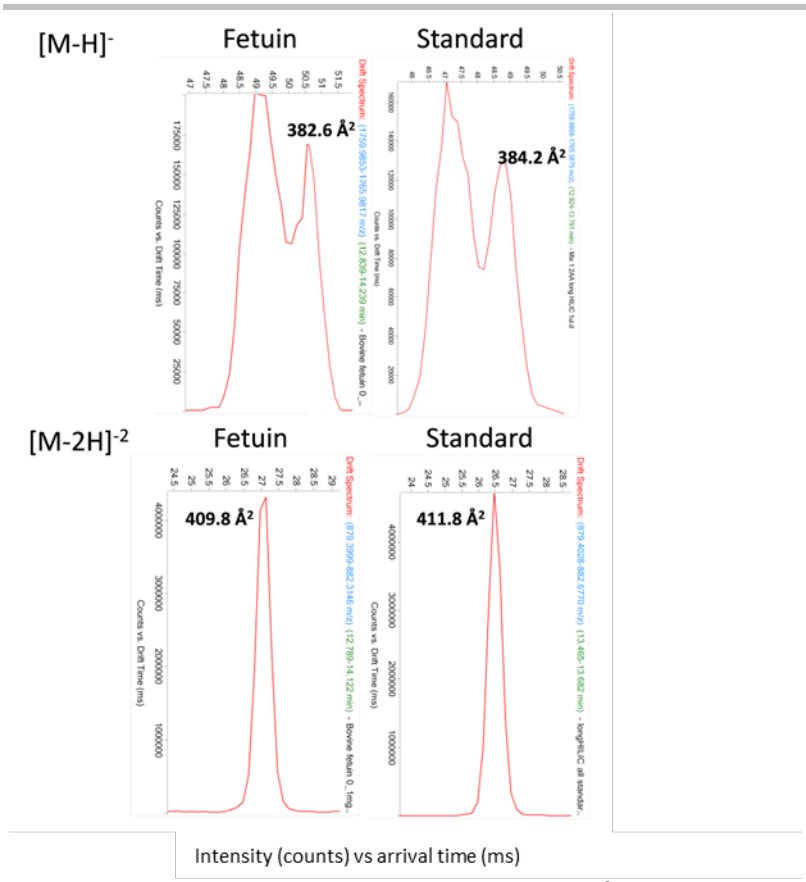

Fig. S113: ATDs of $[M-H]^-$ (highly concentrated) and $[M-2H]^{2-}$ ions from standard **6** compared to the corresponding data from bovine fetuin released glycans. For the $[M-2H]^{2-}$ ions of the standard, averaged CCS values are obtained by stepped field experiments and for $[M-H]^-$ ions by a single field experiment.

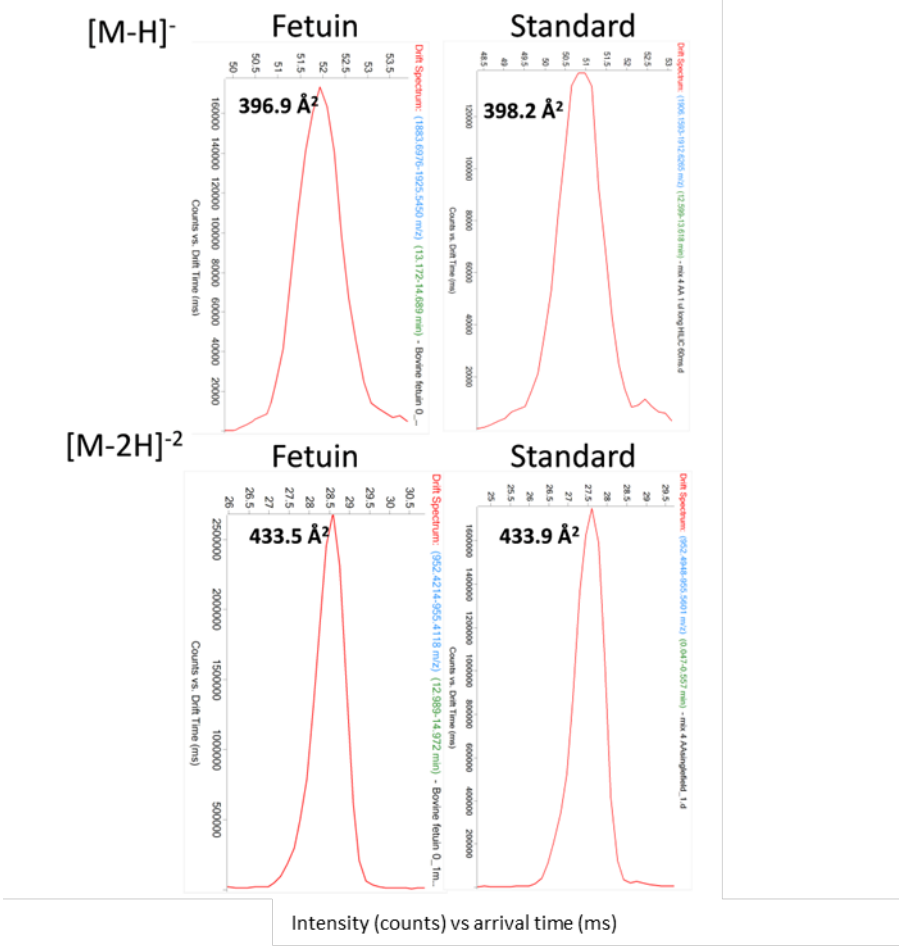

Fig. S114: ATDs of $[M-H]^-$ and $[M-2H]^{2-}$ ions from standard **7** compared to the corresponding data from bovine fetuin released glycans. For the $[M-2H]^{2-}$ ions of the standard, averaged CCS values are obtained by stepped field experiments and for $[M-H]^-$ ions by a single field experiment.

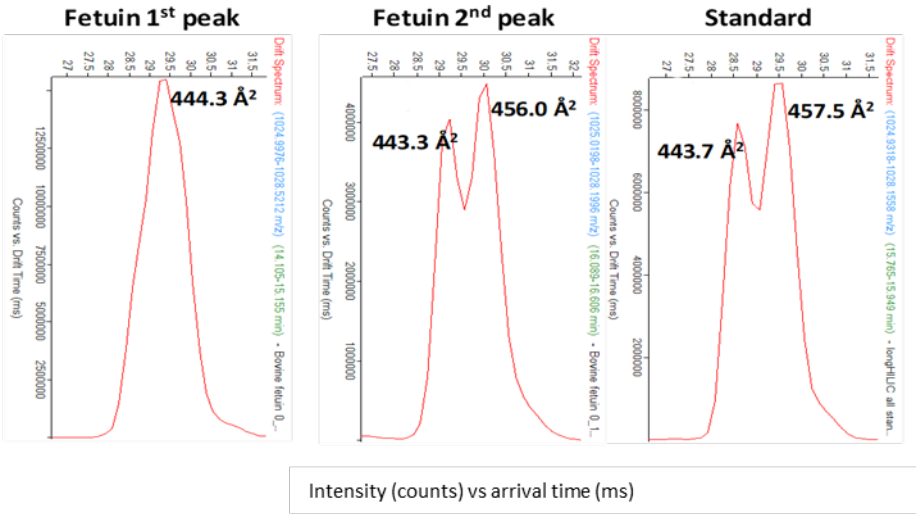

Fig. S115: ATDs of $[M-2H]^{2-}$ ions from standard **8** compared to the corresponding data from bovine fetuin released glycans. Averaged CCS values from interday stepped field experiments are used for the standard.

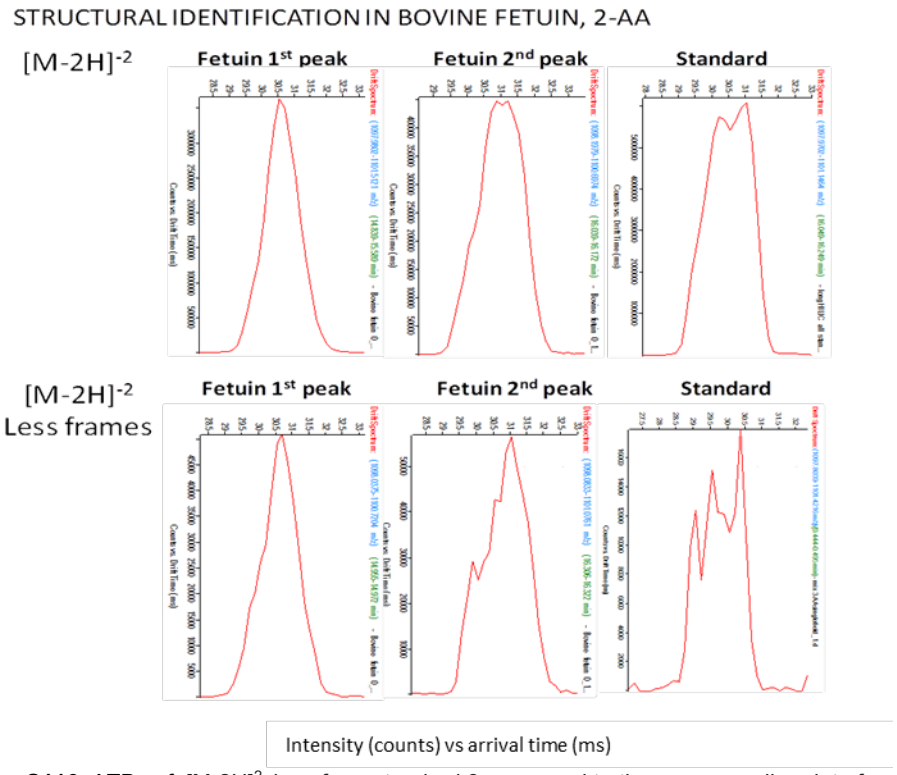

Fig. S116: ATDs of [M-2H]$^{2-}$ ions from standard **9** compared to the corresponding data from bovine fetuin released glycans. Averaged CCS values from interday stepped field experiments are used for the standards.

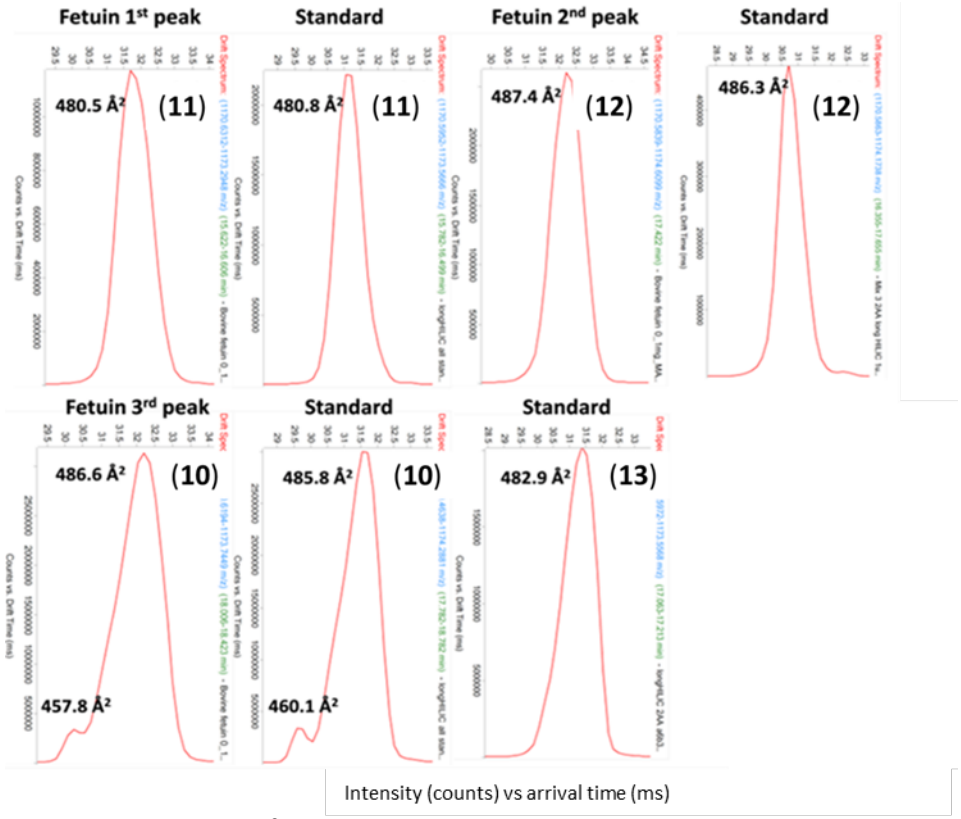

Fig. S117: ATDs of [M-2H]$^{2-}$ ions from regioisomer standards **10, 11, 12** and **13,** compared to the corresponding data from bovine fetuin released glycans, separated by HILIC. Averaged CCS values from interday stepped field experiments are used for the standards.

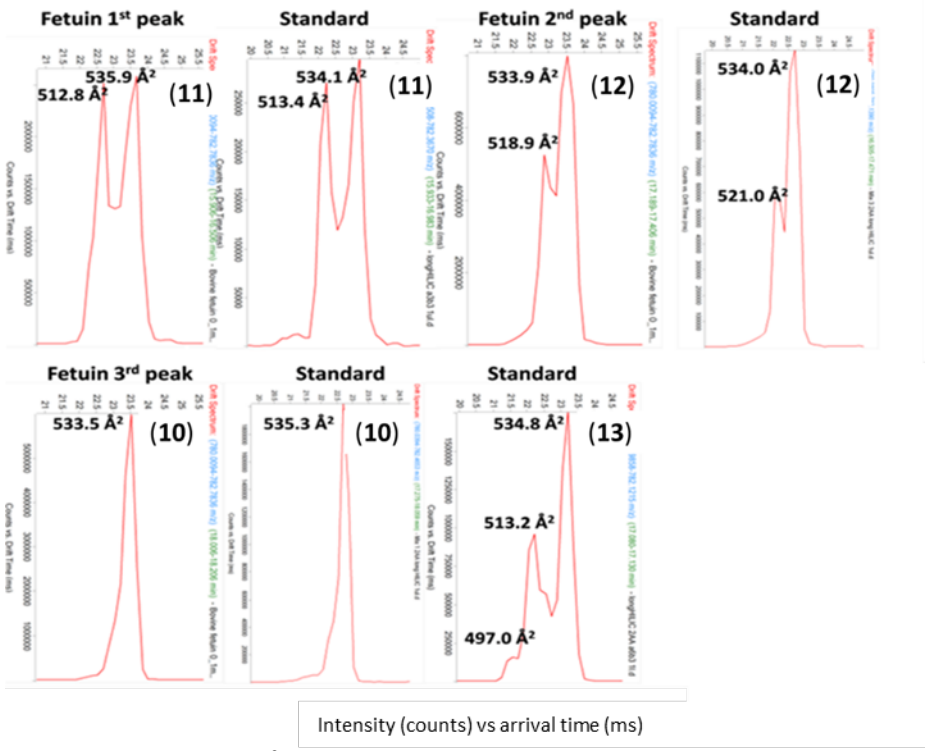

Fig. S118: ATDs of $[M-2H]^{3-}$ ions from regioisomer standards **10, 11, 12** and **13,** compared to the corresponding data from bovine fetuin released glycans, separated by HILIC. Averaged CCS values from interday stepped field experiments are used for the standards.

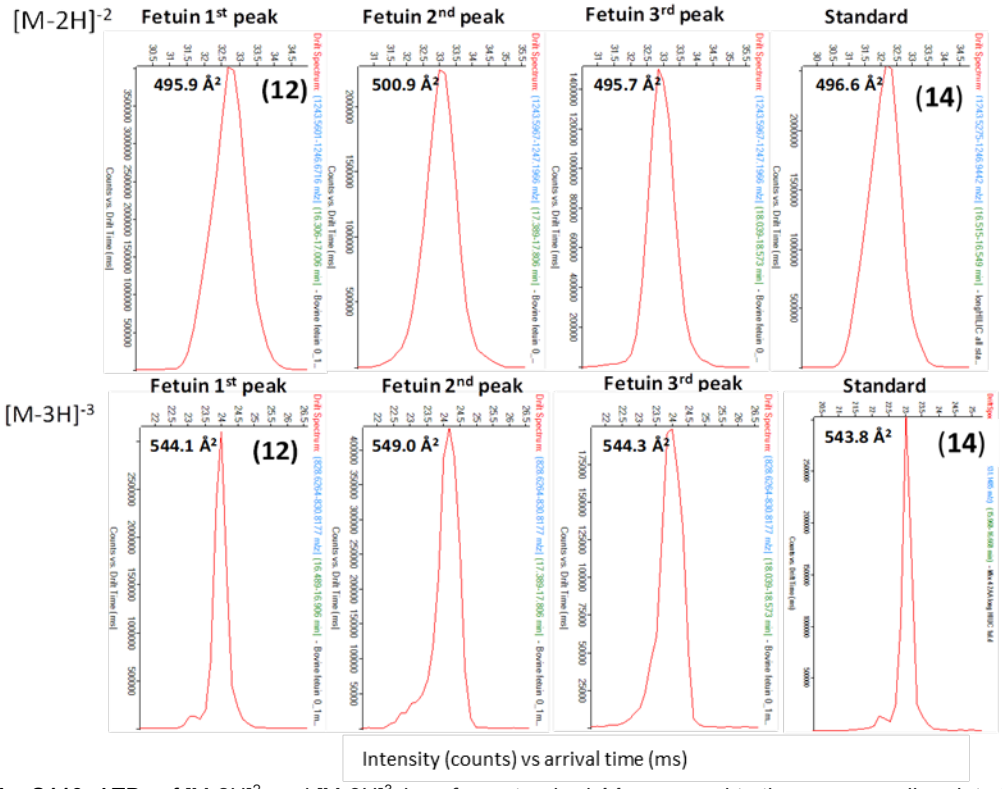

Fig. S119: ATDs of $[M-2H]^{2-}$ and $[M-3H]^{3-}$ ions from standard **14** compared to the corresponding data from bovine fetuin released glycans. For the standards, averaged CCS values from interday stepped field experiments are used for the $[M-2H]^{2-}$ ions and from a single field experiment for the $[M-3H]^{3-}$ ions.

Table S1: HILIC-IMS-QTOF data from bovine fetuin released and 2AA labelled glycand. H = hexose; N = N-acetylhexosamine; F = fucose, S = N-acetylneuraminic acid , G = N-Glycolylneuraminic acid. Linkages are specified in glycans where the structure was elucidated with standards (numbers in bold).

N°	RT (min)	CCS (Å²)	z	m/z	Composition	Error (ppm)	Rel. abund. %	Suggested structure
1	9.53	302.4	1	1176.4280	H3N2F1	2.7	0.007	
2	10.77	307.2	1	1192.4243	H4N2	1.5	0.037	
3	10.54	309.4		1192.4244		1.4	0.014	
4	9.63	320.0	1	1233.4499	H3N3	2.3	0.013	
5	10.13	309.7		1233.4505		1.8	0.025	
6	12.51	369.9	2	676.7346	H5N2	1.8	0.363	
		331.8	1	1354.4779		0.8	0.820	
7	10.56	332.2	1	1379.5061	H3N3F1	3.2	0.004	
		325.2		1379.5065		2.9	0.004	
8	11.52	360.4	2	697.2478	H4N3	1.8	0.008	
		333.0	1	1395.5038		1.2	0.065	
9	11.27	342.2	1	1436.5284	H3N4	2.5	0.014	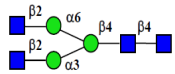
		374.9	2	717.7642		2.5	0.009	
		379.8		717.7639		2.3	0.008	
10	14.02	352.2	1	1516.5291	H6N2	1.7	0.096	
		389.1	2	757.7611		1.5	0.089	
11	11.89	344.8	1	1541.5603	H4N3F1	2.0	0.011	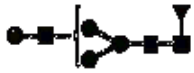
		382.8	2	770.2771		1.2	0.004	
12	12.99	354.7	1	1557.5560	H5N3	1.5	0.049	
		396.9	2	778.2746		1.2	0.001	
		381.2		778.2748		0.9	0.033	
13	11.67	357.3	1	1582.5886	H3N4F1	0.8	0.060	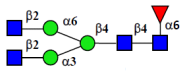
		396	2	790.7909		0.6	0.060	
14	12.51	389.8	2	798.7865	H4N4	2.8	0.008	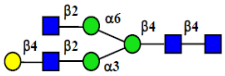
15	15.56	375.3	1	1678.5785	H7N2	3.7	0.003	
		409.2	2	838.7876		1.3	0.047	
16	13.12	400.4	2	842.7954	H4N3S1	1.6	0.234	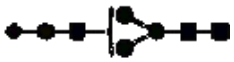
		424.3		842.7946		2.6	0.007	
17	14.14	372.7	1	1686.5961		2.8	0.006	
		403.8	2	842.7953		1.8	0.589	
18	14.14	400.4	2	850.7920	H4N3G1	2.7	0.004	
19	14.95	406.2		850.7929		1.6	0.017	
20	13.30	370	1	1703.6113	H5N3F1	2.9	0.003	
		403.3	2	851.3024		2.4	0.010	
21	14.42	372.2	1	1719.6085	H6N3	1.5	0.032	
		405.6	2	859.3007		1.4	0.113	
22	12.84	377.3	1	1744.6386	H4N4F1	2.4	0.010	
		410	2	871.8166		1.3	0.096	
23	13.59	371	1	1760.6332	H5N4	2.6	0.028	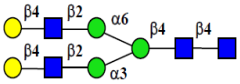
		382.6		1760.6332		2.6	0.012	
		409.8	2	879.8138		1.6	0.201	

N°	RT (min)	CCS (Å²)	z	m/z	Composition	Error (ppm)	Rel. abund. %	Suggested structure
24	14.51	418.5	2	915.8240	H4N3F1S1	1.9	0.008	
25	13.47	420.6		915.8242		1.7	0.030	
26	16.40	422	2	919.8128	H8N2	2.4	0.004	
27	16.71	426.8		919.8130		2.3	0.011	
28	14.46	440.2	2	923.8192	H5N3S1	4.3	0.001	
		419.5		923.8226		0.6	0.278	
29	15.49	418.5		923.8225		0.7	0.627	
30	15.52	428.3	2	940.3274	H7N3	1.0	0.014	
31	14.12	439.5	2	944.3346	H4N4S1	2.0	0.015	
		421.5		944.3352		1.4	0.042	
32	14.99	437.2		944.3354		1.2	0.143	
33	13.71	437.9		944.3367		-0.2	0.010	
34	13.84	396.9	1	1906.6916	H5N4F1	2.1	0.021	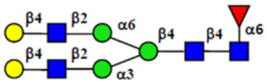
		433.5	2	952.8427		1.5	0.193	
35	14.69	437.2	2	960.8396	H6N4	2.1	0.009	
		426		960.8410		0.6	0.018	
36	15.79	437.4	2	988.3427	H4N3S2	1.9	0.008	
37	15.72	435.2	2	996.8498	H5N3F1S1	2.4	0.002	
38	14.76	443.9		996.8504		1.8	0.016	
	14.76	432.7		996.8517		0.5	0.005	
39	17.69	435.1	2	1000.8397	H9N2	1.7	0.006	
40	15.69	443.9	2	1004.8484	H6N3S1	1.2	0.191	
41	16.69	440.3		1004.8487		0.9	0.318	
42	15.24	446.1	2	1017.3632	H4N4F1S1	2.2	0.003	
43	15.89	443.3	2	1025.3617	H5N4S1	1.1	1.371	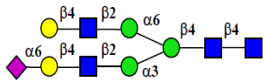
		456.0		1025.3624		0.5	2.603	
44	15.11	444.3		1025.3621		0.8	2.243	
45	16.01	439.6	2	1033.3580	H5N4G1	2.3	0.013	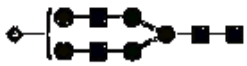
		453.8		1033.3580		2.2	0.013	
46	16.62	447.9		1033.3596		0.7	0.126	
47	14.96	455.3	2	1033.8693	H6N4F1	1.2	0.102	
48	15.74	448.7	2	1041.8634	H7N4	4.4	0.015	
49	14.64	455.6	2	1054.3803	H5N5F1	3.3	0.014	

N°	RT (min)	CCS (Å²)	z	m/z	Composition	Error (ppm)	Rel. abund. %	Suggested structure
50	15.29	449.4	2	1062.3791	H6N5	2.0	0.023	
		436.8		1062.3798		1.4	0.018	
51	18.30	451	2	1069.3682	H5N3S2	2.5	0.011	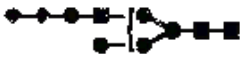
52	17.59	450.6		1069.3687		2.1	0.021	
53	16.89	453.1		1069.3690		1.8	0.017	
54	15.91	461	2	1077.8752	H6N3F1S1	3.2	0.007	
55	16.16	470.3	2	1098.3908	H5N4F1S1	0.9	0.173	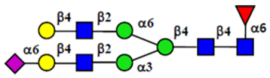
56	15.26	464.3		1098.3913		0.5	0.368	
57	16.10	462.9	2	1106.3878	H6N4S1	1.4	0.087	
58	16.86	468.5		1106.3884		0.8	0.078	
59	15.99	449.4	2	1114.8951	H7N4F1	1.7	0.046	
		475.1		1114.8956		1.2	0.022	
60	14.96	473.4	2	1118.9043	H4N5F1S1	0.8	0.009	
61	15.81	464.2	2	1126.8998	H5N5S1	2.5	0.023	
62	16.48	466.7		1126.9014		1.0	0.023	
63	18.04	457.8	2	1170.9085	H5N4S2	1.8	0.158	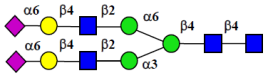
		486.6		1170.9090		1.4	4.758	
		533.5	3	780.2703		1.3	0.374	
64	17.34	487.4	2	1170.9093		1.1	9.347	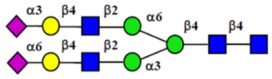
		533.9	3	780.2705		1.0	1.109	
		518.9		780.2705		1.0	0.346	
65	16.51	480.5	2	1170.9097		0.8	1.283	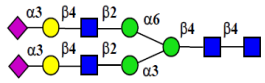
		535.9	3	780.2707		0.8	0.185	
		512.8		780.2708		0.6	0.172	
66	18.76	485.1	2	1178.9062	H5N4S1G1	1.6	0.373	
		530.8	3	785.6021		1.0	0.028	
67	18.16	490.1	2	1178.9064		1.4	0.407	
		530.8	3	785.6021		1.1	0.037	
68	16.17	483.3	2	1179.4171	H6N4F1S1	1.0	0.288	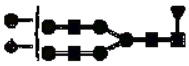
69	18.85	485.4	2	1186.9012	H5N4G2	3.6	0.007	
70	19.38	483.4		1186.9024		2.6	0.009	
71	17.01	483.2	2	1187.4137	H6N4F1G1	1.7	0.034	
72	17.72	487.8		1187.4139		1.6	0.030	
73	17.24	487.8	2	1207.9277	H6N5S1	1.1	0.497	
74	16.59	477.8	2	1207.9278		1.0	1.098	
75	16.72	495.9	2	828.9551	H5N4F1S2	0.8	0.349	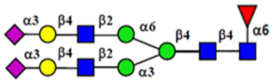
		544.1	3	828.9559		1.2	0.116	
76	17.57	500.9	2	1243.9375		0.7	0.209	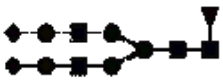
		549.0	3	828.9563		1.7	0.029	
77	18.26	495.9	2	1243.9386		1.6	0.112	
		544.3	3	1243.9387		2.6	0.013	

N°	RT (min)	CCS (Å²)	z	m/z	Composition	Error (ppm)	Rel. abund. %	Suggested structure
78	17.52	492.8	2	1251.934		2.4	0.030	
		544.4	3	834.2872		2.1	0.004	
79	18.39	504.4	2	1251.9346	H5N4F1S1G1	1.9	0.077	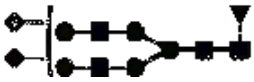
		540.4	3	834.2867		2.7	0.010	
80	18.79	495	2	1251.9343		2.2	0.034	
		537.6	3	834.288		1.1	0.002	
81	18.31	487.9	2	1259.9302		3.3	0.009	
		544.1	3	839.6184		2.5	0.002	
82	18.97	500.3	2	1259.9316	H5N4F1G2	2.2	0.015	
		543.9	3	839.6176		3.5	0.002	
83	19.50	494.9	2	1259.9308		2.9	0.007	
84	17.18	504.2	2	1272.4474		2.3	0.015	
		525.9		1272.4461		3.3	0.004	
		551.2	3	847.9632		1.5	0.002	
		523.1		847.9633		1.4	0.004	
85	17.87	504.3	2	1272.4483	H5N5S2	1.6	0.085	
		538.4	3	847.9622		2.7	0.015	
86	18.65	474.5	2	1272.4473		2.4	0.001	
		496.2		1272.4465		3.0	0.017	
		541.9	3	847.9622		2.6	0.000	
87	17.61	502.2	2	1280.9557	H6N5F1S1	1.8	0.031	
88	16.92	495		1280.9558		1.7	0.064	
89	18.79	508	2	1316.4571		0.9	0.330	
		517.5	3	877.302		1.2	0.015	
		543.8	3	877.3017		1.6	0.240	
		574.9	3	877.3015	H5N4S3	1.9	0.004	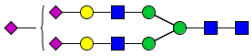
90	19.39	508.4	2	1316.4569		1.1	0.367	
		539.5	3	877.3019		1.4	0.116	
		578.6		877.3026		0.6	0.084	
91	17.08	567.3	3	896.6490	H5N5F1S2	1.5	0.001	
92	17.89	519.4	2	1353.4751		1.2	1.660	
		545.7	3	901.9808		1.4	0.528	
		576.4		901.9813		0.8	0.150	
93	18.61	515.4	2	1353.4742	H6N5S2	1.8	6.974	
		547.8	3	901.9806		1.6	2.186	
94	19.24	510.6	2	1353.4745		1.6	1.965	
		558.4	3	901.981		1.2	0.495	
95	17.04	528.1		1389.4826		1.8	0.017	
96	17.74	523.5		1389.4827		2.2	0.042	
97	18.26	524.7	2	1389.4832	H5N4F1S3	2.9	0.017	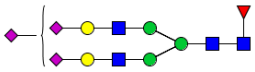
98	18.87	525.3		1389.4842		3.3	0.008	
99	19.48	520.8		1389.4847		3.3	0.003	

N°	RT (min)	CCS (Å²)	z	m/z	Composition	Error (ppm)	Rel. abund. %	Suggested structure
100	19.46	554.4	3	931.3164		4.6	0.002	
	20.01	513.1	2	931.3178		2.9	0.009	
101	20.01	536	3	931.3180		2.9	0.004	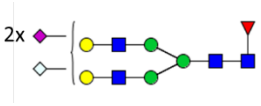
	20.01	560.3		1397.4807	H5N4F1S2G1	2.4	0.003	
102	20.66	515	2	1397.4807		2.9	0.011	
	20.66	550.9	3	931.3181		3.1	0.011	
103	21.26	551.2	3	931.3185		2.8	0.002	
		528.2	2	950.6653		2.3	0.077	
104	18.23	551.3	3	1426.5023		2.9	0.003	
		563.4		1426.5033		1.3	0.010	
105	18.81	535.8	2	1426.5037	H6N5F1S2	1.6	0.345	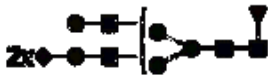
		562.8	3	950.6668		1.3	0.138	
106	19.32	529.8	2	950.6668		1.4	0.114	
		575.8	3	950.6671		0.9	0.044	
107	18.91	553.6	3	955.9965		3.0	0.008	
108	19.40	526.7	2	955.9968	H7N5S2	2.6	0.028	
		540	3	1434.4994		3.3	0.002	
109	18.94	531.9	2	1455.0107		3.9	0.008	
		575.7	3	969.6729	H6N6S2	2.3	0.003	
110	20.74	540.9	2	1462.0024		2.5	0.009	
		576.7	3	974.3331	H5N4S4	1.9	0.017	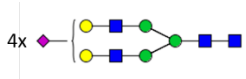
111	19.11	538.4	2	1499.0218		1.7	0.314	
		570.7	3	999.0112		2.7	0.600	
		665.6	4	749.007		2.1	0.011	
112	19.87	536.7	2	1499.022		1.6	3.059	
		566.6	2	1499.0222		1.4	2.137	
		578.2	3	999.0112		2.6	6.566	
		666.4	4	749.0072		1.8	0.102	
		708.4	4	749.0077		1.1	0.018	
113	20.32	542.5	2	1499.0213		2.1	4.316	
		577.5	3	999.0112		2.6	5.744	
		654.9	4	749.0062	H6N5S3	3.2	0.020	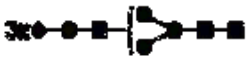
		681.3	4	749.0078		1.0	0.046	
		705.6	4	749.0065		2.8	0.002	
114	21.04	547.9	2	1499.021		2.3	1.054	
		582.4	3	999.011		2.8	1.038	
		623.6	3	999.0115		2.4	0.302	
		641.8	4	749.006		3.4	0.001	
		667.1	4	749.0071		1.9	0.004	
		682.6	4	749.0056		4.0	0.000	
115	21.97	574.2	3	999.0098		4.0	0.054	
116	22.49	575.4	3	999.0102		3.6	0.078	
117	20.94	541.7	2	1507.0193		1.7	1.297	
		682.8	4	753.0063	H6N5S2G1	1.3	0.012	
		579.5	3	1004.3442		1.3	2.033	

N°	RT (min)	CCS (Å²)	z	m/z	Composition	Error (ppm)	Rel. abund. %	Suggested structure
118	18.94	586	3	1018.3564	H6N6F1S2	4.7	0.034	
119	19.47	554.9	2	1572.0496	H6N5F1S3	2.4	0.024	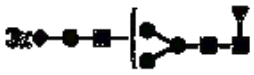
		589.1	3	1047.6982		1.5	0.085	
120	19.92	555.4	2	1572.0498		2.3	0.072	
		597.7	3	1047.6982		1.6	0.150	
		683.5	4	785.5199		4.0	0.002	
121	20.54	599.2	3	1047.698		1.7	0.165	
122	20.67	555.3	2	1580.0459	H6N5F1S2G1	3.1	0.060	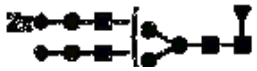
		595.4	3	1053.0294		2.0	0.158	
123	19.29	691.3	4	795.7798	H5N6F1S3	-0.1	0.001	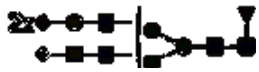
124	22.64	591.1	3	1063.6899	H6N5F1G3	4.5	0.064	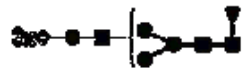
125	20.19	562.4	2	1600.5593	H6N6S3	3.0	0.003	
126	20.72	560.2		1600.558		3.8	0.008	
		601.8	3	1066.7036		3.2	0.027	
127	21.64	571	2	1644.5686	H6N5S4	2.1	2.513	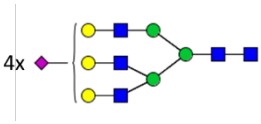
		604.9	3	1096.043		2.4	7.601	
		662.7	4	821.7808		1.9	0.400	
		693.2		821.7811		1.6	0.164	
		718.9		821.7807		2.0	0.030	
128	22.27	572.1	2	1644.5682		2.4	1.413	
		602.1		1644.5678		2.6	0.121	
		603.9	3	1096.0431		2.3	5.210	
		663.3	4	821.7794		3.7	0.002	
		688.7		821.7808		1.9	0.193	
129	22.39	568.9	2	1652.566	H6N5S3G1	2.1	0.237	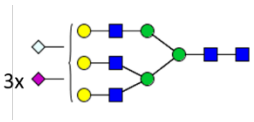
		605.5	3	1101.3752		1.9	1.441	
		664.7	4	825.7788		2.8	0.040	
		692.6		825.7792		2.4	0.023	
130	20.41	608	3	1120.7218	H7N6S3	2.5	0.013	
		645.3		1120.7219		2.4	0.005	
131	21.07	579.7	2	1681.5854		3.0	0.097	
		604	3	1120.7213		2.9	0.379	
132	21.56	634.6	3	1217.753	H7N6S4	2.8	0.037	
		701.6	4	913.0642		1.4	0.005	
133	22.09	613.5	2	1827.1335		2.6	0.080	
		638.1	3	1217.7537		2.2	0.512	
		714	4	913.0636		2.0	0.109	
134	22.54	635.9	3	1217.7539		2.0	0.426	
		709.7	4	913.0636		2.0	0.085	
135	22.04	650.9	3	1266.4384	H7N6F1S4	3.1	0.007	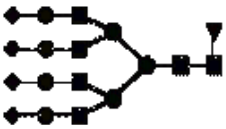

2.7 ATD simulations

Selection of the starting structures for molecular dynamics (MD) simulations

Several rotamers of α- and β-anomers of unlabeled oligosaccharides **10** and **11** were generated with Carbohydrate builder, implemented in GLYCAM-Web (glycam.org). In detail, three staggered conformers of omega dihedral angle (ω) (*gg*, *gt*, and *tg*), together with three staggered conformers of psi dihedral angle (ψ) in which the sialic acid is involved, were used. As a result, a total of 243 α-conformers and 243 β-conformers for unlabeled compound **10,** and 27 α-conformers and 27 β-conformers for unlabeled compound **11** were calculated. These conformers were then ranked in energy. The minimization was performed with AMBER18 package[4] in implicit water (ε =80). Based on the theoretical energy, the Maxwell-Boltzmann distribution was calculated to estimate each conformer population (Tables S2-S5).

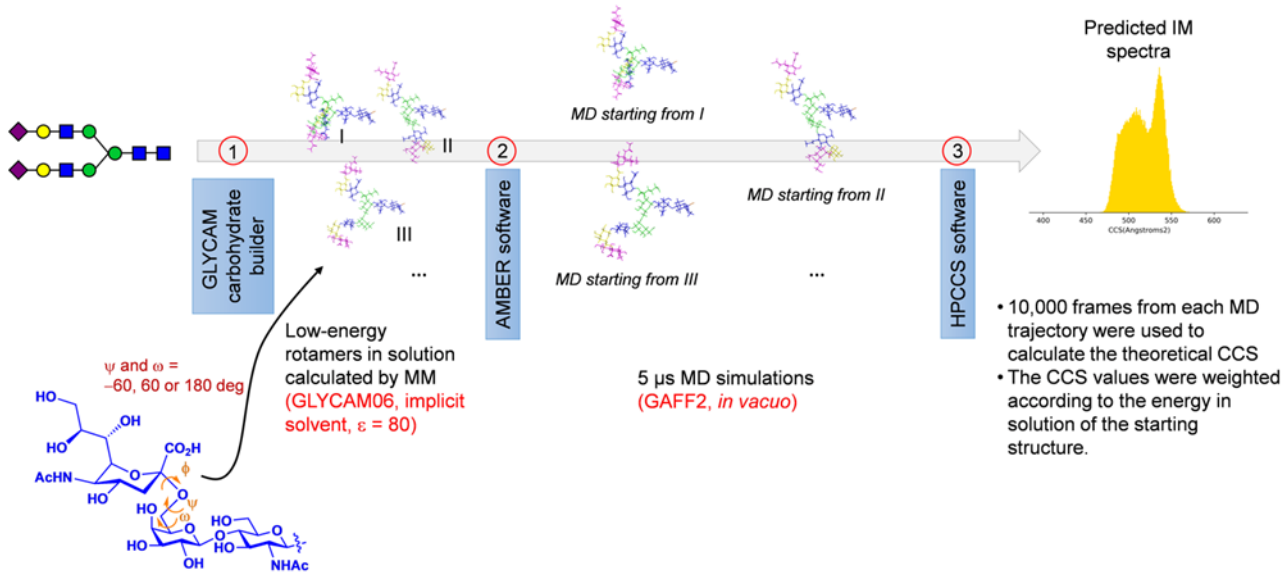

Figure S120. Workflow followed to generate collision cross section distributions (CCSDs).

Table S2: Maxwell-Boltzmann distribution calculated at 300 K for α anomer of unlabeled **10**.

Minimized Energy (Kcal/mol)	Minimized Energy (KJ/mol)	Δ energy (ΔE) (KJ/mol)	-ΔE/RT	$e^{-E/RT}$	fraction	% population
29.49	123.44	0.00	0.00	1.00	0.22	21.96
29.55	123.68	0.25	-0.10	0.90	0.20	19.83
29.77	124.62	1.18	-0.49	0.61	0.13	13.49
29.91	125.18	1.75	-0.72	0.49	0.11	10.68
30.26	126.66	3.22	-1.33	0.26	0.06	5.81
30.38	127.18	3.74	-1.54	0.21	0.05	4.69
30.60	128.11	4.67	-1.93	0.15	0.03	3.19
30.69	128.46	5.02	-2.07	0.13	0.03	2.76
30.82	129.00	5.56	-2.29	0.10	0.02	2.21

30.87	129.22	5.78	-2.39	0.09	0.02	2.02
30.91	129.39	5.96	-2.46	0.09	0.02	1.88
30.94	129.52	6.08	-2.51	0.08	0.02	1.78
31.18	130.52	7.09	-2.93	0.05	0.01	1.18
31.22	130.69	7.25	-2.99	0.05	0.01	1.10
31.22	130.70	7.27	-3.00	0.05	0.01	1.09
31.32	131.08	7.65	-3.16	0.04	0.01	0.93
31.57	132.16	8.72	-3.60	0.03	0.01	0.60
31.62	132.35	8.91	-3.68	0.03	0.01	0.55
31.80	133.11	9.68	-3.99	0.02	0.00	0.40
31.83	133.24	9.81	-4.05	0.02	0.00	0.38
31.85	133.32	9.88	-4.08	0.02	0.00	0.37
31.87	133.40	9.97	-4.11	0.02	0.00	0.36
32.00	133.97	10.53	-4.35	0.01	0.00	0.28
32.10	134.36	10.93	-4.51	0.01	0.00	0.24
32.13	134.48	11.04	-4.56	0.01	0.00	0.23
32.22	134.89	11.45	-4.73	0.01	0.00	0.19
32.33	135.35	11.91	-4.92	0.01	0.00	0.16
32.40	135.61	12.18	-5.03	0.01	0.00	0.14
32.40	135.62	12.19	-5.03	0.01	0.00	0.14
32.58	136.37	12.93	-5.34	0.00	0.00	0.11
32.71	136.91	13.47	-5.56	0.00	0.00	0.08
32.72	136.95	13.52	-5.58	0.00	0.00	0.08
32.77	137.16	13.73	-5.67	0.00	0.00	0.08
32.78	137.23	13.79	-5.69	0.00	0.00	0.07
32.81	137.35	13.91	-5.74	0.00	0.00	0.07
32.84	137.46	14.02	-5.79	0.00	0.00	0.07
32.94	137.87	14.43	-5.96	0.00	0.00	0.06
32.95	137.93	14.50	-5.98	0.00	0.00	0.06
32.97	138.00	14.56	-6.01	0.00	0.00	0.05
33.00	138.14	14.70	-6.07	0.00	0.00	0.05
33.09	138.52	15.08	-6.23	0.00	0.00	0.04
33.10	138.54	15.11	-6.24	0.00	0.00	0.04
33.17	138.85	15.41	-6.36	0.00	0.00	0.04
33.19	138.92	15.48	-6.39	0.00	0.00	0.04
33.29	139.36	15.92	-6.57	0.00	0.00	0.03
33.32	139.48	16.04	-6.62	0.00	0.00	0.03
33.39	139.78	16.34	-6.75	0.00	0.00	0.03
33.44	139.98	16.54	-6.83	0.00	0.00	0.02
33.47	140.11	16.68	-6.88	0.00	0.00	0.02
33.52	140.33	16.89	-6.97	0.00	0.00	0.02
33.58	140.58	17.14	-7.08	0.00	0.00	0.02
33.59	140.62	17.18	-7.09	0.00	0.00	0.02
33.59	140.62	17.19	-7.09	0.00	0.00	0.02

33.68	140.99	17.55	-7.24	0.00	0.00	0.02
33.89	141.86	18.43	-7.61	0.00	0.00	0.01
33.93	142.03	18.59	-7.67	0.00	0.00	0.01
33.93	142.04	18.61	-7.68	0.00	0.00	0.01
34.01	142.38	18.94	-7.82	0.00	0.00	0.01
34.02	142.40	18.96	-7.83	0.00	0.00	0.01
34.12	142.81	19.37	-7.99	0.00	0.00	0.01
34.13	142.88	19.44	-8.02	0.00	0.00	0.01
34.17	143.05	19.62	-8.10	0.00	0.00	0.01
34.26	143.41	19.98	-8.25	0.00	0.00	0.01
34.27	143.45	20.01	-8.26	0.00	0.00	0.01
34.28	143.49	20.05	-8.28	0.00	0.00	0.01
34.31	143.63	20.20	-8.34	0.00	0.00	0.01
34.41	144.03	20.60	-8.50	0.00	0.00	0.00
34.61	144.88	21.44	-8.85	0.00	0.00	0.00
34.62	144.91	21.47	-8.86	0.00	0.00	0.00
34.63	144.97	21.53	-8.89	0.00	0.00	0.00
34.64	145.01	21.57	-8.90	0.00	0.00	0.00
34.66	145.10	21.67	-8.94	0.00	0.00	0.00
34.68	145.18	21.74	-8.97	0.00	0.00	0.00
34.71	145.28	21.84	-9.02	0.00	0.00	0.00
34.72	145.35	21.91	-9.04	0.00	0.00	0.00
34.88	146.00	22.57	-9.31	0.00	0.00	0.00
34.92	146.17	22.73	-9.38	0.00	0.00	0.00
34.97	146.40	22.96	-9.48	0.00	0.00	0.00
35.01	146.55	23.12	-9.54	0.00	0.00	0.00
35.01	146.56	23.13	-9.55	0.00	0.00	0.00
35.04	146.66	23.22	-9.58	0.00	0.00	0.00
35.10	146.92	23.48	-9.69	0.00	0.00	0.00
35.14	147.10	23.67	-9.77	0.00	0.00	0.00
35.17	147.20	23.76	-9.81	0.00	0.00	0.00
35.22	147.44	24.00	-9.91	0.00	0.00	0.00
35.24	147.51	24.07	-9.93	0.00	0.00	0.00
35.39	148.15	24.71	-10.20	0.00	0.00	0.00
35.47	148.46	25.02	-10.33	0.00	0.00	0.00
35.53	148.73	25.29	-10.44	0.00	0.00	0.00
35.53	148.73	25.30	-10.44	0.00	0.00	0.00
35.56	148.85	25.42	-10.49	0.00	0.00	0.00
35.59	148.97	25.53	-10.54	0.00	0.00	0.00
35.60	149.01	25.58	-10.56	0.00	0.00	0.00
35.61	149.05	25.61	-10.57	0.00	0.00	0.00
35.62	149.11	25.67	-10.59	0.00	0.00	0.00
35.64	149.18	25.74	-10.63	0.00	0.00	0.00
35.65	149.24	25.80	-10.65	0.00	0.00	0.00

35.70	149.44	26.00	-10.73	0.00	0.00	0.00
35.71	149.49	26.05	-10.75	0.00	0.00	0.00
35.76	149.67	26.23	-10.83	0.00	0.00	0.00
35.82	149.96	26.52	-10.95	0.00	0.00	0.00
35.85	150.07	26.63	-10.99	0.00	0.00	0.00
35.89	150.23	26.79	-11.06	0.00	0.00	0.00
35.90	150.26	26.82	-11.07	0.00	0.00	0.00
35.92	150.35	26.91	-11.11	0.00	0.00	0.00
35.94	150.44	27.00	-11.15	0.00	0.00	0.00
35.96	150.51	27.08	-11.18	0.00	0.00	0.00
36.06	150.96	27.52	-11.36	0.00	0.00	0.00
36.08	151.02	27.58	-11.38	0.00	0.00	0.00
36.10	151.11	27.68	-11.42	0.00	0.00	0.00
36.11	151.15	27.71	-11.44	0.00	0.00	0.00
36.12	151.19	27.76	-11.46	0.00	0.00	0.00
36.12	151.21	27.77	-11.46	0.00	0.00	0.00
36.15	151.31	27.87	-11.50	0.00	0.00	0.00
36.21	151.58	28.14	-11.61	0.00	0.00	0.00
36.36	152.19	28.75	-11.87	0.00	0.00	0.00
36.41	152.42	28.99	-11.96	0.00	0.00	0.00
36.42	152.44	29.00	-11.97	0.00	0.00	0.00
36.44	152.55	29.12	-12.02	0.00	0.00	0.00
36.57	153.08	29.65	-12.24	0.00	0.00	0.00
36.60	153.19	29.75	-12.28	0.00	0.00	0.00
36.74	153.77	30.34	-12.52	0.00	0.00	0.00
36.84	154.22	30.78	-12.70	0.00	0.00	0.00
36.92	154.53	31.09	-12.83	0.00	0.00	0.00
36.93	154.59	31.15	-12.86	0.00	0.00	0.00
36.98	154.78	31.34	-12.94	0.00	0.00	0.00
37.02	154.97	31.53	-13.01	0.00	0.00	0.00
37.06	155.13	31.69	-13.08	0.00	0.00	0.00
37.08	155.22	31.78	-13.12	0.00	0.00	0.00
37.10	155.29	31.86	-13.15	0.00	0.00	0.00
37.18	155.63	32.19	-13.29	0.00	0.00	0.00
37.20	155.73	32.29	-13.33	0.00	0.00	0.00
37.22	155.79	32.36	-13.36	0.00	0.00	0.00
37.22	155.80	32.36	-13.36	0.00	0.00	0.00
37.27	156.02	32.59	-13.45	0.00	0.00	0.00
37.30	156.15	32.71	-13.50	0.00	0.00	0.00
37.31	156.20	32.76	-13.52	0.00	0.00	0.00
37.42	156.62	33.19	-13.70	0.00	0.00	0.00
37.45	156.74	33.31	-13.75	0.00	0.00	0.00
37.52	157.06	33.63	-13.88	0.00	0.00	0.00
37.54	157.15	33.72	-13.92	0.00	0.00	0.00

37.59	157.35	33.91	-14.00	0.00	0.00	0.00
37.65	157.61	34.17	-14.10	0.00	0.00	0.00
37.67	157.69	34.26	-14.14	0.00	0.00	0.00
37.70	157.80	34.36	-14.18	0.00	0.00	0.00
37.72	157.89	34.45	-14.22	0.00	0.00	0.00
37.73	157.92	34.48	-14.23	0.00	0.00	0.00
37.79	158.18	34.74	-14.34	0.00	0.00	0.00
37.84	158.38	34.94	-14.42	0.00	0.00	0.00
37.85	158.45	35.01	-14.45	0.00	0.00	0.00
37.97	158.93	35.49	-14.65	0.00	0.00	0.00
37.97	158.94	35.51	-14.66	0.00	0.00	0.00
38.00	159.06	35.62	-14.70	0.00	0.00	0.00
38.04	159.24	35.80	-14.78	0.00	0.00	0.00
38.15	159.70	36.26	-14.97	0.00	0.00	0.00
38.26	160.14	36.71	-15.15	0.00	0.00	0.00
38.29	160.29	36.85	-15.21	0.00	0.00	0.00
38.31	160.38	36.95	-15.25	0.00	0.00	0.00
38.38	160.66	37.23	-15.37	0.00	0.00	0.00
38.39	160.72	37.28	-15.39	0.00	0.00	0.00
38.44	160.90	37.46	-15.46	0.00	0.00	0.00
38.45	160.96	37.52	-15.49	0.00	0.00	0.00
38.48	161.06	37.62	-15.53	0.00	0.00	0.00
38.49	161.13	37.69	-15.56	0.00	0.00	0.00
38.53	161.27	37.84	-15.62	0.00	0.00	0.00
38.63	161.71	38.27	-15.80	0.00	0.00	0.00
38.67	161.86	38.42	-15.86	0.00	0.00	0.00
38.77	162.27	38.83	-16.03	0.00	0.00	0.00
38.83	162.53	39.09	-16.13	0.00	0.00	0.00
39.11	163.72	40.29	-16.63	0.00	0.00	0.00
39.13	163.80	40.37	-16.66	0.00	0.00	0.00
39.15	163.86	40.42	-16.69	0.00	0.00	0.00
39.20	164.07	40.63	-16.77	0.00	0.00	0.00
39.20	164.07	40.64	-16.77	0.00	0.00	0.00
39.21	164.12	40.69	-16.79	0.00	0.00	0.00
39.25	164.30	40.87	-16.87	0.00	0.00	0.00
39.27	164.40	40.96	-16.91	0.00	0.00	0.00
39.37	164.81	41.37	-17.08	0.00	0.00	0.00
39.49	165.31	41.87	-17.28	0.00	0.00	0.00
39.53	165.47	42.04	-17.35	0.00	0.00	0.00
39.79	166.56	43.12	-17.80	0.00	0.00	0.00
39.79	166.57	43.13	-17.80	0.00	0.00	0.00
39.87	166.91	43.48	-17.94	0.00	0.00	0.00
39.89	166.99	43.56	-17.98	0.00	0.00	0.00
39.90	167.03	43.60	-17.99	0.00	0.00	0.00

39.98	167.34	43.90	-18.12	0.00	0.00	0.00
40.05	167.65	44.21	-18.25	0.00	0.00	0.00
40.06	167.70	44.26	-18.27	0.00	0.00	0.00
40.12	167.93	44.49	-18.36	0.00	0.00	0.00
40.12	167.94	44.50	-18.37	0.00	0.00	0.00
40.26	168.54	45.10	-18.62	0.00	0.00	0.00
40.32	168.79	45.35	-18.72	0.00	0.00	0.00
40.33	168.82	45.38	-18.73	0.00	0.00	0.00
40.35	168.91	45.47	-18.77	0.00	0.00	0.00
40.56	169.78	46.35	-19.13	0.00	0.00	0.00
40.68	170.28	46.85	-19.34	0.00	0.00	0.00
40.80	170.79	47.35	-19.54	0.00	0.00	0.00
40.82	170.86	47.43	-19.58	0.00	0.00	0.00
40.85	171.01	47.57	-19.63	0.00	0.00	0.00
41.01	171.68	48.24	-19.91	0.00	0.00	0.00
41.19	172.44	49.00	-20.23	0.00	0.00	0.00
41.25	172.67	49.24	-20.32	0.00	0.00	0.00
41.30	172.90	49.46	-20.42	0.00	0.00	0.00
41.35	173.11	49.67	-20.50	0.00	0.00	0.00
41.40	173.31	49.88	-20.59	0.00	0.00	0.00
41.50	173.70	50.26	-20.75	0.00	0.00	0.00
41.50	173.72	50.29	-20.76	0.00	0.00	0.00
41.50	173.73	50.29	-20.76	0.00	0.00	0.00
41.51	173.75	50.32	-20.77	0.00	0.00	0.00
41.63	174.26	50.82	-20.98	0.00	0.00	0.00
41.83	175.10	51.66	-21.32	0.00	0.00	0.00
42.01	175.84	52.40	-21.63	0.00	0.00	0.00
42.06	176.08	52.64	-21.73	0.00	0.00	0.00
42.84	179.34	55.91	-23.08	0.00	0.00	0.00
42.88	179.50	56.06	-23.14	0.00	0.00	0.00
42.89	179.52	56.08	-23.15	0.00	0.00	0.00
42.91	179.63	56.20	-23.20	0.00	0.00	0.00
42.92	179.67	56.23	-23.21	0.00	0.00	0.00
42.96	179.85	56.41	-23.28	0.00	0.00	0.00
43.04	180.16	56.72	-23.41	0.00	0.00	0.00
43.27	181.13	57.69	-23.81	0.00	0.00	0.00
43.29	181.21	57.78	-23.85	0.00	0.00	0.00
43.67	182.81	59.37	-24.51	0.00	0.00	0.00
43.81	183.39	59.95	-24.75	0.00	0.00	0.00
43.83	183.49	60.05	-24.79	0.00	0.00	0.00
43.87	183.63	60.19	-24.85	0.00	0.00	0.00
43.98	184.09	60.65	-25.03	0.00	0.00	0.00
44.11	184.65	61.21	-25.27	0.00	0.00	0.00
44.11	184.65	61.22	-25.27	0.00	0.00	0.00

44.19	184.98	61.55	-25.40	0.00	0.00	0.00
44.76	187.36	63.92	-26.38	0.00	0.00	0.00
44.86	187.78	64.35	-26.56	0.00	0.00	0.00
45.37	189.92	66.49	-27.44	0.00	0.00	0.00
45.49	190.40	66.96	-27.64	0.00	0.00	0.00
45.77	191.61	68.17	-28.14	0.00	0.00	0.00
45.83	191.86	68.42	-28.24	0.00	0.00	0.00
45.92	192.23	68.80	-28.40	0.00	0.00	0.00
46.33	193.95	70.52	-29.11	0.00	0.00	0.00
46.96	196.56	73.12	-30.18	0.00	0.00	0.00
47.30	197.99	74.55	-30.77	0.00	0.00	0.00
47.72	199.75	76.31	-31.50	0.00	0.00	0.00
49.96	209.13	85.69	-35.37	0.00	0.00	0.00
50.80	212.63	89.20	-36.82	0.00	0.00	0.00

Table S3: Maxwell-Boltzmann distribution calculated at 300 K for β anomer of unlabeled **10**.

Minimized Energy (Kcal/mol)	Minimized Energy (KJ/mol)	Δ energy (ΔE) (KJ/mol)	-ΔE/RT	$e^{-E/RT}$	fraction	% population
28.55	119.49	0.00	0.00	1.00	0.19	19.44
28.83	120.69	1.19	-0.49	0.61	0.12	11.88
28.87	120.84	1.35	-0.56	0.57	0.11	11.14
28.89	120.93	1.43	-0.59	0.55	0.11	10.77
29.02	121.47	1.97	-0.81	0.44	0.09	8.62
29.37	122.95	3.45	-1.43	0.24	0.05	4.67
29.38	122.97	3.48	-1.44	0.24	0.05	4.63
29.44	123.24	3.74	-1.54	0.21	0.04	4.15
29.57	123.77	4.27	-1.76	0.17	0.03	3.33
29.65	124.10	4.60	-1.90	0.15	0.03	2.91
29.65	124.10	4.61	-1.90	0.15	0.03	2.90
29.70	124.31	4.82	-1.99	0.14	0.03	2.66
30.16	126.25	6.76	-2.79	0.06	0.01	1.19
30.19	126.38	6.88	-2.84	0.06	0.01	1.14
30.26	126.68	7.18	-2.96	0.05	0.01	1.00
30.30	126.84	7.35	-3.03	0.05	0.01	0.94
30.35	127.03	7.53	-3.11	0.04	0.01	0.87
30.37	127.12	7.63	-3.15	0.04	0.01	0.83
30.37	127.14	7.65	-3.16	0.04	0.01	0.83
30.45	127.45	7.96	-3.28	0.04	0.01	0.73
30.58	128.02	8.52	-3.52	0.03	0.01	0.58
30.73	128.64	9.15	-3.78	0.02	0.00	0.45

30.75	128.74	9.24	-3.81	0.02	0.00	0.43
30.80	128.94	9.45	-3.90	0.02	0.00	0.39
30.97	129.62	10.13	-4.18	0.02	0.00	0.30
31.03	129.90	10.40	-4.29	0.01	0.00	0.27
31.08	130.11	10.62	-4.38	0.01	0.00	0.24
31.14	130.36	10.87	-4.49	0.01	0.00	0.22
31.16	130.44	10.95	-4.52	0.01	0.00	0.21
31.21	130.66	11.16	-4.61	0.01	0.00	0.19
31.26	130.86	11.37	-4.69	0.01	0.00	0.18
31.29	130.97	11.47	-4.74	0.01	0.00	0.17
31.31	131.05	11.56	-4.77	0.01	0.00	0.16
31.43	131.55	12.06	-4.98	0.01	0.00	0.13
31.51	131.90	12.40	-5.12	0.01	0.00	0.12
31.65	132.47	12.98	-5.36	0.00	0.00	0.09
31.66	132.54	13.05	-5.39	0.00	0.00	0.09
31.70	132.71	13.22	-5.45	0.00	0.00	0.08
31.81	133.17	13.67	-5.64	0.00	0.00	0.07
31.86	133.36	13.87	-5.72	0.00	0.00	0.06
31.88	133.43	13.94	-5.75	0.00	0.00	0.06
31.90	133.53	14.03	-5.79	0.00	0.00	0.06
31.90	133.53	14.04	-5.80	0.00	0.00	0.06
31.91	133.57	14.07	-5.81	0.00	0.00	0.06
31.97	133.83	14.34	-5.92	0.00	0.00	0.05
32.01	134.01	14.51	-5.99	0.00	0.00	0.05
32.03	134.09	14.60	-6.03	0.00	0.00	0.05
32.04	134.12	14.62	-6.04	0.00	0.00	0.05
32.06	134.19	14.70	-6.07	0.00	0.00	0.05
32.18	134.70	15.20	-6.28	0.00	0.00	0.04
32.19	134.73	15.23	-6.29	0.00	0.00	0.04
32.20	134.81	15.31	-6.32	0.00	0.00	0.03
32.22	134.86	15.36	-6.34	0.00	0.00	0.03
32.24	134.94	15.45	-6.38	0.00	0.00	0.03
32.31	135.25	15.75	-6.50	0.00	0.00	0.03
32.47	135.94	16.44	-6.79	0.00	0.00	0.02
32.58	136.37	16.88	-6.97	0.00	0.00	0.02
32.62	136.55	17.05	-7.04	0.00	0.00	0.02
32.68	136.79	17.30	-7.14	0.00	0.00	0.02
32.74	137.03	17.54	-7.24	0.00	0.00	0.01
32.76	137.15	17.65	-7.29	0.00	0.00	0.01
32.78	137.20	17.71	-7.31	0.00	0.00	0.01
32.81	137.33	17.84	-7.36	0.00	0.00	0.01
32.82	137.37	17.87	-7.38	0.00	0.00	0.01
32.83	137.41	17.92	-7.39	0.00	0.00	0.01
32.92	137.78	18.29	-7.55	0.00	0.00	0.01

32.99	138.11	18.62	-7.68	0.00	0.00	0.01
33.01	138.16	18.67	-7.70	0.00	0.00	0.01
33.06	138.38	18.88	-7.79	0.00	0.00	0.01
33.18	138.90	19.40	-8.01	0.00	0.00	0.01
33.19	138.91	19.42	-8.02	0.00	0.00	0.01
33.20	138.99	19.50	-8.05	0.00	0.00	0.01
33.35	139.60	20.11	-8.30	0.00	0.00	0.00
33.43	139.92	20.43	-8.43	0.00	0.00	0.00
33.46	140.08	20.58	-8.50	0.00	0.00	0.00
33.54	140.42	20.92	-8.64	0.00	0.00	0.00
33.60	140.65	21.16	-8.73	0.00	0.00	0.00
33.67	140.96	21.47	-8.86	0.00	0.00	0.00
33.72	141.14	21.65	-8.94	0.00	0.00	0.00
33.75	141.27	21.78	-8.99	0.00	0.00	0.00
33.89	141.85	22.35	-9.23	0.00	0.00	0.00
33.94	142.07	22.58	-9.32	0.00	0.00	0.00
33.95	142.12	22.63	-9.34	0.00	0.00	0.00
33.97	142.21	22.71	-9.38	0.00	0.00	0.00
34.00	142.32	22.83	-9.42	0.00	0.00	0.00
34.01	142.36	22.87	-9.44	0.00	0.00	0.00
34.06	142.56	23.06	-9.52	0.00	0.00	0.00
34.09	142.68	23.19	-9.57	0.00	0.00	0.00
34.14	142.91	23.41	-9.66	0.00	0.00	0.00
34.16	142.99	23.50	-9.70	0.00	0.00	0.00
34.17	143.02	23.53	-9.71	0.00	0.00	0.00
34.19	143.12	23.63	-9.75	0.00	0.00	0.00
34.20	143.15	23.66	-9.76	0.00	0.00	0.00
34.21	143.19	23.70	-9.78	0.00	0.00	0.00
34.23	143.29	23.80	-9.82	0.00	0.00	0.00
34.26	143.42	23.93	-9.88	0.00	0.00	0.00
34.27	143.47	23.98	-9.90	0.00	0.00	0.00
34.28	143.48	23.99	-9.90	0.00	0.00	0.00
34.28	143.50	24.01	-9.91	0.00	0.00	0.00
34.29	143.55	24.05	-9.93	0.00	0.00	0.00
34.31	143.63	24.13	-9.96	0.00	0.00	0.00
34.32	143.65	24.16	-9.97	0.00	0.00	0.00
34.32	143.67	24.17	-9.98	0.00	0.00	0.00
34.33	143.70	24.20	-9.99	0.00	0.00	0.00
34.51	144.45	24.96	-10.30	0.00	0.00	0.00
34.53	144.56	25.07	-10.35	0.00	0.00	0.00
34.54	144.57	25.08	-10.35	0.00	0.00	0.00
34.64	145.00	25.51	-10.53	0.00	0.00	0.00
34.64	145.01	25.51	-10.53	0.00	0.00	0.00
34.68	145.15	25.66	-10.59	0.00	0.00	0.00

34.84	145.84	26.35	-10.87	0.00	0.00	0.00
34.90	146.09	26.60	-10.98	0.00	0.00	0.00
35.01	146.55	27.05	-11.17	0.00	0.00	0.00
35.06	146.76	27.26	-11.25	0.00	0.00	0.00
35.07	146.80	27.31	-11.27	0.00	0.00	0.00
35.08	146.86	27.36	-11.29	0.00	0.00	0.00
35.09	146.90	27.41	-11.31	0.00	0.00	0.00
35.10	146.94	27.45	-11.33	0.00	0.00	0.00
35.12	147.00	27.50	-11.35	0.00	0.00	0.00
35.21	147.37	27.88	-11.51	0.00	0.00	0.00
35.22	147.44	27.95	-11.54	0.00	0.00	0.00
35.33	147.90	28.40	-11.72	0.00	0.00	0.00
35.45	148.39	28.89	-11.93	0.00	0.00	0.00
35.48	148.54	29.04	-11.99	0.00	0.00	0.00
35.52	148.69	29.19	-12.05	0.00	0.00	0.00
35.57	148.88	29.38	-12.13	0.00	0.00	0.00
35.65	149.24	29.75	-12.28	0.00	0.00	0.00
35.66	149.28	29.78	-12.29	0.00	0.00	0.00
35.67	149.33	29.83	-12.31	0.00	0.00	0.00
35.71	149.49	30.00	-12.38	0.00	0.00	0.00
35.81	149.91	30.42	-12.55	0.00	0.00	0.00
35.86	150.11	30.61	-12.64	0.00	0.00	0.00
35.86	150.11	30.62	-12.64	0.00	0.00	0.00
35.87	150.16	30.67	-12.66	0.00	0.00	0.00
36.00	150.68	31.19	-12.87	0.00	0.00	0.00
36.06	150.93	31.43	-12.97	0.00	0.00	0.00
36.07	150.99	31.50	-13.00	0.00	0.00	0.00
36.08	151.01	31.52	-13.01	0.00	0.00	0.00
36.08	151.01	31.52	-13.01	0.00	0.00	0.00
36.08	151.02	31.53	-13.01	0.00	0.00	0.00
36.13	151.25	31.76	-13.11	0.00	0.00	0.00
36.19	151.48	31.99	-13.20	0.00	0.00	0.00
36.19	151.50	32.00	-13.21	0.00	0.00	0.00
36.23	151.67	32.17	-13.28	0.00	0.00	0.00
36.28	151.86	32.37	-13.36	0.00	0.00	0.00
36.28	151.88	32.39	-13.37	0.00	0.00	0.00
36.40	152.39	32.89	-13.58	0.00	0.00	0.00
36.42	152.44	32.94	-13.60	0.00	0.00	0.00
36.42	152.46	32.96	-13.61	0.00	0.00	0.00
36.55	152.99	33.49	-13.82	0.00	0.00	0.00
36.55	152.99	33.50	-13.83	0.00	0.00	0.00
36.80	154.03	34.53	-14.25	0.00	0.00	0.00
36.82	154.11	34.61	-14.29	0.00	0.00	0.00
36.84	154.20	34.71	-14.33	0.00	0.00	0.00

36.89	154.41	34.92	-14.41	0.00	0.00	0.00
36.90	154.47	34.98	-14.44	0.00	0.00	0.00
37.01	154.93	35.44	-14.63	0.00	0.00	0.00
37.05	155.10	35.60	-14.69	0.00	0.00	0.00
37.07	155.16	35.66	-14.72	0.00	0.00	0.00
37.22	155.79	36.30	-14.98	0.00	0.00	0.00
37.23	155.84	36.35	-15.00	0.00	0.00	0.00
37.24	155.87	36.38	-15.02	0.00	0.00	0.00
37.26	155.96	36.46	-15.05	0.00	0.00	0.00
37.33	156.25	36.76	-15.17	0.00	0.00	0.00
37.36	156.37	36.87	-15.22	0.00	0.00	0.00
37.39	156.49	37.00	-15.27	0.00	0.00	0.00
37.42	156.65	37.16	-15.34	0.00	0.00	0.00
37.59	157.33	37.84	-15.62	0.00	0.00	0.00
37.60	157.39	37.90	-15.64	0.00	0.00	0.00
37.66	157.64	38.14	-15.74	0.00	0.00	0.00
37.86	158.48	38.99	-16.09	0.00	0.00	0.00
37.86	158.49	39.00	-16.10	0.00	0.00	0.00
37.90	158.65	39.16	-16.16	0.00	0.00	0.00
37.97	158.93	39.44	-16.28	0.00	0.00	0.00
37.97	158.96	39.47	-16.29	0.00	0.00	0.00
38.01	159.12	39.63	-16.36	0.00	0.00	0.00
38.05	159.29	39.80	-16.43	0.00	0.00	0.00
38.06	159.30	39.80	-16.43	0.00	0.00	0.00
38.07	159.34	39.85	-16.45	0.00	0.00	0.00
38.09	159.43	39.93	-16.48	0.00	0.00	0.00
38.09	159.46	39.96	-16.50	0.00	0.00	0.00
38.25	160.11	40.62	-16.76	0.00	0.00	0.00
38.34	160.50	41.01	-16.93	0.00	0.00	0.00
38.41	160.76	41.27	-17.03	0.00	0.00	0.00
38.46	160.98	41.48	-17.12	0.00	0.00	0.00
38.50	161.15	41.65	-17.19	0.00	0.00	0.00
38.52	161.24	41.75	-17.23	0.00	0.00	0.00
38.66	161.84	42.35	-17.48	0.00	0.00	0.00
38.74	162.15	42.66	-17.61	0.00	0.00	0.00
38.76	162.27	42.77	-17.65	0.00	0.00	0.00
38.94	162.99	43.49	-17.95	0.00	0.00	0.00
39.10	163.67	44.18	-18.24	0.00	0.00	0.00
39.41	164.97	45.47	-18.77	0.00	0.00	0.00
39.48	165.28	45.79	-18.90	0.00	0.00	0.00
39.49	165.30	45.81	-18.91	0.00	0.00	0.00
39.50	165.35	45.86	-18.93	0.00	0.00	0.00
39.56	165.59	46.10	-19.03	0.00	0.00	0.00
39.59	165.72	46.23	-19.08	0.00	0.00	0.00

39.64	165.93	46.44	-19.17	0.00	0.00	0.00
39.64	165.94	46.44	-19.17	0.00	0.00	0.00
39.76	166.43	46.94	-19.37	0.00	0.00	0.00
39.81	166.65	47.16	-19.47	0.00	0.00	0.00
39.85	166.82	47.32	-19.53	0.00	0.00	0.00
39.91	167.08	47.58	-19.64	0.00	0.00	0.00
39.98	167.35	47.85	-19.75	0.00	0.00	0.00
40.11	167.89	48.39	-19.98	0.00	0.00	0.00
40.16	168.09	48.60	-20.06	0.00	0.00	0.00
40.24	168.46	48.97	-20.21	0.00	0.00	0.00
40.29	168.67	49.18	-20.30	0.00	0.00	0.00
40.45	169.32	49.83	-20.57	0.00	0.00	0.00
40.47	169.40	49.91	-20.60	0.00	0.00	0.00
40.49	169.47	49.98	-20.63	0.00	0.00	0.00
40.63	170.06	50.57	-20.87	0.00	0.00	0.00
40.96	171.44	51.94	-21.44	0.00	0.00	0.00
41.26	172.70	53.20	-21.96	0.00	0.00	0.00
41.39	173.24	53.74	-22.18	0.00	0.00	0.00
41.45	173.52	54.02	-22.30	0.00	0.00	0.00
41.52	173.79	54.30	-22.41	0.00	0.00	0.00
41.54	173.89	54.40	-22.45	0.00	0.00	0.00
41.58	174.03	54.54	-22.51	0.00	0.00	0.00
41.69	174.51	55.02	-22.71	0.00	0.00	0.00
41.73	174.68	55.19	-22.78	0.00	0.00	0.00
41.91	175.44	55.94	-23.09	0.00	0.00	0.00
41.98	175.71	56.21	-23.20	0.00	0.00	0.00
41.99	175.77	56.28	-23.23	0.00	0.00	0.00
42.35	177.29	57.79	-23.85	0.00	0.00	0.00
42.69	178.68	59.19	-24.43	0.00	0.00	0.00
42.77	179.03	59.53	-24.57	0.00	0.00	0.00
42.93	179.71	60.22	-24.85	0.00	0.00	0.00
43.23	180.95	61.46	-25.37	0.00	0.00	0.00
43.31	181.28	61.79	-25.50	0.00	0.00	0.00
43.39	181.63	62.13	-25.65	0.00	0.00	0.00
43.40	181.66	62.16	-25.66	0.00	0.00	0.00
44.01	184.22	64.72	-26.72	0.00	0.00	0.00
44.19	184.96	65.47	-27.02	0.00	0.00	0.00
44.40	185.86	66.36	-27.39	0.00	0.00	0.00
44.52	186.35	66.85	-27.59	0.00	0.00	0.00
45.08	188.68	69.19	-28.56	0.00	0.00	0.00
45.80	191.71	72.22	-29.81	0.00	0.00	0.00
45.90	192.14	72.64	-29.98	0.00	0.00	0.00
46.20	193.38	73.89	-30.50	0.00	0.00	0.00
48.47	202.89	83.40	-34.42	0.00	0.00	0.00

49.92	208.97	89.47	-36.93	0.00	0.00	0.00

Table S4: Maxwell-Boltzmann distribution calculated at 300 K for α anomer of unlabeled **11**.

Minimized Energy (Kcal/mol)	Minimized Energy (KJ/mol)	Δ energy (ΔE) (KJ/mol)	-ΔE/RT	$e^{-E/RT}$	fraction	% population
20.08	84.04	0.00	0.00	1.00	0.73	72.90
21.17	88.61	4.57	-1.89	0.15	0.11	11.07
21.36	89.43	5.39	-2.22	0.11	0.08	7.89
21.42	89.68	5.63	-2.33	0.10	0.07	7.12
22.91	95.91	11.86	-4.90	0.01	0.01	0.54
23.48	98.30	14.25	-5.88	0.00	0.00	0.20
23.60	98.79	14.75	-6.09	0.00	0.00	0.17
23.98	100.39	16.35	-6.75	0.00	0.00	0.09
25.34	106.09	22.04	-9.10	0.00	0.00	0.01
25.57	107.03	22.99	-9.49	0.00	0.00	0.01
26.01	108.87	24.82	-10.25	0.00	0.00	0.00
26.02	108.90	24.86	-10.26	0.00	0.00	0.00
26.07	109.11	25.07	-10.35	0.00	0.00	0.00
26.12	109.33	25.28	-10.44	0.00	0.00	0.00
26.16	109.50	25.46	-10.51	0.00	0.00	0.00
26.72	111.85	27.80	-11.48	0.00	0.00	0.00
28.54	119.45	35.41	-14.62	0.00	0.00	0.00
29.03	121.50	37.46	-15.46	0.00	0.00	0.00
29.05	121.59	37.54	-15.50	0.00	0.00	0.00
29.15	122.02	37.98	-15.67	0.00	0.00	0.00
29.55	123.70	39.66	-16.37	0.00	0.00	0.00
29.92	125.25	41.21	-17.01	0.00	0.00	0.00
30.54	127.82	43.78	-18.07	0.00	0.00	0.00
30.62	128.18	44.13	-18.22	0.00	0.00	0.00
31.74	132.86	48.81	-20.15	0.00	0.00	0.00
34.24	143.31	59.27	-24.46	0.00	0.00	0.00
35.65	149.21	65.17	-26.90	0.00	0.00	0.00

Table S5: Maxwell-Boltzmann distribution calculated at 300 K for β anomer of unlabeled **11**.

Minimized Energy (Kcal/mol)	Minimized Energy (KJ/mol)	Δ energy (ΔE) (KJ/mol)	-ΔE/RT	$e^{-E/RT}$	fraction	% population
Kcal/mol	KJ/mol	Δ energy (ΔE)	-ΔE/RT	$e^{-E/RT}$	fraction	% population
18.96	79.35	0.00	0.00	1.00	0.73	72.94
20.05	83.94	4.59	-1.90	0.15	0.11	10.96
20.30	84.97	5.63	-2.32	0.10	0.07	7.15
20.36	85.21	5.86	-2.42	0.09	0.06	6.49
21.20	88.73	9.39	-3.88	0.02	0.02	1.51
21.86	91.49	12.14	-5.01	0.01	0.00	0.49
22.24	93.11	13.76	-5.68	0.00	0.00	0.25
22.48	94.09	14.75	-6.09	0.00	0.00	0.17
24.01	100.51	21.16	-8.74	0.00	0.00	0.01
24.02	100.54	21.19	-8.75	0.00	0.00	0.01
24.49	102.53	23.19	-9.57	0.00	0.00	0.01
24.51	102.61	23.26	-9.60	0.00	0.00	0.00
24.73	103.53	24.18	-9.98	0.00	0.00	0.00
24.74	103.57	24.23	-10.00	0.00	0.00	0.00
24.78	103.71	24.36	-10.06	0.00	0.00	0.00
25.06	104.89	25.54	-10.54	0.00	0.00	0.00
26.23	109.79	30.44	-12.56	0.00	0.00	0.00
27.26	114.10	34.76	-14.35	0.00	0.00	0.00
27.55	115.34	35.99	-14.86	0.00	0.00	0.00
27.88	116.69	37.34	-15.41	0.00	0.00	0.00
28.13	117.73	38.39	-15.84	0.00	0.00	0.00
28.95	121.17	41.83	-17.26	0.00	0.00	0.00
29.09	121.75	42.41	-17.50	0.00	0.00	0.00
30.54	127.83	48.49	-20.01	0.00	0.00	0.00
31.16	130.44	51.10	-21.09	0.00	0.00	0.00
33.23	139.09	59.74	-24.66	0.00	0.00	0.00
34.40	143.98	64.63	-26.68	0.00	0.00	0.00

Molecular dynamics (MD) simulations on unlabeled glycans 10 and 11 in vacuum

5 μs MD simulations were performed *in vacuo* on the 14 and the 8 most abundant conformers, involving both anomers for unlabeled compounds **10** and **11,** respectively. These simulations were carried out with the AMBER 18 package.[4] Parameters for the oligosaccharides were generated with the *antechamber* module of AMBER, using GAFF2[5] force field. The partial charges on each atom were generated following a standard protocol. First, HF/6-31G(d) was used to calculate the molecular electrostatic potential (MEP). Secondly, the RESP[6] (Restrained ElectroStatic Potential) algorithm fits this MEP by using an atom-centered point charge model. The charges were calculated according to the Merz-Singh-Kollman scheme using Gaussian 16.[7] Each molecule was minimized in vacuo (500 steps) with a cut-off set to 999 Å for the non-bonded interactions and in the absence of neutralizing ions to better reproduce the ion mobility measurements. The system was subjected then to 5 μs MD simulations in vacuum at a constant temperature of 300K. A weak-coupling algorithm was used to control and equalize the temperature.[8] The time step was kept at 1 fs. Hydrogen atoms were kept fixed through the simulations using the SHAKE algorithm[9] and a cut-off of 999 Å was applied. For each molecule, the trajectory was saved every 10,000 steps, with a total of 5,000,000,000 steps per simulation. The *cpptraj* module of AMBER 18 was employed to extract 10,000 frames from each MD trajectory.

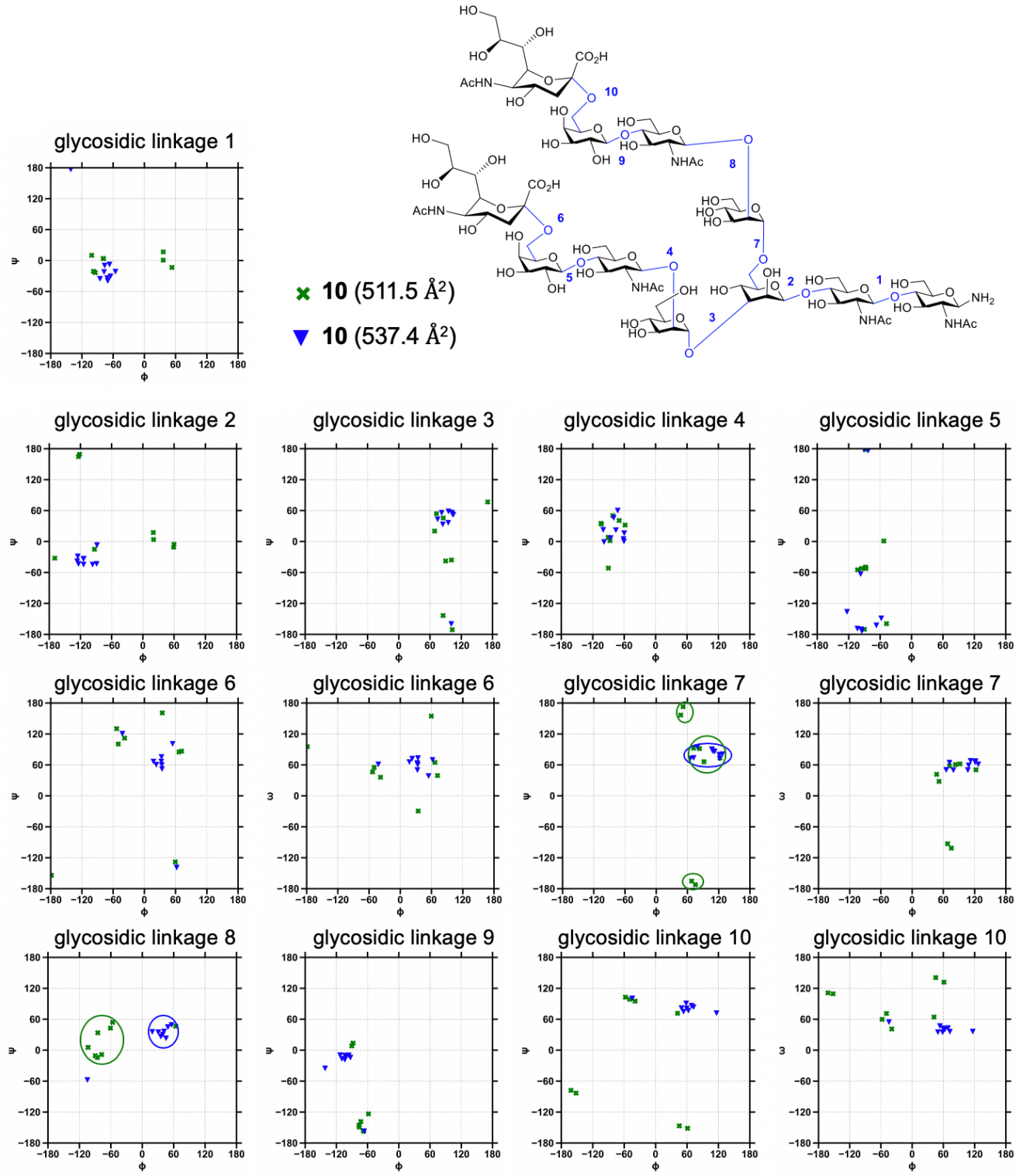

Figure S121. ϕ, ψ and ω dihedral values for all the glycosidic linkages of glycan **10**. Green crosses and blue triangles correspond to the peaks with CCS values of 511.5 A2 and 537.4 A2, respectively. Glycosidic linkage Manα(1,6)Man (glycosidic bond 7) and GlcNAcβ(1,2)Man (glycosidic bond 8) determine the difference between the conformational distributions, as highlighted in the pictures.

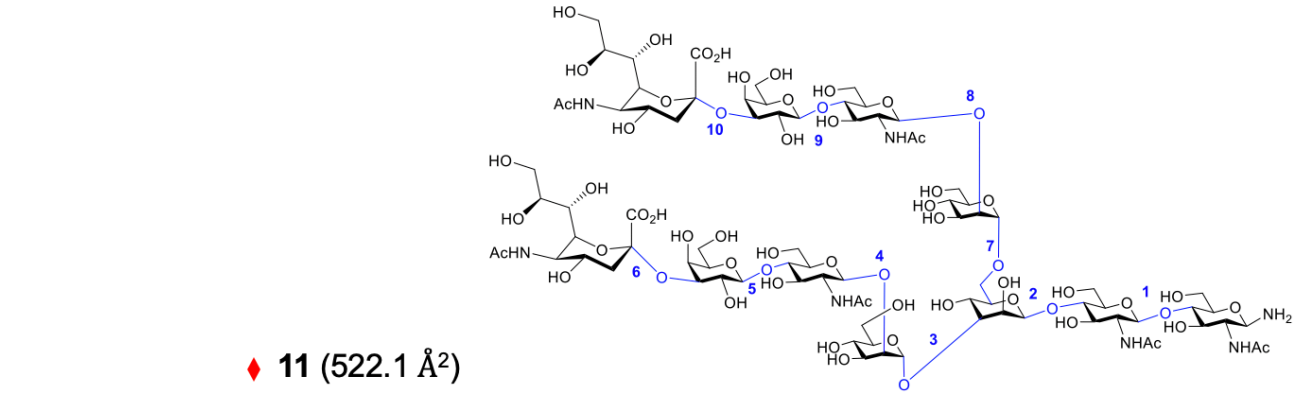

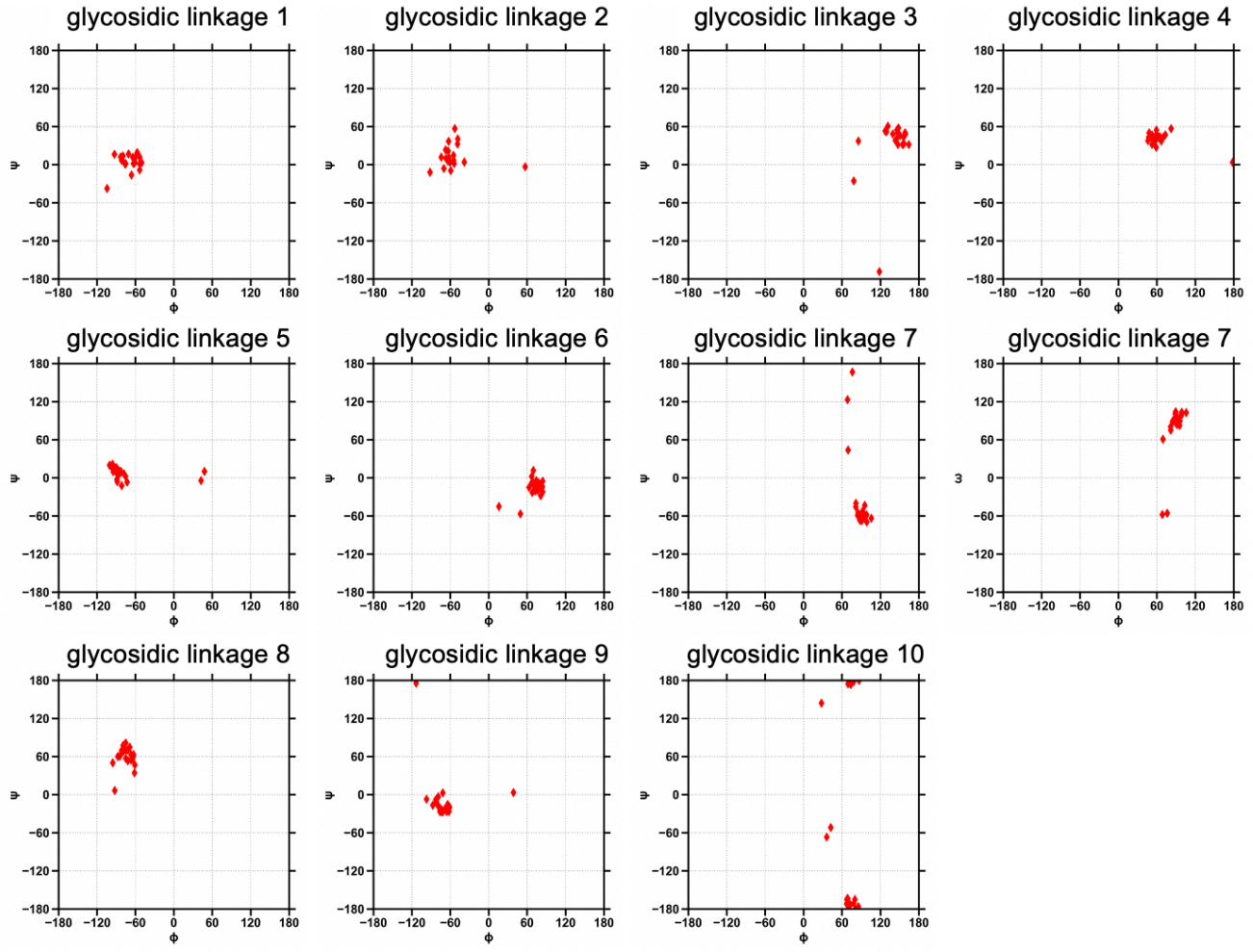

Figure S122. ϕ, ψ and ω dihedral values for all the glycosidic linkages of glycan **11**. The different conformers found for glycan **11** MD simulations in vacuum show higher rigidity, with torsional angles values less disperse, as represented in the figures.

CCS value calculation of each frame

High Performance Collision Cross Section (HPCCS)[10] software was used to estimate the CCS value of each frame using 50 points of integrations for Monte Carlo at 300 K under nitrogen gas. CCS values of each conformer were normalized based on their theoretical abundancy and represented to give the theoretical ATDs of the standards **10'** and **11'**.

References

[1] L. Liu, A. R. Prudden, G. P. Bosman, G. J. Boons, *Carbohydr. Res.* **2017**, DOI 10.1016/j.carres.2017.10.001.

[2] D. H. Joziasse, W. E. Schiphorst, D. H. Van den Eijnden, J. A. Van Kuik, H. Van Halbeek, J. F. Vliegenthart, *J. Biol. Chem.* **1987**, *262*, 2025–33.

[3] D. H. van den Eijnden, W. M. Blanken, A. van Vliet, *Carbohydr. Res.* **1986**, *151*, 329–335.

[4] D.A. Case, S.R. Brozell, D.S. Cerutti, T.E. Cheatham, III, V.W.D. Cruzeiro, T.A. Darden, R.E. Duke, D. Ghoreishi, H. Gohlke, A.W. Goetz, D. Greene, R Harris, N. Homeyer, S. Izadi, A. Kovalenko, T.S. Lee, S. LeGrand, P. Li, C. Lin, J. Liu, T. Luchko, R. Luo, D.J. Mermelstein, K.M. Merz, Y. Miao, G. Monard, H. Nguyen, I. Omelyan, A. Onufriev, F. Pan, R. Qi, D.R. Roe, A. Roitberg, C. Sagui, S. Schott-Verdugo, J. Shen, C.L. Simmerling, J. Smith, J. Swails, R.C. Walker, J. Wang, H. Wei, R.M. Wolf, X. Wu, L. Xiao, D.M. York and P.A. Kollman,. AMBER 2018, *Univ. California, San Fr.* **2018**.

[5] J. Wang, R. M. Wolf, J. W. Caldwell, P. A. Kollman, D. A. Case, *J. Comput. Chem.* **2004**, *25*, 1157–1174.

[6] C. I. Bayly, P. Cieplak, W. Cornell, P. A. Kollman, *J. Phys. Chem.* **1993**, *97*, 10269–10280.

[7] Gaussian 16, Revision C.01, M. J. Frisch, G. W. Trucks, H. B. Schlegel, G. E. Scuseria, M. A. Robb, J. R. Cheeseman, G. Scalmani, V. Barone, G. A. Petersson, H. Nakatsuji, X. Li, M. Caricato, A. V. Marenich, J. Bloino, B. G. Janesko, R. Gomperts, B. Mennucci, H. P. Hratchian, J. V. Ortiz, A. F. Izmaylov, J. L. Sonnenberg, D. Williams-Young, F. Ding, F. Lipparini, F. Egidi, J. Goings, B. Peng, A. Petrone, T. Henderson, D. Ranasinghe, V. G. Zakrzewski, J. Gao, N. Rega, G. Zheng, W. Liang, M. Hada, M. Ehara, K. Toyota, R. Fukuda, J. Hasegawa, M. Ishida, T. Nakajima, Y. Honda, O. Kitao, H. Nakai, T. Vreven, K. Throssell, J. A. Montgomery, Jr., J. E. Peralta, F. Ogliaro, M. J. Bearpark, J. J. Heyd, E. N. Brothers, K. N. Kudin, V. N. Staroverov, T. A. Keith, R. Kobayashi, J. Normand, K. Raghavachari, A. P. Rendell, J. C. Burant, S. S. Iyengar, J. Tomasi, M. Cossi, J. M. Millam, M. Klene, C. Adamo, R. Cammi, J. W. Ochterski, R. L. Martin, K. Morokuma, O. Farkas, J. B. Foresman, and D. J. Fox,. *Gaussian, Inc., Wallingford CT,* **2016**.

[8] H. J. C. Berendsen, J. P. M. Postma, W. F. van Gunsteren, A. DiNola, J. R. Haak, *J. Chem. Phys.* **1984**, *81*, 3684–3690.

[9] S. Miyamoto, P. A. Kollman, *J. Comput. Chem.* **1992**, *13*, 952–962.

[10] L. Zanotto, G. Heerdt, P. C. T. Souza, G. Araujo, M. S. Skaf, *J. Comput. Chem.* **2018**, *39*, 1675–1681.

Author Contributions

O.A.-O., J.S.T. and V.J.S conceived the experiments. N.W, T.L. and G.J.B. designed and synthesized the standards. O.A.-O., J.S.T., V.J.S, F.C. and G.J.O. carried out the experiments. J.S.T., V.J.S., O.A.-O, J.M.F-P,L.U and G.J.B. took the lead in writing the manuscript and designing the figures. All authors provided critical feedback and worked on the manuscript.